Bridge River Project Water Use Plan

Lower Bridge River Aquatic Monitoring

Implementation Year 9

Reference: BRGMON-1

BRGMON-1 Lower Bridge River Aquatic Monitoring, Year 9 (2020) Results

Study Period: April 1 2020 to March 31 2021

Jeff Sneep
Chris Perrin and Shauna Bennett, Limnotek
Josh Korman, Ecometric Research

Field Studies and Data Collection Completed by:
Melissa Evans, Danny O'Farrell, Elijah Michel, Brett Squirrell and Carley Wall, Coldstream Nature-Based Solutions

April 30, 2021

BRGMON-1 Lower Bridge River Aquatic Monitoring, Year 9 (2020) Results

Report Prepared for:
St'at'imc Eco-Resources

Report Prepared by:
Jeff Sneep
Chris Perrin & Shauna Bennett, Limnotek, and
Josh Korman, Ecometric Research

Field Studies and Data Collection Completed by:
Melissa Evans, Danny O'Farrell, Elijah Michel, Brett Squirrell & Carley Wall
Coldstream Nature-Based Solutions

Ref. no. BRGMON-1

April 2021

Executive Summary

Monitoring of juvenile salmonid production, periphyton and benthic communities and their habitat continued in 2020 as part of a long-term process to reduce uncertainty about the ecological response to different flow releases from the Terzaghi Dam. Sampling and measurements in 2020 were the same as in previous years dating to 1996 in Reaches 4, 3, and 2. Twelve fish sampling (juvenile standing stock) sites and four periphyton and benthic sampling sites were added in Reach 1 in 2019 and sampled again in 2020. Two reference sites that were established in the Yalakom River in 2018 have also been sampled each year since.

Flow releases to the Lower Bridge River during the post-high flow years (i.e., 2019 and 2020) were generally the same as under the Trial 2 hydrograph, with slightly earlier timing of ramp up to the peak and ramp down to the summer rearing flows in 2020. This slight difference in flow change timing from the typical Trial 2 hydrograph was not anticipated to have a measurable effect (within detection limits) on the results in 2020. Given this similarity of flow and earlier findings that flow influenced patterns of benthic assemblages and juvenile salmonid production, we focused much of the presentation of results and discussion in this report around comparing the first two Post-high flow years in 2019 and 2020 with the results from the High Flow years (2016-2018) and Trial 2 (2011-2015).

Invertebrate metrics used in the analyses were density of all taxa, density of all chironomids, the sum of mayfly, stonefly, and caddisfly densities (called EPT) that are typically considered a group most sensitive to environmental change, and family richness (the count of families). The set of metrics evaluated for juvenile salmonids (i.e., mykiss fry, mykiss parr, coho fry and Chinook fry) were size (mean weight) and condition factor, abundance and biomass, and stock-recruitment. We also specifically tested for flow effects on juvenile salmonid densities and biomass using a fixed effects model for the first time in 2020, which affirmed that flow and reach are significant determinants. The report includes recommendations on extending this model to incorporate additional covariates, such as nutrient concentrations, benthic invertebrate abundances (as a proxy for fish food availability), and spawner escapements to determine whether changes and variations in these parameters explain some of the differences among years and flow treatments in addition to flow effects. Analysis of fish salvage data were also included to provide guidance for shaping flow ramp down strategies for the low-level outlet release at Terzaghi Dam.

Water temperatures in 2019 and 2020 were largely within the range documented during the Trial 2 years (2011-2015) although temperatures during the winter months in 2019 were at the low end of the range for that season, and summer temperatures in 2019 and 2020 were at the high end of the Trial 2 range. The warmer summer temperatures were within the preferred range for the target salmonid species and likely contributed to conducive rearing conditions in summer.

The fall and winter temperatures resulted in predicted emergence timing for chinook and coho that was on par with the estimated timing for those species under Trial 2. The cooler temperatures in February 2019 extended incubation for chinook alevins by a couple of weeks in

the lower two-thirds of Reach 3 that year but occurred too late in the season to affect timing for eggs incubating in Reach 4 and the upper portion of Reach 3. As documented in previous reports, the majority (71%) of chinook spawning has occurred in the lower portion of Reach 3 with an associated median emergence timing of mid-March to early April and the majority (73%) of coho spawning was in Reach 4 with an associated median emergence timing of mid April. The spawning distribution among monitoring locations within reaches 3 and 4 did not substantively change with inclusion of the 2020 redd location data. The number of redds observed for chinook and coho in 2020 were five and seven, respectively.

Variation in dissolved inorganic nitrogen (DIN) and soluble reactive phosphorus (SRP) concentrations across monitoring years produced shifts in potential limitation of benthic algal growth based on molar N:P ratios at different times and places. During Trial 0 and Trial 1, the molar N:P ratio showed co-limitation by N and P. Molar N:P increased in Reach 2 during and after Trial 2, which showed a progressive time course increase in potential phosphorus deficiency. The Reach 2 N:P in 2020 was the highest measured since monitoring began. It showed greatest potential phosphorus deficiency in Reach 2 on record in the Lower Bridge River, although still lower than in the Yalakom River.

The analytical foundation for testing effects of flow on periphyton peak biomass (PB) and benthic communities was analysis of variance blocked among three categorical variables: Trial, Reach, and Pink salmon presence/absence (due to the observed influence of pink salmon presence on nutrient concentrations in some portions of the study area). There were no significant interactions of Reach, Trial, and Pinks on PB, which meant the main factors could be examined independently. No Pink effect on PB was found. PB in Reach 2 was significantly lower than in Reaches 3 and 4 among all Trials. There was a Trial effect on PB, entirely due to PB in the Post-High Flow years being greater than that in Trial 1. There was no significant difference in PB between all other pairs of Trials.

Like for PB, all interactions of the main effects on total benthos, EPT, or chironomids were not significant, which meant that they could be examined independently. Total benthos, EPT, and chironomid density were significantly lower during the High Flow years compared to the other Trials. Mean densities increased from the High Flow years to Post-High Flow years, resulting in no significant difference in densities between the Post-High Flow years and Trial 2. There was no Reach effect on Total benthos density, largely due to the same outcome on EPT. In contrast, chironomid density was lower in Reach 3 than in the other reaches among all flow periods. Chironomid density was greater when Pink salmon spawners were present compared to when they were absent but the EPT were not affected by Pinks.

Family richness was significantly affected by flow Trial and Reach. Richness declined during High Flow Years compared to during the other flow Trials. Recovery of family richness in the Post-High Flow years was less during Pink-on years than during Pink-off years but with only one sample year in each case during the Post-High Flow years and only one Pink–on sample during the High Flow

Years, this finding is not conclusive. Richness was lowest in Reach 4, highest in Reach 2, and in between in Reach 3 among all flow trials, which showed addition of families with increasing distance from the dam throughout all flow trials.

Mean fish condition factor (Fulton's K value) has decreased over the course of the study period for each target species and age class. Highest values were in the Pre-flow period and Trial 1 and lowest values were in the High flow (2016-2018) or Post-high flow years (2019 and 2020). The mean value (for all species combined) in Trial 2 was 1.15 (±0.05 SD), which dropped to 1.11 (±0.01 SD) during the High flow years and has remained at 1.11 (±0.01 SD) in the Post-high flow years to-date. Interestingly, for reference, the condition factor assessed for Age-0+ and Age-1 rainbow trout in Downton Reservoir (collected under BRGMON-7) was 1.29 and 1.26, respectively, which is on par with the highest condition factor values documented in the Lower Bridge River (i.e., during the Pre-flow period). To be clear, however, the reduced condition factor values in the LBR do not suggest that the condition of the fish is currently poor (i.e., when K values are <1) but may indicate that fish are needing to spend more time and energy foraging to meet their growth needs relative to earlier study years which can have survival implications. The relative trend in condition factor appears to have followed the long-term trend in nutrient concentrations from the release, particularly SRP.

Juvenile fish abundance markedly declined for all target species and age classes during the High flow years, except for chinook, which were already at reduced abundance since early in the flow trials. Results from the Post-high flow years (2019 and 2020) indicate that despite the resumption of lower flow releases (i.e., Trial 2 flow magnitudes and hydrograph shape), juvenile fish abundance and biomass have not recovered. Mean abundance in the post-high flow years was approx. 20,000 more juvenile salmonids than during the high flow years but was still approx. 195,000 fewer fish than the Trial 2 average. The modest increase in abundance was entirely attributable to mykiss and coho fry. Mean biomass in the post-high flow years was the lowest for any flow treatment to-date; approx. 194 kg lower than the high flow period and 773 kg lower than Trial 2. These results suggest that juvenile salmonid abundance and biomass in the Lower Bridge River may not be recovered quickly by the resumption of lower flow releases alone. While flow is clearly an important factor, recovery may require additional actions such as addressing the trend of declining nutrients from the flow release. Additional analyses of different covariates using the mixed effects model may assist in identifying which parameters other than flow are key drivers of juvenile fish abundance and biomass in the study area.

Based on the stock-recruitment data for chinook and coho, the stock sizes for the 2019 and 2020 recruitment years were again at the low end of the range documented across the years of monitoring but were still on par with stock size estimates that produced more juveniles during previous flow treatments. In other words, based on the existing S-R curves, it does not appear that juvenile recruitment in 2019 and 2020 was limited by stock sizes.

For stock-recruitment results, the 2019 and 2020 datapoints were stand-alone points for both coho and Chinook which were not incorporated into any of the existing curves since they represented the first two Post-high flow values (i.e., start of a new treatment) for each species. As such the existing curves (reported in Sneep et al. 2020) did not change. The 2020 datapoint for Chinook reflected another low spawner estimate in 2019 (*n*= 161; 95% CIs: 84–310); though the escapement estimate was likely biased low (possibly by ≥50%) due to the effect of fish fence operations on the spawner surveys that year (White et al. 2021). The Chinook spawner count in 2019 may also have been confounded by an increased incidence of strays due to the migration obstruction on the Fraser River caused by the Big Bar slide. The spawner estimate was close to a cluster of other low escapement values near the origin of the x-axis; however, the juvenile recruitment estimate was lower than values for all the other study years on the y-axis (i.e., 6,000 fry). The 2020 stock-recruitment data point for coho (*n*= 214; 95% CIs: 152–301) was nearest the asymptote of the Pre-flow curve and approx. 45,000 fry below the asymptote of the Trial 2 curve, indicating that recruitment was poor for that spawner stock size compared to the Trial 2 years. The existing set of curves (based on 50% egg-to-fry survival) do not suggest that spawner escapements have been limiting recruitment; however, uncertainty remains about the steepness of the initial slope for these curves.

Salmonid abundance data were collected in Reach 1 for the second time in 2020. Results for this year highlighted that all of the target species and age classes were again present in the reach, of which mykiss fry were the most abundant (~24,000 fish), followed by coho fry (~14,000 fish), Chinook fry (8,000 fish), and then mykiss parr (~3,000 fish). The patterns of abundance among the species in Reach 1 were most similar to their relative contributions in Reach 2, and the same general patterns were apparent during the first year of Reach 1 sampling in 2019 (Sneep et al. 2020); however, abundances for each species and age class were slightly higher in 2020. The total for all species and age classes (~49,000) in 2020 was just over 1/3 of all species in reaches 2, 3 and 4 combined (~87,000). Lineal densities in Reach 1 were on par with Reach 4 for mykiss fry, mykiss parr, and coho fry, and slightly higher than the other reaches for Chinook fry in 2020, at this stage of post-high flow recovery.

Genetic stock analysis was conducted on DNA samples collected from 109 Chinook salmon juveniles in 2020, to test for the incidence of successful spawning by strays in 2019. Two analytical approaches were applied to describe the ancestry of the specimens sampled. The majority of the juveniles were the progeny of pure form Bridge parental pairings. The analysts also determined that at least 13% of the juveniles were admixed and attributed to the successful spawning of mid and upper Fraser River Chinook salmon strays in Bridge River (Wetklo and Sutherland 2021).

Summary of BRGMON-1 Management Questions and Interim (Year 9 – 2020) Status

Primary Objectives	Management Questions	Year 9 (2020) Results To-Date
Core Components: To reduce uncertainty about the relationship between the magnitude of flow release from the dam and the relative productivity of the Lower Bridge River aquatic and riparian ecosystem. To provide comprehensive documentation of the response of key physical and biological indicators to alternative flow regimes to better inform decision on the long term flow regime for the Lower Bridge River. The scope of this program is limited to monitoring the changes in key physical, chemical, and biological productivity indicators in reaches 2, 3, and 4 of the Lower Bridge River aquatic ecosystem.	How does the instream flow regime alter the physical conditions in aquatic and riparian habitats of the Lower Bridge River ecosystem?	• The biggest gains in wetted area were achieved by the wetting of Reach 4 and the augmentation of flows in Reach 3 by the Trial 1 and 2 treatments. 2019 and 2020 were characterized by a return to Trial 2 flows. Increases in wetted area from high flows (>15 $m^3 \cdot s^{-1}$) in 2016 – 2018 were proportionally less substantial and the additional discharge reduced the suitability of mid-channel habitats by increasing flow velocities above suitable thresholds for fish and benthic invertebrates. • Site-specific discharge estimates in 2020 highlighted that flow conditions in reaches 3 and 4 were fairly similar, but that they differed greatly from sites in reaches 2 and 1 due to the contribution of the Yalakom inflows at the top of Reach 2. During years with lower flow releases from Terzaghi Dam (including 2020), the Yalakom River inflow contributes a higher proportion of the total discharge in the lower reaches which dilutes or masks some of the physical and water chemistry characteristics of the release. • Variation in dissolved inorganic nitrogen (DIN) and soluble reactive phosphorus (SRP) concentrations across monitoring years produced shifts in potential limitation of benthic algal growth based on molar N:P ratios at different times and places. The Reach 2 N:P in 2020 was the highest measured since monitoring began. It showed greatest potential phosphorus deficiency in Reach 2 on record in the Lower Bridge River, although still lower than in the Yalakom River. • Water temperatures under all trial flows were cooler in the spring and warmer in fall relative to the Pre-flow (Trial 0) profile. During the High flow years and in 2019 & 2020, water temperatures during the peak flow period were warmer than previous treatments, but still within optimal ranges for rearing (for fish that remained during/after the high flows). There was also a period of warmer temperatures in September 2020 that was particularly evident in reaches 3, 2, 1 and the Yalakom River. The cause of the warmer water temperatures in September 2020 were attributed to ambient temperature influence. There is a gradient of temperature associated with distance from the dam (e.g., Reach 1 temperatures were ~5°C cooler on average than Reach 4 in fall 2020).
	How do differences in physical conditions in aquatic habitat resulting from instream flow regime influence community composition and productivity of primary and secondary producers in Lower Bridge River?	• There is uncertainty about cause of declining SRP concentrations and rising molar N:P over the past 10 years in water released from Carpenter Reservoir, a trend that may be increasing potential phosphorus limitation of biological production mainly in Reach 4. • There was a Trial effect on periphyton peak biomass (PB), entirely due to PB in the Post-High Flow years being greater than that in Trial 1. There was no significant difference in PB between all other pairs of Trials. • Flows during Trials 1 and 2 produced what might be called optimum conditions for the benthic communities. The average 73% decline in invertebrate density and low diversity associated with the High flows showed that physical conditions associated with high peak flow, including scour and bed movement, did not favour the benthic communities. Given that benthos found in the Lower Bridge River includes common fish food organisms, the Trial 3 flows caused a decline in the food available to fish at the time of measurement in the fall months. • Mean benthic invertebrate densities increased from the High Flow years to Post-High Flow years, resulting in no significant difference in densities between the Post-High Flow years and Trial 2.

Primary Objectives	Management Questions	Year 9 (2020) Results To-Date
Core Components: To reduce uncertainty about the relationship between the magnitude of flow release from the dam and the relative productivity of the Lower Bridge River aquatic and riparian ecosystem. To provide comprehensive documentation of the response of key physical and biological indicators to alternative flow regimes to better inform decision on the long term flow regime for the Lower Bridge River. The scope of this program is limited to monitoring the changes in key physical, chemical, and biological productivity indicators in reaches 2, 3, and 4 of the Lower Bridge River aquatic ecosystem.	How do changes in physical conditions and trophic productivity resulting from flow changes together influence the recruitment of fish populations in Lower Bridge River?	• Similar to the results for benthic invertebrates, juvenile salmonid abundance was highest (overall) under the Trial 1 and 2 flow regimes (in general, production between them was near equivalent, but both impacted Chinook recruitment). Relative to Trial 2, the high flows in 2016, 2017 and 2018 reduced salmonid abundance by 76%. Reductions for mykiss and coho fry were by 76% and 89%, respectively. Mykiss parr abundance was 71% lower and Chinook fry abundance remained low (equivalent to Trial 2). • The return to the Trial 2 hydrograph in 2019 and 2020 provided for modest recovery of mykiss and coho fry in Reach 3; however the abundance of mykiss parr in 2020 (the first year-class that recruited post-high flows) and Chinook fry (which are likely affected by temperatures during incubation for all flow trials and may have been impacted by operation of the broodstock collection fence and stray spawners from other systems in 2019) declined relative to the High Flow period. Recovery of all species in reaches 2 and 4 was negligible. Abundances in Reach 1 were higher in 2020 than in 2019 for each species and age class. 2020 lineal densities in Reach 1 were on par with Reach 4 for mykiss fry, mykiss parr, and coho fry, and slightly higher than the other reaches for Chinook fry, at this stage of post-high flow recovery. Reach 1 is the length of reaches 2, 3 and 4 combined and produced 1/3 of the fish from those reaches in 2020. • Mean biomass in the post-high flow years was the lowest for any flow treatment to-date; approx. 194 kg lower than the high flow period and 773 kg lower than Trial 2. • Based on stock-recruit analysis, production for Chinook and coho is characterized by a different curve and asymptote (i.e., carrying capacity) for each flow treatment. It appears that production was not stock-limited in most study years; however, more data at a range of escapements and under modified operations conditions are required to reduce uncertainty in the initial slope and better inform the existing curves. The 2019 and 2020 datapoints for coho and Chinook were compared to the curves and points for Trials 2 and 3 but were not incorporated into the existing curves since they represent the start of a new flow treatment (post-high flows). As such the existing curves remained unchanged. • Genetic stock identity was analyzed for 106 Chinook fry sampled in 2020. Analysis results suggested that the majority were from pure form Bridge River parents and at least 13% were admixed and attributed to the successful spawning of mid and upper Fraser River Chinook salmon strays in the Bridge River in 2019.
	What is the appropriate 'shape' of the descending limb of the 6 cms hydrograph, particularly from 15 cms to 3 cms?	• 2020 flow rampdown monitoring between 15 and 3 $m^3 \cdot s^{-1}$ (i.e., the Trial 2 range) further affirmed what has been learned about fish stranding risk and documented in past reports and the fish stranding protocol. • Modified Operations (2016–2020) results also reaffirmed that ~13 $m^3 \cdot s^{-1}$ is the approx. flow threshold below which stranding risk tends to increase. As such, slower (i.e., WUP) ramp down rates are likely warranted below that level. Above this threshold there is likely flexibility to implement faster ramp rates to reduce flows more quickly without increasing the incidence of stranding significantly.

Table of Contents

1. Introduction

1.1. Background

The context for the Lower Bridge River flow experiment and its associated aquatic monitoring program is only briefly summarized here. It has been more fully described in earlier manuscripts by Failing et al. (2004) and (2013), and Bradford et al. (2011).

The Lower Bridge River (LBR) is a large glacially fed river that has been developed and managed for hydroelectricity generation by BC Hydro and its predecessors since the 1940s. Prior to impoundment, the Bridge River had a mean annual discharge (MAD) of 100 cubic meters per second ($m^3 \cdot s^{-1}$) and maximum flow during spring freshets of up to 900 $m^3 \cdot s^{-1}$ (Hall et al. 2011). Following the completion of Terzaghi Dam in 1960 there was no continuous flow released into the LBR channel due to the complete diversion of water stored in Carpenter Reservoir (upstream of the dam) into Seton Lake in the adjacent valley to the south. This resulted in the dewatering of just over 3 kilometres (km) of Bridge River channel immediately downstream of the dam, other than during periodic mid-summer spills caused by high inflows (Higgins & Bradford 1996). On average, these spill events occurred approximately two to three times per decade (Figure 1.1).

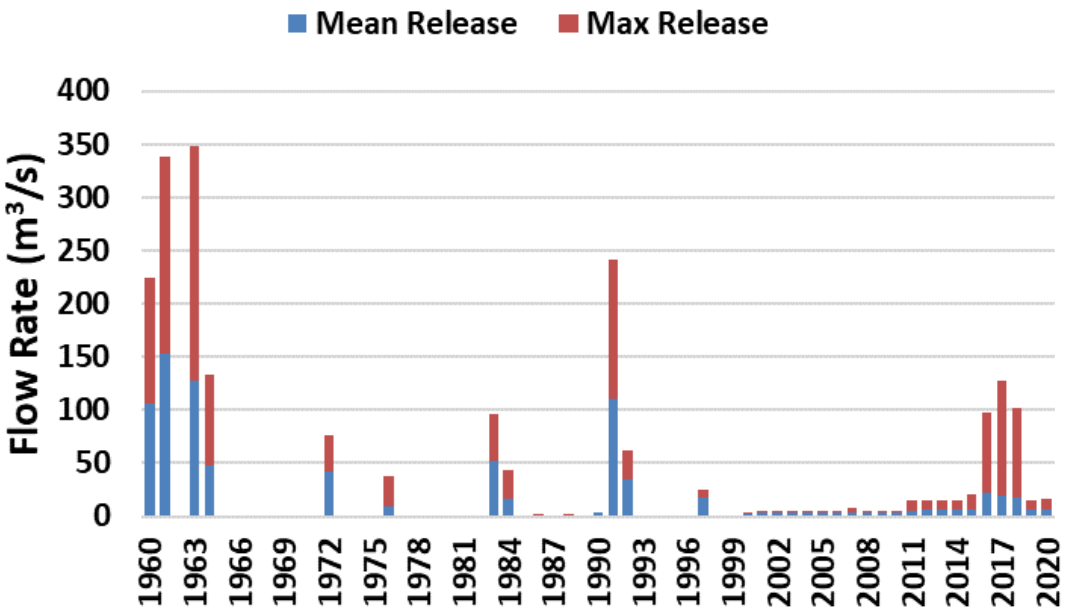

Figure 1.1 Frequency of spill and flow release events from Terzaghi Dam into the Lower Bridge River following impoundment in 1960.

Downstream of the dewatered reach, the river had a low but continuous and relatively stable streamflow, with groundwater and five small tributaries cumulatively providing a MAD of approximately 0.7 $m^3 \cdot s^{-1}$. Fifteen km downstream from the dam, the unregulated Yalakom River joins the Bridge River and supplies, on average, an additional 4.3 $m^3 \cdot s^{-1}$ (range = 1 to 43 $m^3 \cdot s^{-1}$) to the remaining 25 km of Lower Bridge River.

Starting in the 1980s and following spill events from Terzaghi Dam during the 1990s, concerns about impacts of dam operations (particularly the episodic spill events) and the lack of a continuous flow release on the aquatic ecosystem of the Lower Bridge River were raised by First Nations representatives, local stakeholders, and fisheries agencies. According to the magnitude and timing of the spill, the effects of these events likely included: flooding the river channel outside of the typical freshet period, scouring of the streambed, flushing gravels and other sediments, fish entrainment from the reservoir into the river, and fish stranding as the spill flows diminished. Beyond the information provided by fish salvage surveys, the scope of effects from past spills on the aquatic ecosystem were not well understood but were recognized to be significant and warranted mitigation.

In 1998, an agreement between BC Hydro and regulatory agencies (stemming from litigation pertaining to spills in 1991 and 1992) specified that an environmental flow be implemented with the goal of restoring a continuous flow to the dewatered section below the dam and optimizing productivity in the river. However, information was not available to determine what volume of flow and what hydrograph shape would provide optimal conditions for fish production and other ecosystem benefits. This was considered a key uncertainty which precluded the ability to make a flow decision at that time. Therefore, initiation of the continuous release was set up as a flow experiment with an associated monitoring program designed to assess ecosystem response to the introduction of flow from Carpenter Reservoir. The continuous flow release from Terzaghi Dam was initiated by BC Hydro in August 2000.

1.2. The Flow Experiment

The original flow experiment consisted of 2 flow trials: a 3 $m^3 \cdot s^{-1}$ mean annual release (Trial 1; August 2000 to March 2011) and a 6 $m^3 \cdot s^{-1}$ mean annual release (Trial 2; April 2011 to December 2015). The flows for each trial were released according to prescribed hydrographs (Figure 1.2) that were designed by an interagency technical working group. Monthly flows during Trial 1 ranged between a fall/winter low of 2 $m^3 \cdot s^{-1}$ (November to March) to a late spring peak of 5 $m^3 \cdot s^{-1}$ (in June). During Trial 2 the fall/winter low flow was 1.5 $m^3 \cdot s^{-1}$ (October to February) and peak flows were approximately 15 $m^3 \cdot s^{-1}$ for all of June and July.

Reduction of the flow release (ramping) for Trial 1 was conducted in small increments following the peak in mid June down to 3 $m^3 \cdot s^{-1}$ by the end of August, and then down to the fall/winter low in mid to late October. Ramping for the Trial 2 flows occurred ca. weekly during August from 15 to 3 $m^3 \cdot s^{-1}$, and the final ramp down from 3 to 1.5 $m^3 \cdot s^{-1}$ typically occurred in early October (Sneep and Hall 2012b; McHugh and Soverel 2017).

The main intent of this monitoring program was to assess the influence of each of the flow release trials (the flow experiment) on fish resources and the aquatic ecosystem of the Lower Bridge River. Monitoring was also conducted for four years during the Pre-flow period (dubbed “Trial 0”; May 1996 to July 2000) to document baseline conditions when the mean annual release

from the dam was 0 $m^3 \cdot s^{-1}$. Since the wetted portion of the channel between the dam and the Yalakom River confluence was wetted by tributary and groundwater inflows during the pre-flow period, it was important to document existing productivity so the results of the flow trials could be understood in context.

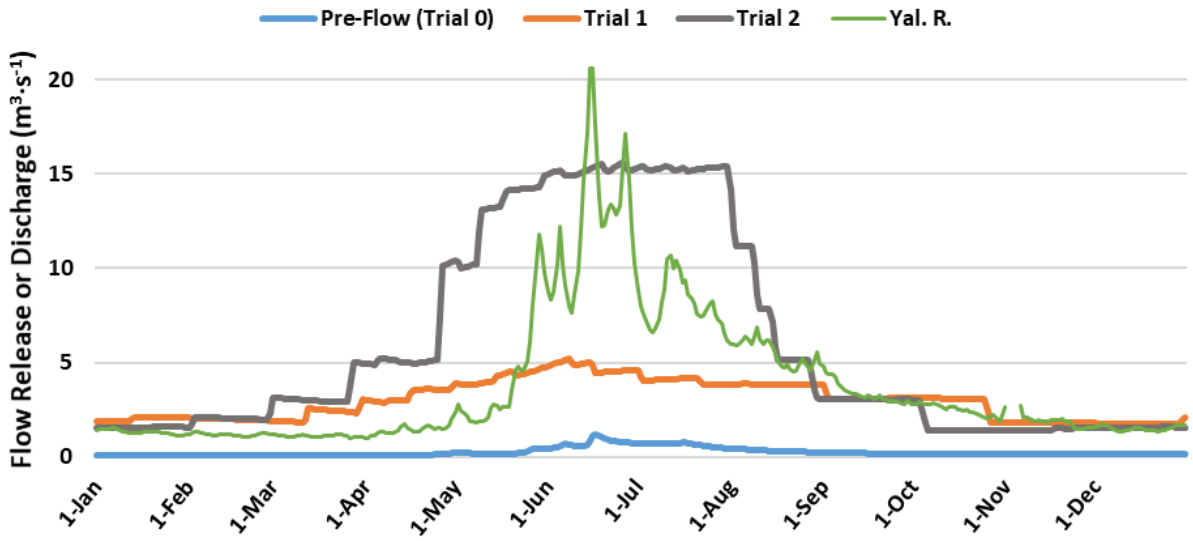

Figure 1.2 Mean daily releases from Terzaghi Dam for Trial 1 and Trial 2 during the flow experiment. Typical hydrograph shapes during the Pre-flow period and for the unregulated Yalakom River discharges are included for reference.

Decisions on the magnitude of peak flows for the flow trials were constrained by morphological characteristics of the channel below Terzaghi Dam. In several areas the channel is confined by narrow canyons and characterized by high gradients; conditions that are not conducive for maintaining spawning substrates or creating rearing habitats at high flows. Prior to impoundment, natural discharges were generally much higher in the Lower Bridge River: summer flows ranged between 100 and 900 $m^3 \cdot s^{-1}$ (mean peak flow was ~400 $m^3 \cdot s^{-1}$; Bradford et al. 2011). However, historical records indicate that most of the best fish habitat (including spawning areas for salmon) were located upstream of the dam site and are now flooded by Carpenter Reservoir. The river below the dam site was primarily used as a migratory corridor for anadromous species (O'Donnell 1988). After construction of Terzaghi Dam, reduced flows in the high-gradient migratory corridor provided spawning and rearing habitat, and habitats above the dam were no longer accessible. Due to this change in the location of habitat, pre-impoundment flows were not considered appropriate benchmarks for the flow trials.

Additionally, available data from the Pre-flow period indicated that the production of salmonids was very high in the groundwater-fed section above the Yalakom River confluence under low flow conditions. Discharge at the top of this section was generally ≤ 1 $m^3 \cdot s^{-1}$, yet spawners of all species were able to reach the upper extent of the inflow and juveniles were distributed throughout the system. Juvenile salmonid densities were among the highest in the province of

BC and average biomass values (g/m^2) were more than double typical values for trout and salmon in western North America (Bradford et al. 2011). This remarkable pre-flow productivity also served as important context for designing the trial flows. The technical working group sought to ideally strike a balance between creating new habitat (by rewetting the previously dry section below the dam and enlarging the wetted area of the river in general) without reducing the exceptional productivity in the wetted section above the Yalakom River confluence.

1.3. Modified Operations

During implementation of the Trial 2 flows, BC Hydro identified issues with some of their infrastructure associated with water storage and flow conveyance within the Bridge-Seton hydroelectric complex. As a result, the storage of water in Downton Reservoir and conveyance of flows from Carpenter Reservoir to Seton Lake (via the diversion tunnels and generating units at Bridge 1 and 2) had to be reduced to allow for the affected infrastructure to be rebuilt or replaced.

The reduction of water storage and flow diversion above Terzaghi Dam meant that additional flow needed to be passed into the Lower Bridge River above the amounts prescribed for the flow experiment (described in Section 1.2) at least in some years according to the timing and magnitude of inflows. In years with normal or below average inflows, the Trial 2 hydrograph would remain the target for flow conveyance. As such, flow magnitudes and hydrograph shapes have tended to be more variable during the period known as “Modified Operations” which began in 2016.

Delivery of higher flows occurred for three consecutive years from 2016 to 2018. For this period of Modified Operation years, mean annual flows from the dam were approximately 22, 19 and 18 $m^3 \cdot s^{-1}$ (peak flows = 97, 127 and 102 $m^3 \cdot s^{-1}$), respectively (Figure 1.3). These peak flows were higher than the Trial 1 and Trial 2 hydrographs but were within the range of spill flows from past events since the completion of Terzaghi Dam in 1960 (Figure 1.1).

The ascending limb of the high flow hydrograph in 2016 started on 17 March, peaked in mid June, and returned to Trial 2 levels by 25 July (2016 high flow duration = 131 days). The high flows in 2017 had a higher peak, but a shorter duration relative to 2016: Flows increased above the Trial 2 hydrograph on 24 May, peaked across the month of June, and were ramped back down to Trial 2 levels on 21 July (2017 high flow duration = 59 days). High flows in 2018 began on 10 May, peaked in late June, and were ramped back down to Trial 2 levels on 1 August (2018 high flow duration = 83 days). Outside of the high flow period in 2016–2018, the flow release from mid summer through fall and winter was identical to the Trial 2 hydrograph shape. The years from 2016 to 2018 are collectively referred to as the “High Flow Years” in this report.

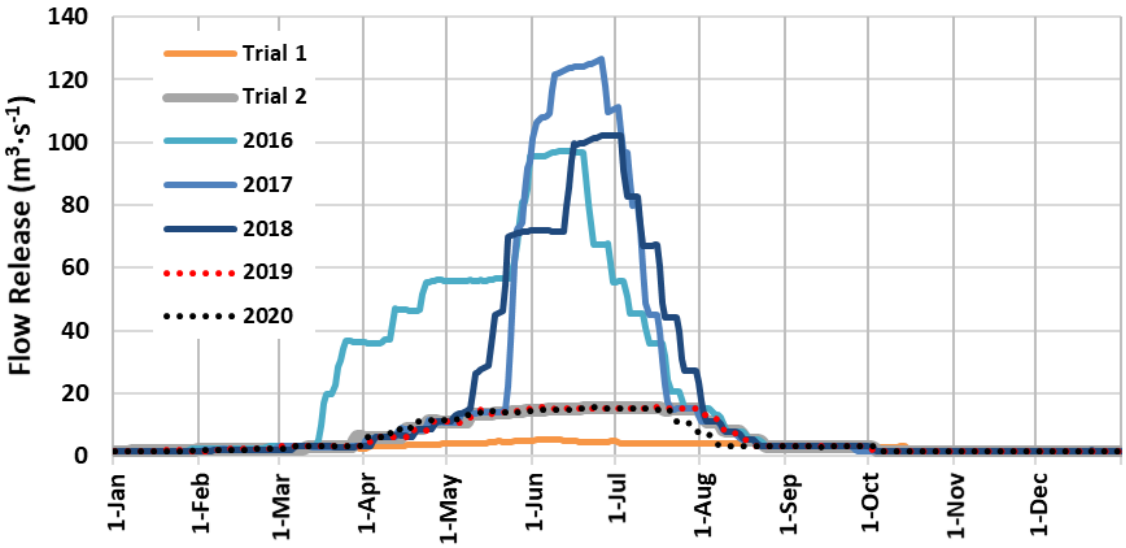

Figure 1.3 Terzaghi Dam flow release hydrograph shapes for Modified Operations years (2016–2020). Mean daily releases for the Trial 1 and Trial 2 hydrographs are shown for reference. Following three consecutive years of high flows, dam releases in 2019 and 2020 returned to the Trial 2 hydrograph.

In 2019 and 2020, reduced snowpack and inflow volumes allowed for a return to the Trial 2 hydrograph in the Lower Bridge River (mean annual flows = ~6 $m^3 \cdot s^{-1}$; peak flows = 15.7 $m^3 \cdot s^{-1}$). As in the other Trial 2 years (2011 to 2015), flows ramped up from the winter lows during April and May (~3 to 15 $m^3 \cdot s^{-1}$), peaked across the months of June and July (~15 $m^3 \cdot s^{-1}$), and were ramped back down to 3 $m^3 \cdot s^{-1}$ between late July and mid August, and then to 1.5 $m^3 \cdot s^{-1}$ at the beginning of October. The timing for the ramp up to the peak flow and ramp down to summer rearing flows were adjusted a couple of weeks earlier in 2020 than in 2019 and the Trial 2 years (2011 to 2015) with the goal of extending the period of post-peak summer rearing flows as much as possible while accommodating the necessary flow conveyance during the typical peak inflow period (Figure 1.3). Flows above the Trial 2 peak were not necessary (2019 and 2020 high flow duration = 0 days). Despite their occurrence during the modified operations period (years ≥2016) and nearly identical flow delivery characteristics to the Trial 2 releases, 2019 and 2020 were considered the start of a new flow treatment (Post-High Flow years) in the analyses and results provided in this report since they represented the return to lower flows following the channel-altering high flows from 2016 to 2018.

Figure 1.4 shows mean trial flows on a logarithmic scale to compare differences in the shapes of the flow release hydrograph between trials. Trial 3 produced a pronounced bell-shaped hydrograph with steep ascending and descending limbs and highest peak release among trials. Trial 1 shape was a flattened bell-shaped hydrograph appearing more like a shallow dome with low slopes on the ascending and descending limbs and lowest peak release among trials. The Trial 2 hydrograph was in between, having a moderate bell shape, moderate rates of ascending

and descending limbs and peak water releases in between Trials 1 and 3. For the reasons noted above, 2019 and 2020 flow releases were characterized by the line representing the Trial 2 mean.

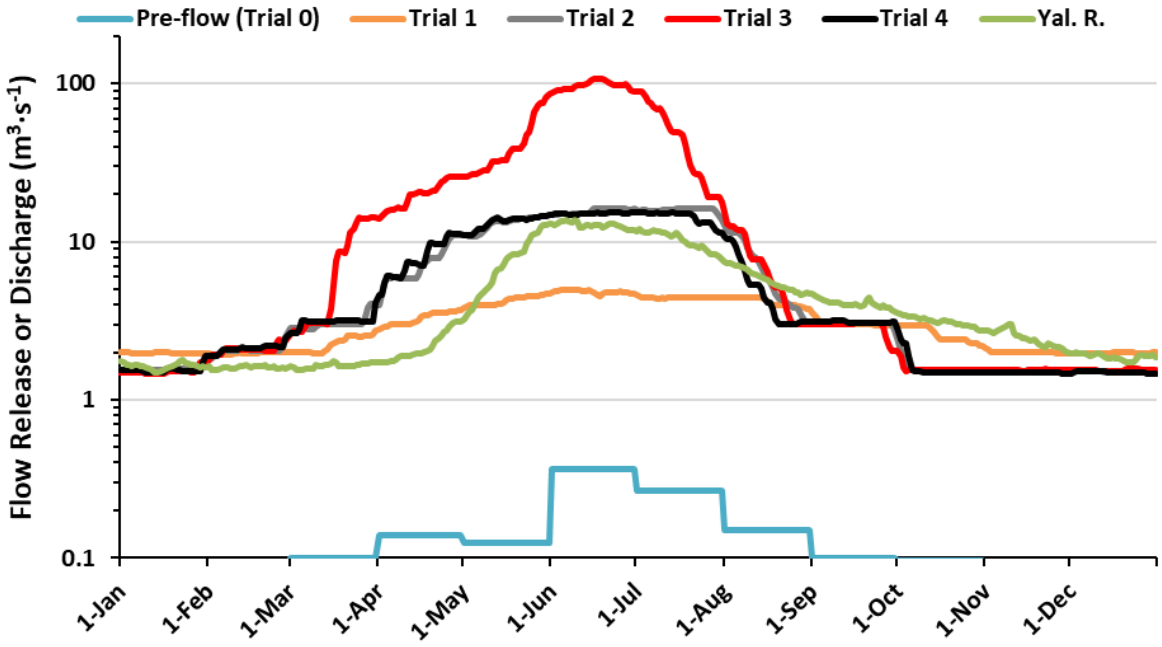

Figure 1.4 Mean daily flow release from the Terzaghi Dam among all years in each flow Trial. Mean daily flow among all years (1996 – 2020) in the Yalakom River is shown for reference. Note the log scale on the Y axis.

The different magnitudes of flow by trial in the Bridge River are compared to those in the Yalakom River, where flow is not regulated (Table 1.1). Mean annual flow in the Yalakom River was 4.2 to 5.2 $m^3 \cdot s^{-1}$ among all trials, which was between the mean annual flow release to the Bridge River in Trials 1 and 2. The average minimum flows were approximately 1 to 2 $m^3 \cdot s^{-1}$ in both the water release to the Bridge River and in the Yalakom River. Average peak flow in the Yalakom River was 22 to 27 $m^3 \cdot s^{-1}$ among all blocks of Trial years, which was about 50% greater than the peak flow release during Trial 2 and the Post-High Flow years (2019 and 2020) in the Bridge River.

Table 1.1 Flow statistics by Trial in the Bridge River and in the Yalakom River.

River	Trial number (years) [a] (sample size)	Flow statistic ± standard deviation		
		Mean annual water release or flow ($m^3 \cdot s^{-1}$)	Average minimum water release or flow ($m^3 \cdot s^{-1}$)	Average peak water release or flow ($m^3 \cdot s^{-1}$)
Lower Bridge	0 (1996–1999) (n=4)	0.6 ± 1.3	0	6.3 ± 12.5
	1 (2001–2010) (n=10)	3.1 ± 0.2	1.8 ± 0.1	5.4 ± 1.1
	2 (2012–2015) (n=4)	6.1 ± 0.3	1.1 ± 0.7	16.8 ± 2.6
	3 (2016–2018) (n=3)	19.5 ± 2.1	1.4 ± 0.1	108.7 ± 15.7
	4 (2019–2020) (n=2)	5.9 ± 0.2	1.4 ± 0.1	15.7 ± 0.0
Yalakom	0 (1996–1999) (n=4)	5.1 ± 1.2	1.2 ± 0.1	25.1 ± 12.7
	1 (2001–2010) (n=10)	4.2 ± 0.9	1.2 ± 0.2	22.5 ± 10.7
	2 (2012–2015) (n=4)	4.5 ± 0.5	0.7 ± 0.4	21.9 ± 5.1
	3 (2016–2018) (n=3)	5.2 ± 0.4	0.9 ± 0.3	25.1 ± 1.8
	4 (2019–2020) (n=2)	4.9 ± 0.2	0.7 ± 0.2	27.3 ± 2.5

[a] Years 2000 and 2011 were omitted because they were transition years between flow treatments and therefore represent incomplete years for calculations of flow statistics.

At least until the end of the Modified Operations period (i.e., until BC Hydro infrastructure is sufficiently rebuilt or replaced to allow a return to normal WUP operations – the timing of which is uncertain at this point), spring flows could continue to be more variable across years than they were under the flow experiment trials and may require discharges above the Trial 2 peak more frequently. Increases in the maximum Terzaghi Dam discharge may have short and long-term effects on the LBR and aquatic productivity. In the short-term, high discharges have caused increased entrainment at Terzaghi Dam, reduced juvenile salmonid rearing habitat area, erosion and sediment deposition throughout the river, and increased the total number of fish stranded during ramp downs from high flows. In both the short- and long-term, high flows may alter primary and secondary productivity, juvenile salmonid growth and abundance, and salmonid habitat suitability.

1.4. Objectives, Management Questions and Study Hypotheses

The objective of the monitoring program was to reduce uncertainty about the long-term ecological response to the release of continuous flows from Terzaghi Dam into the Lower Bridge River channel. This lack of certainty was an impediment to decision-making on an optimal flow regime and centred around the unknown effects of different flows on aquatic ecosystem productivity. A decision about flow release volumes and hydrograph shape based on invalid judgements would have implications for both energy production and the highly valued ecological

resources of the Lower Bridge River. Therefore, the goal of the monitoring program was to resolve the uncertainty by the collection and analysis of scientifically defensible data.

To guide the program, a set of specifically linked "Management Questions" were developed during the Water Use Planning (WUP) process:

1) **How does the instream flow regime alter the physical conditions in aquatic and riparian habitats of the Lower Bridge River ecosystem?**

   Changes in the physical conditions regulate the quantity and quality of habitats for aquatic and riparian organisms. Documenting the functional relationships between river flow and physical conditions in the habitat is fundamental for identifying and developing hypotheses about how physical habitat factors regulate, limit or control trophic productivity and influence habitat conditions in the ecosystem.

2) **How do differences in physical conditions in aquatic habitat resulting from the instream flow regime influence community composition and productivity of primary and secondary producers in the Lower Bridge River?**

   Changes in the flow regime are expected to alter the composition and productivity of periphyton and invertebrate communities. Understanding how these physical changes influence aquatic community structure and productivity are important as they act as indicators to evaluate "ecosystem health" and the trophic status of the aquatic ecosystem in relation to provision of food resources for fish populations.

3) **How do changes in physical conditions and trophic productivity resulting from flow changes together influence the recruitment of fish populations in the Lower Bridge River?**

   Changes in the flow regime can have significant effects on the physical habitat and trophic productivity of the aquatic ecosystem and these two factors are critical determinants of the productive capacity of the aquatic ecosystem for fish. Understanding how the instream flow regime influences abundance, growth, physiological condition, behavior, and survival of stream fish populations helps to explain observations of changes in abundance and diversity of stream fish related to flow alteration.

4) **What is the appropriate 'shape' of the descending limb of the Trial 2 (6 $m^3 \cdot s^{-1}$ MAD) hydrograph, particularly from 15 $m^3 \cdot s^{-1}$ to 3 $m^3 \cdot s^{-1}$?**

   Inherent in the development of the Trial 2 hydrograph, was uncertainty regarding the risk of fish stranding given the relative magnitude of ramp-downs during the months when flows were reduced (i.e., August and October). Some information on the incidence of fish stranding between 8.5 and 2 $m^3 \cdot s^{-1}$ had been documented during the Trial 1 period (Tisdale 2011a, 2011b). However, there was limited existing information on fish stranding in the discharge range from 15 $m^3 \cdot s^{-1}$ to 8.5 $m^3 \cdot s^{-1}$ and the types of habitats in this flow range. The collection of information on the risk of fish stranding at each stage of flow reduction is needed for assigning flow ramping rules during the descending limb of the annual hydrograph.

These management questions were originally intended to improve understanding of LBR aquatic productivity under the Trial 1 and Trial 2 hydrographs. However, the management questions are still considered relevant for understanding the effects of modified operations from Terzaghi Dam (i.e., the high flow years from 2016 to 2018 and the post-high flow years in 2019 and 2020) even though these operations were not within the context of the flow experiment as originally conceived.

Changes to Chinook salmon emergence timing and life history have been observed in the LBR over the course of the flow trials, but these changes were not specifically addressed in the original BRGMON-1 WUP management questions. Two new management questions to address uncertainties about the observed changes were included in a BRGMON-1 Terms of Reference Revision 1 (BC Hydro 2018), as follows:

5) **Do increased water temperatures and early emergence associated with Terzaghi Dam flow releases affect the survival of juvenile Chinook salmon in the Lower Bridge River?**

   BRGMON-1 monitoring results have identified increased fall water temperatures associated with minimum flow releases under the Trial 1, Trial 2 and Trial 3 hydrographs (relative to pre-flow conditions). Based on predicted emergence timing from temperature exposures during incubation under the release coupled with the collection of recently emerged fry during late fall and early winter sampling surveys, the flow release thermal regime has advanced the emergence timing of Chinook salmon fry in the LBR, and most notably in the upper portion of the study area. These changes have also coincided with reduced juvenile abundance for this species. However, there is uncertainty about the extent to which early emergence has affected the survival of Chinook salmon since the observed decline in juvenile Chinook salmon abundance under flow release conditions also coincided with reduced adult returns to the Lower Bridge River and other Mid-Fraser populations.

6) **What freshwater rearing habitats are used by Lower Bridge River juvenile Chinook salmon and is rearing habitat use influenced by Terzaghi Dam flow releases?**

   In addition to potential early emergence effects on Chinook salmon survival described for question #5, other explanations for reduced juvenile abundance in the fall may also include life history changes (e.g., timing of outmigration) or habitat use changes (e.g., rearing in the Fraser River rather than the LBR).

Due to the modified operations resulting from the La Joie Dam and Bridge River Generation issues, additional monitoring programs with new management questions were created in 2016 to guide the short-term high flow monitoring programs and inform the LBR impact assessment and mitigation planning. However, due to manageable inflow volumes in 2019 and 2020, releases above the Trial 2 peak of ~15 $m^3 \cdot s^{-1}$ from Terzaghi Dam were not required during those years. Therefore, most of the additional monitoring activities prescribed for Modified Operations years with high flows (i.e., High Flow Monitoring; Water Quality, Erosion and Entrainment Monitoring; High Flow Fish Salvage and Stranding Risk Assessment; and Substrate Mobilization, Deposition and Composition Monitoring) were not implemented in 2019 or 2020. As such, the management questions pertaining to these Modified Operations (high flows) activities are not included in this report. However, one Modified Operations monitoring component that has continued each year since 2018 is Juvenile Salmonid Habitat Availability and Displacement monitoring within off-channel habitats. The management question included in the ToR revision for this component is:

7) **How does habitat use by juvenile salmonids change with discharge under the modified flow regime?**

   The high flows delivered from 2016 to 2018 impacted juvenile salmonid rearing habitats by introducing higher velocities throughout more of the channel, and mobilizing sediment resulting in additional areas of scour and deposition. The effects of these changes were expected to include potential changes to rearing habitat area, displacement of fish out of the study area, and/or life history changes in the longer term.

1.5. Study Area

The Bridge River drains a large, glaciated region of the Coast Range of British Columbia and flows eastward, joining the Fraser River near the town of Lillooet. The river has been impounded by the La Joie and Terzaghi dams which have segmented the river into three main sections: The Upper Bridge River and Downton Reservoir (above La Joie Dam); the Middle Bridge River and Carpenter Reservoir (above Terzaghi Dam); and the Lower Bridge River (downstream of Terzaghi Dam). The Lower Bridge River between Terzaghi Dam and the confluence with the Fraser River is approximately 41 km long and is currently the only section accessible to anadromous fish.

The Lower Bridge River was divided into four reaches by Matthew and Stewart (1985); their reach breaks are defined in Table 1.2. Monitoring for this program conformed to these reach break designations and from 1996 to 2018 focused on the section of river between Terzaghi Dam and the bridge crossing upstream of Camoo Creek (i.e., reaches 4, 3 and 2). Starting in 2018, measurement of periphyton and benthic invertebrate metrics was extended to include sites in the lower portion of the Yalakom River to allow comparison between the flow controlled Lower Bridge River and the unregulated Yalakom River. In 2019, monitoring was also extended to include Reach 1 (including 4 periphyton and benthic invertebrate monitoring sites and 12 juvenile stock assessment sites), such that all 4 reaches of the Lower Bridge River were covered with comparable monitoring effort. The overall study area is illustrated in Figure 1.5. UTM coordinates for the thirteen index monitoring locations and 61 juvenile stock assessment sites are provided in Appendix A.

Table 1.2 Reach designations and descriptions for the Bridge River below Terzaghi Dam.

Reach	Boundary (Rkm)		Length (km)	Description
	Downstream	Upstream		
1	0.0	19.0	19.0	Fraser River confluence to Camoo Creek
2	19.0	26.0	7.0	Camoo Creek to Yalakom River confluence
3	26.0	37.7	11.7	Yalakom R. confl. to upper extent of groundwater inflow
4	37.7	40.9	3.2	Upper extent of groundwater inflow to Terzaghi Dam

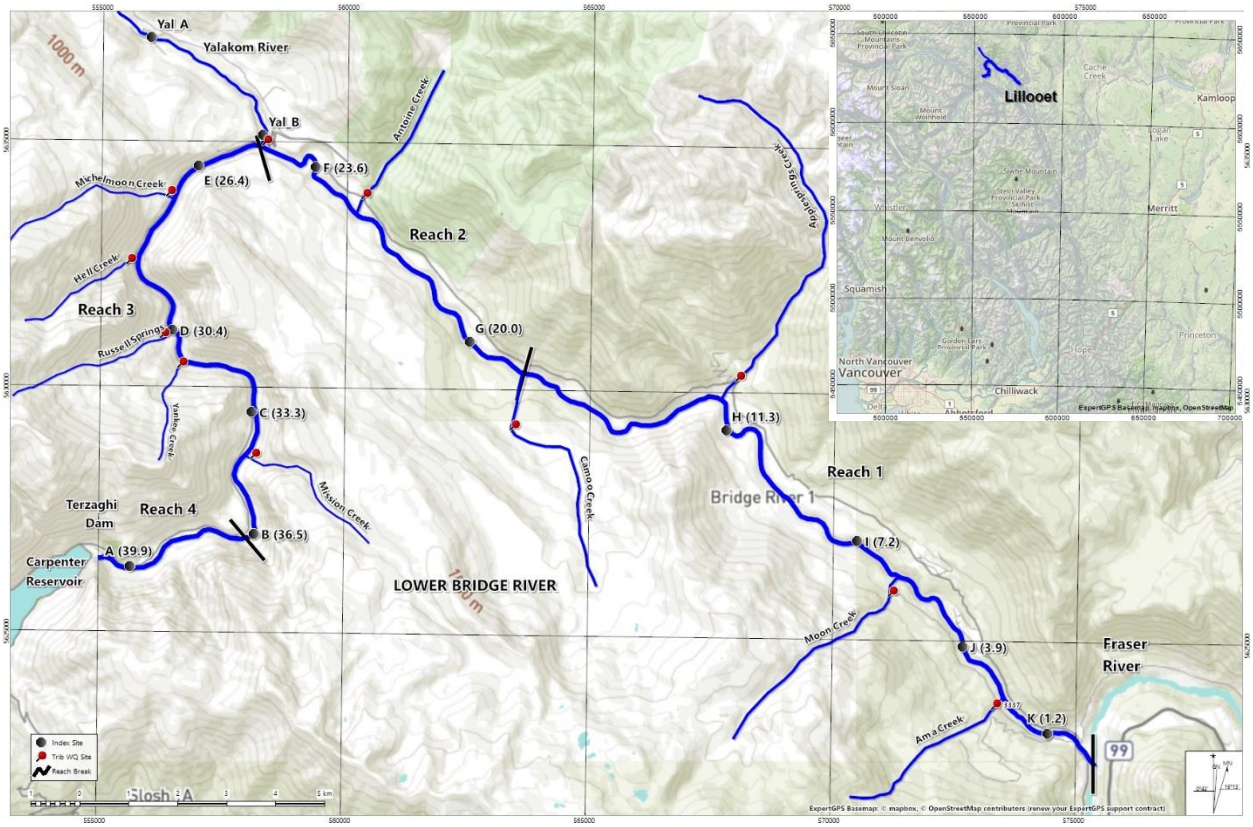

Figure 1.5 The Lower Bridge River downstream of Terzaghi Dam near Lillooet, British Columbia. Reaches are labelled 4 (upstream) through 1 (downstream). Index sampling sites are labelled as distances upstream of the Fraser River and correspond to the following letters: 39.9 km (A), 36.5 km (B), 33.3 km (C), 30.4 km (D), 26.4 km (E), 23.6 km (F), 20.0 km (G), 11.3 km (H), 7.5 km (I), 3.9 km (J) and 1.2 km (K). Yal_A and Yal_B are the two index sites that were established in the Yalakom River in 2018. Tributary water sampling locations are shown as red pins. The inset map in the top-right corner frames the location of the sampling area within the context of southwestern British Columbia.

Prior to initiation of the continuous flow release at the start of the flow experiment (i.e., August 2000), Reach 4 was the previously dry section immediately below the dam (length = 3.2 km). Tributary inflows to this reach were negligible, so flow was mostly from water released at Terzaghi Dam. Reach 3 was the groundwater- and tributary-fed reach extending down to the Yalakom confluence (length = 11.7 km). The tributaries to Reach 3 include: Mission Creek, Yankee Creek, Russell Springs, Hell Creek and Michelmoon Creek. These inflow sources were small, so discharges in this reach prior to the flow release were low (~1% of pre-regulation MAD) and release flows have dominated since the start of the flow trials. Flows in Reach 2 (length = 7.0 km) include the inflow from the Yalakom River, the largest tributary within the study area which contributes between approximately 1 and 45 $m^3 \cdot s^{-1}$ at the top of Reach 2 (mean discharge = 4.6 $m^3 \cdot s^{-1}$). One other small tributary, Antoine Creek, flows into Reach 2. Reach 1 (length = ~19.0 km) receives tributary inflow from Camoo Creek, Applesprings, Moon Creek and Ama

Creek. Relative to the differences among trials in the other reaches, discharge rates in Reach 1 were expected to be fairly similar to Reach 2.

1.6. Study Period

Data collection in 2020 was conducted between March and November according to each monitoring component listed in Table 1.3. Certain components that were measured by loggers (i.e., water temperature, river stage, and discharge from the dam) were recorded year-round. This report focusses on the data collected in 2020; however, comparisons with previous years and flow trials are included where applicable and relevant.

Table 1.3 Summary of data to be included in BRGMON-1 analysis and reporting for monitoring year 9 (2020). Components that have prior years of data are noted.

Task	Components	2020 Period	Prior Years of Data[1]
Physical Parameter Monitoring	Water temperature; river stage; discharge	Year-round	1996 to 2019
	Turbidity	3 Mar to 26 Nov	NA [2]
Water Chemistry	Nutrients; alkalinity; pH	23,24 Jun; 13,14 Jul; 17,18 Aug; 27,28 Sep; 27,28 Oct; 23,24 Nov	1996 to 2007 (Spring/Summer) 1996 to 2019 (Fall)
Primary & Secondary Productivity	Periphyton accrual; benthic invertebrate diversity & abundance	23 Sep to 20 Nov (LBR)	1996 to 2019
		24 Sep to 19 Nov (Yalakom)	2018, 2019
Juvenile Salmonid Abundance	Annual standing stock assessment	25 Aug to 11 Sep	1996 to 2019
	Juvenile fish density in off-channel habitats	15 to 17 Sep	2018, 2019
WUP Ramp Down Monitoring	Stage monitoring; fish salvage	21 Jul to 7 Aug & 5-6 Oct	2011 to 2019
High Flow Monitoring	Kokanee entrainment; water quality sampling; sediment erosion & deposition; fish stranding site reconnaissance	NA	2016 to 2018
Juvenile Salmonid Habitat Availability & Displacement	Single-pass, open site electrofishing at pre-selected rearing sites	13,14 Jun 16,17 Jul	2018, 2019
High Flow Ramp Down & Stranding Risk Assessment	Stage monitoring; fish salvage at flows >15 m^3/s	NA	2016 to 2018

[1] Results of analyses for prior years of monitoring will only be included in this annual report where relevant for providing context to the 2019 results and where this could be supported by the project budget.

[2] Note: While turbidity loggers were deployed in 2019 and data were collected, the loggers were not adequately shielded from ambient light interference so these data were unusable for the analyses and were not included in this report.

2. Methods

2.1. Overview

The purpose of monitoring was to test effects of different flow releases from Terzaghi Dam on benthic assemblages and fish populations among reaches of the Lower Bridge River. Sampling Reaches 2 to 4 was done among all years since 1996 while the Yalakom River was added in 2018 and Reach 1 was added in 2019. Since a control site was not originally included, the study design has relied primarily on before-after comparisons among reaches and examining functional relationships between flow and biological metrics to examine the importance of flow driving biota abundance and diversity. When the flow experiment and associated monitoring program was conceived, the effects of the flow release trials on the aquatic ecosystem were expected to be most strongly observed in reaches 3 and 4. Due to the attenuation of inflows including the Yalakom River inputs, coupled with differences in channel morphology, the effects in reaches 1 and 2 were expected to be more muted. We expected that change in the value of biological metrics or assemblages between trials in reaches 1 and 2 would be less than in reaches 3 and 4 because of interactions from factors other than (or in addition to) flow release from the Terzaghi Dam.

Core sampling methods were the same during all flow treatments and again in 2020. Tasks included: 1) continuous recording of flow release discharge, river stage, temperature and turbidity; 2) monthly sampling of water chemistry parameters (between June and November); 3) assessment of periphyton accrual, and aquatic invertebrate abundance and diversity during fall; 4) a fall standing stock assessment to estimate the relative abundance and distribution of juvenile salmonids in the study area; and 5) flow ramp down monitoring and fish salvage. As in 2018 and 2019, activity 4) also included assessment of fish use of two off-channel habitats during the summer rearing period (June & July) and the fall stock assessment period (September).

Tasks 1) and 2) were conducted at eleven index sites in the LBR and two sites in the Yalakom River in 2020. They included the usual seven index sites located at approximately three-kilometer intervals in the LBR downstream of Terzaghi Dam (i.e., river kilometer (Rkm) 39.9 (Site A), 36.5 (B), 33.3 (C), 30.4 (D), 26.4 (E), 23.6 (F), and 20.0 (G)), as well as 4 new sites in Reach 1 (established in 2019) at Rkm 11.3 (H), 7.5 (I), 3.9 (J), and 1.2 (K). Site A is located in Reach 4; sites B to E are in Reach 3; sites F and G are in Reach 2; and sites H to K are in Reach 1 (see Figure 1.5 and Appendix A). The two sites established in the Yalakom River in 2018 (Yal_A and Yal_B) were sampled again in 2019 and 2020. Inclusion of these sites provided measurements of periphyton accrual and benthic invertebrate diversity and abundance and insight into invertebrate recruitment to lower reaches of the LBR from this important tributary. In addition to the mainstem sites described above, water chemistry sampling was conducted in the following tributaries to characterize nutrient inputs from the various inflow sources: Mission Creek, Yankee Creek, Russell Springs, Hell Creek, Michelmoon Creek (in Reach 3), Yalakom River, Antoine Creek, Camoo Creek (in Reach 2), and Applesprings Creek, Moon Creek and Ama Creek (in Reach 1). The

fall standing stock assessment was conducted at 36 sites distributed among reaches 2 and 3 during the Pre-flow period (Trial 0); at 49-50 sites across reaches 2, 3 and 4 during flow trials 1, 2 and 3; and at 61 sites across reaches 1 to 4 in 2019 and 2020.

Sample collection periods during each flow trial for the water chemistry, periphyton, and benthic invertebrate monitoring components are summarized in Table 2.1. There was a shift in the number of seasons sampled mid way through the flow experiment. Samples were collected during spring (April to June), summer (July to September), and fall (September to December) during the Pre-flow (Trial 0) years and the first half of the Trial 1 period (up to 2005). Starting in the second half of Trial 1 (i.e., 2006) and continuing through Trial 2 and the first four Modified Operations years (i.e., high flow years from 2016-2018; and post-high flows in 2019), samples were collected only in the fall to standardize sampling to a single time of year among all trials.

Table 2.1 Water chemistry, periphyton and benthic invertebrate sample collection by flow trial and season for the Lower Bridge River.

Trial		Years	Reaches	Seasons when samples were collected	Target mean annual flow release from Terzaghi Dam ($m^3 \cdot s^{-1}$ ± %)	Actual mean annual flow release from Terzaghi Dam ($m^3 \cdot s^{-1}$ ± SD)
Trial 0		1996 – July 2000	2, 3	Spring Summer Fall	0	0.5 ± 1.1
Trial 1		August 2000 – 2005	2, 3, 4	Spring Summer Fall	3 ± 5%	3.0 ± 0.3
		2006 – 2010	2, 3, 4	Fall		
Trial 2		2011 – 2015	2, 3, 4	Fall	6 ± 5%	6.2 ± 0.4
Modified Operations [a]	**High Flows**	2016 – 2018	2, 3, 4	Fall	No target [a]	19.5 ± 2.1
		2018	Yalakom		n/a	n/a
	Post-High Flows	2019	1,2,3,4	Fall	6 ± 5%	6.0
			Yalakom		n/a	n/a
		2020	1,2,3,4	Spring [b] Summer [b]	6 ± 5%	5.7
			Yalakom	Fall	n/a	n/a

[a] Modified operations were a variance from Trial 2 resulting from reduction of water storage in Downton Reservoir and issues limiting diversion of flow above Terzaghi Dam to the generating stations at Shalalth. Flow excursions above the Trial 2 hydrograph (in terms of magnitude and duration) depend on snowpack and inflows during each mod. ops. year.

[b] Spring and summer sampling in 2020 applied to water chemistry samples only. As in previous years since 2006, periphyton and benthic invertebrate samples were collected only in fall.

Following on recommendations included in the Year 8 (2019) report, sampling of water chemistry parameters during multiple seasons was resumed in 2020 to document whether the declining

trend in some nutrients (e.g., soluble reactive phosphorus) noted in the annual fall samples were also apparent during the other seasons. However, periphyton and benthic invertebrate sampling continued in the fall only during 2020.

Field data collection in 2020 was conducted by members of Coldstream Nature-Based Solutions and St'at'imc Eco-Resources. Coldstream Nature-Based Solutions (formerly Coldstream Ecology Ltd.) also managed the collection of data, reporting and analysis for most of the Trial 2 years (i.e., 2012 to 2015), and the first high flow (Trial 3) year in 2016 (McHugh and Soverel 2013, 2014, 2015, 2017; McHugh et al. 2017).

2.2. Physical and Chemical Habitat Parameters

2.2.1. Discharge

Discharge rates were either provided or estimated according to location in the study area. Flows in Reach 4 (after initiation of the flow release) were comprised entirely of dam discharge since tributary inputs to this reach are very minor and ephemeral. As such the discharge data for this reach were based on the flow release values alone, which were provided by BC Hydro Power Records (as hourly values). Flows at each index site in reaches 3, 2 and 1 were estimated using a plug-flow approach (described by equations 1 and 2, below) based on tributary drainage area coupled with known Yalakom River discharge data provided by Water Survey of Canada (Gauge 08ME025). The names of the tributaries to the LBR study area are provided in Section 0 and the locations are shown on Figure 1.5. Mean daily, site-specific discharge estimates were calculated for each index site according to the following formulas:

$$(1) \qquad Q_{trib,d} = \left(\frac{Q_{yal,d} \times A_{trib}}{A_{yal}}\right)$$

where

$Q_{trib,\,d}$ = discharge of Lower Bridge River tributary on day (*d*) – see list of tributaries provided in Section 0 and locations shown on Figure 1.5;

$Q_{yal,\,d}$ = discharge of the Yalakom River on day (*d*) -- data provided by Water Survey of Canada;

A_{trib} = drainage area of Lower Bridge River tributary (estimated from a 1:50,000 topographic map); and,

A_{yal} = drainage area of the Yalakom River above the WSC gauge (estimated from a 1:50,000 topographic map).

$$(2) \qquad Q_{i,d} = Q_{i-1,d} + \sum(Q_{trib1,d}, Q_{trib2,d}, \dots)$$

where

$Q_{i,\,d}$ = discharge at Lower Bridge River mainstem index site (*i*) on day (*d*);

$Q_{i\text{-}1,\,d}$ = discharge at the next upstream index site (*i-1*) on day (*d*); and,

$Q_{trib,\ d}$ = discharge of Lower Bridge River tributaries between index site (*i-1*) and index site (*i*) on day (*d*) as calculated by equation (1).

So the daily discharges at the index sites in reaches 3, 2 and 1 (Equation 2) were estimated as the discharge at the next upstream index site plus the sum of the discharge estimates for the tributaries between each index site (Equation 1) as follows:

Site A (km 39.9) = Terzaghi release discharge;
Site B (km 36.5) = Site A discharge + km 36.8 groundwater inflow estimate;
Site C (km 33.3) = Site B discharge + Mission Creek inflow;
Site D (km 30.4) = Site C discharge + Yankee Creek & Russell Springs inflow;
Site E (km 26.4) = Site D discharge + Hell Creek & Michelmoon Creek inflow;
Site F (km 23.6) = Site E discharge + Yalakom River inflow;
Site G (km 20.0) = Site F discharge + Antoine Creek inflow;
Site H (km 11.3) = Site G discharge + Camoo Creek & Applesprings Creek inflow;
Site I (km 7.5) = Site H discharge;
Site J (km 3.9) = Site I discharge + Moon Creek inflow;
Site K (km 1.2) = Site J discharge + Ama Creek inflow.

Three flow metrics contributed to descriptions of benthic habitat. ***Peak flow*** was defined as the peak site-specific flow during March 1 – August 31 preceding the fall periphyton and benthic invertebrate sampling. This metric captured the peak flow at each site during the spring and summer flow release. ***Water depth*** and ***velocity*** at each of the periphyton and benthic invertebrate samplers was measured weekly during the periods of sampler incubation (Section 2.3 and Section 2.4) using a top-set wading rod and velocity meter (Swoffer Instruments, Inc.).

2.2.2. Wetted habitat area

Surveys of hydraulic conditions were conducted during water releases at the dam ranging from 0 $m^3 \cdot s^{-1}$ to 15 $m^3 \cdot s^{-1}$ among the flow trials. Wetted width and length was measured with a laser distance meter (Leica Geosystems, Model Disto X4) and a laser rangefinder (Bushnell Corporation, Model Legend 1200 ARC), respectively, for each habitat type (cascades, runs, riffles, pools, rapids, and side channels). Wetted widths were measured at 10-20 m intervals within each habitat unit from one wetted edge across the channel (perpendicular to the stream axis) to the wetted edge on the other side. A minimum of 2 width measurements, and a maximum of 15 width measurements were recorded for each unit, according to unit length. Habitat unit lengths were measured along the stream axis (in mid-channel) from the upstream to downstream extents of each unit by aiming the rangefinder at a target (white, reflective board held by a crew member) and recording the distance. One length measurement was sufficient for shorter habitat units, and multiple measurements were necessary for longer units or around bends in the channel.

Water depths and velocities (at 0.6 of depth) were measured using a top-set wading rod and Swoffer Instruments, Inc. Model 2100 velocity meter at a minimum of 2 and a maximum of 18 locations along the thalweg in each habitat unit, according to unit length. Wetted area for a whole reach was calculated as the sum of wetted areas among habitat units within a reach wherein wetted area was unit length multiplied by mean wetted width within that unit. A model was fitted to the data and used to show change in wetted area as a function of the mean site-specific flows for each reach. Mean site-specific flow for a reach was the arithmetic mean flow calculated among sampling sites within a given reach.

2.2.3. Sediment Particle Size Distribution

Sediment particle size distribution was measured in 2019 by conducting pebble counts to measure the composition of the stone matrix at each of the periphyton and benthic invertebrate sampling sites (Figure 1.5; Sections 2.3 and 2.4). A 100-particle Wolman Pebble Count (Wolman 1954) was completed at each site, where the intermediate diameter of 100 randomly selected particles was measured using calipers. A crew member entered the stream. Without looking, he or she picked up a stone and measured its intermediate diameter using calipers, moved two or three steps in any direction and repeated the measurement on another stone. This process was repeated to measure 100 stones. Measurements were done at each site except at sites H and I where safety risk prevented access on the day of sampling. From sizing of the 100 stones, the 50^{th} percentile called D50 was calculated as the median particle size among the 100 measurements (Eaton et al. 2019). Sediment particle size measurements were not repeated in 2020 due to budget limitations.

2.2.4. River Stage

The relative stage of the river was continuously monitored and recorded at seven stations: Terzaghi Plunge Pool (km 40.9), Reach 3/4 Boundary (km 36.8), Bottom of Reach 3 (km 26.1), Top of Reach 2 (km 23.6), Bottom of Reach 2 (km 20.0), Top of Reach 1 (km 11.3), and Bottom of Reach 1 (km 3.9). BC Hydro maintained the river stage monitoring equipment at Rkm 36.8, which is considered the compliance point for measurement of stage changes associated with flow ramp down events. River stage data for this site was recorded every 5 minutes throughout the year and was provided by BC Hydro Generation Operations. The stage data for the remaining sites were recorded every half-hour by water level data loggers manufactured by Onset Computer Corporation (Model: U20-001-01), which were maintained by the BRGMON-1 field crews. The Onset loggers were deployed from 3 March to 30 November 2020 in reaches 2, 3 and 4, and from 11 March to 1 December 2020 in Reach 1. During the deployment period, these loggers were retrieved and downloaded on 11-12 August and 19-20 October 2020.

Since the depths where the loggers were placed varied at each site and among deployments, the resulting stage values needed to be standardized so that relative changes across the year could

be compared among the monitored locations. The stage data for each site were calibrated to 0.5 m at low flows (i.e., on 1 November 2020) using the following formula:

$$Stage(cal)_{i,d} = Stage(raw)_{i,d} + \left(0.5 - Stage(raw)_{i,Nov1}\right)$$

where $Stage(cal)_{i,d}$ is the calibrated stage value at site (*i*) on day (*d*), $Stage(raw)_{i,d}$ is the original stage value at site (*i*) on day (*d*), and $Stage(raw)_{i,Nov1}$ is the original stage value at site (*i*) on 1 November 2020. This approach ensured that the absolute differences in stage value remained unchanged, but they were all anchored to the same y-axis base point at low flows.

2.2.5. Water Temperature

Water temperature was recorded hourly throughout 2020 using Onset Model UTBI-001 data loggers (Onset Computer Corporation (Cape Cod, Massachusetts)). The temperature loggers were deployed at each of the eleven index sites in the LBR (including the four new sites in Reach 1) and at one location in the Yalakom River, approx. 100 m upstream of its confluence with the Bridge River. The loggers were anchored to the river substrate so they remained continuously submerged, and were checked and downloaded at ca. 3- to 4-month intervals to reduce the potential for data loss.

To evaluate the effects of flow releases on the timing of emergence of Chinook and coho salmon fry from spawning gravels we calculated accumulated thermal units (ATU), defined as the sum of daily temperatures above 0°C from the observed average date of peak spawning, using average surface water temperatures for each monitoring station. Median emergence was assumed to occur at 1000 ATU for Chinook salmon (Groves et al. 2008) and 500 ATU for coho salmon (Murray et al. 1990; based on development data for 2-5°C water). Peak of spawning was set at September 8 and November 15 for Chinook and coho salmon, respectively, based on LBR run-timing distributions from streamwalk survey data collected under BRGMON-3 (White et al. 2018).

2.2.6. Turbidity

Turbidity was continuously monitored for a period of the year in 2020 at each of the following locations (in upstream to downstream order): 1) Rkm 40.9 (Terzaghi Plunge Pool); 2) Rkm 36.8 (Reach 3/4 Boundary); 3) Rkm 26.1 (downstream end of Reach 3); 4) Yalakom River (near confluence with the Bridge River; Site Yal_B); 5) Rkm 20.0 (downstream end of Reach 2; Site G); and 6) Rkm 1.2 (downstream end of Reach 1; Site K). We used RBRsolo Tu loggers equipped with a Seapoint sensor and sensor wiper (RBR Ltd. Ottawa, ON). Due to variation in timing of logger installation, the logging period was March 3 to November 26 at Rkm 40.9, 26.1, and 20.0; April 30 to November 26 at Yalakom; August 13 to November 26 at Rkm 1.2; and August 14 to November 26 at 36.8. The logging interval was 10 minutes, and the sensors were wiped once an hour. Each logger and wiper assembly was installed inside an ABS pipe housing that was bolted to a large boulder or other anchor point (Photo 2.1). A cut-out on the pipe exposed the sensor to flowing water and allowed free movement of the wiper arm. To avoid sunlight affecting

saturation of the photodiode amplifier on the sensor that can produce negative readings (J. Mather, Seapoint Sensors Inc. Pers Comm. May 11, 2020), the sensor was shielded using a plastic cover fixed in position above the pipe cut-out as shown in Photo 2.1 (the green cover). Despite the sensor shading, some negative values remained. These occurrences were deleted from the data frame.

Photo 2.1 The turbidity logger housing installed at Rkm 36.8. The green shield was installed over the sensor to limit exposure to sunlight that can produce faulty readings.

Numerous high values were found, which represented voltage spikes potentially caused by artifacts on the sensor or other interference not associated with the general time course change in turbidity. These values were removed by assigning a rule that any value exceeding 70 NTU was deleted. No trend in turbidity reached 70 NTU, making that a safe value that did not affect the true time course variability in turbidity. A further rule was applied that if the absolute value of the difference between a measured value (value A) and the average of the previous 6 values (a time period of 1 hour) was greater than 5 NTU then the average of those previous 6 values was assumed for value A. This action removed spurious anomalies that did not conform to a time course trend and were less than 70 NTU.

2.2.7. Water Chemistry

Water samples for analysis of nutrient concentrations were collected monthly between June and November 2020 using standard grab methods. Sample locations were each of the mainstem index sites (A to K; Figure 1.5; Appendix A) as well as tributaries to each reach (shown as red pins on Figure 1.5). Sampling dates in 2020 were: 23-24 June; 13-14 July; 17-18 August; 27-28 September; 27-28 October; and 23-24 November. Sampling in June, July and August was intended to characterize water chemistry during spring and summer at each station. The samples

collected in September, October and November were intended to characterize water chemistry conditions during the periphyton and benthic invertebrate sampling time series in fall (Sections 2.3 and 2.4).

All samples were kept cool and shipped to ALS Environmental in Burnaby, B.C. for analysis of ammonium (NH_4-N), nitrate (NO_3-N), soluble reactive phosphorus (SRP), total dissolved phosphorus (TDP), total phosphorus (TP), total alkalinity, total dissolved solids (TDS) concentration, conductivity, and pH using standard methods (APHA 2011). The sum of NH_4-N and NO_3-N was called dissolved inorganic N (DIN) that can be taken up by biota and used in photosynthetic production.

The molar ratio of DIN:SRP was used to show potential change in N and P limitation of benthic algal growth (Bothwell 1989, Perrin and Richardson 1997, Biggs 2000, Nelson et al. 2013). Rhee (1978) showed that for a given species of algae there is a sharp transition between P-limited and N-limited growth. The particular N:P ratio at which the transition between N and P-limitation occurs is species dependent, varying from as low as 7:1 for some diatoms (Rhee and Gotham 1980) to as high as 45:1 for some blue-greens (Healey 1985). Below a molar N:P of 20, the growth of most algal species will be limited by N whereas P-deficient growth is prevalent at molar N:P ratios greater than 50 (Guildford and Hecky, 2000). Because an optimum N:P ratio (above which P limitation occurs and below which N limitation occurs) can vary widely among freshwater algae, the range between 20 and 50 was regarded as a transition range in a community where the growth of some species will be P-limited and the growth of others will be N-limited.

2.3. Periphyton Biomass and Composition

Periphyton was sampled during the fall (September – November) in 2020 from riffle or run habitats at each of stations A to K in the LBR and at both Yalakom River stations (see Figure 1.5 and Appendix A for locations). The two stations in the Yalakom (Yal_A and Yal_B) and the four stations in Reach 1 (Sites H – K) were added in 2018 and 2019, respectively. The sampling locations in reaches 2 to 4 were the same during the earlier flow trials as described by Bradford and Higgins (2001) and Decker et al. (2008). Periphyton sampling methods in 2020 were the same as those used in all previous years of BRGMON-1, summarized as follows.

Artificial substrata called “periphyton plates” were used to sample periphyton assemblages (Photo 2.2). Each plate was a 30 x 30 x 0.64 cm sheet of open-cell Styrofoam (Floracraft Corp., Pomona CA) attached to a plywood plate that was bolted to a concrete block. Styrofoam is a good substratum because its rough texture allows for rapid seeding by algal cells, and the adhered biomass is easily sampled (Perrin et al. 1987). Use of the plates standardized the substrate at all stations and removed variation in biomass accrual due to differences in substrata roughness, shape, and aspect.

Photo 2.2 An installed periphyton plate.

Periphyton biomass was sampled weekly from each of three replicate plates at each location for 57 days between 23 September and 20 November 2020, which was generally the same period of incubation used in previous years. Each biomass sample was a 2 cm diameter core of the Styrofoam and adhered biomass that was removed as a punch from a random location on each plate using the open end of a 7-dram plastic vial. The samples were kept frozen from the end of each sampling day until they were analyzed at ALS Environmental (Burnaby, B.C.) for chlorophyll-a concentration using fluorometric methods reported by Holm-Hansen et al (1965) and Nusch (1980). Units were µg chlorophyll-a·cm^{-2}. Chlorophyll-a is a plant pigment commonly used as a measure of biomass of photosynthetic algae (e.g., Stevenson 1996). This measure is preferred over something like dry weight that can include non-biological material in the stream substratum or non-photosynthetic organic matter (e.g., bacteria, fungi, detritus of terrestrial origin). The highest chlorophyll-a concentration accruing on each plate during the incubation period was called peak biomass (PB), which is related to cellular growth rate (Bothwell 1989) and was used as a standard metric of periphyton production.

Depth and velocity was measured weekly at each the time of sampling for each plate using a top-set wading rod and Swoffer Instruments velocity meter. On the final periphyton sampling day (November 20, 2020), an additional core was removed from each plate and preserved in Lugol's solution, for later cell counts and biovolume by taxon. During shipping from the field to the lab in Vancouver, these samples were lost due to faulty packaging, which resulted in no data describing taxonomic composition of periphyton in 2020.

2.4. Benthic Invertebrate Abundance and Composition

Three replicate benthic invertebrate samples were collected from the same 11 sites in the LBR and two sites in the Yalakom River that were used for the periphyton sampling (Section 2.3). Each

invertebrate sample was collected from 25–50 mm size gravel enclosed in a wire basket measuring 30 cm long x 14 cm wide x 14 cm deep (Photo 2.3), with 2 cm openings that was installed in the river for 54 days (between 23 September and 18 November 2020). The basket was similar to that shown by Merritt et al. (2008). The baskets were filled with clean material that was collected from the stream bed or bank and closed using cable ties.

Photo 2.3 Basket sampler before installation in the Lower Bridge River. Baskets used in 2020 were longer than those from previous years. To ensure consistency of data among years, a baffle was installed in each basket so that it contained the same volume of packed stones as previous samplers.

At the start of each colonization period, the baskets with contained stones were placed among the natural river substrata in riffle or run habitat. The baskets remained undisturbed for the duration of the ca. eight-week colonization period. Water depth and velocity was measured weekly during the incubation period at the upstream end of each benthic invertebrate sampling basket using a top-set wading rod equipped with a velocity sensor manufactured by Swoffer Instruments.

Following incubation, the baskets were carefully removed from the streambed and placed into individual buckets. The basket was opened by clipping the cable ties, and invertebrates were brushed from the gravel using nylon brushes. Removed material was filtered through a 250 µm Nitex screen (to remove excess water), transferred to a sample jar, and preserved in 10% formalin. Following sample collection, the preserved invertebrates were submitted to Stamford Environmental for sorting, identification to Family, and enumeration.

In the laboratory, formalin was removed from the samples by washing with water through a 250 µm filter then neutralized with FORMEX (sodium metabisulfite) before discarding. Animals were picked from twigs, grasses, clumps of algae, and other large organic debris. These animals and remaining material were washed through 2 mm and 250 µm mesh sieves to separate the

macro portion (>2 mm) from the micro portion (<2 mm and >250 µm). Animals in the macro portion were picked and placed in vials containing 70% ethanol. The micro portions were subsampled according to the following four steps:

1) Suspended specimens and substrate were decanted from the micro portions in preparation for subsampling. The remaining sandy heavy portion was then examined under a microscope and all specimens (e.g., stone-cased caddis fly larvae) were picked out and added to the decanted volume.

2) Suspended micro portions were each homogenized by stirring then subsampled using a four-chambered Folsom-type plankton splitter: an apparatus designed to collect random proportions from volumes of suspended invertebrates. Approximately 300 specimens (minimum 200) were used for guiding subsample sizes. Simulations suggest random subsamples containing >200 specimens encompass the diversity present in a sample and provide accurate estimates of abundance (Vinson and Hawkins 1996; Barbour and Gerritsen 1996; Walsh 1997; King and Richardson 2001). Micro portions were split into half portions repeatedly until the resultant splits contained about 300 specimens.

3) A random selection of three samples (10%) were sorted twice to ensure picking efficiency was consistently maintained at 95%.

4) Counts from the micro portions were multiplied by the inverse of the split proportion to obtain estimates of abundance in the micro portions. These values were added to the direct counts from the macro portion to obtain the estimated abundance in the whole sample. All animals were preserved and retained in 70% ethanol.

For taxonomic identification and enumeration, the animals were identified to family except *Acari* (mites), *Clitellata/Oligochaeta* (earthworms), *Nematomorpha* (horsehair worms), *Platyhelminthes/Turbellaria* (flatworms), and *Ostracoda* (ostracods). Enumeration at the family level was based on findings by Reynoldson et al. (2001), Bailey et al. (2001), Arscott et al. (2006), and Chessman et al. (2007) that family assemblage data are equally sensitive to lower taxonomic levels for evaluating invertebrate response to change in habitat condition in resource management applications. Higher level taxonomy (e.g., class, order) was applied for non-insect aquatic invertebrates and terrestrial taxa. Taxonomy was based on keys in Merritt and Cummins (1996) and Thorpe and Coviche (2001).

Benthic invertebrates were quantified as counts of animals in aquatic life stages (mainly larval forms of aquatic insects). Individuals from terrestrial habitats or adults of aquatic insects were not included in the animal counts. All invertebrate data were expressed as number of individuals per basket sampler or per unit area where the planar areal dimension of the basket lying on the stream substratum was the area of sample. Biomass of the benthic invertebrates was not measured.

2.5. Juvenile Fish Production: Size, Abundance, Biomass and Habitat Use

For fish sampling, the focus of the program has been on the juvenile lifestage (i.e., fry and parr) of Chinook salmon (*Oncorhynchus tshawytscha*), coho salmon (*O. kisutch*) and steelhead (*O. mykiss*), because it was expected that instream flows and associated freshwater productivity could have a measurable influence on the recruitment and survival of these species. It is understood that both resident rainbow trout and anadromous steelhead reside in the Lower Bridge River. Based on the results of otolith microchemistry analysis in 2015, a higher proportion of the recruited juveniles are steelhead (King and Clarke 2015); however, potential changes in the relative proportions were not routinely assessed across each of the flow trials. As such, juvenile steelhead/rainbow trout are referred to collectively as "mykiss" in the text and represented by the abbreviation "RB" in tables and figures throughout this report.

Juvenile Fish Size

Monthly growth sampling was discontinued in 2018 – refer to the Year 7 report for the rationale (Sneep et al. 2019). As a result, the analysis of fish size among flow treatments included in this report is based solely on fish sampled during the annual stock assessment (see description of this method under "Abundance and Biomass", below). During this task, a sufficient sample size ($n \geq 30$) of each target species and age class has been more consistently acquired for each reach, and the sample timing has been very consistent across years. Forklength (mm) and weight (g) has been recorded for captured fish since 1996.

Abundance and Biomass

The abundance and biomass contributions of juvenile salmonids were estimated by conducting an annual closed-site, depletion-type electrofishing survey. For 1996 to 1998, sampling was conducted between late September and mid October, but for the remainder of the experiment, sampling generally occurred between early and late September (Table 2.2). The selection of sampling sites for the flow trials was based on habitat surveys that were conducted in reaches 2 and 3 in 1993, and in Reach 4 in 2000 (after initiation of the flow release re-wetted that reach) that inventoried all major meso-habitat types (e.g., runs, riffles, pools).

At the start of the program, 18 sampling units were randomly selected for each of reaches 2 and 3 from the inventory of habitat units in proportion to their occurrence in the inventory. Although the original intent was to use these sites throughout the entire flow experiment, some sites had to be relocated slightly owing to changes in the channel morphology resulting from debris flows and spills from the dam. New sites were chosen to have the same characteristics as the altered sites to maintain the same distribution of habitat types being sampled. Two additional sites were added to the upper region of Reach 3 in 1998, bringing the total number of sites for Reach 3 to 20. In 2000, an additional 12 sites were selected in the rewetted Reach 4 by the same procedure that was used for reaches 2 and 3, bringing the total number of sites for all three study reaches to 50. Starting in Trial 2, 1 – 2 sites in Reach 2 were dropped, reducing the number for that reach

to 16 or 17 and the total for reaches 2 – 4 to 48 or 49 since 2012. Starting in 2019, 12 new sites were established in Reach 1 bringing the total number of sites to 61 and extending the spatial scope of monitoring to the confluence with the Fraser River (Figure 2.1 and Appendix A).

Table 2.2 Years used to compute average abundance and biomass for each flow regime in the Lower Bridge River for Chinook, coho, and mykiss fry (Age-0+) and mykiss parr (Age-1).

Year	Flow Treatment (MAD)		Sampled Reaches	Total # of Sites	Sampling Dates
1996	Trial 0 – Pre-Flow (0 $m^3 \cdot s^{-1}$)		2-3	36	8 – 16 Oct
1997				36	2 – 13 Oct
1998				38	29 Sep – 9 Oct
1999				38	3 – 10 Sep
2000	Transition Year [a]		2-3	50	30 Aug – 10 Sep
2001	Trial 1 (3 $m^3 \cdot s^{-1}$)		2-4	50	27 Aug – 10 Sep
2002				50	28 Aug – 5 Sep
2003				50	2 – 11 Sep
2004				50	7 – 15 Sep
2005				50	6 – 16 Sep
2006				50	5 – 14 Sep
2007				50	5 – 19 Sep
2008				50	3 – 18 Sep
2009				49	8 – 24 Sep
2010				50	7 Sep – 19 Oct [b]
2011	Trial 2 (6 $m^3 \cdot s^{-1}$)		2-4	50	6 – 22 Sep
2012				45	5 – 27 Sep
2013				47	4 – 26 Sep
2014				48	2 – 24 Sep
2015				48	1 – 28 Sep
2016	Modified Operations	High Flows (>18 $m^3 \cdot s^{-1}$)	2-4	48	1 – 21 Sep
2017				49	5 – 20 Sep
2018				49	4 – 15 Sep
2019		Post-High flow (6 $m^3 \cdot s^{-1}$)	1-4	61	29 Aug – 18 Sep
2020				61	25 Aug – 11 Sep

[a] The year 2000 was considered a transition year because the flow release started on 1 Aug that year, only one month before the annual stock assessment timing. As such, this year was not included in any trial averages.

[b] In 2010, 4 sites were completed in mid-October (3 in Reach 2; 1 in Reach 4); The other 46 sites were completed by 19 September.

At each site, the area to be sampled was enclosed with block nets constructed of 6 mm mesh. The average size of a sampled area in 2020 was 87 m^2 (range: 47 to 127 m^2 among sites, based on the amount of suitable habitat at each location). Total catches were derived using a depletion method based on three or four passes of backpack electrofishing. A minimum of 30 minutes elapsed between passes. After each pass, captured fish were identified and forklength (nearest

mm) and weight (0.1 g) of all salmonids were recorded before being released outside the enclosure. Ages (i.e., Age-0+, Age-1, etc.) were assigned to all captured fish according to identifiable size ranges based on analysis of length-frequency histograms for each reach.

During the Pre-flow period, nets were used to block off the full width of the stream in Reach 3; therefore, the sampled areas included the entire channel. This was not possible in reaches 1 and 2 during any monitoring year, or in reaches 3 and 4 after the flow release because of the greater depths and velocities associated with the increased flows. In these cases, sampling was conducted in three-sided enclosures along shore instead. These enclosures averaged 5.1 m in width. Flows from the dam during the depletion sampling period in September were the same (i.e., 3 $m^3 \cdot s^{-1}$) for all of the flow release monitoring years (2000 to 2020; see September period on Figure 1.3).

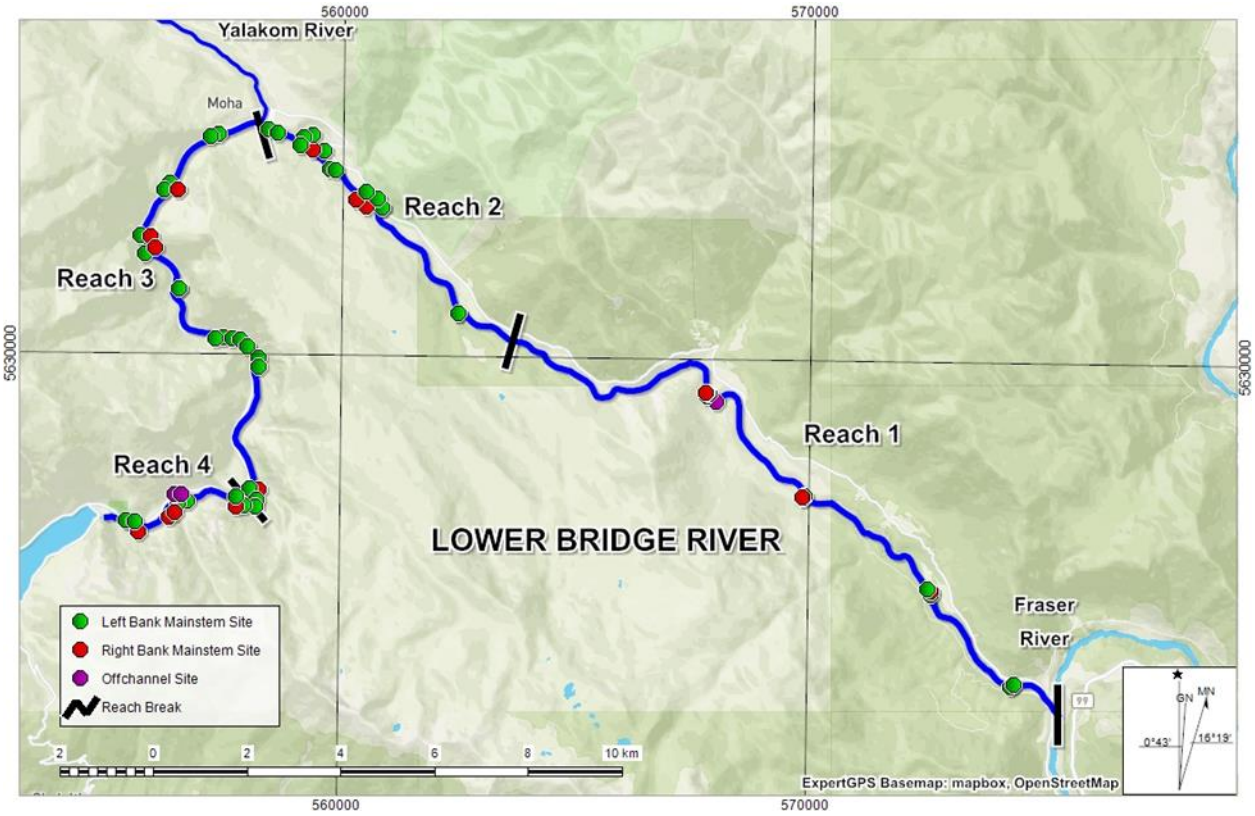

Figure 2.1 Distribution of Juvenile Stock Assessment Sites in the Lower Bridge River study area in 2020.

For the locations where three-sided sites were used, there was potential for some fish (e.g., parr) to be located further offshore and inaccessible to the gear. Therefore, the proportion of the population that was vulnerable to this sampling method was estimated using data that was collected as part of a separate Lower Bridge River microhabitat use study. In that study, divers located the position of juvenile salmonids during the day relative to the shoreline at two sites in Reach 2 and two sites in Reach 3 during August 1999, October 1999 and July 2000, prior to the flow release, and in August 2000 after the flow release.

For Reach 2, where the flow release from the dam had little impact on habitat conditions, observations from the August 1999 and August 2000 surveys were combined for estimating the distribution of fish from shore. The data collected in Reach 3 in late August 2000, approx. one month after the start of the flow release, was used to estimate the post-flow release distribution for reaches 3 and 4. The location of fish concealed in the substrate could not be determined by the daytime surveys, so the assumption was made that the distribution of fish observed during the microhabitat study would be a reasonable approximation of the location of all fish in the channel (either concealed in the substrate or swimming in the water column).

Enhanced Off-channel Sites – Juvenile Salmonid Seasonal Habitat Use

Following from pilot efforts during high flow releases in 2018, fish sampling was undertaken in a couple of enhanced off-channel sites in spring (i.e., June) and summer (i.e., July or August) to characterize fish use of these habitats during the peak period and descending limb of the LBR hydrograph in 2019 and 2020. There is interest in understanding the relative importance of these habitats for providing refuge when high discharges limit the suitability of fish habitat in the mainstem. Data collection in non-high flow years (i.e., 2019 and 2020) was intended to provide context and background information against which the high flow results can be compared in future reports. By repeat-sampling the same set of sites on two dates in the same year, the intent was to assess changes in use of those sites by juvenile salmonids at different flow release discharges and seasonal periods (i.e., spring vs. summer).

2020 surveys were conducted on 13 and 14 June, and 16 and 17 July. The surveys targeted peak flows for the Trial 2 hydrograph (i.e., 15 $m^3 \cdot s^{-1}$ on both June and July dates). Two sites were selected in the off-channel habitat at Bluenose (Bluenose Outflow Channel and Bluenose Pond & Upper Intake Channel) and four sites were in the off-channel habitat at Applesprings (Applesprings Outflow Channel, Applesprings Upper Sidechannel, Middle Sidechannel and Lower Sidechannel) (see Appendix A for locations).

Each site was sampled in an upstream direction and spanned the full width of the channel. Fish sampling was conducted by open-site electrofishing. As such, catch results for these surveys represented a minimum estimate of fish presence at the time of each survey. Juvenile (Age-0+ and Age-1) coho, Chinook, and *O. mykiss* were the target species and age classes. Site length and electrofishing effort varied depending on the amount of habitat available at the selected sites.

All fish collected during sampling were identified to species and age class (estimated), measured for length and weight, and a sub-set were photographed. Electrofishing effort (seconds) and the number of crew members carrying out sampling was recorded. The locations of the upper and lower extent of each site were recorded with a GPS, the length of shoreline, and the general

characteristics of the site (habitat type, dominant/sub-dominant substrate, water visibility) were also recorded.

Enhanced Off-channel Sites – Juvenile Salmonid Stock Assessment

Enhanced side channel sites were also sampled for juvenile salmonids in fall of 2018, 2019 and 2020. During 2020, two sites in riffle habitat and one site in pool habitat were sampled at the Applesprings enhanced side channel located in Reach 1, and one site in riffle habitat and two sites in pool habitat were sampled at the enhanced Bluenose side channel in Reach 4 (refer to Appendix A for maps and UTM coordinates) for a total of three sites in each off-channel. Fish sampling methods applied at these locations were the same as those used during the mainstem fall standing stock assessment (described in the Abundance and Biomass sub-section above. Sample timing in 2020 was 15-17 September for the enhanced off-channel sites, which was just after the mainstem depletion sample timing. A multi-pass electrofishing depletion approach was used to estimate density, biomass and abundance. Estimates of density and biomass were compared to averages from mainstem sites during 2020 and the average across trials 1 and 2. The area of each enhanced side channel site by habitat type was multiplied by the estimated densities and summed to determine the total abundance at each site. We compared the abundance from these enhanced side channels relative to the total abundance in the mainstem to determine the extent to which they potentially mitigate impacts of high flows. Note: the abundance estimates for the off-channel sites were not included in the total estimates for the mainstem reaches presented in this report in order to maintain consistency with the results and analysis from previous years and flow treatments.

2.6. Adult Escapement

Adult spawner count data for the Lower Bridge River (up to 2019) were provided by Instream Fisheries Research (IFR) who are conducting the Lower Bridge River Adult Salmon and Steelhead Enumeration program (ref. BRGMON-3). As a part of their work, IFR have compiled and analyzed historical data to supplement their own data collection which began in 2012.

Visual counts for Chinook and coho were conducted annually by helicopter overflights or streamwalks during the flow experiment period (i.e., Pre-flow (Trial 0), Trial 1 and Trial 2 years), as well as the high flow years from 2016 to 2018, and the post-high flow years in 2019 and 2020. Counts by helicopter overflight were conducted in all reaches from 1997 to 2004 (missing 2000, 2002 and 2003 for Chinook Salmon, 2000 and 2002 for Coho Salmon). Visual streamside counts have been used since 2005 to enumerate both Chinook and Coho Salmon in Reach 3 and 4 (missing 2007 for Coho Salmon). Count data obtained from DFO was used to reconstruct AUC estimates for Chinook and coho salmon from the Yalakom confluence to Terzaghi Dam (Reach 3 and 4) since the start of monitoring. However, IFR has noted a caveat that the historical estimates are highly uncertain given changes in methods over time, the low number of surveys in some years, and the lack of measurements for observer efficiency and survey life prior to 2012 (White et al. 2021).

Visual surveys (streamwalks) conducted under the BRGMON-3 program (2012 to the present) followed methods used in previous years, where two observers walked in a downstream direction on the riverbank, counted spawners and recorded species and location. Viewing conditions, cloud cover, and secchi depth were also recorded (White et al. 2021). Visual counts occurred weekly for Chinook and coho salmon in Reaches 3 and 4. Starting in 2018, the streamwalks for spawner enumeration were expanded to include sections of Reach 2 and spot counts at the downstream end of Reach 1 (White et al. 2021). However, for consistency with BRGMON-1 reporting from previous years, only counts for reaches 3 and 4 were used in the stock-recruitment analyses (note: low numbers of Chinook (number unreported) and one coho salmon were observed during streamwalks in Reach 2 during 2019, but spawning behaviour was not confirmed).

In 2019, the visual survey period for Chinook was from 2 August to 15 October, and the survey period for coho was from 11 October to 3 December. **However, as noted in the BRGMON-3 report, there was an important factor constraining the reliability of the survey data for enumerating Chinook spawners in 2019: A channel-spanning fish fence (for broodstock collection) was installed at the downstream end of Reach 3 on 20 August, so the surveys were only able to assess fish that passed the fence site before this date, or fish that were released upstream by the fence crews.** Another important factor for salmon runs in 2019 was the Big Bar Slide on the Fraser River. The slide reportedly occurred in November 2018 and may have increased the proportion of stray spawners from other systems entering the Bridge River (see Section **Error! Reference source not found.** for DNA-based stock identification results for adult Chinook captured at the broodstock collection fence). Surveys for steelhead were deemed ineffective in past years due to high turbidity and flow volumes in the LBR during their migration and spawning period; thus, visual surveys have not been completed for steelhead.

Escapement estimates from these visual surveys were generated using area under the curve (AUC) estimation which relied on observer efficiencies and residence times determined by radio telemetry and visual surveys, including marked fish, which have been conducted since 2011 (White et al. 2021). However, as noted by the authors, generating accurate and precise AUC estimates from the historic data was hampered by inconsistent sampling methodology and survey area across flow treatments, and a lack of historic observer efficiency data. A key assumption in AUC estimates is that the mean observer efficiency documented by the BRGMON-3 program reflects conditions both before and after the flow release. It is likely that observer efficiency prior to the flow release was higher owing to lower and clearer flows. Thus, escapements prior to the flow release are likely overestimated due to this assumption. **Also, due to the effect of the broodstock collection fence (described above), the visual counts and AUC estimates for Chinook in 2019 were incomplete and may represent <50% of the true AUC since the peak count typically occurs after 20 August, when the fence was installed** (White et al. 2021).

A fish enumeration facility (resistivity counter) was constructed by IFR in October 2013 near the downstream end of Reach 3 to obtain more precise escapement estimates for coho, Chinook and steelhead above the Yalakom confluence going forward. Based on results in other systems, resistivity counters can provide accurate estimates (with confidence limits +/- 10% of true abundance). In future, these counter-based estimates can be compared to the estimates based on visual methods as a means of calibrating the historic estimates (though such a comparison would only apply to post-flow release counting conditions and would not address the bias described in the preceding paragraph). However, at the time of this report, the time series of data available from the resistivity counter were insufficient for incorporation in the stock-recruitment analyses.

For more detailed information on the collection of the adult salmon and steelhead escapement data and the associated analyses for generating the annual abundance estimates, refer to the IFR BRGMON-3 report (White et al. 2021).

2.7. Genetic Stock Identification of Bridge River Chinook Salmon Juveniles

The Big Bar Slide, located on the Fraser River approximately 60 km northeast of Lillooet, BC, created a fish passage impediment for migrating salmon spawners and was considered a complete blockage at some discharge levels, particularly affecting spring and early summer runs (DFO unpublished info.). The Lower Bridge River is the first significant spawning tributary downstream of the slide and more stray spawners from other systems were expected to migrate into the Lower Bridge River as a result of the slide and potentially spawn there. To assess the incidence of straying and the recruitment of progeny from admixed pairings for spawning events in 2019, genetic stock identification was completed for juvenile Chinook salmon sampled in 2020.

Tissue samples collected from 117 Chinook juveniles were submitted for genetic stock identification by the Molecular Genetics Lab at Pacific Biological Station (PBS). Two analytical approaches were completed to describe the genetic ancestry of these juveniles and infer which stocks successfully spawned in the Lower Bridge River in 2020. Following is a description of the analytical methods provided in a summary report from PBS (Wetklo and Sutherland 2021):

> *"To identify the stocks present in the juvenile sample of 2020 Bridge River Chinook, 117 juveniles were genotyped with a panel of 15 microsatellites. Genetic Stock Identification (GSI) analysis was then conducted using a microsatellite baseline of 76 Chinook populations (see PID20200112_Bridge_20_juv_2021-02-09.xlsx). Where possible, GSI for individuals is reported to the population level. In cases where genetically similar populations cannot be resolved, these populations are reported to the level of a Genetic Unit (GU). The GU level was developed in 2020 and found to be reliably identified based on simulations, and reflects the resolution limits of the current real-time genotyping method for Chinook in the mid and upper Fraser River. Stocks identified in the juvenile samples with probabilities greater than 75% at the individual*

ID level were considered reliable and selected as baseline samples to be used in a second analysis using the program Structure [Appendix E, Table E1] (Pritchard et al., 2000). Structure is routinely used to infer population structure, identify hybrids of two species or admixed individuals of two or more populations. For our analysis, the number of populations (k) assumed by Structure was determined empirically and set at 10. Here, each k population is characterized by a particular set of allele frequencies. Generally, juveniles with a Structure inferred Bridge ancestry greater than 75% and stray ancestry less than 20% were considered to have primarily Bridge River ancestry (i.e., the offspring of two local Bridge River spawning adults). Admixed juveniles were reported when a single stray stock ancestry was 20% or greater. Ten iterations of the Structure analysis were performed and the mean Bridge ancestry (%) and consensus stock assignments or admixture sources were reported.

Parentage analysis using the program Colony (Jones and Wang, 2010) was also performed to identify related juveniles."

2.8. WUP Ramp Down Monitoring and Fish Salvage

Flow ramping and fish salvage data were collected across the range of flow releases in 2020 (15 to 1.5 $m^3 \cdot s^{-1}$ – same as the Trial 2 hydrograph). The methods described in this section are based on documentation provided by Coldstream Nature-Based Solutions. 2020 discharge data for Terzaghi Dam and river stage data for Rkm 36.8 (~4 km downstream from the dam; a.k.a. the compliance location) were provided by BC Hydro Power Records. The data were available as hourly values.

On each ramping date before any flow changes were initiated, field reconnaissance of the survey area was completed at an overview level to identify and rank specific locations with potential fish stranding risk. Once the flow changes from the dam began, fish salvage crews were dispatched to the areas deemed to have the most immediate risk first, and then moved as the degree of risk shifted from location to location. Site and habitat information was recorded for each identified stranding location on each ramping day, which included: Date, flow release rate at the dam, approximate river kilometre (upstream of the confluence with the Fraser River), GPS coordinates, bank, area (in m^2 based on length and width measurements), habitat type, substrate composition, and weather.

For fish salvaging, backpack electrofishing (EF) and hand collection were the methods employed. Parameters recorded for the fish salvaging included: Sampling effort (EF seconds), number of passes, species and age class (i.e., fry or parr), and number salvaged. Forklengths (in mm) and weights (g) were measured for a subset of salvaged fish and DNA was collected from a sample of Chinook and coho juveniles for stock identification. Fish salvage efforts focussed on fish that were already isolated, stranded or mortalities. As per the direction of BC Hydro's Scope of Services (BC Hydro 2019), fish in habitats that were not yet isolated or stranded (i.e., incidental catches)

were not to be sampled. This was to ensure that salvage totals reflected the actual numbers of fish that were stranded from the main channel flow by the ramp down event.

Analyses of the flow ramp down and fish salvage results were based on the risk assessment approach outlined in BC Hydro's Lower Bridge River Adaptive Stranding Protocol to determine risk ratings for the identified stranding sites at each river stage change. Where possible, fish stranding data from 2020 were compared with the results from previous study years to better inform the risk of fish stranding across the flow ramp down range.

2.9. Data Analysis

2.9.1. Benthic Communities

Stacked bar graphs were drawn to descriptively show the taxonomic composition of periphyton and benthic invertebrates by Trial and Reach and from the Yalakom River. The stacked segments of the bars were algal divisions or invertebrate orders to give a general description of composition over time and space.

We tested Trial, Reach, and Pink effects on several response variables using three-way analysis of variance (ANOVA). The response variables were algal PB and the count per sample of all invertebrates, Chironomidae, EPT (sum of Ephemeroptera (mayflies), Plecoptera (stoneflies), and Tricoptera (caddisflies)), and family richness (number of invertebrate families in a sample). The chironomids and EPT represented most individuals among the invertebrate assemblages found in previous analyses (Sneep et al. 2020) and are sensitive indicators of habitat disturbance (Holt et al. 2015, Kennedy et al. 2016). Both the chironomid and EPT larvae are fish food organisms (Quinn 2018).

"Trial" corresponded to each of the flow treatment blocks (refer to Sections 1.2 and 1.3) plus 2019 and 2020 occurring after the High Flow years (called "Post-High Flow years"). "Reach" blocked the response variables by physically different places in the river. "Pink" was a surrogate for nutrient pulsing caused by salmon spawning and carcass decomposition (e.g., Harding and Reynolds 2014, Albers and Petticrew 2012). In the Bridge River, Pink salmon spawn in odd years and are absent in even years. This bi-annual sequence may produce greater benthic production in odd years (the on years for Pink spawning) and lower production in even years according to nutrient releases from the salmon. The overall layout allowed for testing effects of Trial, Reach, and Pinks on each of the response variables using the compiled data of response variables dating back to 1996 when benthos monitoring started in the Bridge River.

Each observation was the mean value of a response variable among all samplers and stations, by reach, in a given year. Years were replicates. This approach overcame pseudoreplication within a station and stations within a reach. Normality was tested using the Shapiro-Wilks test. If sample distributions were non-normal, the data were $\log_{10}$ transformed to achieve normality. The significant probability level was set at 0.05 (an effect was considered present if the probability value was <0.05). If a significant interaction between Trial, Reach, and Pink was found, the results

were interpreted using graphs and the Tukey test was applied to examine significance of interacting pairs of each level of Trial (1 to 4), Reach (2 to 4), and Pink (0 and 1). If no significant interaction of Trial and Reach was found, then each factor (Trial or Reach or Pink) was examined independently. If any one of the factors was found to have a significant effect on a response variable ($p<0.05$), the Tukey test was run on the significant factor to determine what level or levels of that factor differed significantly from the others. Significant probability was $p<0.05$.

Periphyton and benthic invertebrates were not measured in Reach 4 during Trial 0 due to no flow release, which meant that the combination of Trial 0 and Reach 4 was missing from the layout and would not allow testing of Trial effects and Reach effects (an overall ANOVA could still be run but individual effects of Trial and Reach could not be examined). Either Trial 0 or Reach 4 had to be omitted to allow testing of Trial and Reach effects. We elected to omit Trial 0 on the premise that some flow release rather than no flow release was more important for management decisions than omitting Reach 4 because it is unlikely that a future flow scenario would consider no flow release from the dam. In Reach 1, periphyton and benthic invertebrates were only measured in 2019 and 2020. Without observations from Trials 1 to 3, Reach 1 could not be included in the ANOVA's. Based on these criteria Trial had 4 levels (Trials 1 to 4), Reach had 3 levels (Reaches 2 to 4), and Pink had two levels (0 for off years and 1 for on years).

2.9.2. Juvenile Fish Production: Size and Condition

We evaluated effects of flow on juvenile salmonid growth based on weight samples taken during the annual fall stock assessment. As in the analysis for periphyton and benthic communities described above, 2019 and 2020 were considered a new modified operations flow treatment which we refer to as the "Post-High Flow years". The results as presented for the previous flow treatments did not change. Mean weight is also the metric used to transform abundance estimates to biomass estimates for each flow treatment, so understanding changes in mean weights in addition to changes in abundance is important for explaining why abundance and biomass trends may differ.

Using weight as a surrogate for growth assumes that the interval between emergence date and sampling date are relatively consistent among years, or at least among flow treatments. There was some variation in sampling dates for stock assessment among years, particularly between the first three years of the Pre-flow period (early to mid October from 1996 to 1998) and the subsequent flow treatments (late August to late September from 1999 to 2019; see Table 2.2, above). Generally, the variation within the flow trial years was low. Owing to changes in water temperatures due to differences in flow treatments, emergence timing was likely different, especially for Chinook where water temperature differences over the incubation period between the pre-treatment and later flow treatments have been large (Section 3.1.1). Thus, using weight data to make inferences about growth is problematic, especially for Chinook. Nevertheless, we computed average weight (and standard deviation) by reach and flow treatment for Age-0+ mykiss, coho, and Chinook, and also for Age-1 mykiss.

We did not use formal tests to determine whether average weights in a particular reach were statistically different among flow treatments for two reasons. First, this would involve a large number of comparisons. There are 10 potential flow treatment comparisons (Pre-flow to Trial 1, Pre-flow to Trial 2, Pre-flow to High flow period, Pre-flow to the Post-high flow period, Trial 1 to Trial 2, Trial 1 to High flow period, Trial 1 to the Post-high flow period, Trial 2 to High flow period, Trial 2 to the Post-high flow period, and High flow period to Post-high flow period) for both reaches 2 and 3, and 6 flow comparisons for Reach 4. This results in 26 different flow treatment comparisons for each of four species-age classes for a total of 104 statistical comparisons. Second, statistical tests provide no information on whether a statistically significant result is biologically meaningful. For example, mean weight across two treatments could be significantly different but their means may be very close if the amount of variation in mean weight within each treatment is small.

Thus, our assessment of differences in mean weight across flow treatments is based on an examination of differences in the mean values for each treatment, and the extent to which the error bars at one standard deviation overlap. When these standard deviation error bars do not overlap, it's likely that the difference may be statistically significant. Given uncertainty about the criteria used to define biologically relevant difference in mean weights, and errors associated with whether those differences are related to growth or habitat (as opposed to differences in sample timing or emergence), we did not test for statistical significance in these cases. The graphical comparison of mean weights and their errors provides an efficient way to identify trends or any major differences in treatment effects.

Differences in mean weight (or length) of fish among flow treatments can also be influenced by factors that select for size (e.g., under high flows the incidence of displacement out of the study area may be higher for smaller fish than larger fish, introducing a bias in the estimate of mean size based on fork lengths or weights). This effect was noted as one of the possible explanations for the higher mean weights observed during the High Flow years (2016-2018) in the Year 7 monitoring report (Sneep et al. 2019). To overcome this potential bias and assess the relative fitness of individuals under the different flows, we calculated Fulton's Condition Factor (K) to characterize the body condition of each juvenile salmonid measured for length and weight according to the following equation (Anderson and Neumann 1996):

$$K = \frac{W \times 10^N}{L^3}$$

Where:

W is weight in grams;
L is forklength in millimeters; and
N is an integer that scales the condition factor close to a value of 1 (*N*=5 for LBR).

We then calculated the mean condition factor by species and age class for each flow trial and reach, as well as the standard deviations.

2.9.3. Juvenile Fish Production: Abundance & Biomass

The abundance and biomass of juvenile salmon in each reach was estimated with a hierarchical Bayesian model (HBM) described in Bradford et al. (2011) and Appendix B. Note that minor modifications to priors used in Bradford et al. (2011) were made to account for sparse catches which began in 2015. These modifications are summarized in Appendix B. The HBM provided annual estimates of abundance for Chinook, coho, and mykiss fry (Age-0+) as well as for mykiss parr (Age-1). We also computed means under five flow regimes which included the original annual average flow release treatments of 0 (Trial 0 - Pre-flow), 3 (Trial 1), and 6 $m^3 \cdot s^{-1}$ (Trial 2), as well as the unplanned high flows from 2016 – 2018 (High Flows) and the two years (2019, 2020) of Post-high Flows, to-date.

As described in detail in Appendix B, the effect of each flow treatment was determined based on mean abundance and biomass by reach for each regime. The years used to calculate average abundance and biomass for each treatment are provided in Table 2.3.

Table 2.3 Range of years used to compute average abundance and biomass for each flow treatment in the Lower Bridge River for Chinook, coho, and mykiss fry (Age-0+) and mykiss parr (Age-1).

Treatment	Mean Release	Age-0+	Age-1
Trial 0 – Pre-Flow	0 $m^3 \cdot s^{-1}$	1996-1999	1996-1999
Trial 1	3 $m^3 \cdot s^{-1}$	2001-2010	2002-2010
Trial 2	6 $m^3 \cdot s^{-1}$	2011-2015	2012-2015
High Flows	>18 $m^3 \cdot s^{-1}$	2016-2018	2017-2018
Post-High Flows	6 $m^3 \cdot s^{-1}$	2019-2020	2020

Note that data from 2000 was not used in the average for the Pre-flow or Trial 1 treatments because the change in flow occurred midway through the growing season and it is unclear how juvenile fish (both fry and parr) would have been affected in that year. There was no need to skip a year during the transition from the Trial 1 to Trial 2 treatments because flow changes occurred at the start of the growing season and prior to the emergence of mykiss fry in that year (2011). Despite a higher peak flow in 2015 (i.e., 20 $m^3 \cdot s^{-1}$ instead of 15 $m^3 \cdot s^{-1}$) owing to particular conditions and reservoir management decisions in that year, 2015 was included in the Trial 2 treatment because the yearly average (i.e., 6.6 $m^3 \cdot s^{-1}$) was still very close to the average for other years in this treatment (i.e., 5.3 to 6.1 $m^3 \cdot s^{-1}$). Age-0+ abundances from 2016 – 2018 were used

to compute the average abundance and biomass for the High flow regime, and 2019 – 2020 results were used to characterize the Post-high flow period.

For Age-1 mykiss we did not use data from 2000 or 2001 in the average abundance and biomass for the Trial 1 treatment period. Same as for the fry, the effects of the transition from base flows to the Trial 1 release in August 2000 on that year class of Age-1 fish was unknown. The Age-1 fish in 2001 would have experienced baseline flows during their first 2-3 months after emergence from spawning gravels (as Age-0+ fish in spring 2000), which may have affected survival during this important early life stage. Due to this off-set year effect for Age-1 fish, the first year of transition from Trial 1 to Trial 2 (i.e., 2011), Trial 2 to High flow (i.e., 2016), and High flow to Post-high flows (i.e., 2019) were also not included in the treatment averages for mykiss parr.

2.9.4. Mixed Effects Models for Predicting Log Density or Biomass

We used the following mixed effects models to predict the density (fish/m) and biomass (g/m) for each species and age class:

$$\text{1a)} \quad \hat{d}_{r,y} = \rho_r + \phi_f + \gamma_y + \varepsilon_{r,y}$$

or,

$$\text{1b)} \quad \hat{d}_{r,y} = \rho_r + \phi_{f,r} + \gamma_y + \varepsilon_{r,y}$$

where $\hat{d}_{r,y}$ is the predicted density (or biomass) in reach *r* in year *y* in log space, ρ_r is a fixed effect of reach (log density when no flow was released from the dam under Trial 0), ϕ_f is a fixed effect for flow treatments *f* (trials 1, 2, and 3) that is common to all reaches (eqn. 1a), $\phi_{f,r}$ is a reach-specific flow treatment effect (eqn. 1b), γ_y is a random effect of year, and $\varepsilon_{r,y}$ is the remaining process error. Random year and process error effects are drawn from a zero-centered normal distributions with estimated standard deviations σ_y and σ_p, respectively (i.e., $\beta_y \sim \text{dnorm}(0, \sigma_y)$). Under Trial 0 (0 $m^3 \cdot s^{-1}$) β_F and β_{Fr} are set to zero, which is why ρ_r is the average log density or biomass for reach r over years in Trial 0. ρ_r for Reach 4 is set to zero because there was no water in this reach during Trial 0.

The Age-0+ (fry) data consists of 68 density and biomass estimates across all year-reach combinations over 24 separate years. Data from 2000 were excluded because the year was influenced by both trials 1 and 2. The rainbow trout Age-1 (parr) data consists of 61 density and biomass estimates over 20 separate years. Data from 2001, 2011, 2016 and 2019 were excluded because Age-0+ fish were influenced by the previous treatment relative to the one these fish were captured in at Age-1. A total of 99 and 90 parameters are estimated when fitting the unstratified flow effect model (eqn. 1a) to Age-0+ and Age-1 data, respectively, and 105 and 96 parameters are estimated when fitting the reach-stratified flow effect model (eqn. 1b) to Age-0+ and Age-1 data, respectively. There are more parameters estimated than observations, but the

parameters are identifiable because the random year and process error effects are constrained by their prior distributions. Owing to the penalty associated with these priors, the model will attempt to explain as much of the variation as possible using the fixed effects.

The likelihood of the data given the predictions was calculated by comparing the observed ($d_{r,y}$) and predicted log density or biomass (eqn. 1) using,

$$2) \qquad d_{r,y} \sim dnorm(\hat{d}_{r,y}, \sigma_{o_{r,y}}^{-2})$$

where $\sigma_{o_{r,y}}^{-2}$ is the inverse of the observation error variance (i.e., precision) in the log density or biomass for each reach and year. These values were estimated by the hierarchical Bayesian model (Bradford et al. 2011) and treated as data in the mixed effects model. As some deviation between predictions and observations are expected due to observation error, predictions of log density or biomass are not expected to match the observed values perfectly. In essence, the process variance (σ_p^2) only needs to be large enough to explain the predictions after observation error has been accounted for via eqn. 2. The model was fit in winBUGS using uninformative uniform prior distributions for all fixed effects and variance terms. To achieve adequate model convergence, as assessed by the Gelman-Rubin convergence statistic (Gelman et. al. 2004, $\hat{r} \leq 1.05$), we saved every 10th MCMC sample from a total of 25,000 for each of 3 chains initialized with random starting values, after discarding the first 10,000 samples to eliminate initialization effects.

Multi-level R^2 statistics (Gelman and Pardoe 2006, Recchia 2010) were used to describe fit and quantify the explanatory ability of fixed effects. At the data level, the familiar square of the Pearson correlation coefficient indicates how much of the total variation in observed log density or biomass is explained by the model, as determined by both fixed and random effects (e.g., via eqn. 1a or 1b. We refer to this coefficient as the data r^2. At the next level, the ratio of the variation in predicted log density or biomass across reach and year strata explained by fixed effects, relative to its total variation resulting from both fixed and random effects, is used to quantify the explanatory power of fixed effects. We refer to this coefficient as the fixed effects r^2 (FE_r^2). Unstratified and stratified flow effect models were compared using the Deviance Information Criteria (DIC) which is a Bayesian analog of the Akaike Information Criteria (Spiegelhalter et al. 2002). The source code for the unstratified model is provided in Appendix C.

2.9.5. Stock-Recruitment Analysis

Estimates of juvenile salmonid abundance and biomass reflect the productive capacity of reaches in the LBR if they are adequately 'seeded'. That is, if the escapement to these reaches is sufficient so that fry and parr numbers are not limited by the number of fertilized eggs deposited in the gravel. If escapement is not sufficient to fully seed the habitat, fry and parr abundance and biomass will not reflect habitat conditions in the LBR (as affected by flow and other factors). The effect of escapement on fry production can be examined using a stock-recruitment (S-R) analysis, where the escapement in one calendar year is related to the fry produced from that escapement which is measured in the following calendar year.

Currently, escapement estimates for Chinook, coho and steelhead are generated by the BRGMON-3 Lower Bridge River Adult Salmon and Steelhead program (conducted by Instream Fisheries Research). However, a historical time series of escapement estimates (i.e., covering an equivalent time frame as the juvenile abundance data) are only available for Chinook and coho. As such, we were able to conduct stock-recruitment analysis for coho and Chinook salmon using annual estimates of escapement to evaluate the assumption of full seeding. However, the time series of escapement data for steelhead is too sparse to support stock-recruit analysis for this species at this point.

Escapement estimates for Chinook and coho in the mainstem LBR upstream of the confluence with the Yalakom River were derived from a modified area-under-the-curve (AUC) method (White et al. 2021). Escapement estimates for these species represent abundance in reaches 3 and 4 only as this is where the longest time series of stream walks have been conducted. Counts were expanded to estimates of the number present based on estimates of observer efficiency, which were determined from mark-resight data. A normal distribution was fitted to the expanded count data from each year, and the total escapement was determined by dividing the area under the normal curve by the survey life. The escapement estimates for each calendar year were plotted against fry abundance the following calendar year (e.g., Chinook spawning in September of 2019 produced fry that were sampled in the fall of 2020). We then fit the following Beverton-Holt model to these data,

$$F_{y+1} = \frac{\alpha \cdot E_y}{1 + \frac{\alpha}{\beta} \cdot E_y} \cdot e^{\lambda_j}$$

where F is fry abundance in year *y*+1, E is escapement in year *y*, α is the maximum productivity (fecundity/female * proportion of females * maximum egg-fry survival rate) which occurs when escapement is very low, β is the carrying capacity for fry, and λ is a parameter reflecting the effect of flow treatment *j* on the stock-recruitment relationship. For Trial 0 (0 $m^3 \cdot s^{-1}$ pre-flow period), $\lambda_{j=1}$ was fixed at 0. As $e^0=1$, α and β therefore represent the stock-recruitment curve under the pre-treatment conditions. Estimates of $e^{\lambda j}$ for j=2,3, and 4 represent how much the stock-

recruitment curve shifts under the 3 and 6 $m^3 \cdot s^{-1}$ treatments, and under high flow conditions (2016 to 2018), respectively. This approach for modelling habitat effects on freshwater stock-recruitment relationships is the same as used by Bradford et al. (2005) in their power analysis of evaluating the response of salmon populations to experimental habitat alterations.

The S-R data for 2018 and 2019 (i.e., 2019 and 2020 recruitment years) were not incorporated into any of the existing curves since these years represent the start of a new flow treatment (i.e., Post-high flows) and because the escapement estimates in 2019 were likely affected by strays due to the Big Bar Slide (Chinook + coho) and the operation of the broodstock collection fence (Chinook only). See Sections 2.6 and 2.7 for further information on these factors. There were not enough S-R datapoints for the Post-High Flow years (n= 2) to define an additional curve for this latest flow treatment.

Parameters of the stock-recruitment model were estimated in R using the optim non-linear search routine (R Core Development Team 2009) by maximizing the log-likelihood returned from a normal distribution comparing predicted and observed log-transformed fry abundances (i.e., recruitments). Chinook and coho escapements used in the analysis represent the number of fish spawning in the LBR upstream of the Yalakom River confluence. Fry abundance estimates used in the analysis represent the total abundance across reaches 2 and 3 (pre-treatment condition) and 2, 3, and 4 (other treatments and high flows). Thus, we assume that: 1) there is minimal spawning in the LBR downstream of the Yalakom River confluence; and that; 2) fry in Reach 2 are produced from fish that spawned upstream of the Yalakom River confluence.

Owing to the pattern in escapement-fry data, the estimated initial slope (α) of the unconstrained stock-recruitment model was unrealistically large. This occurred because observations of escapement near the origin still produced relatively high fry numbers. The initial slope of the escapement-fry stock-recruitment curve is the product of fecundity-sex ratio, and the maximum egg-fry survival rate at low density (from fertilization until the fall standing stock assessment). We constrained the initial slope based on assumed fecundity (5000 eggs/female for Chinook, 1500 eggs/female for coho), sex ratio (0.5), and maximum egg-fry survival rates (0.5 to 0.05). These estimates cover the wide range of values reported in Bradford (1995). We compared the fit of these alternate stock-recruitment models based on the difference in their log-likelihood values.

3. Results

3.1. Physical and Chemical Habitat Parameters

3.1.1. Discharge and Site-specific Flow

In 2020, the flow release from Terzaghi Dam generally conformed to the Trial 2 hydrograph for the entire year, but with slightly earlier timing for the ramp down to summer rearing flows than in 2019 and the Trial 2 years (2011 to 2015) (see Figure 1.3 in Section 1.3). Minimum flows were 1.5 – 2.2 $m^3 \cdot s^{-1}$ from 1 January to 3 March, and 5 October to 31 December. Flows were ramped up from the winter lows in a series of steps between 4 March and 13 May and reached a stable peak of ~15 $m^3 \cdot s^{-1}$ from 14 May to 20 July. Flows were ramped down from 15 to 3 $m^3 \cdot s^{-1}$ in a series of eight steps between 21 July and 7 August, and then down to the minimum release (i.e., 1.5 $m^3 \cdot s^{-1}$) in two steps on 5 and 6 October. Mean annual discharge from the dam in 2020 was 5.7 $m^3 \cdot s^{-1}$. 2020 was the second year of lower flows following the three consecutive years of high flows from 2016 to 2018 (MAD >18 $m^3 \cdot s^{-1}$; see Section 1.3).

Within the study area, estimated flow volumes across the index monitoring sites in reaches 3 and 4 (i.e., sites A to E) were the most consistent across the year and followed the shape of the release hydrograph quite closely, reflecting the small amount of tributary inflow to this section (Figure 3.1). The maximum difference in flow volume between Site A (top of Reach 4) and Site E (bottom of Reach 3) was 4.3 $m^3 \cdot s^{-1}$ at the peak of freshet. Between the bottom of Reach 3 (i.e., Site E) and the top of Reach 2 (i.e., Site F), differences in flow volumes were greater, particularly during the freshet period between early May and early August. This difference reflected the influence of the Yalakom River inflows at the top of Reach 2. The maximum difference between Site E (bottom of Reach 3) and Site F (top of Reach 2) was 25.5 $m^3 \cdot s^{-1}$ in 2020. The difference in flows across sites in reaches 2 and 1 was moderate (i.e., 2020 max. = 9.9 $m^3 \cdot s^{-1}$).

The Yalakom hydrograph in 2020 had two main peaks: an initial peak in late-May (up to 13.5 $m^3 \cdot s^{-1}$), followed by a higher peak in early July (up to 25.5 $m^3 \cdot s^{-1}$) (Figure 3.2). The second, higher peak represented a substantial discharge rate (i.e., 99th percentile) for the Yalakom River during that early July period based on the record from 1996 to 2020, although it was brief. The only other higher peaks in the month of July occurred in 2019 (i.e., 29.0 $m^3 \cdot s^{-1}$ on 8 July) and 1999 (i.e., 42.1 $m^3 \cdot s^{-1}$ on 15 July). MAD for the Yalakom River in 2020 was 4.8 $m^3 \cdot s^{-1}$, which was near the median value (i.e., 4.7 $m^3 \cdot s^{-1}$) for the 25-year monitoring period. The peak release flows from Terzaghi Dam (i.e., from 14 May to 20 July 2020) overlapped the timing of the peak period on the Yalakom River (i.e., from approx. 9 May to 12 July 2020), although the LBR flows started ramping up about a month earlier and were ramped down about two weeks later (Figure 3.1).

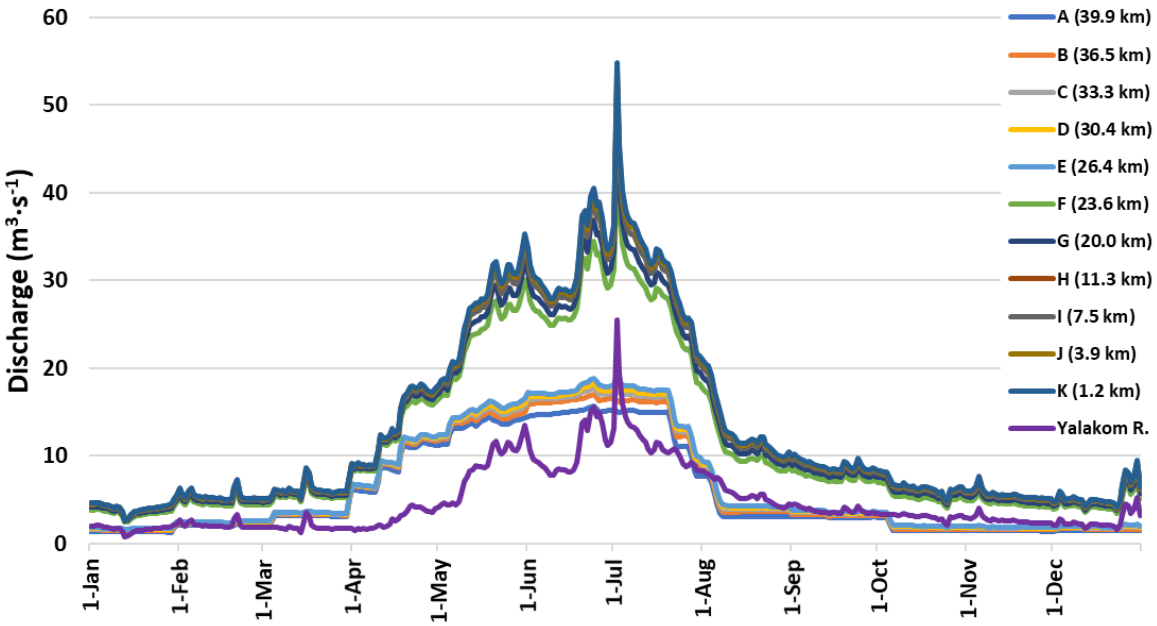

Figure 3.1 **Site-specific discharge estimates (shown as mean daily values) in the Lower Bridge River during 2020. Site A is in Reach 4, sites B to E are in Reach 3, sites F and G are in Reach 2, and sites H to K are in Reach 1. 2020 Yalakom River discharge is also shown.**

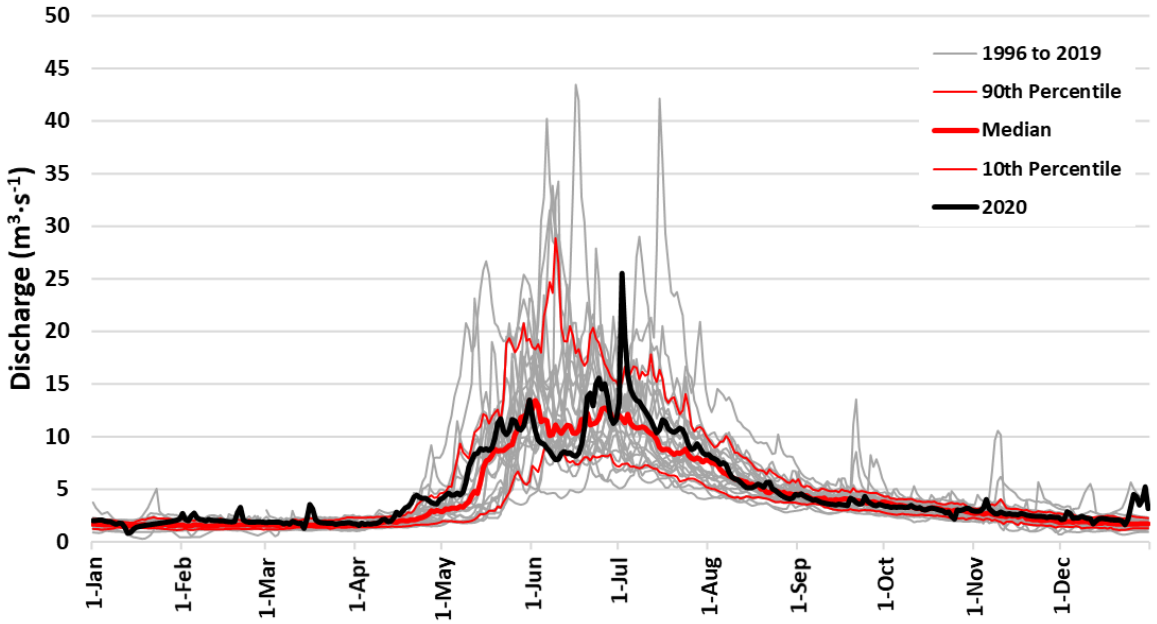

Figure 3.2 **Mean daily discharge in the Yalakom River for the period 1996 to 2020. The 10th and 90th percentiles are represented by the thin red lines (lower and upper, respectively) and the median is the bolded red line. The 2020 hydrograph is shown as the bolded black line.**

Site-specific mean peak flow recorded between 1 March and 31 August of each year among flow treatments increased from Trial 0 to Trial 3, reaching a maximum of 109 $m^3 \cdot s^{-1}$ in Reach 4 and 130 $m^3 \cdot s^{-1}$ in Reach 2 (Table 3.1). In 2019 and 2020, the summer peak flow preceding the fall biological sampling was similar to that during Trial 2.

Mean water depths and velocities at the periphyton and benthic invertebrate samplers were set according to placement of the samplers (Table 3.1). Velocities were 0.05 – 0.42 $m \cdot s^{-1}$ in both the Lower Bridge River and the Yalakom River. Water depths were 0.17 – 0.33 m in the Lower Bridge River and up to a mean value of 0.37 m in the Yalakom River (Table 3.1). These ranges were representative of river margins where current was adequate to maintain water exchange but not high enough to cause physical disturbance during all flow trials.

Table 3.1 Mean values (± standard error) of peak flow, water depth, and water velocity at the benthic invertebrate samplers among flow trials.

Variable and units	Reach	Mean value of flow variables ± standard error of arithmetic mean				
		Trial 0 (May 1996 – Jul 2000)	Trial 1 (Aug 2000 – Mar 2011)	Trial 2 (Apr 2011–Dec 2015)	High Flow Years (2016 – 2018)	Post High Flow Years (2019 – 2020)
Peak flow ($m^3 \cdot s^{-1}$)	Reach 4	No flow	5.0 ± 0.1	16.6 ± 0.6	108.7 ± 4.5	15.7 ± 0.02
	Reach 3	10.2 ± 1.9	6.3 ± 0.1	18.9 ± 0.3	110.9 ± 2.2	18.3 ± 0.4
	Reach 2	36.2 ± 3.4	26.1 ± 1.4	44.5 ± 1.4	130.0 ± 2.7	49.1 ± 1.8
	Reach 1	Not measured	Not measured	Not measured	Not measured	55.9 ± 1.1
	Yalakom River	Not measured	Not measured	Not measured	26.7*	27.1 ± 1.1
Water depth at benthic invertebrate samplers (cm)	Reach 4	No flow	0.27 ± 0.02	0.29 ± 0.04	0.20 ± 0.02	0.17 ± 0.01
	Reach 3	0.17 ± 0.01	0.30 ± 0.01	0.33 ± 0.02	0.31 ± 0.02	0.31 ± 0.03
	Reach 2	0.17 ± 0.02	0.26 ± 0.01	0.30 ± 0.03	0.27 ± 0.03	0.3 ± 0.04
	Reach 1	Not measured	Not measured	Not measured	Not measured	0.27 ± 0.03
	Yalakom River	Not measured	Not measured	Not measured	0.32*	0.37 ± 0.05
Water velocity at benthic invertebrate samplers ($m^3 \cdot s^{-1}$)	Reach 4	No flow	0.26 ± 0.03	0.26 ± 0.06	0.05 ± 0.02	0.15 ± 0.03
	Reach 3	0.27 ± 0.02	0.34 ± 0.02	0.21 ± 0.04	0.17 ± 0.03	0.2 ± 0.03
	Reach 2	0.42 ± 0.05	0.35 ± 0.02	0.42 ± 0.05	0.15 ± 0.03	0.22 ± 0.06
	Reach 1	Not measured	Not measured	Not measured	Not measured	0.18 ± 0.05
	Yalakom River	Not measured	Not measured	Not measured	0.20*	0.17 ± 0.03

3.1.2. Wetted habitat area

Wetted habitat area was a logarithmic function of site-specific flow in all reaches (Figure 3.3). Without correction for reach length, the curves show wetted areas in Reach 3 > Reach 2 > Reach 4 (Figure 3.3 A). With correction for reach length, the curves show smaller wetted areas per km in Reach 3 than in Reaches 2 and 4 for a given flow (Figure 3.3 B). This difference was due to greater confinement of the channel in the Reach 3 canyon than in the other reaches. Given that wetted

area was measured over different ranges of flows between reaches, change in wetted area among flows was only comparable between reaches where flows were the same: 5 – 15 $m^3 \cdot s^{-1}$. Application of the models in Figure 3.3 showed that this 300% increase in flow (5 – 15 $m^3 \cdot s^{-1}$) produced an increase in wetted area of 9.3% in Reach 2, 14.5% in Reach 3, and 17.2% in Reach 4.

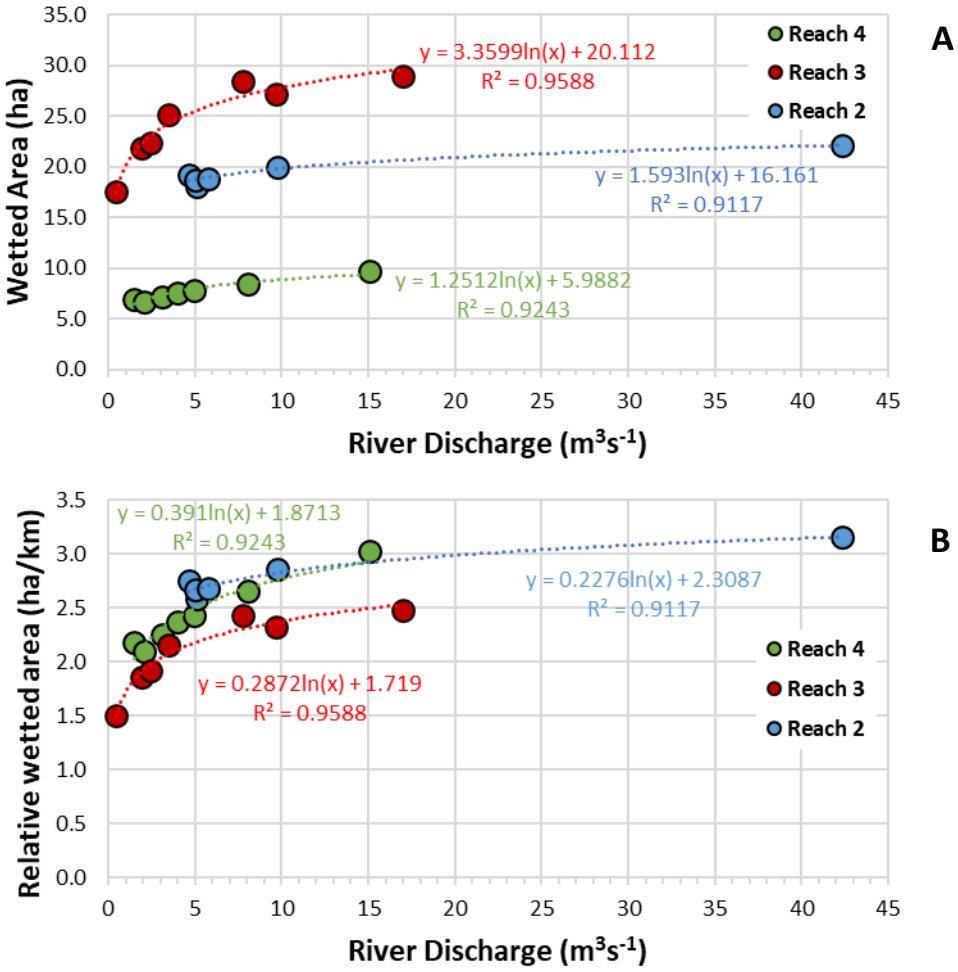

Figure 3.3 Relationships between river discharge and wetted habitat area, by reach, (A) and between discharge and relative wetted area (wetted area divided by reach length) (B) in the lower Bridge River.

3.1.3. Sediment Particle Size Distribution

The median particle size of river substrata (D50) measured in 2019 was 11.7 cm in Reach 4, declining to 7 cm in Reach 1. These sizes were larger than the 3.5 cm size measured in the Yalakom River.

Table 3.2 Sediment particle size summarized as D50 among sites within the Lower Bridge River reaches and the Yalakom River (measured in 2019).

Reach number	D50 mean ± standard error of arithmetic mean in 2019 (cm)
Reach 4	11.7 ± 0
Reach 3	7.6 ± 0.6
Reach 2	9.1 ± 0.2
Reach 1	7.0 ± 0.6
Yalakom River	3.5 ± 0.4

3.1.4. River Stage

Relative stage levels across the year varied among locations according to proximity to the dam, the attenuation of tributary inflows and the degree of channel confinement at each monitored location (Figure 3.4).

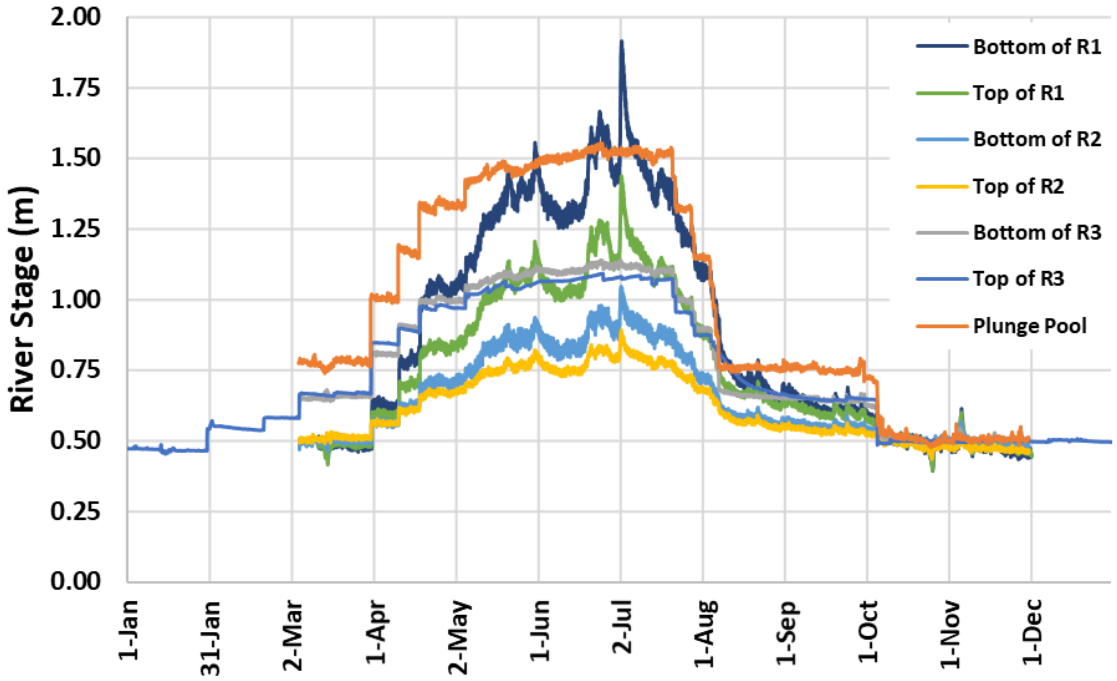

Figure 3.4 Relative river stage levels (m) according to location in the Lower Bridge River in 2020.

For reaches 3 and 4 (i.e., upstream of the Yalakom River confluence), the stage elevation changes tracked with the timing and shape of the flow release hydrograph quite closely and the Plunge Pool site was the most sensitive to flow changes from the dam (mean stage change = 7.3 cm for every 1 $m^3 \cdot s^{-1}$ flow change under the 2020 hydrograph at this location (Table 3.3). The stage elevation changes at the top and bottom of Reach 3 were lower and very similar at both locations

(i.e., 3.8 cm and 3.5 cm per 1 $m^3 \cdot s^{-1}$ flow change, respectively). The river stage profiles for monitoring locations in reaches 1 and 2 closely followed the discharge profile of the Yalakom River, reflecting the dominant influence of this major inflow source in the lower reaches under the Trial 2 flow release hydrograph. The mean stage change was <3 cm per 1 $m^3 \cdot s^{-1}$ flow change at all monitoring locations below the Yalakom confluence (i.e., 1.0, 1.2, 2.0, and 2.9 cm per 1 $m^3 \cdot s^{-1}$ flow change at the top and bottom of Reach 2 and Reach 1, respectively). The slightly higher values in Reach 1 (relative to Reach 2) are likely due to greater channel confinement at the monitoring locations in this reach.

Table 3.3 Summary of flow changes, stage changes and rate of stage change per flow increment at various locations in the Lower Bridge River under the Trial 2 Hydrograph in 2020.

Location	River km	Site-specific Discharge ($m^3 \cdot s^{-1}$)			Site-specific Stage (m)			Mean Stage Change per Flow Increment ($cm/m^3 \cdot s^{-1}$)
		Min.	Max.	Diff.	Min.	Max.	Diff.	
Plunge Pool	40.9	1.4	15.7	14.2	0.50	1.54	1.04	7.3
Top of Reach 3	36.8	1.6	17.0	15.4	0.50	1.09	0.59	3.8
Bottom of Reach 3	26.1	1.9	19.4	17.5	0.51	1.13	0.62	3.5
Top of Reach 2	23.6	4.1	44.9	40.8	0.45	0.87	0.42	1.0
Bottom of Reach 2	20.0	4.4	48.9	44.5	0.47	1.02	0.55	1.2
Top of Reach 1	11.3	4.7	52.3	47.6	0.43	1.40	0.97	2.0
Bottom of Reach 1	3.9	4.9	53.9	49.0	0.43	1.86	1.43	2.9

Specific stage changes associated with flow ramp down events at Terzaghi Dam are discussed further in Section 3.5.

3.1.5. Water Temperature

Relative to the Pre-flow period (Trial 0), dam releases have caused water temperatures to be cooler in the early spring period (Mar-Apr), and warmer throughout the fall (Figure 3.5). These effects were most evident in reaches 4 and 3, with a gradient of effect among stations associated with proximity to the dam. In addition to continuation of these effects, Trial 3 flows from 2016 to 2018 were also characterized by warmer temperatures in January and February, and during the period of the year when the high flows were delivered, typically from May to July. The flow release in 2019 and 2020 followed the Trial 2 hydrograph and the temperature profiles by reach generally followed the patterns observed in 2011-2015. However, there were a few exceptions: the temperatures in winter 2019 (i.e., January to March) were among the lowest of the range for the Trial 2 hydrograph and temperatures in summer 2019 and 2020 (i.e., June to September) were among the highest of the Trial 2 range (Appendix D). There was also a period of warmer water temperatures in September 2020 that was particularly evident in reaches 3, 2 and 1.

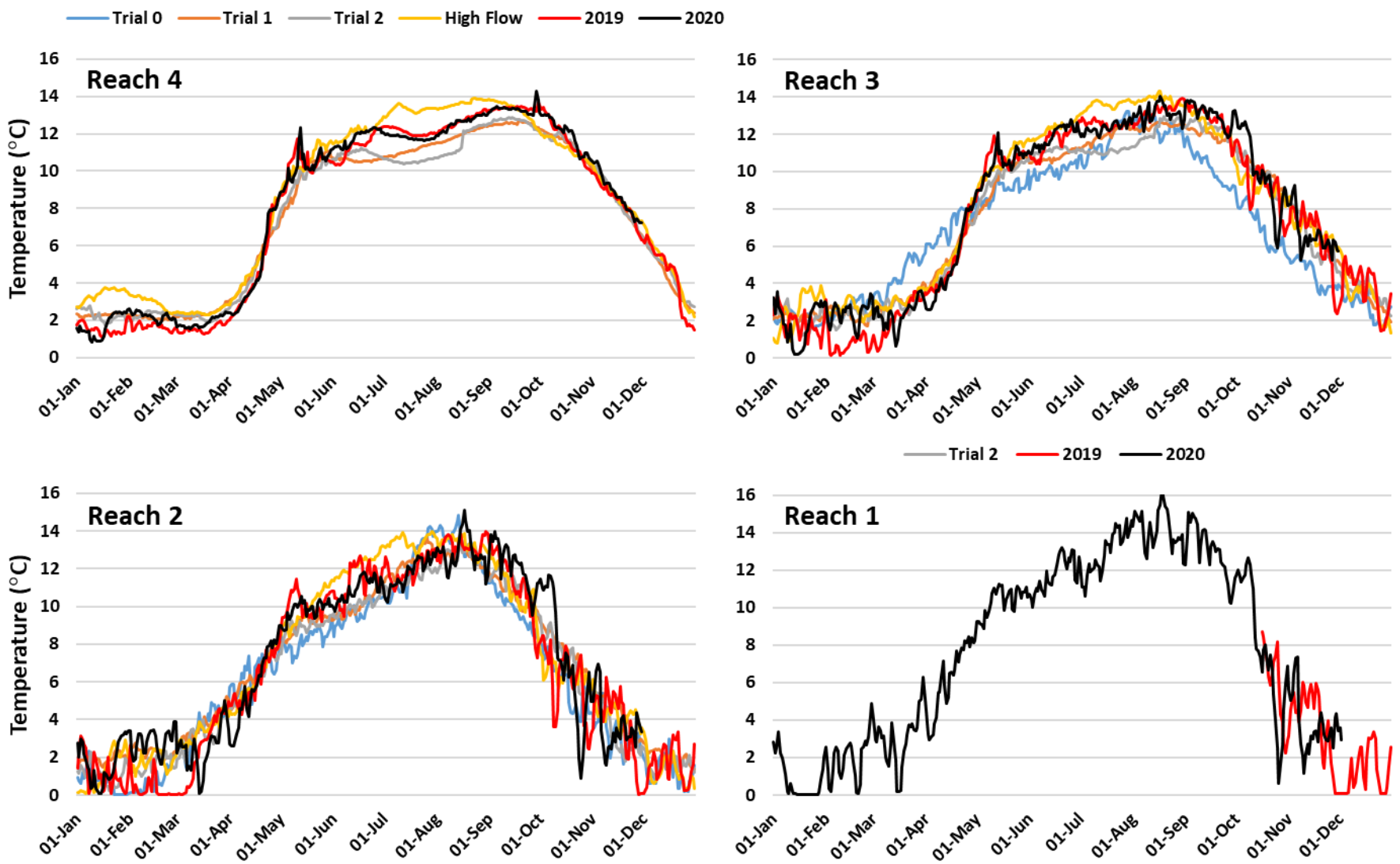

Figure 3.5 **Mean daily water temperatures during Trial 0 (pre-flow), Trial 1 (3 $m^3 \cdot s^{-1}$), Trial 2 (6 $m^3 \cdot s^{-1}$), High Flow years (2016-2018), and the Post-High Flow years (2019, 2020) for Reach 4 (top left), Reach 3 (top right), Reach 2 (bottom left) and Reach 1 (bottom right). Note the temperature loggers in Reach 1 were installed on 16 October 2019.**

Due to the influence of tributary inflows (particularly the Yalakom River at the top of Reach 2), water temperatures tended to be more widely variable on a day-to-day basis in the lower reaches.

The cause of the cooler water temperatures in February 2019 and the warmer temperatures in September 2020 were likely due to ambient temperature influence since these effects were apparent in most of the reaches and the Yalakom River (Appendix D). Mean monthly air temperatures were colder in February 2019 and warmer in September 2020 than they were in those months during the previous flow treatment periods (Table 3.4; Data provided by Environment Canada).

Table 3.4 Mean monthly air temperatures for Lillooet, BC summarized by LBR flow trial/period (data provided by Environment Canada).

Flow Period	Mean Monthly Air Temperatures (± SD)												Period Average
	Jan	Feb	Mar	Apr	May	Jun	Jul	Aug	Sep	Oct	Nov	Dec	
Trial 0	-1.8 (±3.0)	3.4 (±0.2)	5.8 (±1.1)	10.4 (±0.6)	15.4 (±3.0)	19.2 (±1.7)	22.4 (±3.2)	23.0 (±1.1)	17.9 (±1.6)	9.5 (±0.5)	4.6 (±0.5)	0.7 (±1.4)	10.9 (±0.8)
Trial 1	-1.6 (±2.0)	1.3 (±1.3)	5.3 (±2.2)	10.3 (±1.3)	15.2 (±1.2)	19.4 (±1.5)	23.4 (±1.2)	22.0 (±0.9)	16.9 (±1.2)	9.7 (±0.9)	2.8 (±2.9)	-2.3 (±2.9)	10.2 (±0.4)
Trial 2	-1.1 (±1.5)	1.3 (±3.4)	5.8 (±1.9)	10.0 (±1.0)	15.6 (±1.7)	19.5 (±1.9)	23.5 (±1.9)	22.9 (±0.6)	17.6 (±1.5)	10.5 (±1.3)	2.1 (±0.8)	-0.4 (±0.6)	10.6 (±0.7)
Trial 3	-2.2 (±1.6)	0.6 (±2.9)	6.3 (±1.6)	11.3 (±2.4)	17.3 (±1.6)	19.9 (±0.7)	23.2 (±1.4)	22.7 (±1.3)	16.2 (±1.9)	8.9 (±0.7)	4.8 (±2.0)	-2.4 (±3.1)	10.6 (±0.5)
2019	0.6	-6.4	5.2	10.2	18.0	19.6	21.4	22.7	16.9	8.7	3.4	0.1	10.0
2020	-1.4	2.9	4.8	10.0	16.3	18.3	22.0	22.4	19.2	9.9	3.8	1.4	10.8

The warmer water temperatures during the June to August period in 2019 and 2020 may be due to upstream operations as the effect was also observed during the other modified operations years (2016-2018) and ambient temperatures were not notably warmer during this period than in the previous flow trials. These warmer summer water temperatures were likely caused by: 1) higher conveyance of water through Terzaghi Dam, which may affect draw from the various thermal layers in Carpenter Reservoir (high flow years only); 2) deeper drawdown of Carpenter Reservoir in the spring, which reduces the depth of water above the intake for the low-level outlet (observed in 2017 to 2020); or 3) some combination of 1) and 2). The CE-QUAL temperature model developed for Carpenter Reservoir under BRGMON-10 could be consulted to better understand the relationship between reservoir operation and release temperatures. However, the analyses required to determine the cause and mechanism of the observed effects were beyond the scope of this report.

Mean water temperature during the periphyton and benthic invertebrate sampling periods declined upstream to downstream (Table 3.5). Relatively high temperatures in Reach 4 during fall were due to the release of warm hypolimnetic water from Carpenter Reservoir caused by mixing of epilimnetic water that had temperatures exceeding 20°C and cooler hypolimnetic water in the

fall (Limnotek 2019). The water cooled with downstream flow. Water temperature was relatively consistent among trials in a given reach except in reaches 2 and 3 during Trial 2 and the High Flow years. Mean water temperatures for the sampler colonization period were lower due to later installation of the plates and baskets in those years, which affected these reaches more than Reach 4 because the tributary inflows are cooling rapidly across this seasonal period (and there are no year-round tributary inflows to Reach 4).

Table 3.5 Mean temperature values ± standard error by reach and trial for the periphyton and benthic invertebrate sampling periods.

Reach	Mean temperature ± standard error of arithmetic mean				
	Trial 0 (May 1996 – Jul 2000)	**Trial 1 (Aug 2000 – Mar 2011)**	**Trial 2 (Apr 2011 – Dec 2015)**	**High Flow Years (2016 – 2018)**	**Post-High Flow Years (2019 – 2020)**
Reach 4	No flow	10.8 ± 0.3	10.0 ± 0.2	10.2 ± 0.3	10.9 ± 0.3
Reach 3	10.2 ± 1.2	10.7 ± 0.5	8.1 ± 0.4	8.3 ± 0.6	9.0 ± 0.6
Reach 2	9.3 ± 1.0	9.6 ± 0.8	5.6 ± 0.3	5.9 ± 0.3	6.0 ± 0.3
Reach 1	Not measured				6.3 ± 0.6
Yalakom R.	4.7 ± 0.3	4.7 ± 0.1	4.6 ± 0.6	4.1 ± 0.0	4.7 ± 0.4

Water temperatures during the early part of the salmon incubation period in fall (i.e., Sep to Dec) have been elevated during all flow trial years (2000 to 2020) by up to 4°C at the top of Reach 3 (relative to the pre-flow period - Trial 0). Differences among the flow trials during that seasonal period were small, as were differences among years within trials (refer to Reach 4 figure in Appendix D). Release flows among all flow trial years have been very similar across the fall period (3.0 $m^3 \cdot s^{-1}$ in Sep; and between 1.5 and 2.0 $m^3 \cdot s^{-1}$ from Oct to Dec in all cases – Figure 1.3 in Section 1.3). Changes to the thermal regime have caused large differences in the timing of juvenile salmon emergence from the spawning beds (based on modelled ATU data and qualitative sampling observations). Prior to the flow release the predicted median date of both coho and Chinook salmon fry emergence was late April or early May, with a trend to slightly later timing at downstream sites due to the cooling of water as it flows downstream in the fall months when air temperatures are falling (Figure 3.6). The estimated peak spawning dates for Chinook and coho salmon were September 8 and November 15, respectively, based on observations made during streamwalk surveys conducted as part of BRGMON-3 (White et al. 2018).

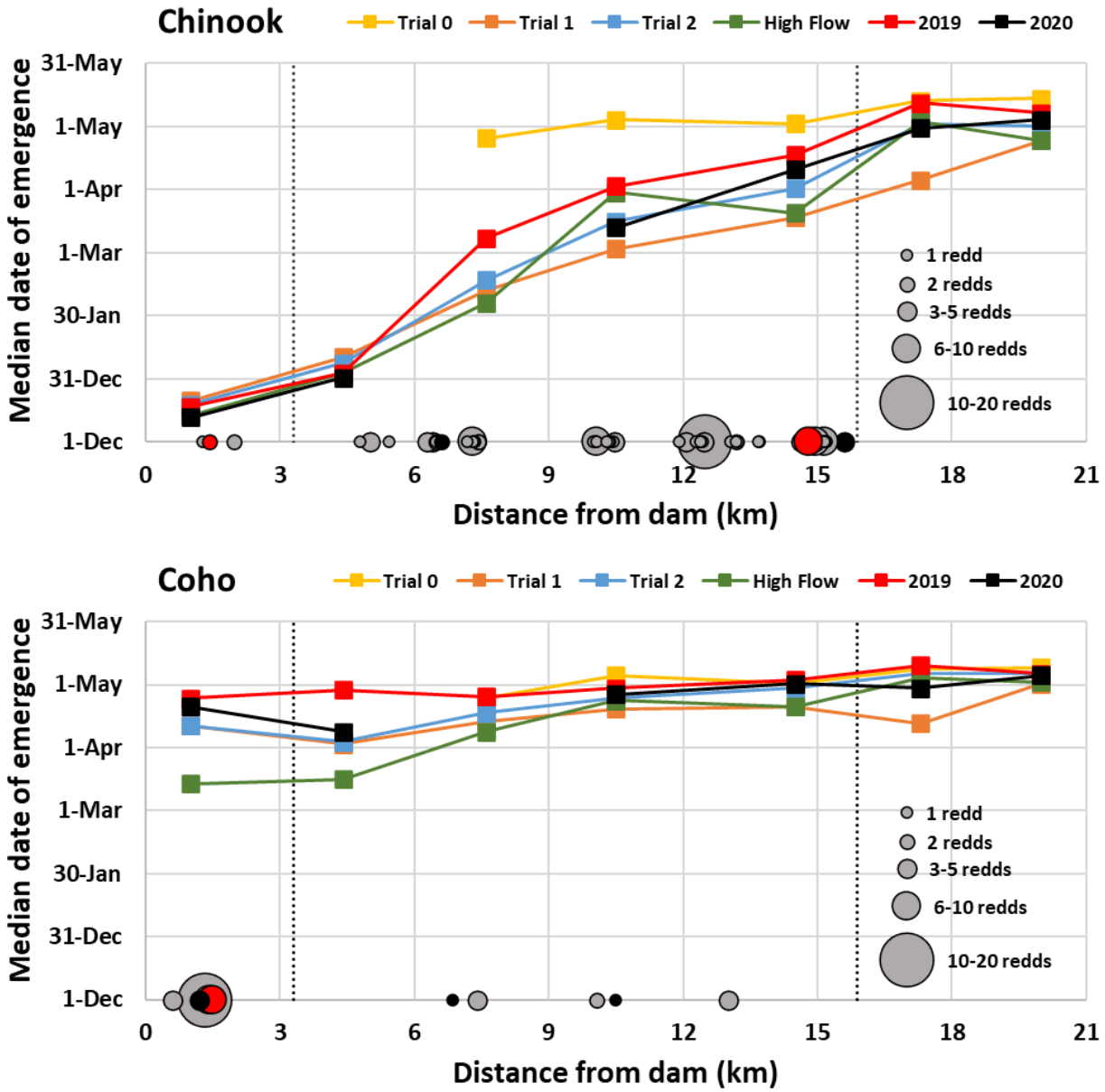

Figure 3.6 **Modelled median emergence dates for Chinook (top) and coho (bottom) fry at varying distances below Terzaghi Dam based on observed daily mean temperatures for each flow treatment. The vertical dotted lines indicate the location of reach breaks. The locations of redds observed for each species during the available period (2014 - 2020) are represented by the dots along the x-axis on each plot (data provided by BRGMON-3). The colour of dot reflects the period (black = 2020; red = 2019; grey = 2014-2018) and the size of dot indicates the relative number of redds at each location.**

As noted above, there is a gradient of temperature across the length of the study area during fall, and this gradient influences the predicted timing of emergence according to distance from the dam (Figure 3.6), particularly for Chinook (due to their earlier spawn timing in the fall). For both

Chinook and coho, the predicted emergence timing at each monitoring location in 2020 was very similar to the average estimates for Trial 2 (black and blue points in Figure 3.6). The predicted timing for Chinook in 2019 at sites 7.6 km, 10.5 km and 14.5 km downstream of the dam (in Reach 3) was approx. 2 weeks later than the Trial 2 average because of the colder water temperatures in February that year (see Figure 3.5). Alevins incubating closer to the dam emerged in December and January so their emergence timing was not influenced by the cold spell in February 2019.

Since location-specific spawning information became available starting in Trial 2 (collected under BRGMON-3), Chinook and coho spawners have utilized spawning areas in both reaches 3 and 4, but the distribution of redds among those reaches has been different for the two species (Figure 3.6 and Table 3.6). The total number of Chinook redds observed from 2014 to 2020 was 138. Five percent of the total (*n*= 7) were observed in Reach 4, and the remaining 95% (*n*= 131) were distributed across Reach 3. Based on these findings, and assuming equivalent survival among locations, approx. 5% of the spawned eggs would have been associated with a predicted median emergence (PME) timing of mid-December (near temperature monitoring site A), and a further 24% would have had a PME timing between early January and mid February (near sites B and C). The remaining 71% would have had a PME of mid- March to early April in the bottom portion of Reach 3.

In 2019 and 2020, only eight redds and five redds were observed, respectively, for Chinook although spawning distributions and collection of these data were affected by the operation of a broodstock collection fence installed early in the spawning period at the bottom of Reach 3 (White et al. 2021). Of the observed redds in these two years, 15% (*n*= 2) were observed in Reach 4, 15% (*n*= 2) were observed in the upper portion of Reach 3, and 70% (*n*= 6) were observed at the bottom of Reach 3 near the fence. It is also important to note that, due to the effects of the Big Bar slide on Chinook migration in the Fraser River (upstream of the Bridge River confluence), there was likely an increased incidence of straying into the Bridge River by Chinook from other populations in 2019 and 2020.

Observations for coho redd locations were available for 2018 to 2020, and the total number of coho redds observed in those years was 44 (2018 *n*= 31; 2019 *n*= 6; 2020 *n*= 7). Unlike Chinook, a much higher proportion of coho spawning was observed in Reach 4 (73%), with an associated PME timing of mid- April for this species. The remaining 27% of redds were observed in Reach 3 with corresponding PME timing between 17 and 29 April, according to location (Table 3.6).

Table 3.6 Proportion of Chinook and coho spawning, according to observed redd locations (2014 to 2020), by distance from dam and predicted median emergence timing in reaches 3 and 4.

Species	Reach	Station (Rkm)	Dist. From Dam (km)	Predicted Median Emergence Date	*n*	Percentage of observed redds [a,b]
Chinook	4	A (39.9)	1.0	16-Dec	7	5% (5%)
	3	B (36.5)	4.4	3-Jan	17	12% (17%)
		C (33.3)	7.6	20-Feb	17	12% (30%)
		D (30.4)	10.5	24-Mar	54	39% (69%)
		E (26.4)	14.5	5-Apr	43	31% (100%)
Coho	4	A (39.9)	1.0	10-Apr	32	73% (73%)
	3	B (36.5)	4.4	8-Apr	0	0% (73%)
		C (33.3)	7.6	17-Apr	5	11% (84%)
		D (30.4)	10.5	27-Apr	3	7% (91%)
		E (26.4)	14.5	29-Apr	4	9% (100%)

[a] Values in brackets represent the cumulative percentage of redds observed at, and upstream of, each station.

[b] Values for coho are based on data collected in 2018-2020 only, as these were the only years of redd count data available for this species.

3.1.6. Turbidity

Turbidity in 2020 for each of the six stations with a RBR logger (Plunge pool, Boundary, Fish fence, Yalakom, Camoo, and Bridge) is shown in Figure 3.7.

Turbidity at the Plunge pool, Fish fence, and Camoo showed “flat lining” at 22 NTU as early as March and it continued through July. This error occurred when turbidity bridged 22 NTU. Consultation with RBR staff in May 2020 about similar observations in 2019 data showed this anomaly was due to an error in firmware that affected the instrument auto-ranging calculations. A fix was supplied by RBR, but it could not be installed until the loggers could be safely removed from the river at low flow in August 2020. Once the fix was applied and the loggers were re-installed, no flat lining occurred.

Despite data corrections that were described in Section 2.2.6, some turbidity spikes (a high value not found 10 minutes before and after the anomaly) were found at all stations (Figure 3.7). These artifacts are common, even with the sensor wiping, and are not part of time course turbidity variability. The more densely packed values that represent a narrow band of variability related to the 10-minute frequency of logging represented actual turbidity.

With consideration of the firmware errors, corrections to those errors, and removal of anomalies, the following time course changes in turbidity were found in 2020 (Figure 3.7). In March and early April, turbidity was <10 NTU in all reaches, which is related to winter conditions before snowmelt and before filling of Carpenter Reservoir. Turbidity increased in April as watershed snowmelt began. Most data from the spring were not useable because of the firmware error (flatlining

during bridging at 22 NTU) but a spring peak was expected based on known spring peaks in hypolimnetic turbidity in Carpenter Reservoir of 30-40 NTU (Limnotek 2019).

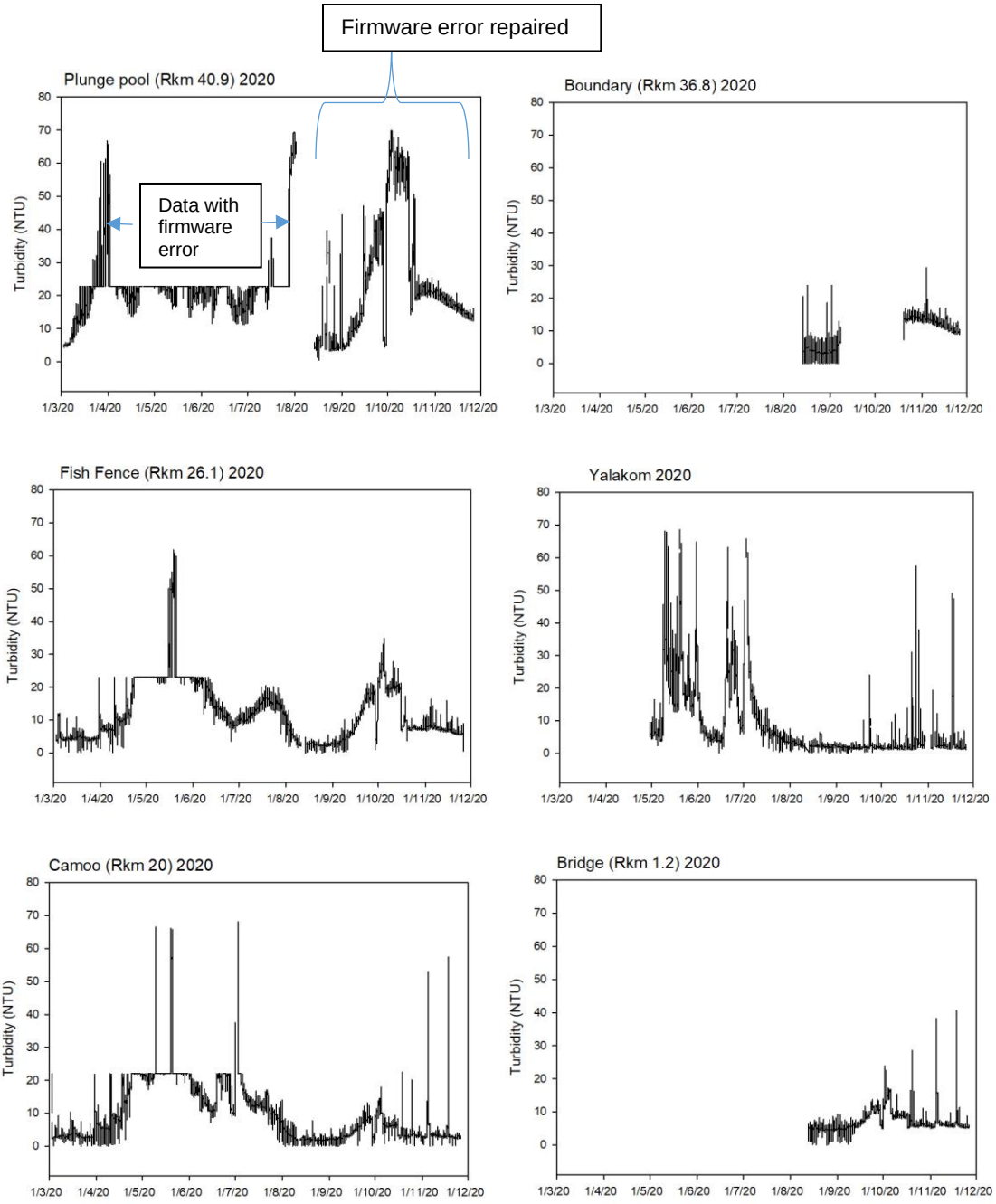

Figure 3.7 Turbidity in 2020 at sites from the dam plunge pool downstream to the bridge near the confluence with the Fraser River and in the Yalakom River. Firmware errors found in March through July were corrected in August (see Plunge pool image for notation). These errors and fixes occurred at the Plunge pool, Fish fence, and Camoo. Only values <22 NTU were reliable at these sites in the affected period of March through July.

In June, both the Bridge River and Yalakom River turbidity declined to values <20 NTU. A secondary peak close to 20 NTU in the Bridge River and 30-40 NTU in the Yalakom River occurred in July with much greater variability in the Yalakom than in the Bridge River. This was likely related to the second, higher discharge peak in the Yalakom and other tributaries in July (see Figure 3.1 in Section 3.1.1). Lower turbidity of <10 NTU was found in August at all locations. It stayed at that level in the Yalakom River with episodic higher turbidity possibly associated with precipitation events in the watershed. In the Bridge River, turbidity in September and October increased to values near 60 NTU in water released from the dam and 20-30 NTU further downstream but upstream of the Yalakom confluence. While an increase in turbidity was found downstream of the Yalakom inflow, it was about half that found upstream of the confluence due to dilution from low turbidity in the Yalakom. This increase in turbidity in the Bridge River in the early fall is due to mixing in Carpenter Reservoir that produces turbidity of 40 NTU or higher in the hypolimnetic water that is released to the Bridge River, which is more than double the values occurring in summer (Limnotek 2019). In November and December turbidity declined from 20 NTU to 10 NTU in Reach 4 while values were consistently <10 NTU further downstream.

3.1.7. Water Chemistry

Total alkalinity and pH increased upstream to downstream in all trials (Table 3.7). This pattern showed inorganic carbon was added to the Bridge River with distance from the Terzaghi Dam. The tributaries were a major source of that alkalinity (a Values with a "≤" symbol were at or below the detection limit.

Table 3.8). At the pH's of 7.5 to 8.1 found among all tributaries, mainstem reaches, and trials, bicarbonate (HCO_3) was the expected dominant form of inorganic carbon (Stumm and Morgan 1996). Separate measurements of bicarbonate, carbonate, and hydroxide alkalinity (data not shown) confirmed bicarbonate dominance.

Total dissolved solids (TDS) have been measured infrequently during the project despite its importance for interpreting chemical conditions. Routine measurement during the post – High Flow Years (2019 and 2020) showed increasing TDS upstream to downstream, with tributaries being an important source which is consistent with addition of bicarbonate as inferred from alkalinity and pH. Addition of major base cations may also have contributed to this pattern.

With one exception, DIN concentrations (sum of NO_3-N and NH_4-N) increased upstream to downstream (Table 3.7). The exception was during Trial 0 when Bridge River flow upstream of the Yalakom confluence was limited to cumulative seepage. DIN was mainly comprised of NO_3-N in Trial 0 and the High Flow Years but during Trials 1 and 2, NH_4-N and NO_3-N concentrations were about the same, mainly in Reaches 3 and 2. Tributaries flowing into Reach 3 were an important source of the NO_3-N but the small tributary in Reach 2 (Antoine Creek) had very low concentrations of NO_3-N, indicating unusual demand for or loss of N in that stream. The loading of NO_3-N from tributaries in Reach 3 combined with that from the Yalakom River were the primary sources of NO_3-N in Reach 3 and Reach 2.

Table 3.7 Bridge River mainstem and Yalakom River mean chemical concentrations or values ± standard error of the arithmetic mean by reach and trial.

Chemical variable and units	Reach	Mainstem Bridge River and Yalakom River mean value ± standard error of arithmetic mean [a]				
		Trial 0 (May 1996 – Jul 2000)	Trial 1 (Aug 2000 – Mar 2011)	Trial 2 (Apr 2011–Dec 2015)	High Flow Years (2016 – 2018)	Post High Flow Years (2019 – 2020)
Total alkalinity ($mg \cdot L^{-1}$ as $CaCO_3$)	Reach 4	No flow	56.1 ± 0.7	42.4 ± 4.4	28.2 ± 0.3	30.3 ± 3.3
	Reach 3	168 ± 3.5	72.4 ± 0.9	55.3 ± 3.0	41.2 ± 0.9	38.8 ± 1.9
	Reach 2	192 ± 2.6	140.7 ± 1.2	110.6 ± 8.5	85.6 ± 0.3	87.5 ± 6.0
	Reach 1	Not measured	Not measured	Not measured	Not measured	84.1 ± 2.1
	Yalakom River	Not measured	Not measured	Not measured	113 ± 0	106 ± 3.8
pH	Reach 4	No flow	7.5 ± 0.05	7.6 ± 0.06	7.7 ± 0.008	7.5 ± 0
	Reach 3	8.1 ± 0.03	7.5 ± 0.02	7.7 ± 0.02	7.8 ± 0.02	7.6 ± 0
	Reach 2	8.1 ± 0.03	7.8 ± 0.03	8.0 ± 0.02	8.1 ± 0.005	8.0 ± 0
	Reach 1	Not measured	Not measured	Not measured	Not measured	8.1 ± 0
	Yalakom River	Not measured	Not measured	Not measured	8.2 ± 0	8.0 ± 0
Total dissolved solids ($mg \cdot L^{-1}$)	Reach 4	Not measured	63.7 (no replicates)	Not measured	Not measured	53.5 (no replicates)
	Reach 3	103 ± 2.7	54.8 ± 2.6	Not measured	Not measured	64.4 ± 4.0
	Reach 2	103 ± 1.2	89.5 ± 2.6	Not measured	Not measured	131 ± 19.8
	Reach 1	Not measured	Not measured	Not measured	Not measured	118 ± 2.2
	Yalakom River	Not measured	Not measured	Not measured	Not measured	127 ± 0
NH_4-N ($\mu g \cdot L^{-1}$)	Reach 4	No flow	5.4 ± 0.6	11.0 ± 2.3	5.5 ± 0.3	7.4 ± 0.4
	Reach 3	6.1 ± 0.5	28.4 ± 4.3	57.8 ± 10.0	5.8 ± 0.2	15.9 ± 4.9
	Reach 2	8.2 ± 0.6	50.8 ± 8.0	70.2 ± 16.1	5.4 ± 0.2	17.6 ± 1.4
	Reach 1	Not measured	Not measured	Not measured	Not measured	17.3 ± 3.6
	Yalakom River	Not measured	Not measured	Not measured	<5.0	10.1 ± 2.9
NO_3-N ($\mu g \cdot L^{-1}$)	Reach 4	No flow	19.0 ± 1.3	17.6 ± 2.2	10.2 ± 0.7	12.6 ± 0.6
	Reach 3	39.2 ± 4.5	30.5 ± 1.8	68.9 ± 7.5	20.9 ± 1.3	29.5 ± 7.3
	Reach 2	23.6 ± 1.6	46.9 ± 3.5	81.0 ± 7.4	49.6 ± 0.8	61.4 ± 8.4
	Reach 1	Not measured	Not measured	Not measured	Not measured	46.8 ± 6.4
	Yalakom River	Not measured	Not measured	Not measured	76.5 ± 0	65.7 ± 3.6
DIN ($\mu g \cdot L^{-1}$)	Reach 4	No flow	24.4 ± 1.6	28.6 ± 3.8	15.7 ± 0.7	20 ± 0.2
	Reach 3	45.3 ± 4.6	58.9 ± 5.8	126.7 ± 17	26.7 ± 1.3	45.4 ± 12.1
	Reach 2	31.8 ± 1.8	97.6 ± 10.9	151.2 ± 22.6	55.0 ± 0.7	78.9 ± 9.8
	Reach 1	Not measured	Not measured	Not measured	Not measured	64.0 ± 9.7
	Yalakom River	Not measured	Not measured	Not measured	81.5 ± 0	75.8 ± 0.7
SRP ($\mu g \cdot L^{-1}$)	Reach 4	No flow	3.1 ± 0.2	2.7 ± 0.2	1.5 ± 0.2	1.5 ± 0.5
	Reach 3	3.5 ± 0.1	6.6 ± 0.9	10.2 ± 1.4	1.7 ±0.1	4.7 ± 1.6
	Reach 2	3.7 ± 0.4	9.5 ± 1.7	9.2 ± 2.2	1.1 ± 0	2.5 ± 0.9
	Reach 1	Not measured	Not measured	Not measured	Not measured	3.8 ± 0.9
	Yalakom River	Not measured	Not measured	Not measured	≤1.0	1.1 ± 0.1

[a] Values with a "≤" symbol were at or below the detection limit.

Table 3.8 Mean chemical concentrations or values ± standard error in Bridge River tributaries partitioned within mainstem reaches by reach and trial. Reach 4 is omitted because no tributaries flow into that reach.

Chemical variable and units	Reach receiving flow from sampled tributaries	Mean concentration or value ± standard error of arithmetic mean among tributaries [a]				
		Trial 0 (May 1996 – Jul 2000)	Trial 1 (Aug 2000 – Mar 2011)	Trial 2 (Apr 2011–Dec 2015)	High Flow Years (2016 – 2018)	Post High Flow Years (2019 – 2020)
Total alkalinity ($mg \cdot L^{-1}$ as $CaCO_3$)	Reach 3	214 ± 11	211 ± 5.4	161 ± 9.5	117 ± 5.4	118 ± 6.0
	Reach 2	351 ± 54	334 ± 15	238 ± 26	183 ± 19	181 ± 20
	Reach 1	Not measured	Not measured	Not measured	Not measured	170 ± 19
pH	Reach 3	8.0 ± 0.05	8.0 ± 0.03	8.2 ± 0.02	8.2 ± 0.02	8.1 ± 0.03
	Reach 2	8.2 ± 0.02	8.0 ± 0.03	8.2 ± 0.02	8.3 ± 0.02	8.2 ± 0.03
	Reach 1	Not measured	Not measured	Not measured	Not measured	8.3 ± 0.05
Total dissolved solids ($mg \cdot L^{-1}$)	Reach 3	120 ± 7.7	128 ± 13.1	Not measured	Not measured	162 ± 12.4
	Reach 2	196 ± 32	209 ± 30	Not measured	Not measured	264 ± 29
	Reach 1	Not measured	Not measured	Not measured	Not measured	234 ± 18
Turbidity (NTU)	Reach 3	Not measured	Not measured	0.7 ± 0.08	0.5 ± 0.07	0.4 ± 0.17
	Reach 2	Not measured	Not measured	0.8 ± 0.2	0.5 ± 0.1	0.7 ± 0.3
	Reach 1	Not measured	Not measured	Not measured	Not measured	6.1 ± 2.6
NH_4-N ($\mu g \cdot L^{-1}$)	Reach 3	5.3 ± 0.6	3.8 ± 0.5	3.5 ± 0.3	≤5.0	7.5 ± 1.0
	Reach 2	7.2 ± 2.4	8.1 ± 1.0	7.0 ± 1.6	6.0 ± 0.5	6.0 ± 0.4
	Reach 1	Not measured	Not measured	Not measured	Not measured	8.6 ± 1.5
NO_3-N ($\mu g \cdot L^{-1}$)	Reach 3	102 ± 29	104 ± 13	225 ± 45	187 ± 40	156 ± 37
	Reach 2	4.8 ± 1.4	3.6 ± 0.5	14.8 ± 4.8	7.9 ± 1.3	6.7 ± 1.1
	Reach 1	Not measured	Not measured	Not measured	Not measured	20.5 ± 5.7
SRP ($\mu g \cdot L^{-1}$)	Reach 3	4.3 ± 0.5	2.4 ± 0.1	3.5 ± 0.3	3.0 ± 0.4	2.4 ± 0.4
	Reach 2	5.0 ± 1.0	2.2 ± 0.2	2.3 ± 0.3	1.3 ± 0.1	1.1 ± 0.1
	Reach 1	Not measured	Not measured	Not measured	Not measured	3.0 ± 0.8

[a] Values with a "≤" symbol were at or below the detection limit.

Relatively high NH_4-N concentrations in Reaches 2 and 3 during Trials 1 and 2 showed addition of reduced forms of nitrogen that would ultimately be oxidized to NO_3-N via nitrification given expected high oxygen saturation. Absence of disturbance and no forest silvicultural activities in the drainage of Reaches 2 and 3 eliminated an inorganic source of NH_4-N. Concentrations of NH_4-N less than 8.5 $\mu g \cdot L^{-1}$ in tributaries (a Values with a "≤" symbol were at or below the detection limit.

Table 3.8) were low as expected in the absence of landscape disturbance The prevalence of high mainstem NH_4-N concentrations in the mainstem during Trials 1 and 2 must have come from enrichment by organic matter containing nitrogen that did not occur or was less apparent in Trial 0 and during the High Flow Years and post – High Flow Years. In 2019 and 2020, the NH_4-N concentrations were 7 – 18 $\mu g \cdot L^{-1}$, which was up to 3 times greater than during the High Flow Years but about three times less than those during Trials 1 and 2. These 2019 and 2020 NH_4-N

concentrations infer smaller organic nitrogen enrichment than during Trials 1 and 2 but more than in the High Flow Years.

SRP concentration differed by reach and trial (Table 3.7). SRP in Reach 4 declined over time from a peak of 3.1 $\mu g \cdot L^{-1}$ in Trial 1 to 1.5 $\mu g \cdot L^{-1}$ in 2019 and 2020 (Table 3.7 and Figure 3.8). In contrast, SRP concentration in Reach 3 increased between Trial 0 (3.5 $\mu g \cdot L^{-1}$) and Trial 2 (10.2 $\mu g \cdot L^{-1}$). Reach 3 values were several times greater than in Reach 4 in Trials 0 to 2, indicating addition of phosphorus in Reach 3. The tributaries flowing into Reach 3 carried low and consistent concentrations of SRP, eliminating them as a major source of phosphorus in Reach 3 at any time.

The greater SRP concentrations in Reach 3 compared to Reach 4 must have come from another mainstem specific source, such as spawning salmon during Trials 1 and 2. The same pattern occurred in Reach 2. Then during High Flow Years, mean SRP concentrations in both of reaches 3 and 2 declined to <2 $\mu g \cdot L^{-1}$, showing absence of phosphorus enrichment that was apparent during Trials 1 and 2. In the post – High Flow Years, SRP concentration in Reach 3 more than doubled that in High Flow Years while in Reach 4 the SRP concentrations were the same as during the High Flow Years (Figure 3.8). This increase in SRP concentration in the Post – High Flow Years compared to the High Flow Years did not come from tributaries because they carried relatively unchanged SRP concentrations over the same time periods (a Values with a "≤" symbol were at or below the detection limit.

Table 3.8). Reach 3 SRP concentrations were diluted by the Yalakom inflow that had some of the lowest SRP concentrations in the whole study area at any time. This mixing produced lower SRP concentrations in Reach 2 compared to Reach 3 during the High Flow Years and the post – High Flow Years. SRP concentrations in Reach 1 were marginally greater than those in Reach 2 during 2019 and 2020, the only years of chemical measurements in Reach 1, in part due to tributary inflows carrying relatively high SRP concentrations.

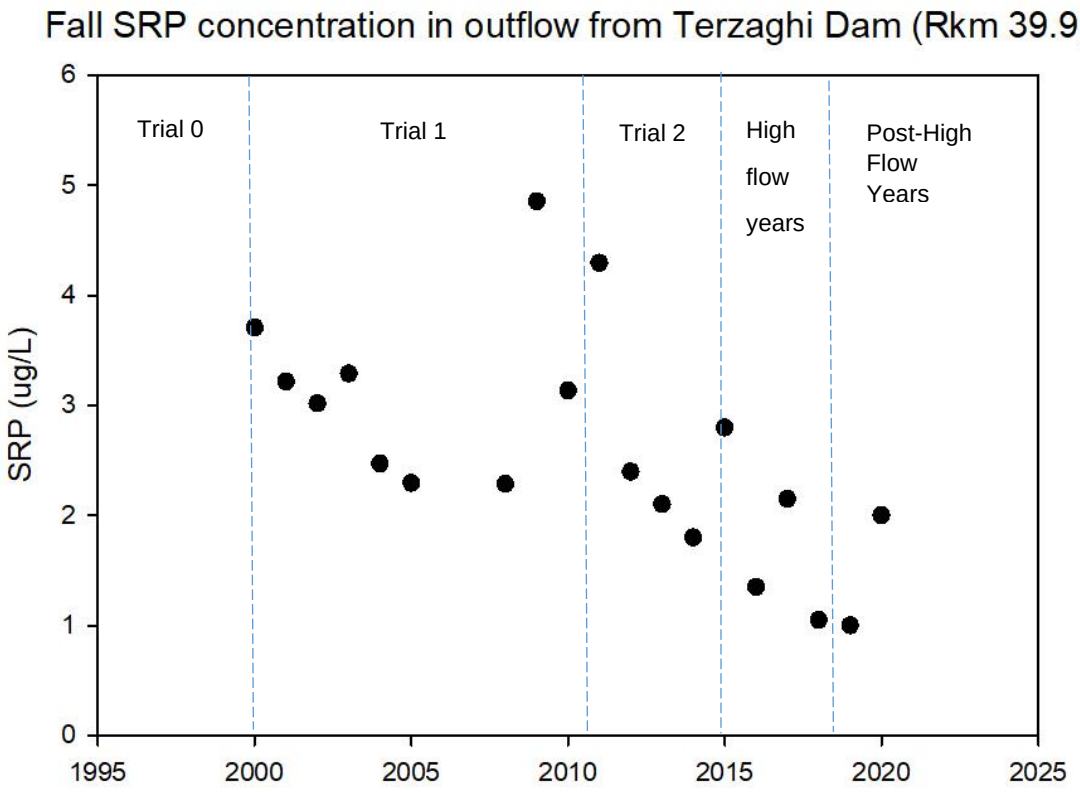

Figure 3.8 Fall SRP concentration in water released from Terzaghi Dam (Rkm 39.9) among years of all flow trials.

Relatively high mean SRP and NH_4-N concentrations in Reaches 3 and 2 during Trials 1 and 2 resulted from high concentrations in many of the odd years but low concentrations in even years (Figure 3.9). These interannual differences coincided with the timing of the pink salmon spawning runs that were dominant in odd years and absent in even years (Grant et al. 2014). The coincidences were pronounced in 2003, 2005, 2009, 2011, and 2013. Attempts were made to access DFO data describing the size of pink runs in this part of the Fraser River system (J. Harding, DFO, Kamloops, Pers. Comm.) but surprisingly nothing has turned up. These run size data would be advantageous to see if there is a correlation between run size and these odd year high SRP and NH_4-N concentrations in Reaches 2 and 3, where most of the pink spawning is thought to occur.

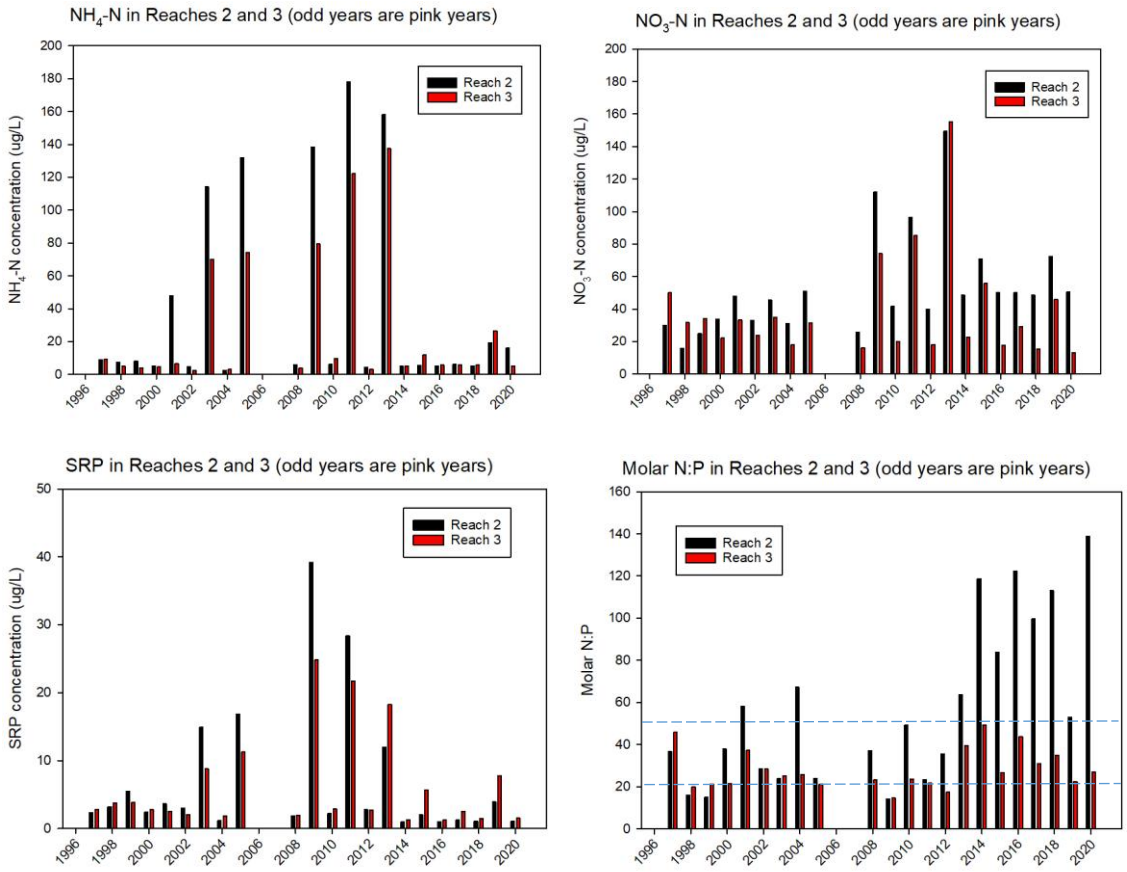

Figure 3.9 Concentration of NH_4-N (top left), NO_3-N (top right), and SRP (bottom left) with molar N:P (bottom right) among years in Reaches 2 and 3 with reference to pink salmon spawning in odd years. In the N:P figure, values above the top dashed line show potential P-limitation of algal growth; values below the bottom dashed line show potential N-limitation; values in between the dashed lines indicate potential co-limitation by N and P of algal growth.

The variation in DIN and SRP concentration produced shifts in potential limitation of benthic algal growth based on molar N:P ratios at different times and places (Figure 3.9, Figure 3.10). During Trial 0, the N:P was 20 - 30 in Reaches 3 and 2, the only reaches monitored at that time, showing co-limitation by N and P. During and after Trial 1, molar N:P remained about the same in Reach 3, again showing co-limitation by N and P. In contrast, N:P in Reach 2 increased during and after Trial 2, which showed a progressive time course increase in potential phosphorus deficiency. The Reach 2 N:P in 2020 was the highest measured since monitoring began in 1997 (Figure 3.9). It showed greatest potential phosphorus deficiency in Reach 2 on record in the Lower Bridge River, although still lower than in the Yalakom River (Figure 3.10).

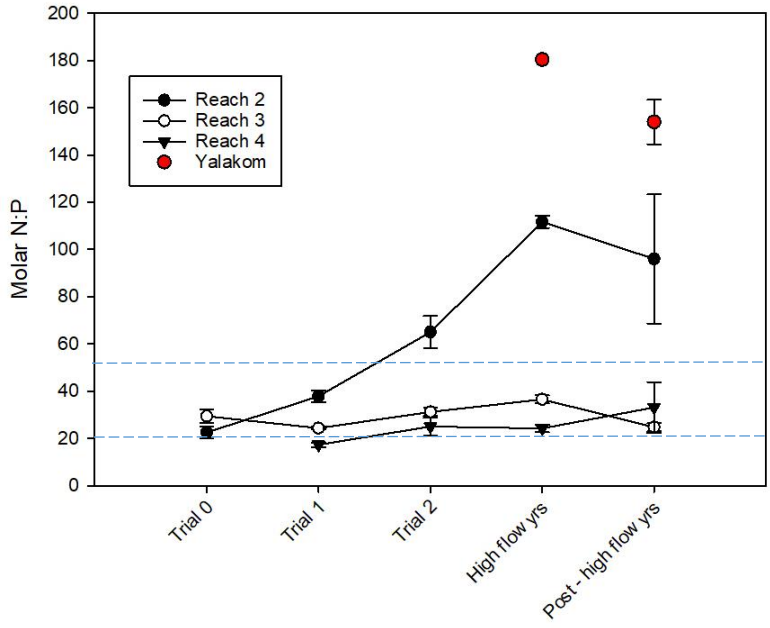

Figure 3.10 Mean molar N:P (±standard error) by reach among trials. N:P values above the top dashed line show potential P-limitation of algal growth. Values below the bottom dashed line show potential N-limitation. Values in between the dashed lines indicate potential co-limitation by N and P of algal growth.

3.2. Periphyton

Mean periphyton PB was 5.6 – 16.3 µg chl-a·cm^{-2} among Trials and Reaches (Figure 3.11). PB values were normally distributed so no transformations were applied prior to running the ANOVA's to test for Trial, Reach, and Pink effects. PB data for Reach 1 and the Yalakom River and for Trial 0 were excluded from the ANOVA because observations for those factor levels were incomplete among all combinations of Trial, Reach, and Pink. The ANOVA output is shown in Table 3.9. All interactions of the main effects were not significant ($p \geq 0.08$), which meant that Trial, Reach, and Pink effects on PB could be examined independently. No Pink effect on PB was found ($p=0.1$). PB in Reach 2 was significantly lower than in Reaches 3 and 4 among all Trials ($p=0.002$, Tukey pairwise contrast $p=0.002$ for Reach 2 x Reach 3 and $p=0.047$ for Reach 2 x Reach 4). There was a Trial effect on PB ($p=0.005$), entirely due to PB in the Post-High Flow years being greater than that in Trial 1 (Tukey $p=0.01$). There was no significant difference in PB between all other pairs of Trials (Tukey $p>0.05$).

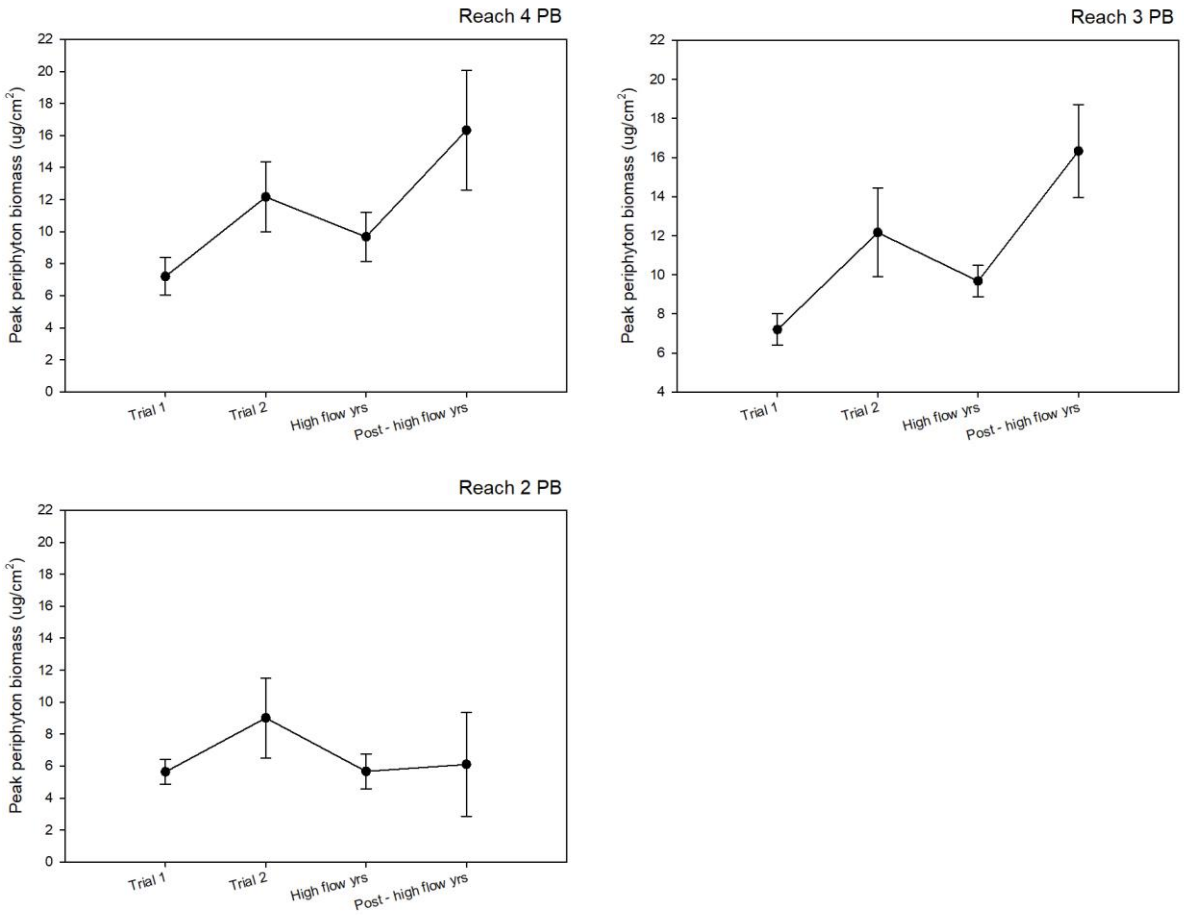

Figure 3.11 Mean periphyton peak biomass ± standard error of arithmetic mean by trial and reach. Years were replicates for calculation of the statistics.

Table 3.9 PB ANOVA table showing portioning of variance between main effects (trial, reach, pink) and residual variance (error). P values less than 0.05 showed a significant effect.

Source	Sums of squares	Degrees of freedom	Mean Squares	F-Value	p-Value
Trial	166.9	3	55.6	4.9	0.005
Reach	163.0	2	81.5	7.2	0.002
Pink	29.4	1	29.4	2.6	0.115
Trial*Reach	88.4	6	14.7	1.3	0.277
Trial*Pink	82.2	3	27.4	2.4	0.08
Reach*Pink	56.6	2	29.3	2.6	0.087
Trial*Reach*Pink	48.3	6	8.0	0.7	0.641
Error	440.1	39	11.3		

Periphyton biomass was measured in Reach 1 only during the Post-High Flow years. Table 3.10 shows mean PB with standard errors for the Yalakom River, Reach 2 and Reach 1. If we double the standard errors to arrive at approximately the 95% confidence interval, mean PB in Reach 1 was approximately the same as in Reach 2. This biomass was 10 times greater than upstream in the Yalakom River at the same time.

Table 3.10 Mean PB during Post – High Flow Years ± standard error in the Yalakom River and Reaches 2 and 1 of the Lower Bridge River.

Reach	Mean PB during Post – High Flow Years ± standard error
Yalakom River	0.92 ± 0.02
Lower Bridge River Reach 2	6.1 ± 3.2
Lower Bridge River Reach 1	11.7 ± 6.7

3.3. Benthic Invertebrates

Benthic invertebrates in the Lower Bridge River included Ephemeroptera (mayflies), Plecoptera (stoneflies), Tricoptera (caddisflies), Diptera (true flies, including chironomids) and "Other" taxa including Hemiptera, Podocopida, Coleoptera, Gordea, Haplotaxida, Tricladida, Basommatophora, Taeniopterygidae, terrestrial taxa from the riparian zone, and zooplankton from Carpenter Reservoir. Mean density of all taxa in the basket samplers was 71,000 animals·m^{-2} in Trial 0, 95,000 animals·m^{-2} in Trial 1, 94,000 animals·m^{-2} in Trial 2, a decline of 69% to 29,000 animals·m^{-2} in High Flow Years, and a subsequent increase to 74,000 animals·m^{-2} in the Post-High Flow years. Yalakom River samples included the same taxa found in the Lower Bridge River (Figure 3.12) with a mean invertebrate density of 47,625 animals·m^{-2} in 2018 (only one year of data available during High Flow Years) and 35,500 animals·m^{-2} in Post-High Flow years. Mean invertebrate density in Reach 1 during the Post-High Flow years was 35,114 animals·m^{-2}. Taxa in Reach 1 were similar to those in the other Bridge River reaches.

There were no significant interactions of Reach, Trial, and Pinks on total benthos, EPT, or chironomids, which meant the main factors could be examined independently (Table 3.11, Table 3.12, Table 3.13). Total benthos, EPT, and chironomid density were significantly lower during the High Flow years compared to the other Trials ($p<0.001$ to 0.006). Mean densities increased from the High Flow years to Post-High Flow years, resulting in no significant difference in densities between the Post-High Flow years and Trial 2. There was no Reach effect on Total benthos density ($p=0.85$), largely due to the same outcome on EPT ($p=0.34$). In contrast, chironomid density was lower in Reach 3 than in the other reaches among all flow periods ($p=0.02$). Chironomid density was greater when Pink salmon spawners were present compared to when they were absent ($p=0.025$) but the EPT were not affected by Pinks ($p=0.31$).

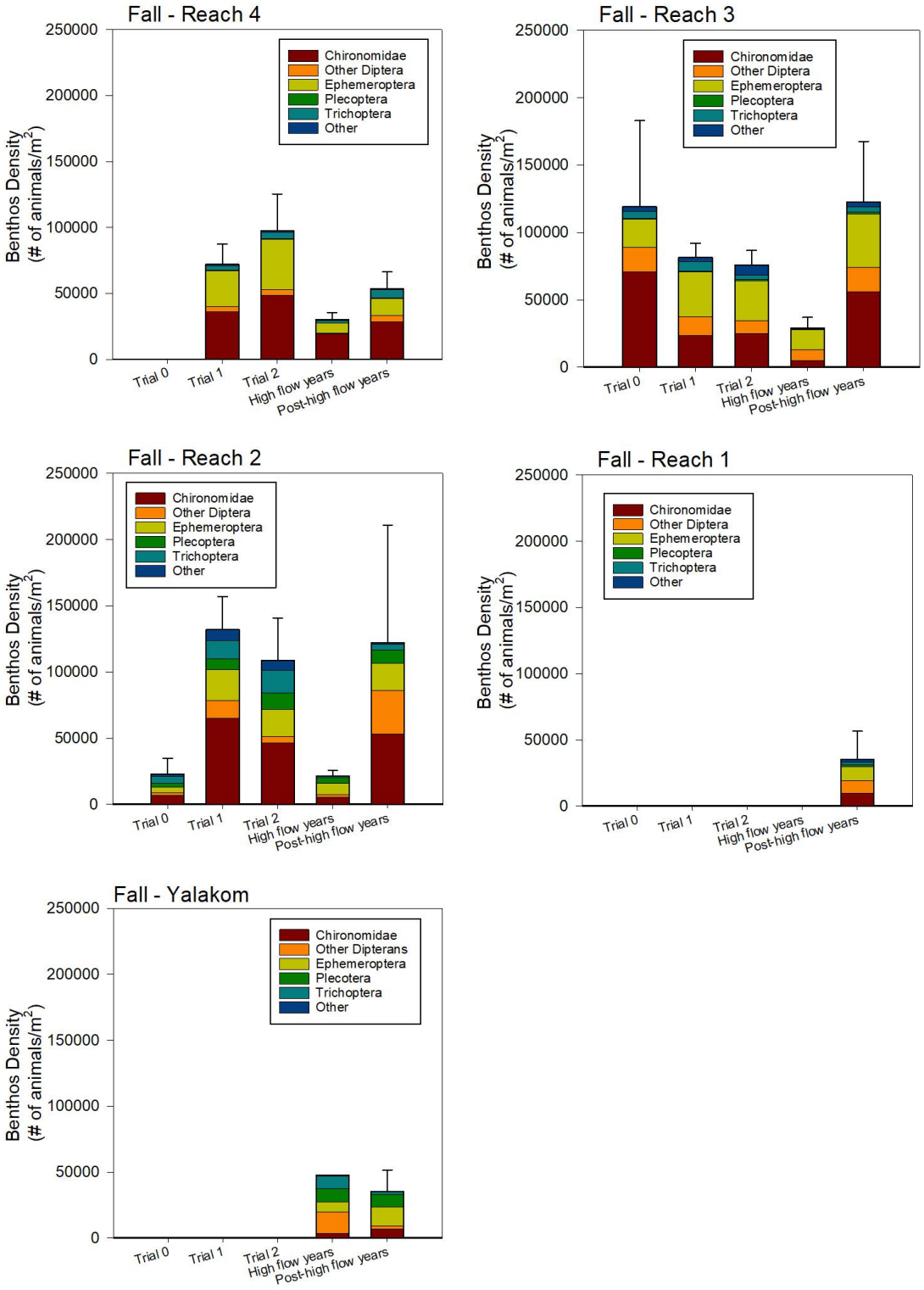

Figure 3.12 Mean density (years are replicates) of invertebrate orders in the fall among Trials in Reach 4 (top left), Reach 3 (top right), Reach 2 (middle left), Reach 1 (middle right), and the Yalakom River (bottom left). Error bars are standard error of the arithmetic mean of total density.

Table 3.11 Analysis of variance table for test of Trial, Reach, and Pink effects on total benthos. Where a factor showed a significant effect, results of the Tukey test of pairwise contrasts are shown to indicate what factor levels were significantly different from the others (p<0.05).

Analysis of variance statistics (Log_{10} total benthos+1)						Tukey test
Source	SS	df	Mean Squares	F-Ratio	p-Value	
Trial	1.687	3	0.562	7.910	<0.001	High Flow Years<Trial 1=Trial 2= post High Flow Years
Reach	0.024	2	0.012	0.167	0.847	Not applicable
Pink	0.012	1	0.012	0.176	0.678	Not applicable
Trial*Reach	0.297	6	0.050	0.697	0.654	Not applicable
Trial*Pink	0.566	3	0.189	2.654	0.065	Not applicable
Reach*Pink	0.017	2	0.009	0.120	0.887	Not applicable
Trial*Reach*Pink	0.228	6	0.038	0.534	0.778	Not applicable
Error	2.345	33	0.071			

Table 3.12 Analysis of variance table for test of Trial, Reach, and Pink effects on Ephemeroptera + Plecoptera + Tricoptera (EPT). Where a factor showed a significant effect, results of the Tukey test of pairwise contrasts are shown to indicate what factor levels were significantly different from the others (p<0.05).

Analysis of variance statistics (Log_{10} EPT+1)						Tukey test
Source	SS	df	Mean Squares	F-Ratio	p-Value	
Trial	1.463	3	0.488	4.938	0.006	High Flow Years<Trial 1=Trial 2= post High Flow Years
Reach	0.219	2	0.110	1.109	0.342	Not applicable
Pink	0.106	1	0.106	1.068	0.309	Not applicable
Trial*Reach	0.083	6	0.014	0.141	0.990	Not applicable
Trial*Pink	0.542	3	0.181	1.829	0.161	Not applicable
Reach*Pink	0.115	2	0.057	0.582	0.565	Not applicable
Trial*Reach*Pink	0.421	6	0.070	0.710	0.644	Not applicable
Error	3.260	33	0.099			

Table 3.13 Analysis of variance table for test of Trial, Reach, and Pink effects on Chironomidae. Where a factor showed a significant effect, results of the Tukey test of pairwise contrasts are shown to indicate what factor levels were significantly different from the others (p<0.05).

Analysis of variance statistics (Log_{10} Chironomidae+1)						Tukey test
Source	SS	df	Mean Squares	F-Ratio	p-Value	
Trial	2.335	3	0.778	6.045	0.002	High Flow Years<Trial 1=Trial 2= post High Flow Years
Reach	1.111	2	0.556	4.315	0.022	Reach 3<Reach 4= Reach 2
Pink	0.714	1	0.714	5.547	0.025	Pink on years > Pink off years
Trial*Reach	1.331	6	0.222	1.723	0.147	Not applicable
Trial*Pink	0.827	3	0.276	2.142	0.114	Not applicable
Reach*Pink	0.100	2	0.050	0.387	0.682	Not applicable
Trial*Reach*Pink	0.397	6	0.066	0.514	0.793	Not applicable
Error	4.249	33	0.129			

Family richness was significantly affected by flow Trial and Reach (Table 3.14, Figure 3.13). Richness declined during High Flow Years compared to during the other flow Trials (p<0.001). Recovery of family richness in the Post-High Flow years was less during Pink – on years than during Pink – off years but with only one sample year in each case during the Post-High Flow years and only one Pink – on sample during the High Flow Years, this finding is not conclusive. Richness was lowest in Reach 4, highest in Reach 2, and in between in Reach 3 among all flow trials (p<0.001), which showed addition of families with increasing distance from the dam throughout all flow trials.

Table 3.14 Analysis of variance table for test of Trial, Reach, and Pink effects on Family Richness. Where a factor showed a significant effect, results of the Tukey test of pairwise contrasts are shown to indicate what factor levels were significantly different from the others (p<0.05).

Analysis of variance statistics (Family richness)						Tukey test
Source	SS	df	Mean Squares	F-Ratio	p-Value	
Trial	117.131	3	39.044	12.797	<0.001	High Flow Years<Trial 1=Trial 2= post High Flow Years
Reach	158.745	2	79.372	26.014	<0.001	Reach 2 >Reach3>Reach 4
Pink	0.320	1	0.320	0.105	0.748	Not applicable
Trial*Reach	12.606	6	2.101	0.689	0.660	Not applicable
Trial*Pink	29.003	3	9.668	3.169	0.037	Not applicable
Reach*Pink	0.179	2	0.090	0.029	0.971	Not applicable
Trial*Reach*Pink	4.370	6	0.728	0.239	0.960	Not applicable
Error	100.686	33	3.051			

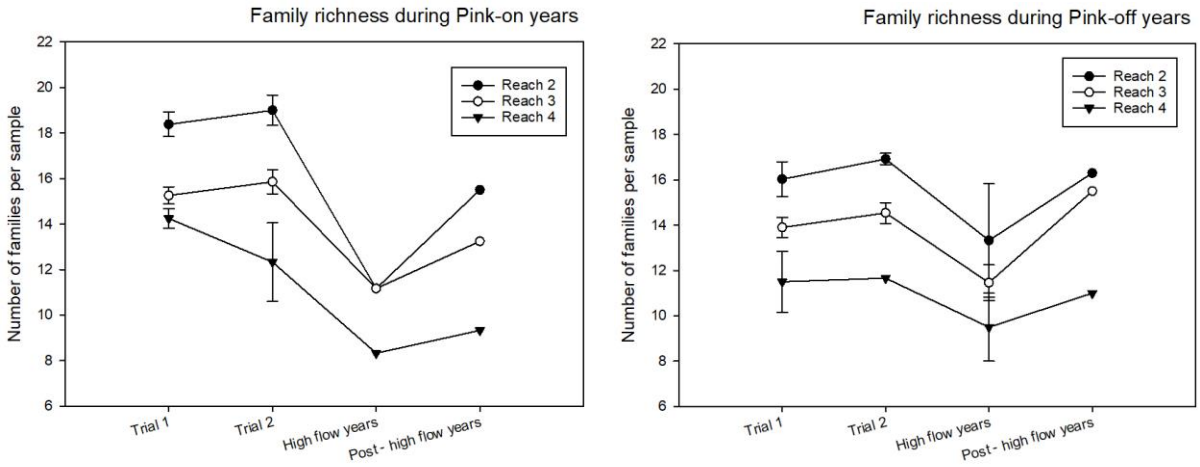

Figure 3.13 Mean family richness ± standard error of the arithmetic mean stratified by Trial and Reach in Pink-on years (left) and Pink-off years (right).

Benthic invertebrates were sampled in Reach 1 only during the Post-High Flow years. Table 3.15 shows mean densities with standard errors among the same groups tested for Trial and Reach effects in reaches 2 to 4 with comparisons made to the Yalakom River and Reach 2. If we double the standard errors to arrive at approximately the 95% confidence interval, mean densities in Reach 1 were approximately the same as in Reach 2 and the Yalakom River despite large differences among means. Using the same approach for family richness, Reach 1 richness was about the same as in the Yalakom River, which supported about 1 family per sample less than in Reach 2.

Table 3.15 Mean benthic invertebrate abundance during Post – High Flow Years ± standard error in the Yalakom River and Reaches 2 and 1 of the Lower Bridge River.

Reach	Mean invertebrate abundance ± standard error (number/m^2)			Family richness (number of families per sample)
	Total abundance	EPT	Chironomids	
Yalakom River	35,496 ± 16,192	26,192 ± 10,629	6,685 ± 3,369	14 ± 0.5
Lower Bridge River Reach 2	122,315 ± 88,335	34,950 ± 23,783	53,298 ± 35,515	16 ± 0.4
Lower Bridge River Reach 1	35,115 ± 21,325	13,572 ± 9,459	9,841 ± 4,076	13 ± 0.9

3.4. Juvenile Fish Production

3.4.1. Size and Condition

Mean weight of mykiss fry (Age-0+) in all reaches was highest during the High Flow period (2016-2018) compared to the other treatment periods (Figure 3.14). This likely occurred for a few possible reasons: 1) reduced density (see Figure 3.19 in Section 3.4.2) which reduced competition for available food; 2) warmer temperatures during the summer rearing period (see Figure 3.5) which may have facilitated growth; or 3) the high flows selected for larger fish since they are more mobile and capable of competing for habitat space, while smaller fish may be more readily displaced downstream. Mean weight during the Post -high flow years (2019-2020) was also high, most likely due to reasons 1) and 2) above, which have continued to some extent, but also due to recovered benthic invertebrate abundance (see Figure 3.12 in Section 3.3) after two years of a return to Trial 2 flows. Growth in reach 3 during the Trial 0 pre-flow period (0 $m^3 \cdot s^{-1}$) was also high likely due to ample benthic invertebrate abundance, combined with the quality rearing conditions in this reach prior to the flow release. Size of mykiss fry among the reaches was fairly equivalent within each flow treatment period.

Mean size for mykiss parr (Age-1+) was also greatest during the High flow and Post-high flow periods, and equivalent among them (i.e., there was complete overlap in the standard deviation error bars for these two periods). Mykiss parr tended to be largest in reaches 3 and 4 during the High flow and Post-high flow years, whereas they had been more equivalent among the reaches during the previous treatment periods. However, these results for mykiss parr were based on only two years available for the High flow period and one year for the Post-high flow period (see Table 2.3 and rationale provided in Section 2.9.3).

Patterns in mean weight for coho fry across flow treatments in reaches 2, 3 and 4 closely matched the patterns seen for mykiss fry which reflected increased size during the High flow and Post-high flow periods, and higher growth in Reach 3 during Trial 0, likely for the same set of reasons provided for mykiss fry, above. On average, the coho fry were consistently larger than the mykiss fry at the time of sampling due to their earlier emergence timing in the year (i.e., longer period of growth). Coho fry have typically been largest in Reach 4 among each of the flow treatments. However, as with mykiss, there was also considerable overlap in the standard error bars among some reaches and flow treatment periods.

In Reach 2, mean weight of Chinook fry was higher under the Trial 2 (6 $m^3 \cdot s^{-1}$), High flow and Post-high flow years relative to the Trial 0 (0 $m^3 \cdot s^{-1}$) and Trial 1 (3 $m^3 \cdot s^{-1}$) treatments, probably due to lower density. In reaches 3 and 4, mean weights were higher than in Reach 2 (for all flow treatments) and were highest under the High flow and Post-high flow treatments (and equivalent among them). The Chinook fry were the largest of the target species and the size gradient among the reaches corresponded with the patterns of abundance and predicted emergence timing for Chinook which likely resulted in reduced competition and a longer growing period in reaches 3 and 4 than in Reach 2.

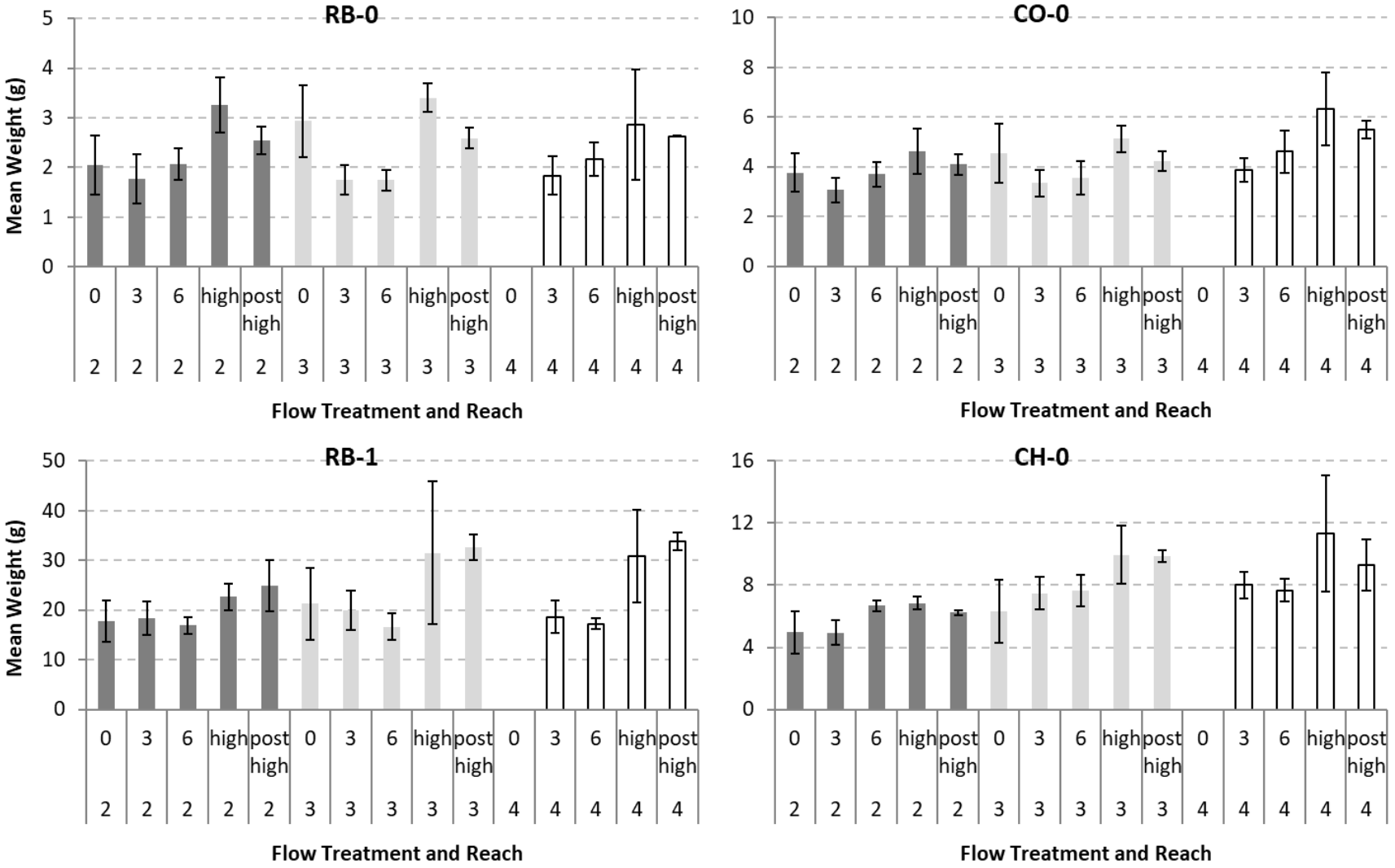

Figure 3.14 Mean juvenile salmonid weight during fall standing stock assessments across flow treatments (0, 3, and 6 $m^3 \cdot s^{-1}$ trials and the high and post-high flow periods) and reaches (2, 3, and 4). RB-0, RB-1, CO-0, and CH-0 denote mykiss fry, mykiss parr, coho fry, and Chinook fry, respectively. Height of bars represents the means of annual values for each reach-flow treatment combination and error bars denote 1 standard deviation (variation in annual values within treatments).

Given uncertainty in the factors driving differences in mean weight among the flow trials (particularly for the Trial 3 high flow years when food availability was dramatically reduced), we calculated mean condition factor values since this better reflects actual body condition of the fish sampled (i.e., expressed as Fulton's Condition Factor, K), rather than just size (Figure 3.15). Interestingly, the condition factor values showed a different pattern among flow trials than the mean weight data: For each target species and age class there has been a general trend of declining condition factor values across the study period. This was true for mykiss fry, coho fry and Chinook fry, particularly in reaches 2 and 3. Exceptions for coho and Chinook fry were in Reach 4 where condition factor has either not changed (i.e., for coho), or highest K values were during the High flow years (i.e., for Chinook; however, this K value was also based on the smallest sample size in the analysis (*n*= 13 fish)). For mykiss parr, lowest K values were during the Post-high flow years (with only 1 year-replicate to-date), but highest K values for this age class were in flow trials 0 and 1 (with substantial overlap in standard error bars among flow trials 0 to 2). Condition factors in Trial 1 vs. Trial 2 were generally very similar for all species and age class combinations.

We also plotted condition factor values from 2019 and 2020 with the Trial 2 mean (± SD; based on 2011 to 2015 values) to compare relative values before and after the high flow years (Figure 3.16). These comparisons showed that, despite the same flow release volumes throughout the year, K values in 2019 and 2020 were generally within or below the Trial 2 lower standard deviation line for each species and age class in each reach. Exceptions were in Reach 3 for 2019 mykiss parr and Chinook fry and 2020 mykiss fry which were equivalent to the respective Trial 2 means, and in Reach 4 for Chinook fry in 2019 and coho fry in 2020 which had higher K values than the Trial 2 mean. Overall, for all reaches combined, K values were notably lower than Trial 2 values for mykiss fry (Age-0+), coho fry and Chinook fry in 2019 and for mykiss parr (Age-1) and Chinook fry in 2020. Condition factor for mykiss fry and coho fry increased slightly in 2020 relative to 2019 and decreased for mykiss parr and Chinook fry.

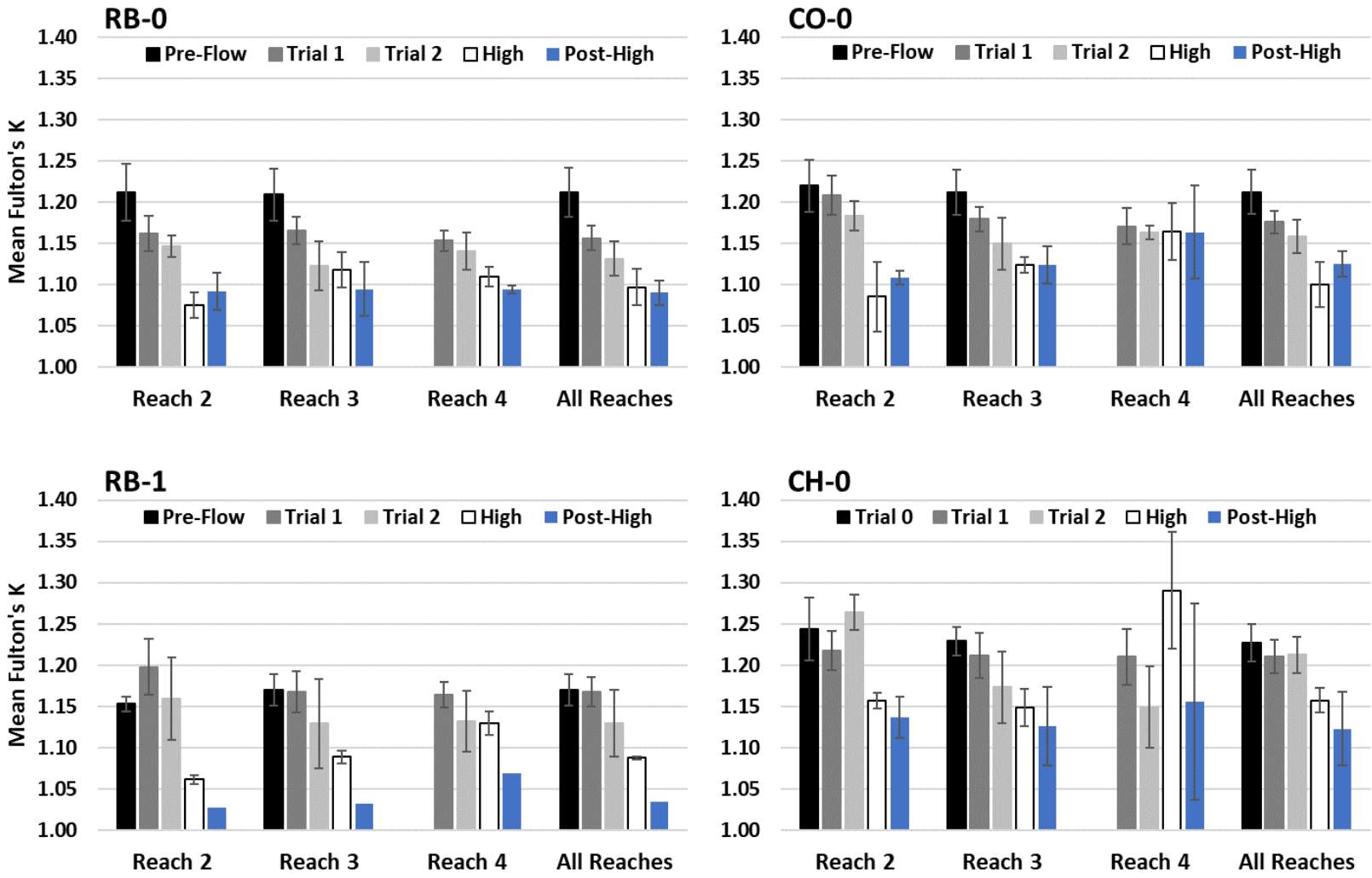

Figure 3.15 Mean condition factor for juvenile salmonids during fall standing stock assessments across flow treatments (0, 3, and 6 $m^3 \cdot s^{-1}$ trials and the high and post-high flow periods) and reaches (2, 3 and 4). Species and age designations are the same as described for Figure 3.14. Height of bars represents the means of annual values for each reach-flow treatment combination and error bars denote 1 standard deviation (variation in annual values within treatments).

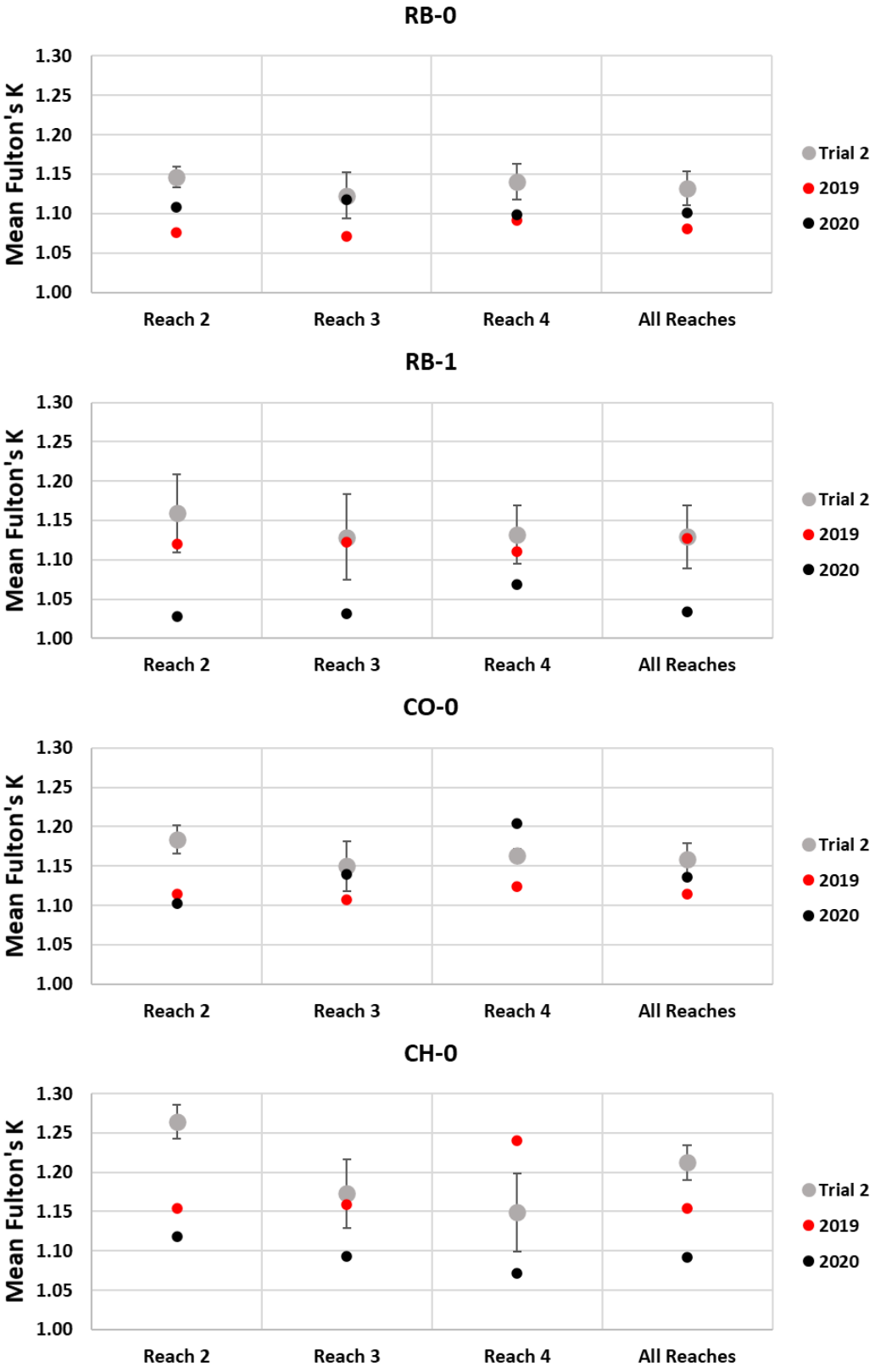

Figure 3.16 Mean condition factor (Fulton's K value) between 2019, 2020 and all Trial 2 years for mykiss fry, mykiss parr, coho fry and Chinook fry in reaches 2, 3 and 4.

3.4.2. Abundance and Biomass

For all juvenile salmonid species combined, abundance and biomass increased from Trial 0 (the Pre-flow period) to Trial 1, decreased slightly in Trial 2 and then decreased substantially under high flows (Figure 3.17). Relative to the values from the earlier trials, abundance and biomass estimates in 2019 and 2020 were low (abundance and biomass were substantially lower than the Trial 2 average under equivalent flow release discharges). The abundance and biomass values in Figure 3.17 are shown relative to the average flow release discharge in summer (i.e., June-July) since this was the period of the year when discharges varied the most among the trials (see Figure 1.3 in Section 1.3).

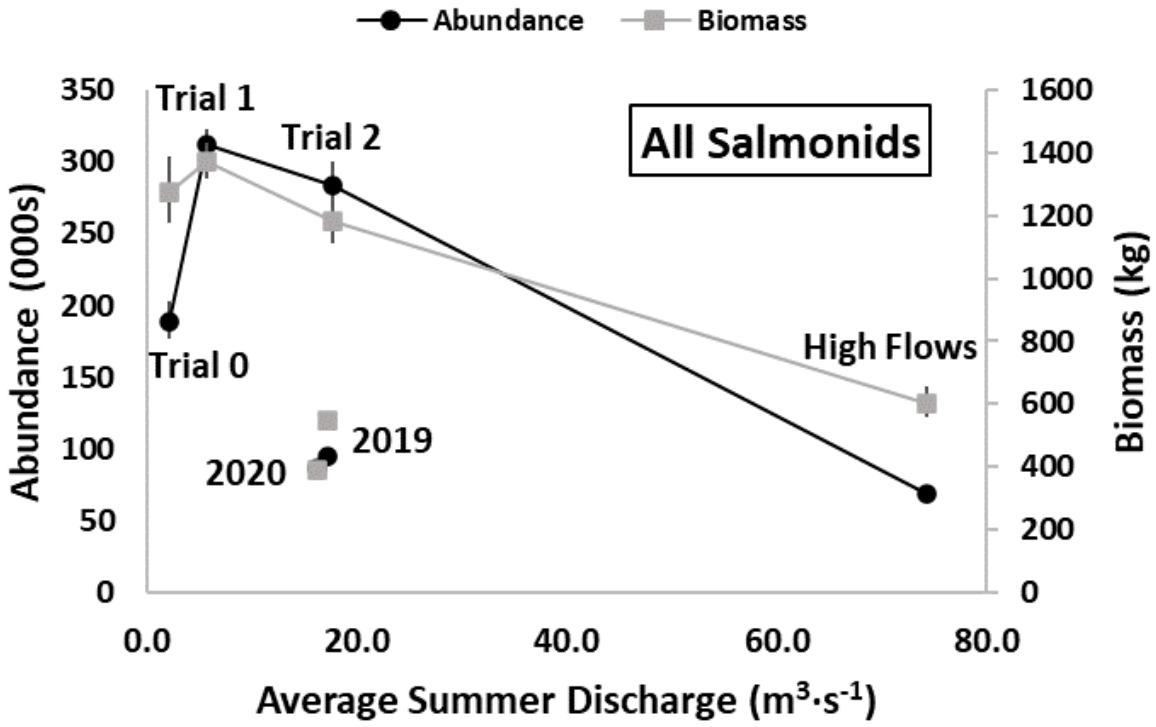

Figure 3.17 Juvenile salmonid abundance (1° y-axis) and biomass (2° y-axis) in the Lower Bridge River as a function of the average June-July flow releases from Terzaghi Dam for each flow treatment (with 95% credible intervals). The individual data points for 2019 and 2020 are also shown.

Among the flow treatments, fish production response to flow (abundance and biomass) varied by species and age class (Table 3.16, In terms of recovery post-high flows (i.e., in 2019 and 2020), all species and age classes have fared relatively poorly to-date. Since the return to low flow releases (i.e., the Trial 2 flow magnitudes and hydrograph shape) following the High flow years, mykiss fry and coho fry abundance and biomass increased modestly (+14K fish for each); however, the estimates for mykiss parr and Chinook fry actually decreased relative to the High flow period (-4K and -3K on average, respectively) (Table 3.16 and Table 3.17). The abundance

and biomass estimates were fairly equivalent between 2019 and 2020 for all species/age classes and substantially lower than the Trial 2 estimates, particularly for mykiss (fry and parr) and coho fry (Figure 3.18). For Chinook, the 2019 and 2020 estimates were lower, but the Trial 2 estimates were already low (compared to the Pre-flow estimates) for this species.

Table 3.17 and Figure 3.18). Mykiss fry and coho fry responded the most favourably to the initial flow release trials (Trial 1 and Trial 2) and, proportionately, decreased the most under the High flows. Mykiss parr were highest (and relatively equivalent) among the Pre-flow, Trial 1 and Trial 2 periods, and then decreased substantially under High flows. Chinook fry decreased during Trial 1 and remained low during Trial 2 and High flows.

Table 3.16 Average total abundance (a, '000s) and biomass (b, kg) of juvenile salmonids in the Lower Bridge River across all reaches by flow treatment (2019 and 2020 included as stand-alone columns). RB-0, RB-1, CO-0, and CH-0 denote Age-0+ mykiss, Age-1 mykiss, Age-0+ coho, and Age-0+ Chinook, respectively.

a) Abundance

Species-Age	Trial 0	Trial 1	Trial 2	High Flow	Post-High Flow	
					2019	2020
RB-0	90	174	162	38	51	53
RB-1	36	35	33	10	8	6
CO-0	25	81	76	8	23	21
CH-0	38	22	13	13	12	7

b) Biomass

Species-Age	Trial 0	Trial 1	Trial 2	High Flow	Post-High Flow	
					2019	2020
RB-0	249	305	282	124	141	125
RB-1	690	653	554	326	243	127
CO-0	108	281	255	39	89	94
CH-0	228	134	91	114	72	43

In terms of recovery post-high flows (i.e., in 2019 and 2020), all species and age classes have fared relatively poorly to-date. Since the return to low flow releases (i.e., the Trial 2 flow magnitudes and hydrograph shape) following the High flow years, mykiss fry and coho fry abundance and biomass increased modestly (+14K fish for each); however, the estimates for

mykiss parr and Chinook fry actually decreased relative to the High flow period (-4K and -3K on average, respectively) (Table 3.16 and Table 3.17). The abundance and biomass estimates were fairly equivalent between 2019 and 2020 for all species/age classes and substantially lower than the Trial 2 estimates, particularly for mykiss (fry and parr) and coho fry (Figure 3.18). For Chinook, the 2019 and 2020 estimates were lower, but the Trial 2 estimates were already low (compared to the Pre-flow estimates) for this species.

Table 3.17 Relative number of fish produced (by species and age class) under each flow treatment (2019 and 2020 included as stand-alone columns). Each value reflects production by the flow treatment (or year) in the column label relative to the flow treatment in the row label (1.0 = equivalent production). Matrix cells comparing 2019 and 2020 values to the Trial 2 averages are highlighted yellow.

Species-Age Class		Flow Treatment (Mean Annual Release)				
		Trial 1 (3 $m^3 \cdot s^{-1}$)	Trial 2 (6 $m^3 \cdot s^{-1}$)	High Flows (>18 $m^3 \cdot s^{-1}$)	Post-High Flows (6 $m^3 \cdot s^{-1}$)	
					2019	2020
RB Age-0+	Pre-Flow	1.9	1.8	0.4	0.6	0.6
	Trial 1		0.9	0.2	0.3	0.3
	Trial 2			0.2	0.3	0.3
	High Flows				1.3	1.4
RB Age-1	Pre-Flow	1.0	0.9	0.3	0.2	0.2
	Trial 1		0.9	0.3	0.2	0.2
	Trial 2			0.3	0.2	0.2
	High Flows				0.9	0.6
CO Age-0+	Pre-Flow	3.3	3.1	0.3	0.9	0.9
	Trial 1		0.9	0.1	0.3	0.3
	Trial 2			0.1	0.3	0.3
	High Flows				2.9	2.7
CH Age-0+	Pre-Flow	0.6	0.3	0.3	0.3	0.2
	Trial 1		0.6	0.6	0.5	0.3
	Trial 2			1.0	0.9	0.5
	High Flows				0.9	0.5
All Salmonids	Pre-Flow	1.7	1.5	0.4	0.5	0.5
	Trial 1		0.9	0.2	0.3	0.3
	Trial 2			0.2	0.3	0.3
	High Flows				1.4	1.3

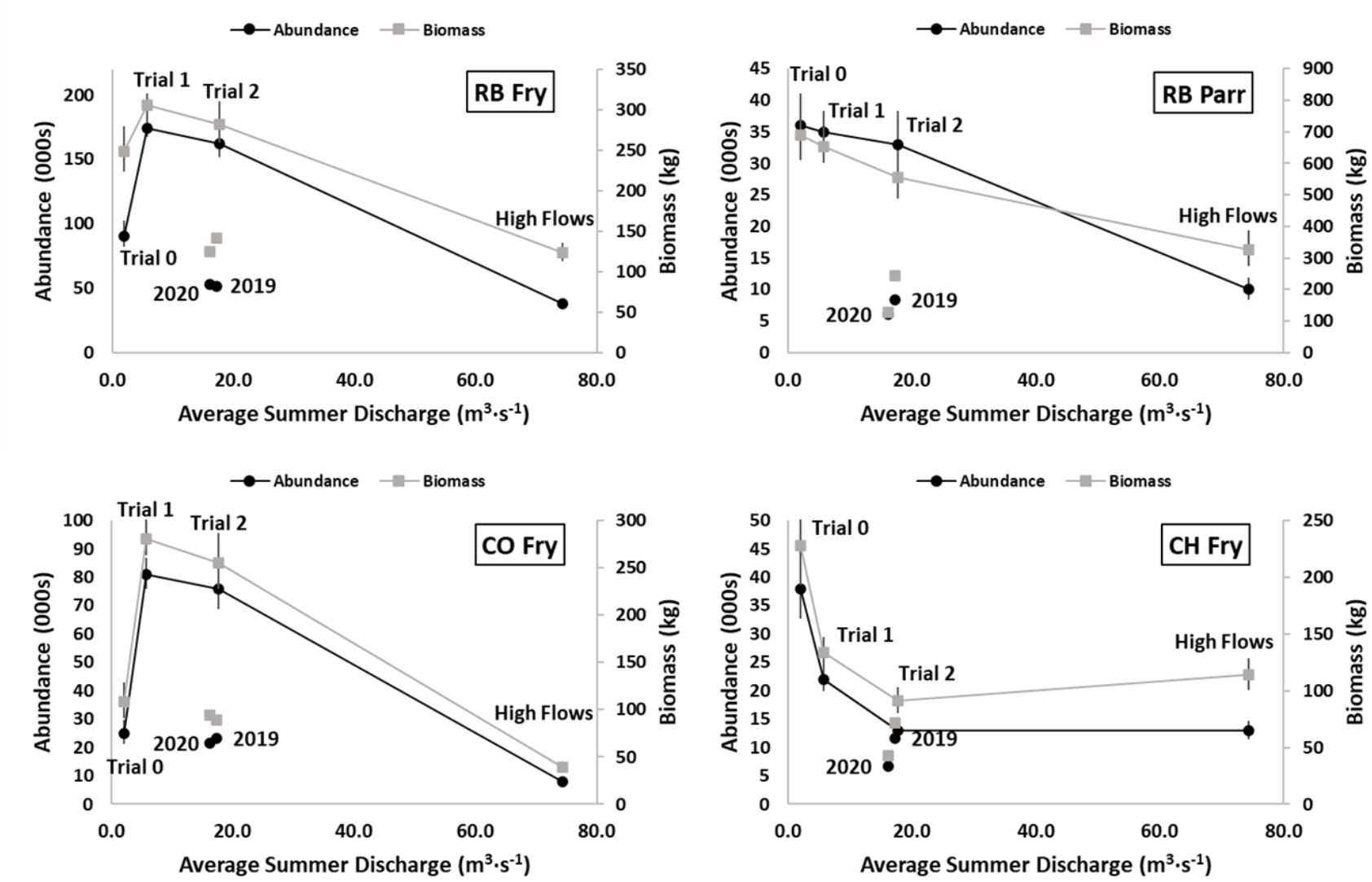

Figure 3.18 Abundance (1° y-axis) and biomass (2° y-axis) for mykiss fry (top left), mykiss parr (top right), coho fry (bottom left) and Chinook fry (bottom right) as a function of the average June-July flow releases from Terzaghi Dam for each flow treatment (with 95% credible intervals). The individual data points for 2019 and 2020 are also shown on each plot.

On a reach basis, increasing flow from Trial 0 (0 $m^3 \cdot s^{-1}$ release) to the Trial 1 (3 $m^3 \cdot s^{-1}$) treatment led to increases in abundance of mykiss fry in reaches 2 (+13K fish) and 3 (+24K fish) and there was substantial new production in Reach 4 (+46K fish)(Figure 3.19). Production under Trial 2 (6 $m^3 \cdot s^{-1}$) was nearly equivalent, with Reach 4 contributing a little less (-12K), Reach 3 contributing about the same (-3K), and Reach 2 contributing slightly more (+3K) than during Trial 1. Under high flows, when abundance was substantially reduced, all of the study reaches were affected. Mykiss fry production decreased by 31K, 71K and 21K relative to the Trial 2 abundances in reaches 4, 3 and 2, respectively. During the Post-high flow years (2019 and 2020), the recovery was strongest in Reach 3 (+11K relative to the High flow abundance), and more modest in reaches 4 (+1K) and 2 (+1K). However, relative to the Trial 2 averages, the abundances for mykiss fry during the Post-high flow years (when flow releases were the same as Trial 2) were -30K, -60K, and -19K for reaches 4, 3 and 2, respectively.

Mykiss parr abundance increased by 1K in Reach 2 from Trial 0 to Trial 1 while there was a large decrease by 13K in Reach 3. However, Trial 1 also produced about 11K additional parr in Reach 4, which compensated for the losses in Reach 3. Under Trial 2, mykiss parr abundance increased in Reach 3 (by 4K relative to the Trial 1 abundance), decreased in Reach 4 (by 5K), and stayed the same in Reach 2. For the study area as whole (i.e., reaches 2, 3 and 4 combined) the production of mykiss parr was equivalent for trials 0, 1 and 2. Under the high flows, the response of mykiss parr followed a similar pattern to the fry: Reaches 3 and 4 were hit the hardest (-20K and -5K relative to the Trial 2 abundance), whereas Reach 2 abundance increased slightly (by ~1K). During the Post-high flow period, mykiss parr abundance has actually dropped further with abundances in reaches 4, 3 and 2 being -1K, -2K and -1K relative to the High flow production, respectively. Relative to the Trial 2 years, there are ~21K fewer mykiss parr in Reach 3, ~6K fewer in Reach 4, and about the same production in Reach 2. Although it must be noted for these comparisons that the Post-high flow production is currently based on one year of data (2020) since 2019 was a transition year between flow treatments for this age class.

Coho fry abundance trends followed those for mykiss fry with increases in reaches 2 (+3K fish) and 3 (+32K) between Trial 0 and Trial 1 and substantial gains in Reach 4 (+21K), and little change in abundance under Trial 2 (i.e., -6K, +1K and +1K for reaches 4, 3 and 2, respectively) (Figure 3.19**Error! Reference source not found.**). Like the mykiss fry, coho fry abundance was substantially reduced by the high flows: -14K in Reach 4, -50K in Reach 3, and -3K in Reach 2. During the Post-high flow period to-date, coho fry production has increased modestly (i.e., +3K in Reach 4, +10K in Reach 3, and +1K in Reach 2) relative to the abundances during the High flow years. However, these abundances are still substantively less than the Trial 2 production, particularly in reaches 3 and 4 which were -40K and -11K relative to the Trial 2 averages for these reaches. Post-high flow abundance in Reach 2 was 2K less than the Trial 2 average for this reach which has not been a big contributor to coho production during any of the flow treatments.

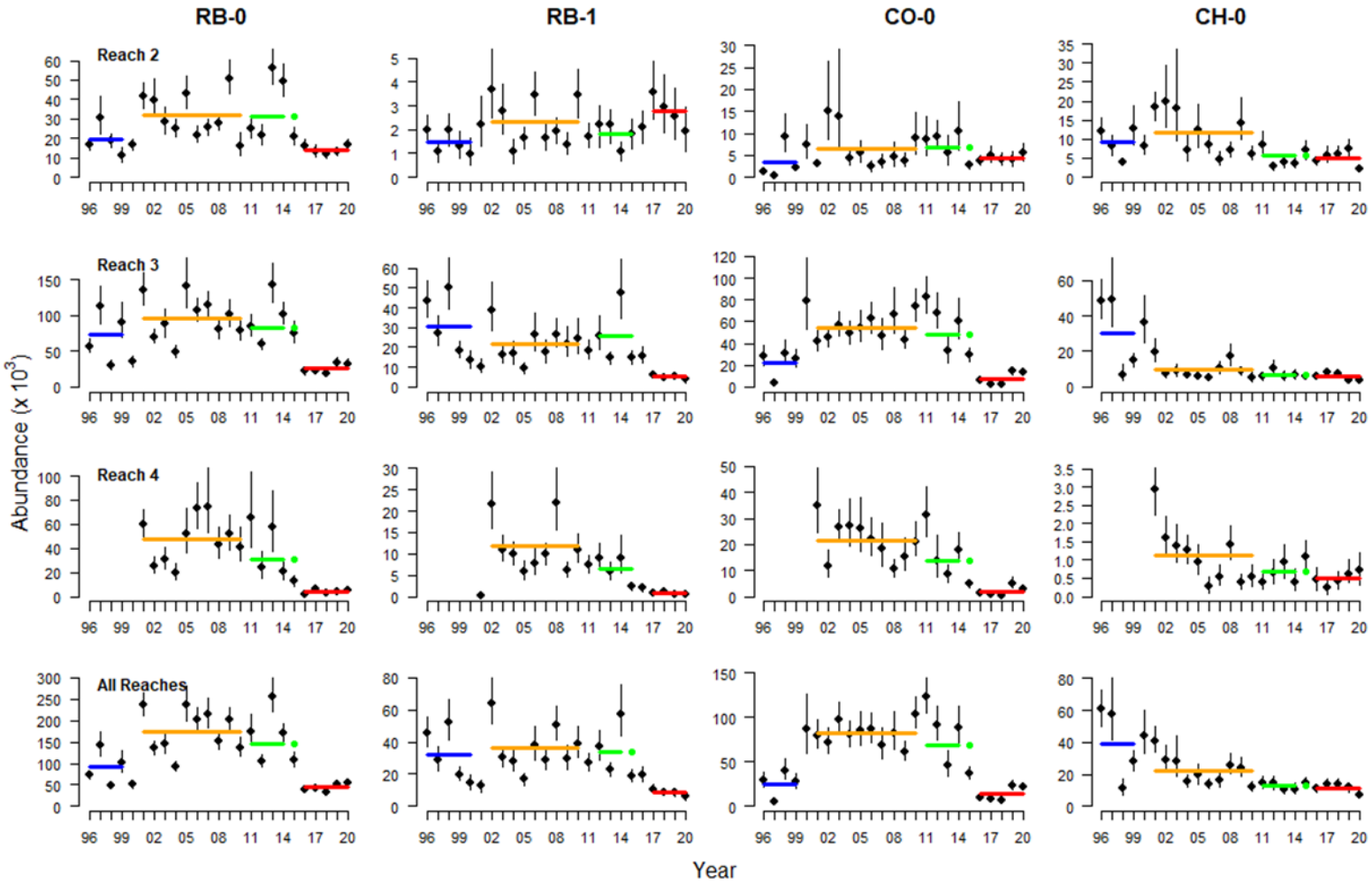

Figure 3.19 Abundance (in thousands) of juvenile salmonids in the lower Bridge River by reach (row) and species-age class (column). Points and vertical lines show mean values and 90% credible intervals from posterior distributions of abundance for each year from the hierarchical Bayesian model, respectively. Blue, orange, green and red lines show the mean values for trials 0, 1, 2, and high flow treatments, respectively. RB-0, RB-1, CO-0, and CH-0 denote age-0 mykiss, age-1+ mykiss, age-0 coho, and age-0 Chinook, respectively.

Chinook fry abundance increased slightly in Reach 2 (+2K) under the Trial 1 treatment relative to Trial 0, but declined in Reach 3 (-19K) likely owing to higher incubation temperatures which result in premature emergence in that reach (Figure 3.19 and Figure 3.6 in Section 3.1.5**Error! Reference source not found.**). Chinook recruitment in Reach 4 has been low (~0.3 to 3K) across all flow treatments. Due to a continuation of these temperature conditions from the release (and similar release discharges) during the incubation period for Chinook, abundances during stock assessment sampling have remained low within reaches and among flow treatments since Trial 1 for this species. Unlike the case for mykiss and coho fry, the high flows from 2016–2018 did not result in a further decline in Chinook fry abundance (relative to Trial 2) within the study area, perhaps because their abundance was already reduced. Post-high flow abundances were ~3K lower in Reach 3 and ~1K lower in Reach 2 relative to the Trial 2 and High Flow production in these reaches. The continued depressed production of Chinook fry across multiple flow treatments suggests that, under current constraints, flow volumes may be less a driving factor for recruitment of this species within the study area than the incubation issue.

So, for the species and age classes that increased, the change was largely attributable to Reach 3 (Figure 3.19). For mykiss fry, the ~11K additional fish in Reach 3 accounted for ~79% of the Post-high flow increase for that species-age class; and for coho fry, the additional ~10K fish in Reach 3 accounted for ~71% of the Post-high flow increase for that species-age class. The ~3K increase in coho fry in Reach 4 accounted for ~21% of the Post-high flow increase. As noted above, the contributions by reach for mykiss parr and Chinook fry were generally equivalent to the distribution during the high flow years.

Despite some differences in mean weights among species and age classes under the different flow treatments described in Section 3.4.1 (see Figure 3.14), the trends in biomass among flow treatments generally followed those based on abundance (Table 3.16b, Figure 3.18 and Figure 3.20**Error! Reference source not found.**). This was because the changes in abundance were more substantial than the relative changes in mean weights among treatments. However, the higher mean weights during the High flow and Post-high flow years had a slight moderating effect on the change in biomass (relative to Trial 2) than the change in abundance. This moderating effect was evident for each species and age class during the High flow and Post-high flow treatments and was most notable for mykiss (fry and parr) since the increases in mean weights were more substantial for this species. As such, the biomass estimates during the Post-high flow years were 47%, 23%, 36% and 63% of the Trial 2 estimates for mykiss fry, mykiss parr, coho fry and Chinook fry, respectively (compared to 32%, 18%, 29% and 73%, respectively, for abundance).

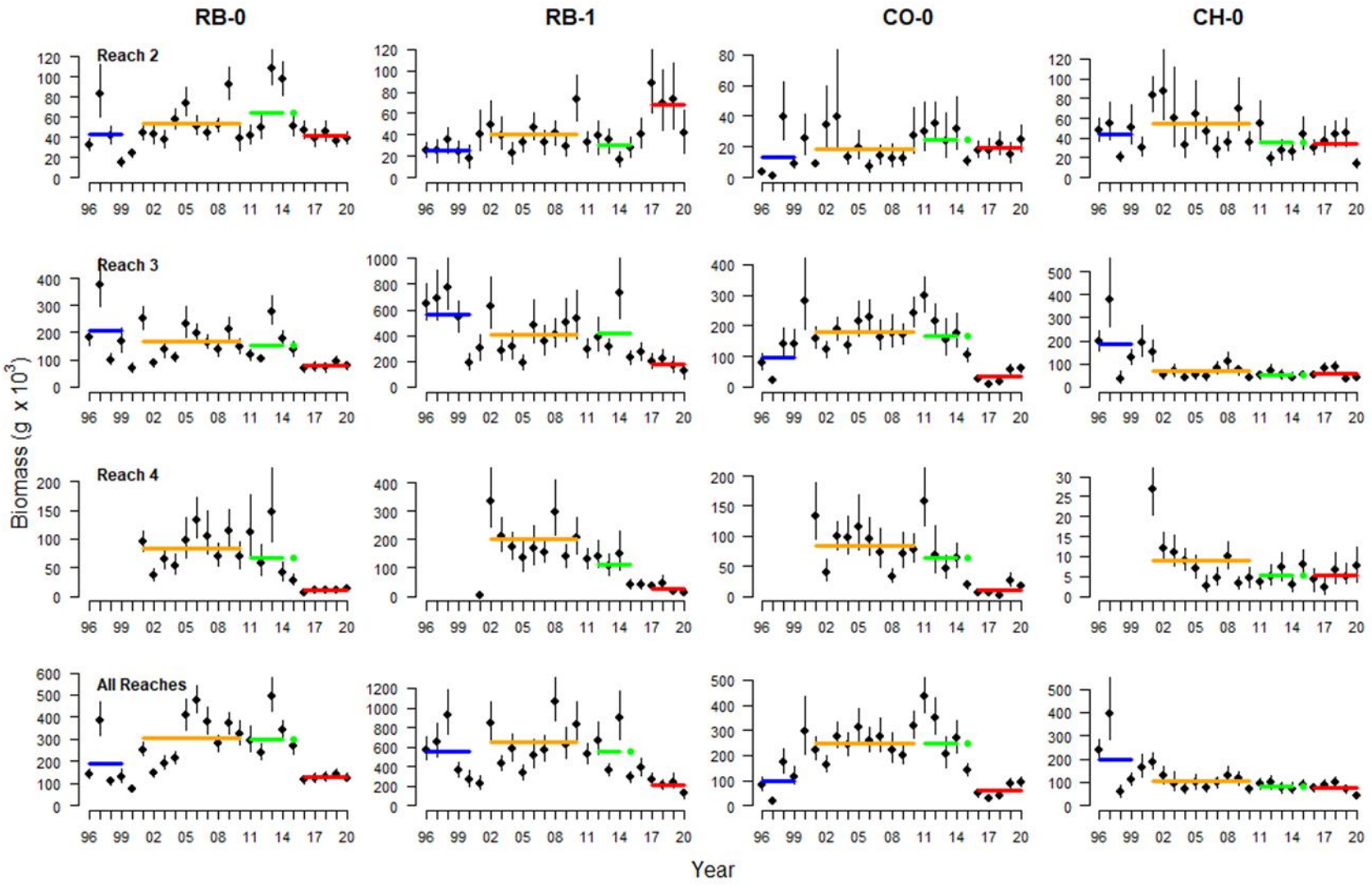

Figure 3.20 Biomass (in thousands of grams or kilograms) of juvenile salmonids in the Lower Bridge River by reach (row) and species-age class (column). See caption for Figure 3.19 for details.

Mixed Effects Model Results

We used a mixed effects model to formally test for flow effects (according to the various flow treatments from Terzaghi Dam) on the density and biomass of juvenile salmonids in the study area across the years of monitoring to-date. One approach assessed flow effects that were not stratified by reach (Equation 1a in Section 2.9.4) and another where they were stratified by reach (Equation 1b). The intent of the two approaches was to determine if the effects of the various flow releases on each target species and age class could be adequately characterized for the study area as a whole or if there were reach-specific effects. The added parameters in Equation 1b ($\phi_{f,r}$) add complexity and are only beneficial if reach is informative for explaining the variation among years and treatments (e.g., where the credible intervals for flow effects don't overlap among reaches).

For the unstratified flow effect model (eqn. 1a), where the flow effects are assumed to be the same for all reaches, this means the flow effect includes the added production in Reach 4 once it was rewetted (going from a density of zero during the Pre-flow period) as well as any effects of the additional discharge added to reaches 2 and 3. These effects cannot be teased apart using this model. Furthermore, a potentially large effect in one reach (e.g., Reach 4) could be masked by a large counter-effect in another reach (e.g., due to Yalakom influence on Reach 2) and this would not be detected by the unstratified approach. Nevertheless, the unstratified approach is a simpler model that can provide a less complex picture of flow effects on juvenile salmonid production in the study area (including both rewetting and added-water effects). However, the plotted results for the unstratified model are not included here, but are available upon request (see rationale on selecting between the models below).

These two effects (wetting vs. adding more water) are separated when using the reach-stratified model (eqn. 1b). The β_F values produced by the stratified model for Reach 4 represent the rewetting effect, while the β_F values for reaches 2 and 3 are the effect of adding varying amounts of extra water during Trial 1, Trial 2, High flow, and Post-high flow treatments (Figure 3.21 and Figure 3.22). The rewetting effect on log density and biomass in Reach 4 was much greater than the added water effect in reaches 2 and 3, particularly for biomass (blue points; Figure 3.22). Given the results of this monitoring program reported to-date, this result is intuitive: more water in already wetted reaches does not produce more fish, whereas rewetting the previously dry reach clearly provides fish production benefits (relative to no water).

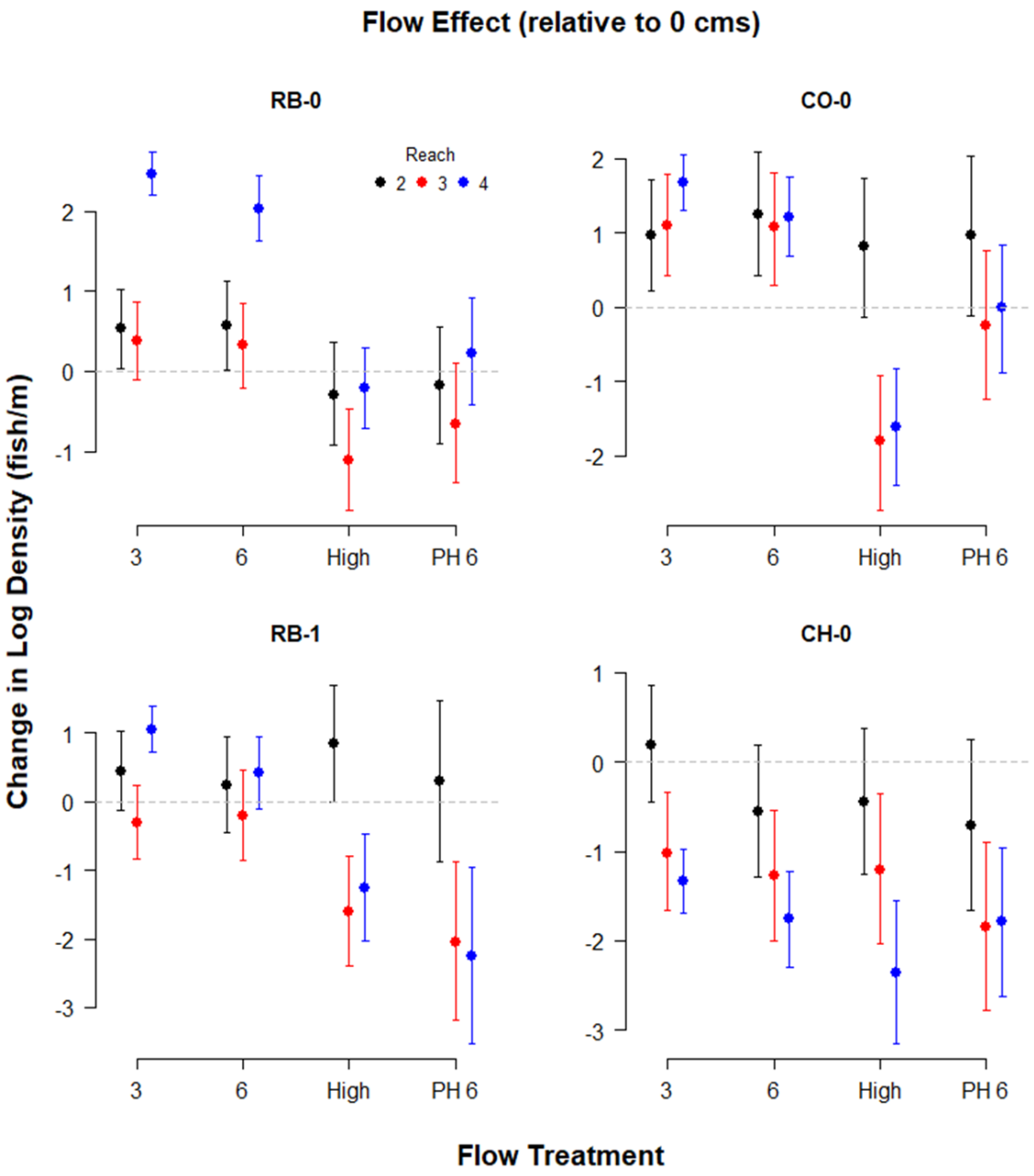

Figure 3.21 **Results of the mixed effect model showing the reach-stratified flow effects (β_F values ±95% credible intervals) on log density (fish/m) for mykiss fry (RB-0; top left), mykiss parr (RB-1; bottom left), coho fry (CO-0; top right), and Chinook fry (CH-0; bottom right). For the flow treatments, 3 $m^3 \cdot s^{-1}$ = Trial 1, 6 $m^3 \cdot s^{-1}$ = Trial 2, High = High flows, and PH6 = Post-high (6 $m^3 \cdot s^{-1}$) flows. Each point depicts the change relative to Trial 0 (0 $m^3 \cdot s^{-1}$ release), shown as a dotted horizontal line.**

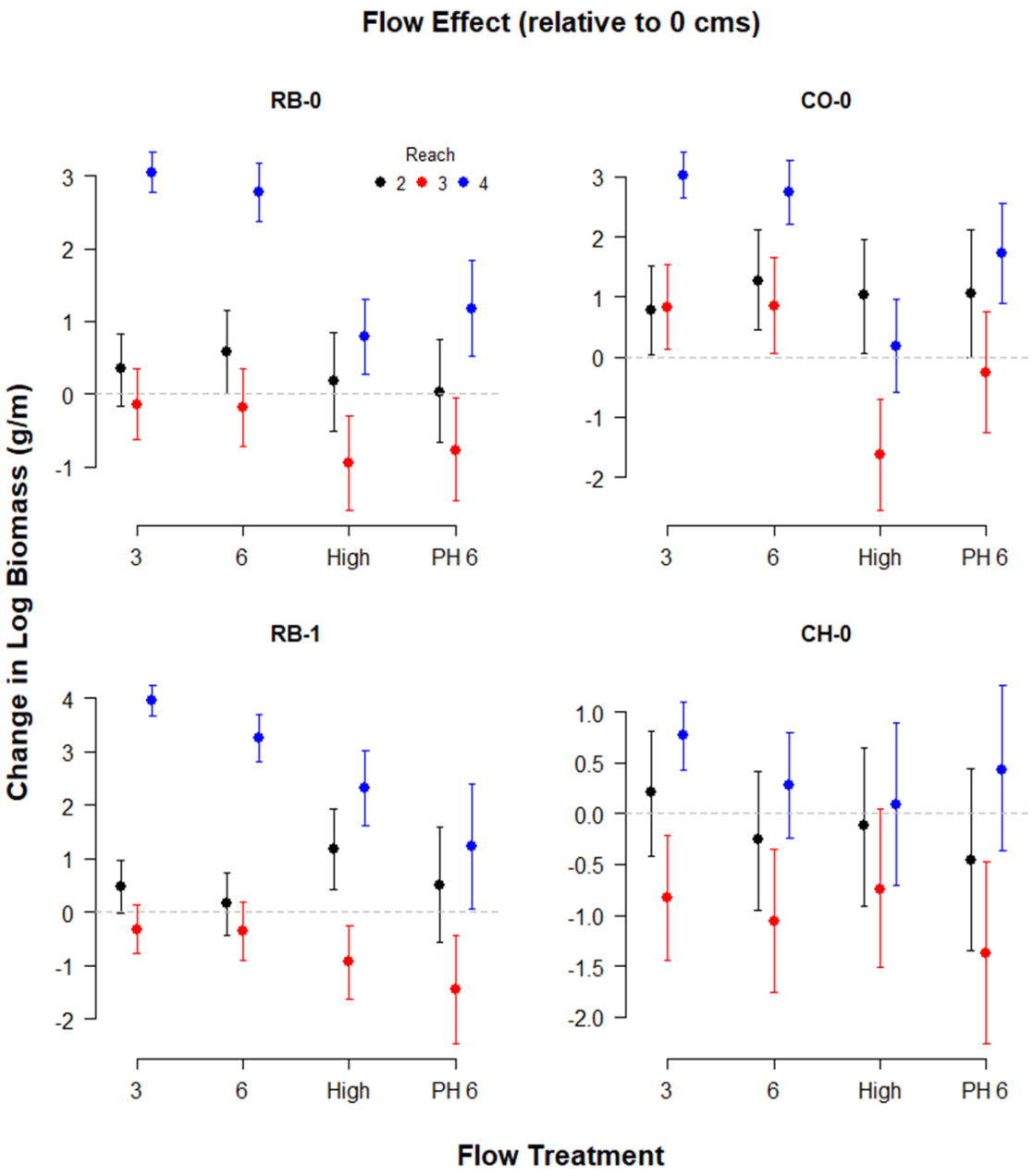

Figure 3.22 Results of the mixed effect model showing the reach-stratified flow effects (β_F values ±95% credible intervals) on log biomass (g/m) for each species and age class. See Figure 3.21 caption for details.

In addition to differentiating the rewetting vs. added-water effects, there are a number of indicators in the mixed effect analysis which shows the reach-stratified flow model is better than the unstratified model for interpreting the BRGMON-1 results (Table 3.18 and Table 3.19). The Deviance Information Criteria (DIC) scores the predictive ability of each model. This is a Bayesian equivalent of AIC and weighs the benefits of the improvement in fit from adding more parameters (e.g., more β_F values for the stratified vs. unstratified models) and the costs to

precision of adding extra parameters. A model that has a DIC score that is lower by two units or more than another model is considered to have better predictive power. For log density, the stratified model is better for mykiss fry (RB-0), mykiss parr (RB-1), and coho fry (CO-0), and for log biomass the stratified model is better for mykiss fry and parr (so 5 of 8 cases) (Table 3.18). This result makes sense considering the flow effect sizes and their error bars in Figure 3.21 and Figure 3.22. Consider log density as an example: For mykiss fry, Reach 4 has much larger flow effects for Trials 1 and 2 compared to these effects in reaches 2 and 3. For mykiss parr and coho fry, reaches 3 and 4 show much bigger negative effects of the High flows compared to Reach 2.

Table 3.18 Deviance Information Criteria (DIC) scores for flow effects on log density and log biomass from the unstratified model (F) and the reach-stratified model (FR). Green highlighted cells indicate the better model (based on a DIC score lower than other model by 2 or more units)

Species-Age	Log Density (fish/m)			Log Biomass (g/m)		
	F	FR	ΔDIC	F	FR	ΔDIC
RB-0	-9.34	-12.88	-3.54	-9.88	-15.17	-5.29
RB-1	41.14	30.48	-10.66	42.59	28.62	-13.96
CO-0	56.59	53.16	-3.43	53.79	52.45	-1.34
CH-0	53.59	52.91	-0.68	48.96	51.37	+2.41

Table 3.19 Data r^2 (square of the Pearson correlation coefficient) and fixed effects r^2 (FE_r^2; see description in Section 2.9.4) values for describing fit and quantifying the explanatory ability of fixed effects. Orange highlight indicates negative FE_ r^2 values – due to model mis-specification (e.g., flow effect among reaches greater than effect across treatments – see Recchia 2010).

Species-Age	Log Density (fish/m)				Log Biomass (g/m)			
	Data_r^2		FE_r^2		Data_r^2		FE_r^2	
	F	FR	F	FR	F	FR	F	FR
RB-0	0.96	0.96	0.30	0.78	0.95	0.94	-0.95	0.72
RB-1	0.95	0.96	0.68	0.87	0.95	0.95	-0.66	0.89
CO-0	0.91	0.91	0.65	0.77	0.93	0.91	0.46	0.77
CH-0	0.90	0.90	0.56	0.70	0.88	0.86	0.44	0.62

Chinook fry (CH-0) was the only case where the DIC scores for unstratified and stratified models were close (i.e., each model had equivalent predictive power). This occurred because the differences in flow effects among reaches was smaller. Essentially, Chinook fry production was impacted in each reach since the start of the flow trials, so the extra parameters of the reach-stratified model were not necessary to predict the pattern for this species.

We can also use the FE_r^2 statistic to compare unstratified and stratified flow effect models (Table 3.19). This statistic is the proportion of the variation in the predicted log density (or

biomass) across the 68 (fry) or 61 (parr) reach-year strata that is explained by the fixed effects (i.e., the reach and flow effects ρ_r and ϕ_f). For density, FE_r^2 for the stratified model (FR) is much higher than for the unstratified model (F). This is also the case for log biomass. The negative FE_r^2 values for mykiss fry and parr for log biomass is not an error. This can happen when there is a mis-specified model (see an explanation of this phenomenon in Recchia 2010). In these cases, the effects in Reach 4 relative to the other reaches are much greater for some treatments (e.g., Trials 1 and 2) but not others (e.g., High and Post-high flows) (Figure 3.22).

The reach-stratified model also highlights the reach-specific losses in fish density and biomass under the high flows for mykiss fry (in all reaches), mykiss parr (in reaches 3 and 4), and coho fry (in reaches 3 and 4), relative to the previous flow trials (Figure 3.21 and Figure 3.22). And it shows the relative degree of recovery for mykiss fry and coho fry (and lack of recovery for mykiss parr and Chinook fry) among reaches since the return to the Trial 2 hydrograph in 2019 and 2020 (shown as "PH 6" on the plots). These differences (calculated as $\Delta\beta_F$) can be readily determined from model outputs among any of the flow treatments (e.g., PH 6 vs Trial 2) for each species and reach as a means of quantifying the relative changes.

Reach 1 Results

Two years of stock assessment sampling results were available for Reach 1 (2019 and 2020) which enabled comparison of abundance results among all four reaches of the Lower Bridge River for the Post-high flow years (Figure 3.23). Analysis of 2020 sampling data from Reach 1 yielded abundance results by species/age class of approx. 24,000, 3,000, 14,000, and 8,000 for mykiss fry, mykiss parr, coho fry and Chinook fry, respectively (Figure 3.23 Top Right). The abundance pattern among species-age classes in 2020 was similar to 2019, but numbers were up slightly from the 17,000, 1,000, 10,000, and 4,000 reported for those species-ages for that year (Figure 3.23 Top Left).

The totals for all species in Reach 1 were ~32,000 fish in 2019 and ~49,000 fish in 2020, which represented one-quarter and just over one-third of the total juvenile salmonid production (i.e., ~127,000 in 2019 and ~136,000 in 2020) in the study area as a whole for those years, respectively. However, Reach 1 constitutes nearly half (i.e., 20 km) of the total length of the study area (i.e., 40.9 km). Therefore, lineal densities (# of fish per km) were the lowest in Reach 1 for each species and age class among all the reaches in 2019 (Figure 3.23 Bottom Left). However, lineal densities in Reach 1 were on par with Reach 4 for mykiss fry, mykiss parr, and coho fry, and slightly higher than the other reaches for Chinook fry in 2020, at this stage of post-high flow recovery (Figure 3.23 Bottom Right).

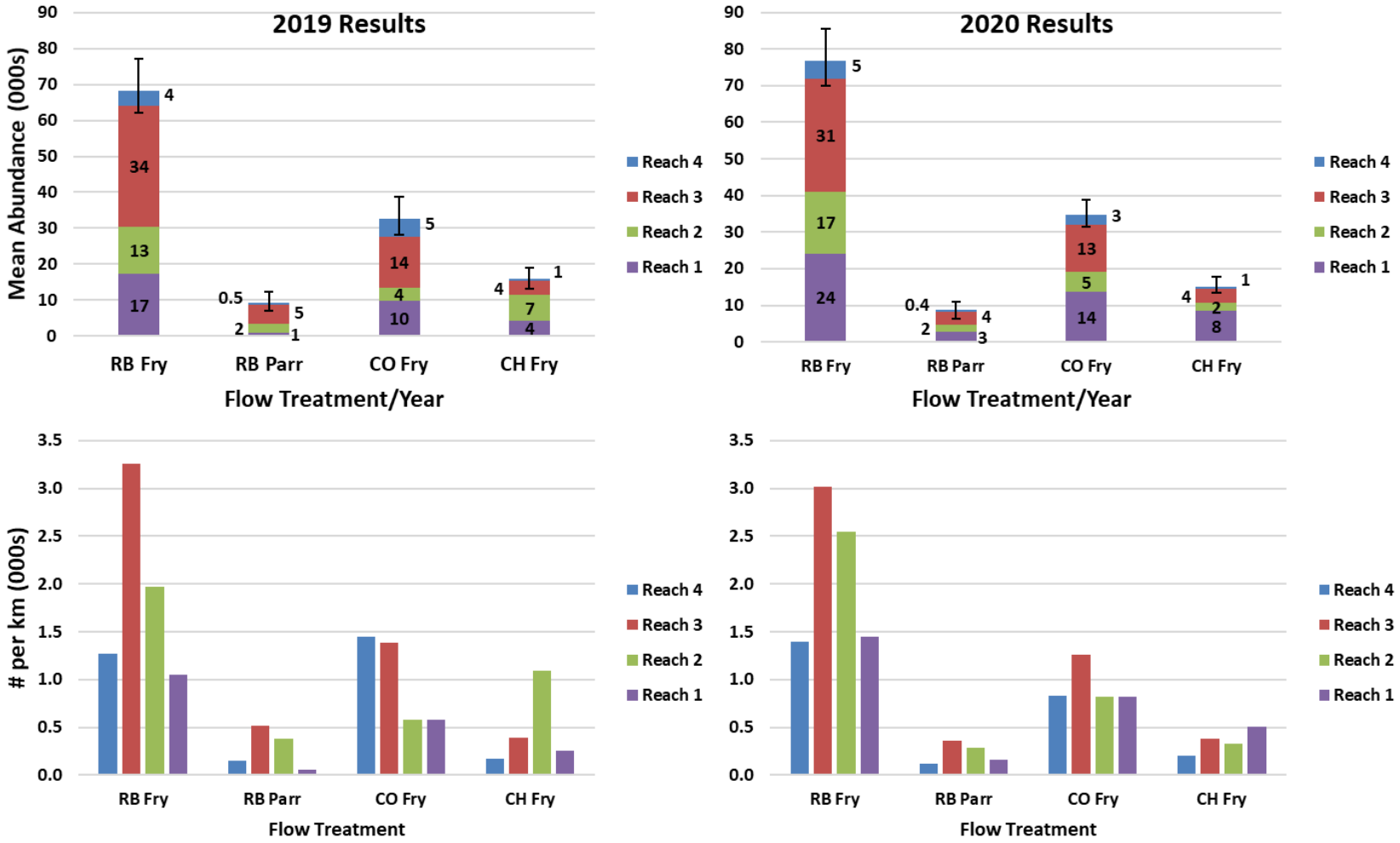

Figure 3.23 **Abundance (in thousands) of mykiss fry (RB-0), mykiss parr (RB-1), coho fry (CO-0) and Chinook fry (CH-0) among reaches of the Lower Bridge River (Top), and lineal densities (# of fish per km) by species and reach (Bottom). The left-side plots show 2019 results and the right-side plots show 2020 results. Vertical lines in the top plot show 90% credible intervals from posterior distributions of abundance for each year from the hierarchical Bayesian model.**

3.4.3. Enhanced Off-channel Habitats

Juvenile Salmonid Seasonal Habitat Use

A set of pre-selected sites were sampled for juvenile salmonids in two off-channel habitats (Bluenose in Reach 4 and Applesprings in Reach 1; see Appendix A for locations and maps of these sites) at the peak of the Post-high flow hydrograph in late spring (13-14 June) and early summer (16-17 July) in 2020. Sites were open and sampled in a single pass so there was no way of determining differences in capture probability among sites or sample sessions, but we divided the 1-pass catch by the distance sampled to generate relative lineal densities (# of fish per 100 m) for each species and age class by site to facilitate some comparisons (Figure 3.24). These data are also intended to serve as a "baseline" for lower flow releases (i.e., the Trial 2 peak) against which results collected during any future high(er) flow releases can be compared for addressing Management Question #7 (see Section 0). A potential shift in habitat use (from mainstem to off-channel) would be determined by detecting an increase in the lineal density of fish in the off-channel habitats that coincides with the timing of the flow increase from Terzaghi Dam and is different than the patterns in lineal densities documented under baseline conditions.

For juvenile salmonids in the off-channel habitats, coho densities were the highest, particularly in the Applesprings habitat in June (Figure 3.24, middle plot). Site-specific densities in June 2020 were: 209, 0, 327 and 132 fish/100 m in the upper, middle, lower, and outflow channels at Applesprings, respectively, and 0 and 152 fish/100 m in the pond and outflow channel at Bluenose, respectively. Site-specific densities for coho in July 2020 were: 234, 72, 114 and 20 fish/100 m in the upper, middle, lower, and outflow channels at Applesprings, respectively, and 2 and 87 fish/100 m in the pond and outflow channel at Bluenose, respectively. In general, the densities of juvenile coho declined from June to July at both habitats: from an average of 167 to 110 fish/100 m at Applesprings and 76 to 45 fish/100 m at Bluenose. The vast majority of coho juveniles in these off-channel habitats were fry (*n*= 370 out of 373 or 99%); however, three were coho parr based on size (*n*= 1 in June and *n*= 2 in July).

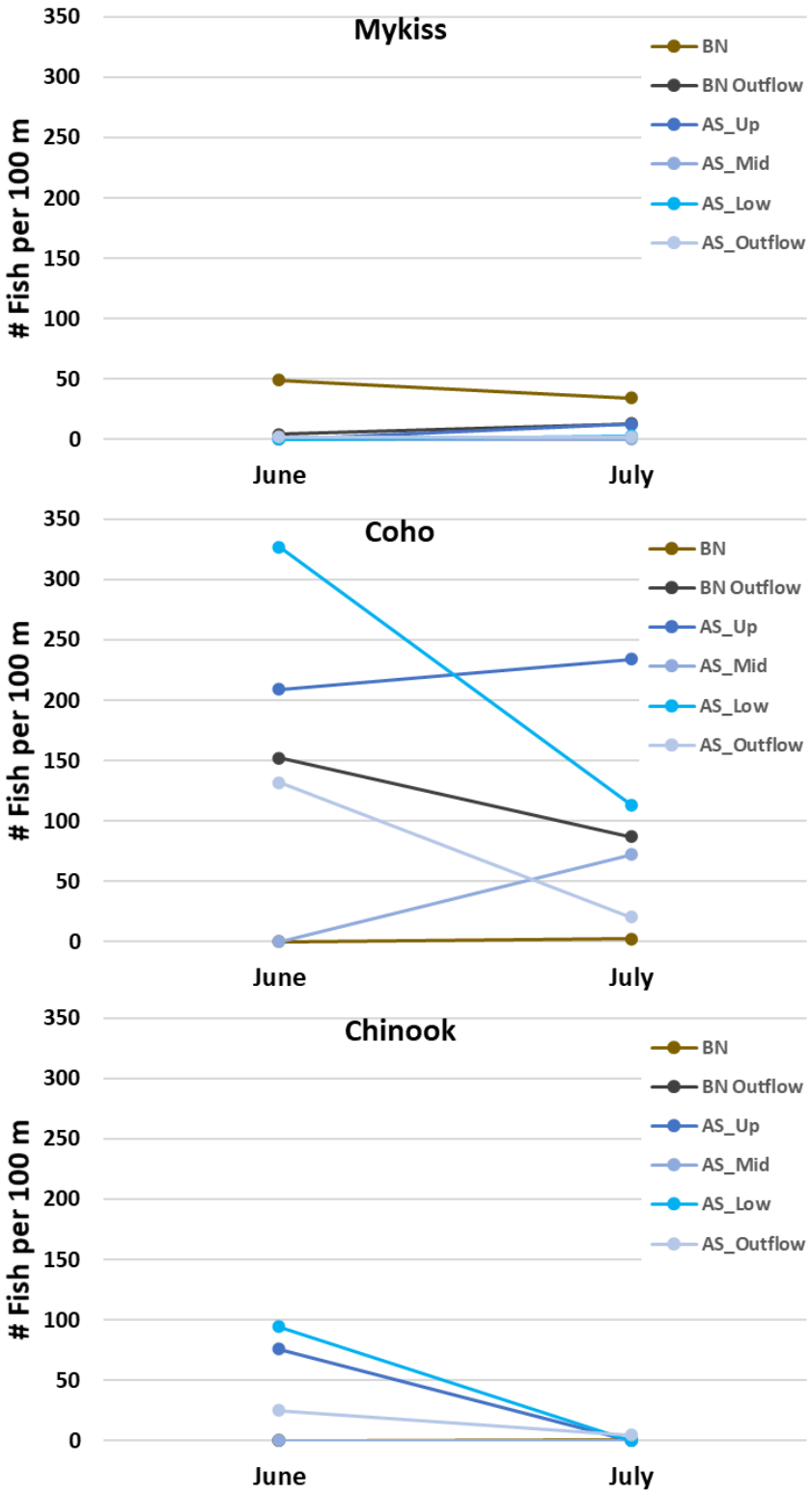

Figure 3.24 Relative numbers of mykiss (top), coho (middle), and Chinook (bottom) juveniles in various sections of two off-channel habitats during peak flow releases (i.e., 15 $m^3 \cdot s^{-1}$) from Terzaghi Dam (BN = Bluenose; AS = Applesprings). Sampling occurred in mid-June and mid-July 2020 to represent spring and summer rearing.

Chinook juveniles were the next most abundant species in the off-channel habitats in June, although their densities were substantially lower than for coho, and they were almost exclusively in the Applesprings habitat (Figure 3.24, lower plot). Site-specific densities in June 2020 were: 76, 0, 94 and 25 fish/100 m in the upper, middle, lower, and outflow channels at Applesprings, respectively, and 0 fish/100 m at both sites in the Bluenose habitat. Site-specific densities for Chinook in July 2020 were: 5 fish/100 m in the Applesprings outflow channel, 1 fish/100 m in the Bluenose pond, and 0 fish/100 m at every other site. Overall, the densities of juvenile Chinook declined substantially from June to July at Applesprings (from an average of 49 to 1 fish/100 m) and were very low at Bluenose during both sessions (0 and <1 fish/100 m). All of the Chinook were fry based on size.

Mykiss juveniles tended to show a different pattern than the other two species (Figure 3.24, top plot). They were the least abundant in the sample in June, were more prevalent in the Bluenose habitat, and their densities remained about the same between the June and July sessions overall. Site-specific densities in June 2020 were: 0 fish/100 m in the upper, middle and lower channels, 2 fish/100 m in the outflow channel at Applesprings, and 49 and 4 fish/100 m in the pond and outflow channels at Bluenose, respectively. Site-specific densities for mykiss in July 2020 were: 13, 0, 3 and 2 fish/100 m in the upper, middle, lower, and outflow channels at Applesprings, respectively, and 35 and 13 fish/100 m in the pond and outflow channel at Bluenose, respectively. Overall, the densities of juvenile mykiss did not change substantially between the June and July sessions at both habitats: from an average of 1 to 4 fish/100 m at Applesprings and 27 to 24 fish/100 m at Bluenose. The vast majority of mykiss sampled in the off-channel habitats during these sessions were parr (*n*= 112 out of 118, or 95%); however, the slight increase in density at some sites in July was due to the arrival of the new year-class of mykiss fry (*n*= 6) which had emerged and begun colonizing the sites by the time of the July sample. This was similar to the timing of emergence noted for this species during flow trials 1 and 2 (Sneep and Hall 2012a).

Other species captured in the off-channel habitats were: redside shiner (*n*= 42), mountain whitefish (*n*= 33), dace sp. (*n*= 15), sucker sp. (*n*= 12), and sculpin sp. (*n*= 2), which constituted 16% of the total fish sampled (n= 656, all species combined). Densities and trends were not evaluated for these other species since analysis is focussed on the change in habitat use by target species (mykiss, coho and Chinook).

Juvenile Salmonid Density and Biomass

The Bluenose off-channel habitat located in Reach 4 had high densities of mykiss fry (RB-0; Table 3.20), as well as a decent number of mykiss parr (RB-1). Densities of juvenile coho (CO-0) were very low at Bluenose, and no Chinook juveniles (CH-0) were caught. The Applesprings habitat in Reach 1 had high densities of juvenile coho and lower densities of juvenile Chinook and mykiss. The Bluenose site had much higher densities of mykiss fry and parr compared to the mainstem in fall of 2020, while the Applesprings site had much higher densities of coho fry compared to densities in the mainstem of Reach 1 in 2020 (Figure 3.25, top and bottom panels).

Table 3.20 Catch, capture probability (pCap), abundance, density, and biomass of juvenile salmonids at enhanced side channel sites in fall of 2020. Note: the suffix "RI" and "PO" in the site names denotes riffle and pool habitats, respectively.

Sp-Age	Site	Catch	pCap (per pass)	Abundance	Density (#/100 m^2)	Biomass (g/100 m^2)
RB-0	Bluenose_RI	40	0.62	42	78	131
	Bluenose_PO	99	0.62	105	140	449
	Applesprings_RI	30	0.81	30	24	150
	Applesprings_PO	0				
RB-1	Bluenose_RI	6	0.27	9	17	358
	Bluenose_PO	7	0.44	8	11	426
	Applesprings_RI	6	0.67	7	6	216
	Applesprings_PO	0				
CO-0	Bluenose_RI	3	0.60	3	6	35
	Bluenose_PO	5	0.63	6	8	81
	Applesprings_RI	82	0.85	82	66	764
	Applesprings_PO	48	0.25	83	116	750
CH-0	Bluenose_RI	0				
	Bluenose_PO	0				
	Applesprings_RI	16	0.63	17	14	261
	Applesprings_PO	0				

The densities in these enhanced off-channel sites in 2020 were very similar to the average densities for each species and age class in these sites in 2018 (i.e., the last high flow year), higher than in 2019 (the other Post-high flow year), and the same or higher than densities in the mainstem LBR during trials 1 and 2 (see Figure 3.17 in Sneep et al. 2020).

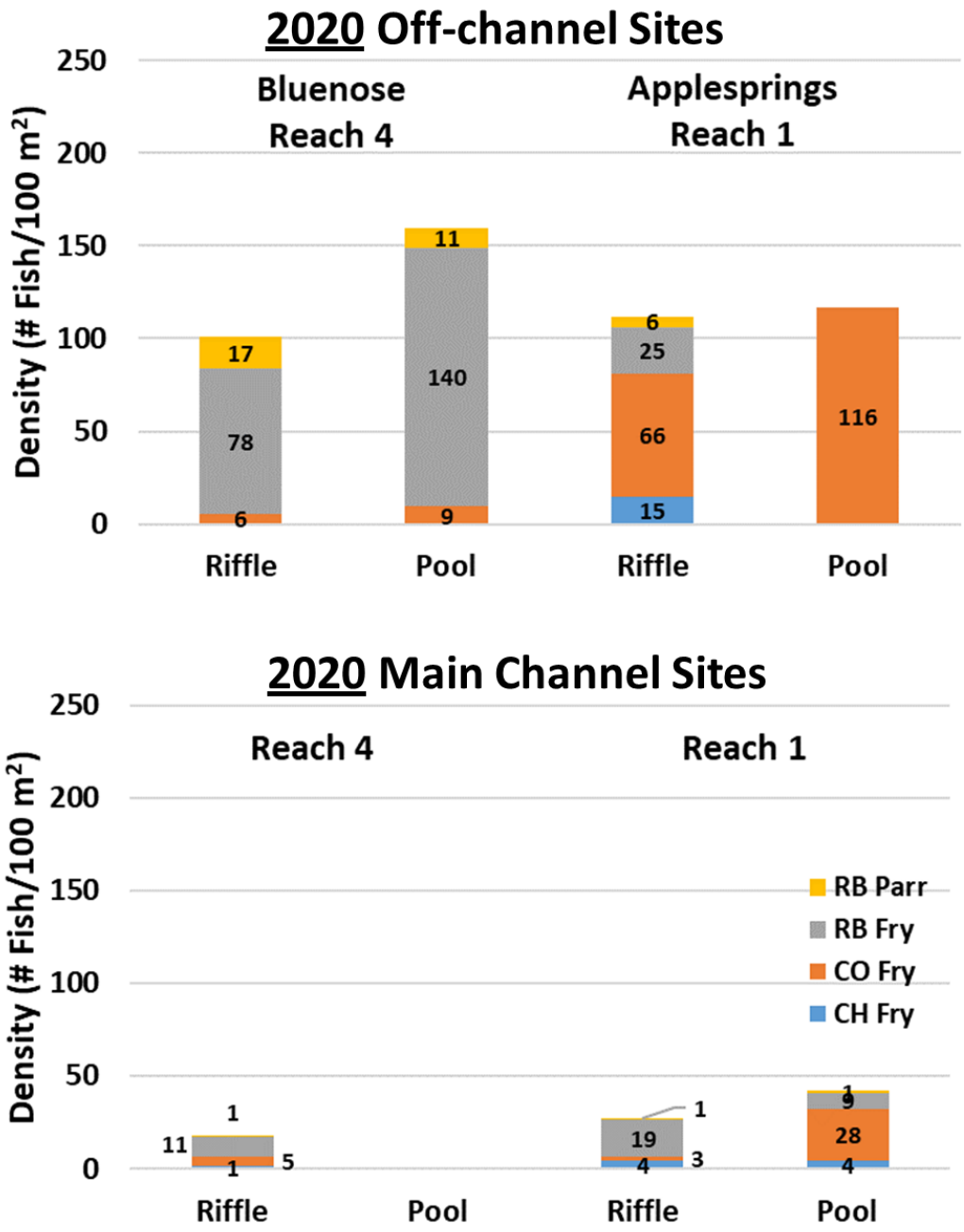

Figure 3.25 Density of juvenile salmonids in off-channel habitats in fall of 2020 (left) by habitat type compared to mainstem densities during the same time period in 2020 (right).

The sum of abundance estimates for juvenile salmonids in 2020 at Bluenose (~1,500) and Applesprings (~10,000) was ~11,500 fish, which was ~8% of the number of fish in the mainstem across reaches 1 – 4 in 2020 (~136,000) (Figure 3.26). This off-channel abundance estimate was higher than in 2018 (~6,500 fish) and 2019 (~1,100 fish) and represented a fair contribution considering the difference in wetted area (i.e., ~1 ha for the off-channel habitats vs. ~100 ha in the mainstem for reaches 1 to 4). However, this also reveals that an area significantly larger than

the Applesprings and Bluenose offchannel habitats would be required to meaningfully contribute to fish production in the Lower Bridge River and compensate for lost production in the main channel caused by high flows.

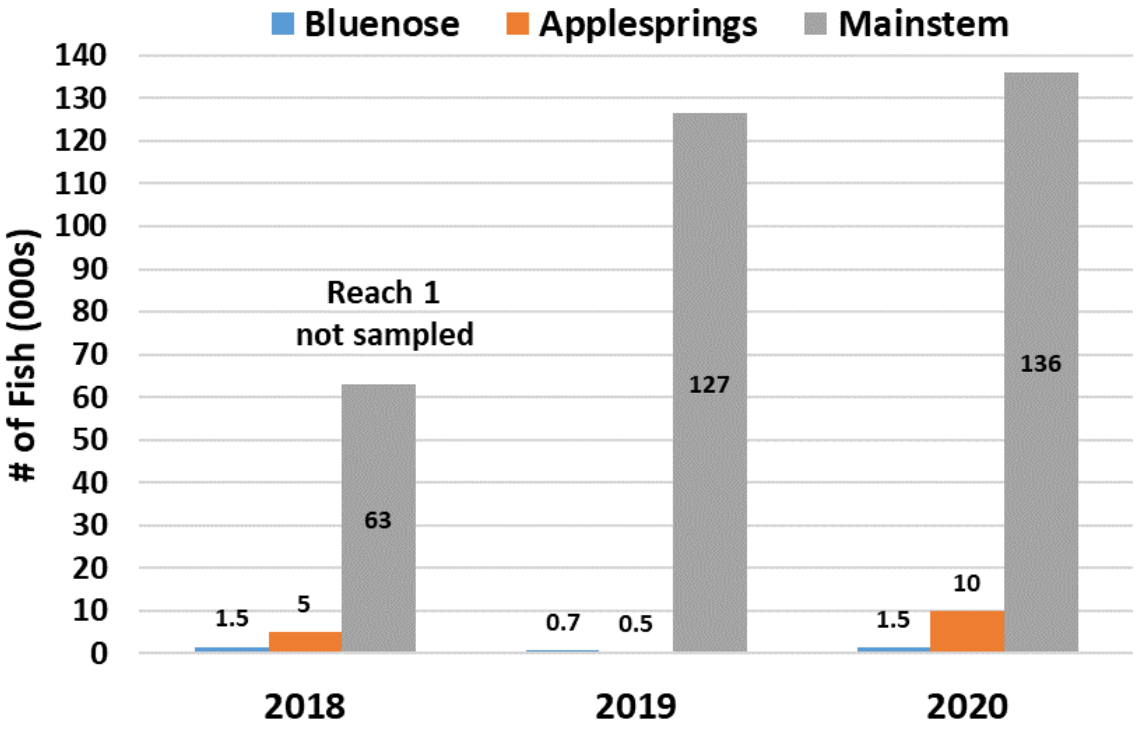

Figure 3.26 Total juvenile salmonid abundance estimates for the two off-channel habitats and the mainstem LBR (reaches 1 to 4 combined) in the three years since stock assessment sampling in the off-channel habitats began. 2018 was the last high flow year and 2019 & 2020 were Post-high flow years. Note: The 2018 mainstem abundance does not include Reach 1 which was sampled for the first time in 2019.

3.4.4. Stock-Recruitment

As noted in previous annual reports, the shift in escapement-fry stock-recruitment curves for coho and Chinook across different flow treatments reflected the changes in fry abundance seen in the juvenile abundance analysis. The newest data points reflecting the 2019 and 2020 fry abundance estimates which corresponded to the 2018 and 2019 spawner escapements for coho and Chinook were not applied to any of the existing curves since they reflect the first two years of post-high flow conditions (considered a new treatment). As such they are shown as stand-alone points on the plots and we simply compare them to the other existing curves for this analysis.

The maximum likelihood estimate for coho spawner escapement in 2019 was 214 (95% confidence intervals: 152–301) for reaches 3 and 4 (White et al. 2021). This was the lowest AUC-based estimate for coho since 2015 (174). It was paired with the 2020 coho fry abundance estimate of 21,430 (90% credible intervals: 17,900–25,500). The maximum likelihood estimate for Chinook spawners in 2019 was 161 (95% confidence intervals: 84–310) for reaches 3 and 4 (White et al. 2021). This estimate was on par with previous estimates in 2008 (164), 2013 (168), 2015 (158), and 2017 (120). However, as White et al. 2021 report, there were insufficient radio tag and visual tag data to estimate observer efficiency and survey life for 2019, so average values were used. As was the case in 2018, Chinook spawner estimates were again influenced by the operation of a broodstock collection fence installed at the bottom of Reach 3 on 20 August 2019. The fence caused substantial up and down cycling below it as well as handling and removals for broodstock collection which may have affected the number of spawner observations during the streamwalks after it was installed. Also, the migration obstruction in the Fraser River caused by the Big Bar slide resulted in increased prevalence of Chinook salmon from other watersheds straying into the LBR (more on this in Section 0). Each of these factors had the potential of confounding the reliability of the Chinook escapement estimate for both 2018 (fence) and 2019 (fence + strays). The 2019 escapement estimate was paired with the 2020 Chinook fry estimate of 6,710 (90% credible intervals: 4,940–9,340), which was the lowest recruitment value for this species since monitoring began in 1996.

It must be noted that the reliability of the stock-recruit analysis for estimating production capacity within the study area and determining when stock size may be limiting juvenile recruitment for each flow treatment is wholly dependent on the quality of both the stock and recruit estimates. If the installation of the broodstock collection fence will continue to preclude the collection of reliable spawner escapement data, as was the case in 2018 and 2019, then we will not have reliable data for updating the stock-recruitment curves going forward. If the operation of the fence can be compatible with the MON-3 spawner escapement monitoring (i.e., through effective collaboration between these programs) such that reliable estimates are still possible then these curves can continue to be updated.

Coho fry abundance increased under the Trial 1 and Trial 2 treatments relative to the Trial 0 pre-flow period (Figure 3.27). The magnitude in the shift of the stock-recruitment curve for coho fry (e^{λ}) was 2.9, 2.3, and 0.35 for Trial 1, Trial 2, and the Modified Operations High Flow years, respectively. That is, for a given level of escapement, the stock-recruitment model indicates an approximate 2- to 3-fold increase under trials 1 and 2 relative to pre-flow conditions, respectively, and a reduction by 65% under high flows. The 2020 datapoint for coho was near the origin of the x-axis and below the escapements for the Trial 2 years (range: 410 – 3,563), which had the same hydrograph, but within the low-end of escapements during Trial 1 that produced many more fry (see 2005 and 2009 datapoints in Figure 3.27). The 2020 datapoint was also near the asymptote of the Pre-flow curve and recruitment each year since the start of the high flows in 2016 have been low relative to the previous flow trials. Taken together, and given the uncertainty in the escapement estimate, we cannot readily rule out whether the 2019 spawner escapement could have been a contributing factor limiting coho fry recruitment in 2020, in addition to other possible factors such as in-river habitat conditions, nutrient supply, or food source availability.

The points in Figure 3.27 result in a steep initial slope which is not uncommon for coho populations where escapement and smolt production has been monitored (Korman and Tompkins 2014). However, it is important to note that the estimated initial slope for this set of curves hit the boundary of our maximum assumed value (1500 egg/female x 0.5 females/total spawners x 50% egg-fry survival rate = 375 fry/spawner) and would be unrealistically steep if we had not constrained this parameter.

Assuming a lower maximum initial slope (e.g., 37.5 fry/spawner based on a 5% egg-fry survival rate) constrains the curves to a much greater extent (Figure 3.28). In this case, there are many data points that have escapements that are less than required to maximize fry production. These more constrained curves are rather different than the set described above yet provide a near equivalent fit to the data (due to the wide scatter of points and limited *n* size for defining each curve). The difference in log-likelihood measuring the fit of the curves in Figure 3.27 and Figure 3.28 is less than 2 units and therefore one set of curves cannot be considered more reliable than the other based on fit alone. The stock-recruitment curve in Figure 3.28 implies that the population has been under-seeded during the High flow years and in 2020 (as it would be for several Trial 1 and 2 years also). More data are required (i.e., at a range of escapement levels) to better define the initial slope of the stock-recruitment relationship to strengthen inferences about potential spawning stock limitation and determine which set of curves are a more reliable indicator of flow effects on coho fry production in the LBR.

The escapement-fry stock-recruitment curve for Chinook also had a very steep initial slope that was constrained by our assumption that it could not exceed 1250 fry/spawner (5000 eggs/female x 0.5 females/spawner x 50% egg-fry survival rate, Figure 3.29). The stock-recruitment λ values indicate that recruitment under the Trial 1 and Trial 2 flow treatments and during the Modified Operations High Flow years were 0.74-fold, 0.46-fold, and 0.44-fold lower than under the pre-

flow conditions (Figure 3.29). Owing to the steep initial slope on this set of curves (based on 50% egg-to-fry survival) there is no clear indication that Chinook escapements have been limiting fry abundance among the flow treatments, and the 2020 datapoint was within a large cluster of datapoints near the origin on the x-axis. However, like the case for coho, the initial slope of the stock-recruitment curve for Chinook depends on the maximum initial slope constraint. When we lower egg-fry survival to 5% (initial slope constraint = 5000 x 0.5 x 0.05 = 125 fry/spawner) the model makes the unlikely prediction of a positive effect of the flow treatments on Chinook production capacity relative to the pre-flow conditions (Figure 3.30). Yet, again, this more constrained curve provides a near equivalent fit to the data (the likelihood difference between fits is less than 2 units), which highlights the limitations on drawing firmer conclusions based on the available data.

Given the current uncertainty regarding which set of curves (i.e., based on 50% vs 5% egg-fry survival) are more reliable for both of these species, the stock-recruit data are not yet ideal for allowing us to confidently differentiate flow effects from potential stock size effects (escapement). Though there is a fairly large sample size overall (*n*= 20 data points for coho and *n*= 22 datapoints for Chinook), the data must be parsed according to flow treatment because we have observed different levels of production due to variable incubation and rearing conditions under the different flow trials (i.e., a flow treatment effect; see Section 3.4.2). As a result, there is a much smaller *n* size for defining the initial slope of each individual curve. Characterization of fecundity, male:female spawner proportion, and egg-to-fry survival for the LBR populations would provide in-situ data to address the set of assumptions currently applied to the stock-recruitment model; however, we would not have these data for past years and flow treatments to understand how these parameters may also have changed over time.

As such, though the stock-recruitment analysis is a bit of a crude tool for the purposes of this program, it does suggest that changes in escapements among years may have been a less significant driver than flow treatment effects on juvenile production for these species to-date, but that escapements at the low end of the range during the Modified Operations years (High flows and Post-high flows) could be contributing to slower recovery from the effects of the high flows. Applying the annual escapement estimates as an additional covariate in the mixed effects model (described in Sections 2.9.4 and 3.4.2) could be another means of formally testing the effects of spawner stock size and the degree to which it accounts for the variability in the annual juvenile abundance estimates within and among the flow treatments. This could be an appropriate approach for the Year 10 final synthesis report (see Section 5 – Recommendations).

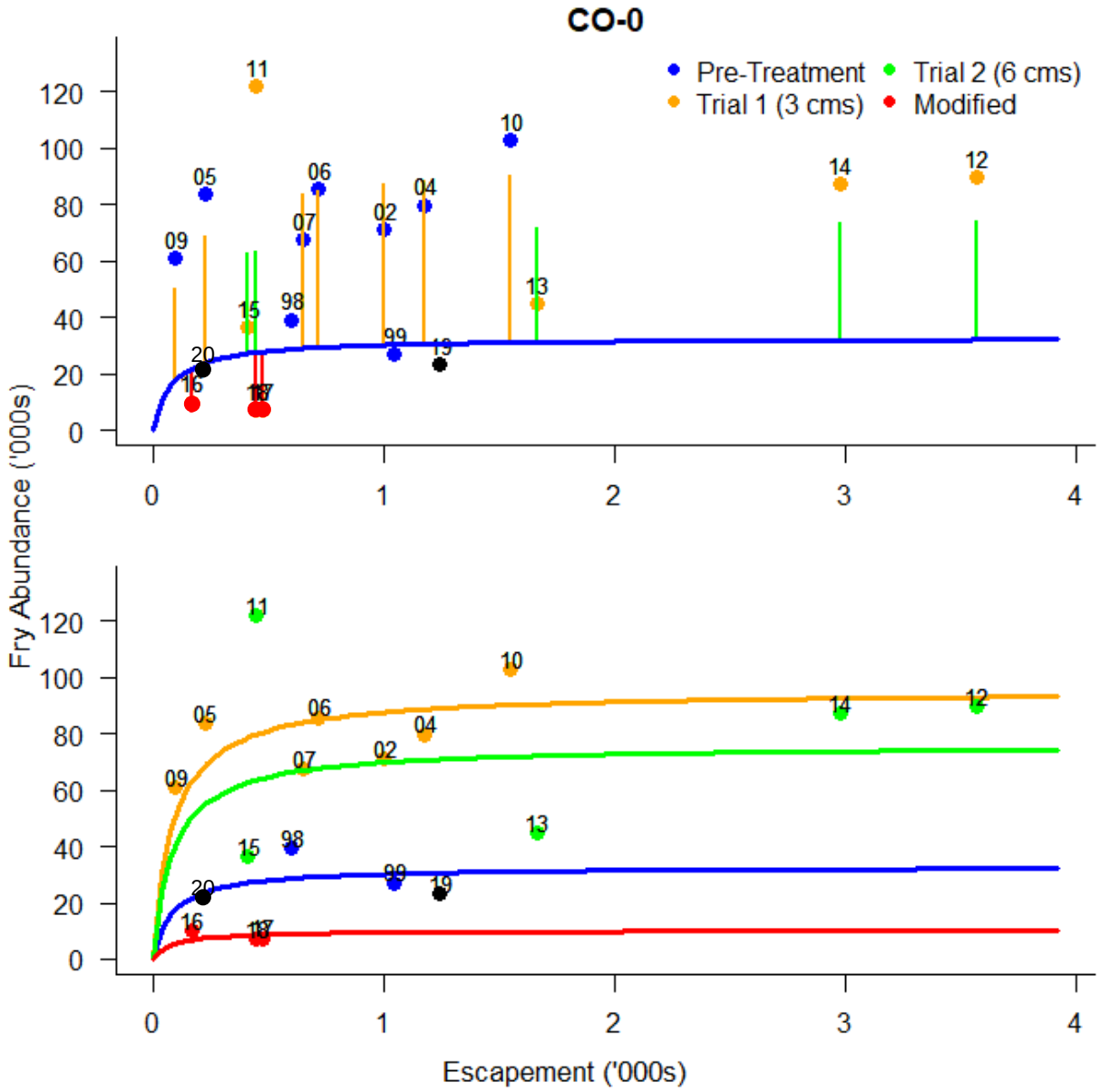

Figure 3.27 Spawner-fry coho Beverton-Holt stock-recruitment curves fit assuming a maximum initial slope of 375 fry/spawner (50% egg-fry survival rate). Points show annual estimates of escapement and fry abundance with the label beside each point showing the recruitment year. The blue line in the top plot shows the base stock-recruitment curve under pre-flow conditions (Trial 0). The vertical lines in the top plot show the shift of the base stock-recruitment curve for the other three flow treatments. The bottom plot shows the treatment-specific stock-recruitment curves (e.g. the curve that results from drawing a line through the ends of the vertical lines in the top plot). The 2019 and 2020 points (black dots) were not used in fitting any of the existing curves since they represent the start of a new flow treatment (Post-high flows).

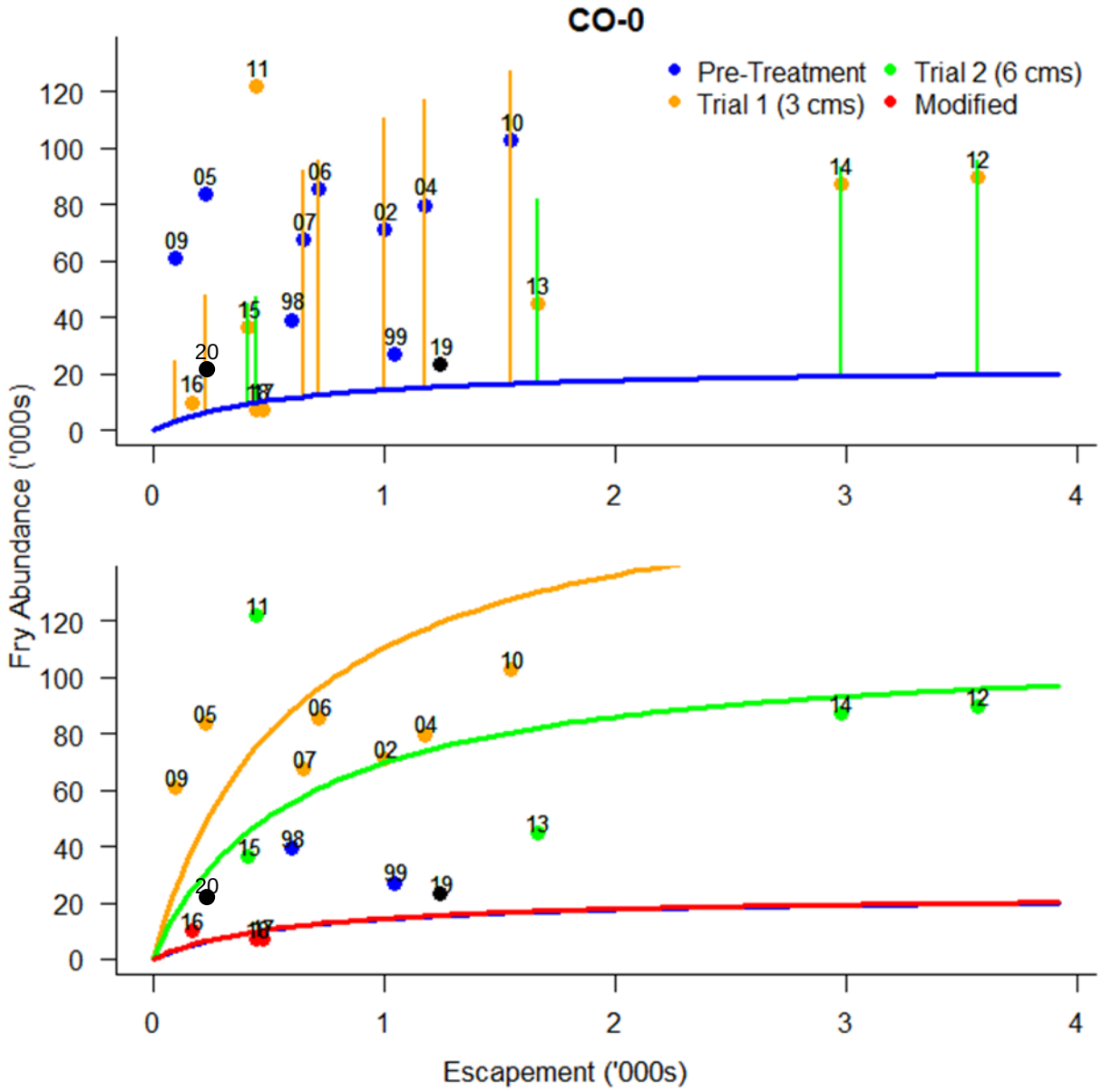

Figure 3.28 Spawner-fry coho Beverton-Holt stock-recruitment curves fit assuming a maximum initial slope of 37.5 fry/spawner (5% egg-fry survival rate). See caption for Figure 3.27 for additional details.

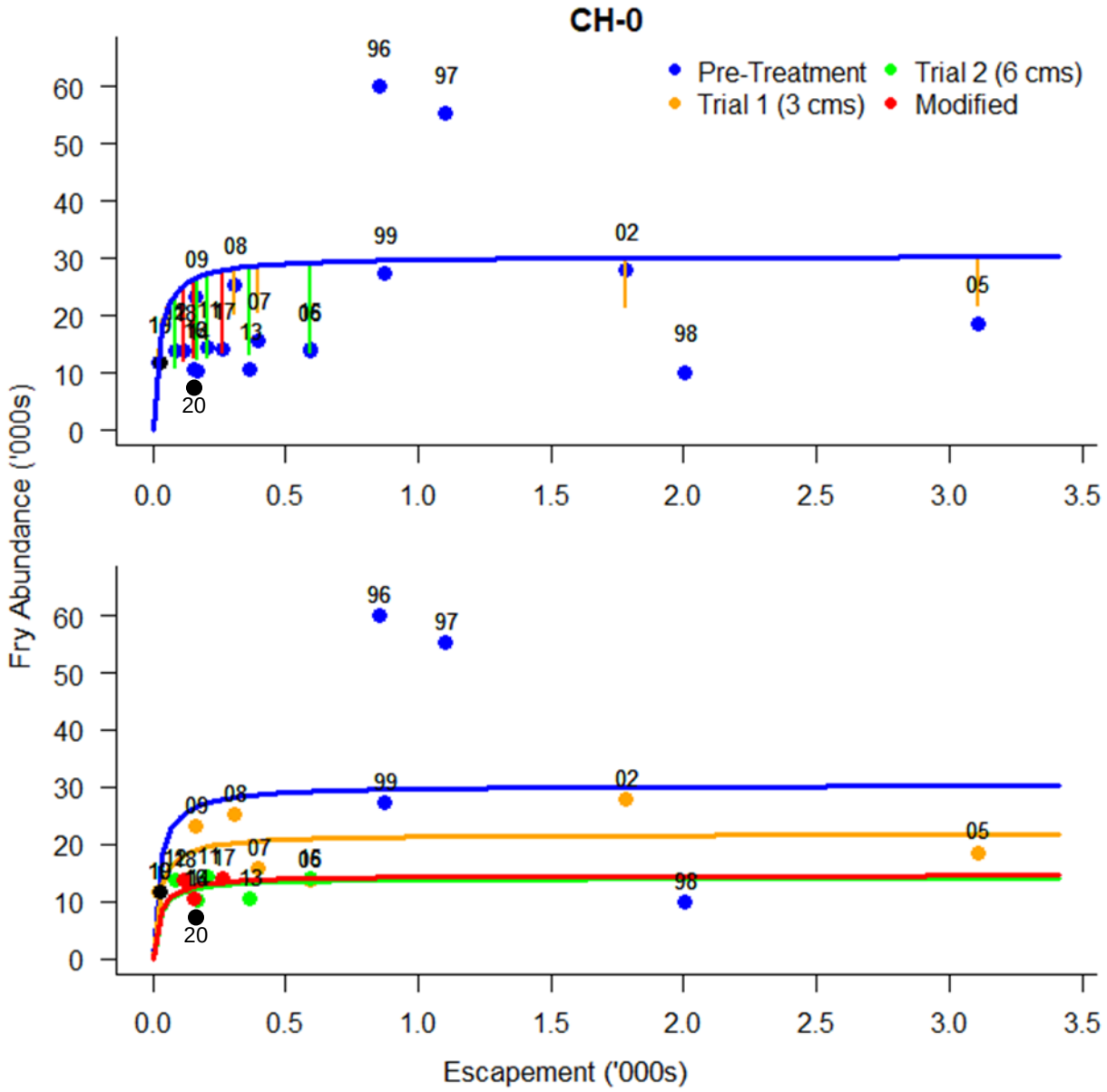

Figure 3.29 Spawner-fry Chinook Beverton-Holt stock-recruitment curves fit with a constraint that assumes a maximum egg-fry survival rate of 50% (maximum initial slope of 1250 fry/spawner). See caption for Figure 3.27 for details.

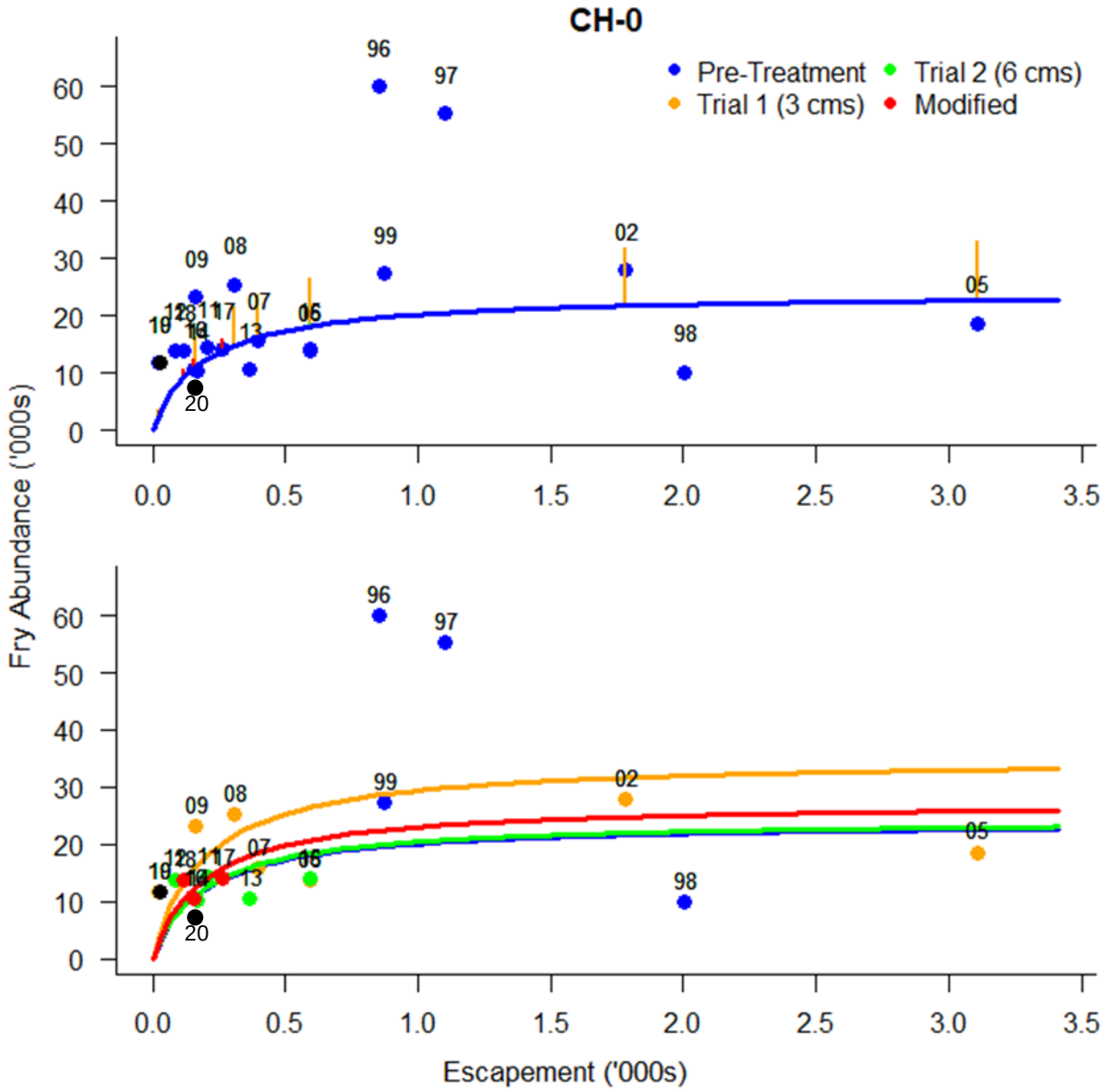

Figure 3.30 Spawner-fry Chinook Beverton-Holt stock-recruitment curves fit with a constraint that assumes a maximum egg-fry survival rate of 5% (maximum initial slope of 125 fry/spawner). See caption for Figure 3.27 for details.

3.4.5. Genetic Stock Identification of Bridge River Chinook Salmon Juveniles

The following are the results of the genetic stock identification analyses that were done on juvenile Chinook salmon collected from the Lower Bridge River. These results were taken directly from the summary report provided by PBS (Wetklo and Sutherland 2021):

> *"Genetic stock identification (GSI) by cBayes (Neaves et al., 2005) of the 2020 Bridge River juveniles identified eight stocks or GUs [Appendix E, Table E2]. In this sample of 117, three individuals failed to genotype and eight were identified as non-Chinook. Of the remaining 106 samples, almost half (45.7%) were assigned to Bridge, 11.4 % were assigned to GU1, 1.9% to GU2, and 36% of the GSI assignments were rejected since their probabilities were less than 75%. It was not surprising that many of the assignments by GSI were of low probability since this approach assumes pure form stocks and not admixed stocks for its baseline populations. For this reason it is best suited to the identification of pure form individuals. The individual GSI results are found in [Appendix E, Table E3].*
>
> *The graphical outputs from the Structure analysis are shown in [Appendix E, Figure E1]; baseline or juvenile individuals are each represented by a coloured vertical bar that depicts their Structure inferred genetic ancestry. Differentiated populations or GUs were each assigned a single dominant colour (k): North Thompson Mainstem is light blue; Bridge River is green; Taseko River is yellow; Tete Jaune is medium blue; GU3 is magenta; GU2 is red; GU1 is sky blue; and GU4b is navy blue) [Appendix E, Table E1]. While each population or GU was characterized by a dominant Structure inferred genetic ancestry, in some cases this ancestry was shared between populations and/or GUs (eg. the dominant Structure inferred genetic ancestry in GU1 was observed in GU2 populations Nazko and West Road as well but to a lesser extent). The two remaining "populations" (i.e., mustard and orange) were seen exclusively in the Bridge juvenile samples and were attributed to related individuals. Parentage analysis confirmed that there were at least three full-sib families with between three and four progeny each; two of the families also shared one common parent (i.e., mustard). The Structure inferred mean Bridge ancestry for the 10 iterations and consensus stock assignment (or admixture source) for individual juveniles are given in [Appendix E, Table E3].*
>
> *While the 1996 Bridge baseline and 2020 juvenile samples both contained individuals with primarily Bridge ancestry, the juvenile sample was distinguished by it admixed nature [Appendix E, Figure E1]. Using Structure, it was estimated that as many as 71.7% of the 2020 juveniles had primarily Bridge ancestry and were most likely the progeny of two pure form Bridge Chinook spawners [Appendix E, Table E2]. The remainder of the juveniles showed evidence of admixture resulting from stray Chinook spawning with pure form Bridge spawners. The most common parental pairing implicated was GU1 strays spawning with pure form Bridge Chinook; 12 of the 106 juveniles (11.3%) had GU1 ancestry [Appendix E, Table E2].*
>
> *The two analytical approaches applied in this study of Bridge River Chinook juveniles were found to be in agreement 77.6% of the time (i.e., in 67 comparisons; [Appendix E, Table E4]). These comparisons give us the most reliable estimate of the proportion of juveniles*

with Bridge ancestry and those with admixed ancestry. Thus we would estimate that at least 64% of the Chinook juveniles sampled in 2020 were the progeny of pure form Bridge spawners. In addition, there is good evidence to suggest that Mid-Fraser (i.e., Taseko, GU3, GU2, and GU1) and Upper Fraser (i.e., GU4b) strays were successful spawners in Bridge River, producing admixed progeny. GU1 Chinook were the most successful stray spawners in terms of numbers of juveniles, accounting for 7.5% of the admixed Bridge juvenile Chinook."

3.5. WUP Ramp Down Monitoring and Fish Salvage

In several of the tables and figures throughout this section, comparable ramping information from the other modified operations years (i.e., ≥2016), as well as ramping results from the Trial 2 years (i.e., rampdown range 15 to 1.5 $m^3 \cdot s^{-1}$) have been included along with the 2020 results, for reference.

Ramp downs from peak flows (i.e., between 15.1 and 3.0 $m^3 \cdot s^{-1}$) occurred on eight days between 21 July and 7 August 2020, representing a total flow reduction of 12.1 $m^3 \cdot s^{-1}$ across that period (Figure 3.31 and Table 3.21). This rampdown timing occurred approx. 2 weeks earlier than the comparable rampdowns in 2019 and during Trial 2 (2011 to 2015). Final ramp downs from 3.0 to 1.5 $m^3 \cdot s^{-1}$ (i.e., flow reduction of 1.5 $m^3 \cdot s^{-1}$) were completed on 5 and 6 October 2020, which was similar to the usual timing from previous years. For additional information on flow and stage changes for each rampdown event, refer to the tables in Appendix F. Total stage change at the 36.8 km compliance location was 57 cm, and the maximum daily stage change rate implemented was 2.7 cm/hr (Table 3.22). Some higher hourly ramp rates compared to other years (between 4.0 and 4.6 cm/h) were implemented in 2017, 2018 and 2019, with the intent of determining whether there is a correlation between ramping rate and the incidence of fish stranding within the survey area.

Based on stage monitoring conducted during ramp events by the field crews and the hourly stage elevation data recorded by loggers deployed in reaches 2, 3 and 4, a gradient of stage change across the length of the study area was evident (Table 3.21). Within the flow range released from the dam in 2020 (max = 15.1 $m^3 \cdot s^{-1}$; min = 1.5 $m^3 \cdot s^{-1}$), the total stage change was 92 cm at the Terzaghi Dam plunge pool (Reach 4; Rkm 40.9), 57 cm near the Reach3/Reach 4 boundary (a.k.a. the compliance location; Rkm 36.8), 51 cm at the fish fence site (bottom of Reach 3; Rkm 26.1), 17 cm at the horseshoe bend (Reach 2; Rkm 23.6), and 24 cm at Camoo (Reach 2; Rkm 20.0). The gradient was similarly evident on each individual ramping date (and in the stage change data from 2019). The substantial reduction in stage elevation changes in Reach 2, relative to reaches 3 and 4, highlights the moderating effect of the Yalakom inflows on stage changes associated with flow reductions at the dam (within the Trial 2 hydrograph range). This finding supports the understanding that fish stranding risk is lower in reaches 1 and 2 due to the moderated stage changes and that fish salvage at discharges ≤15 $m^3 \cdot s^{-1}$ is not required in these reaches.

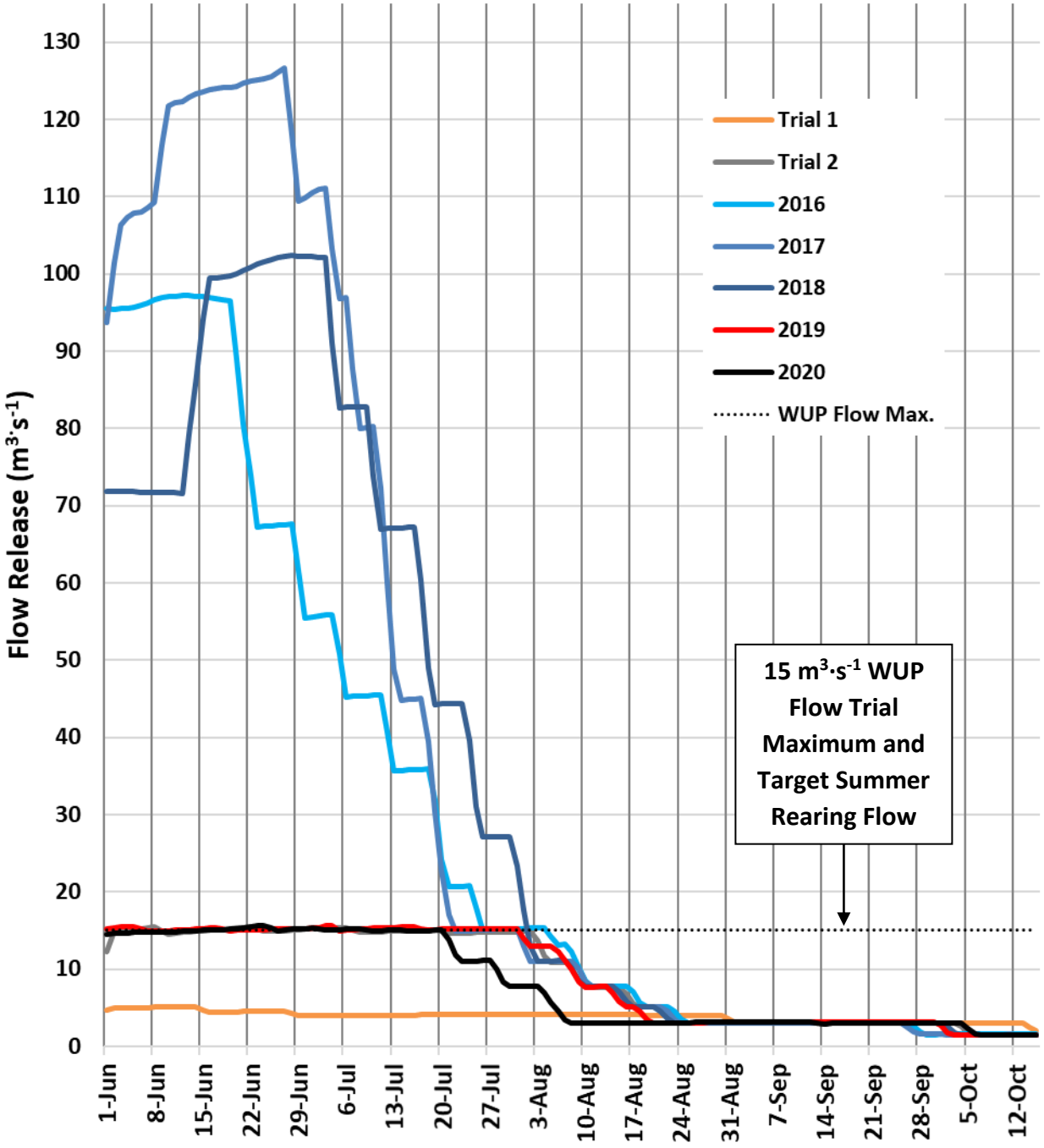

Figure 3.31 Schedule of flow releases and ramp downs from the peak period to the start of the fall low flow period in 2019 and 2020. For reference, WUP Trial 1 and 2 flow releases as well as the 2016–2018 high flow years are shown for the same period.

Table 3.21 Summary of stage changes at available monitoring locations in reaches 2, 3 and 4 for each rampdown event in 2019 and 2020 (under the Trial 2 hydrograph).

Year	Date	Event #	Start Flow ($m^3 \cdot s^{-1}$)	End Flow ($m^3 \cdot s^{-1}$)	Flow Change ($m^3 \cdot s^{-1}$)	Stage Change (cm)				
						Plunge Pool (Rkm 40.9)	Top of Reach 3 (Rkm 36.8)[a]	Bottom of Reach 3 (Rkm 26.0)	Horseshoe Bend (Rkm 23.6)	Bottom of Reach 2 (Rkm 20.0)
2019	1 Aug	1	15.2	12.9	-2.3	-11	-6	-5	-3	-4
	6 Aug	2	13.0	11.1	-1.9	-11	-5	-6	-1	-3
	8 Aug	3	11.1	9.3	-1.8	-9	-5	-5	-2	-2
	9 Aug	4	9.3	7.7	-1.6	-9	-5	-5	-1	-3
	14 Aug	5	7.7	6.4	-1.3	-8	-5	-4	-1	-3
	15 Aug	6	6.4	5.1	-1.3	-9	-6	-6	-2	-3
	18 Aug	7	5.1	4.1	-1.1	-10	-5	-5	-1	-2
	19 Aug	8	4.1	3.0	-1.1	-9	-6	-6	-1	-2
	1 Oct	9	3.2	2.1	-1.0	-11	-8	-6	-1	-2
	2 Oct	10	2.1	1.5	-0.6	-10	-6	-5	-1	-1
2019 Rampdown Summary			**15.2**	**1.5**	**-13.7**	**-96**	**-60**	**-51**	**-15**	**-25**
2020	21 Jul	1	15.1	12.9	-2.2	-9	-6	-5	-2	-3
	22 Jul	2	13.0	11.0	-2.0	-10	-6	-6	-2	-4
	28 Jul	3	11.1	9.3	-1.8	-9	-3	-5	-2	-3
	29 Jul	4	9.3	7.7	-1.6	-8	-4	-5	-2	-3
	4 Aug	5	7.7	6.4	-1.3	-8	-4	-4	-2	-3
	5 Aug	6	6.4	5.1	-1.3	-8	-6	-5	-2	-2
	6 Aug	7	5.1	4.1	-1.0	-9	-5	-4	-1	-1
	7 Aug	8	4.1	3.0	-1.1	-11	-6	-7	-3	-3
	5 Oct	9	3.0	1.7	-1.3	-14	-11	-8	-2	-3
	6 Oct	10	1.7	1.5	-0.2	-6	-3	-2	0	-1
2020 Rampdown Summary			**15.1**	**1.5**	**-13.6**	**-92**	**-57**	**-51**	**-17**	**-24**

[a] This location represents the compliance location for stage changes associated with ramp down events.

Table 3.22 Summary of flow ramp down events across the high flow range (>15 $m^3 \cdot s^{-1}$) and "normal" Trial 2 range (≤15 $m^3 \cdot s^{-1}$) during Modified Operations years (2016–2020). Note: Flow releases did not exceed the WUP flow targets in 2019 or 2020 so high flow ramp downs were not required in those years. For more details on individual events refer to the tables provided in Appendix F.

Period	Year	Month(s)	# of Ramping Days	Total Flow Reduction ($m^3 \cdot s^{-1}$)	Total Stage Change (cm)	Maximum Hourly Rate (cm/hr)
High Flow Ramp Events (>15 $m^3 \cdot s^{-1}$)	2018	Jul	8	-86.9	-122	-4.0
	2017	Jun – Jul	9	-96.5	-143	-4.1
	2016	Jun – Jul	8	-81.4	-108	-2.3
"Normal" Ramp Events (≤15 $m^3 \cdot s^{-1}$)	**2020**	**Jul/Aug, Oct**	**10**	**-13.6**	**-57**	**-2.7**
	2019	Aug, Oct	10	-13.7	-60	-4.6
	2018	Aug, Oct	9	-13.6	-62	-2.0
	2017	Aug, Sep	9	-13.7	-67	-2.6
	2016	Aug, Sep	10	-13.8	-67	-3.0

Coupling the BC Hydro flow release records with the continuous river stage level recorded at 36.8 km (known as the compliance location for tracking ramp rates) enabled characterization of the discharge-stage relationship at that location (Figure 3.32). The plot includes the stage-discharge data points for every year since 2016 (the start of the high flows).

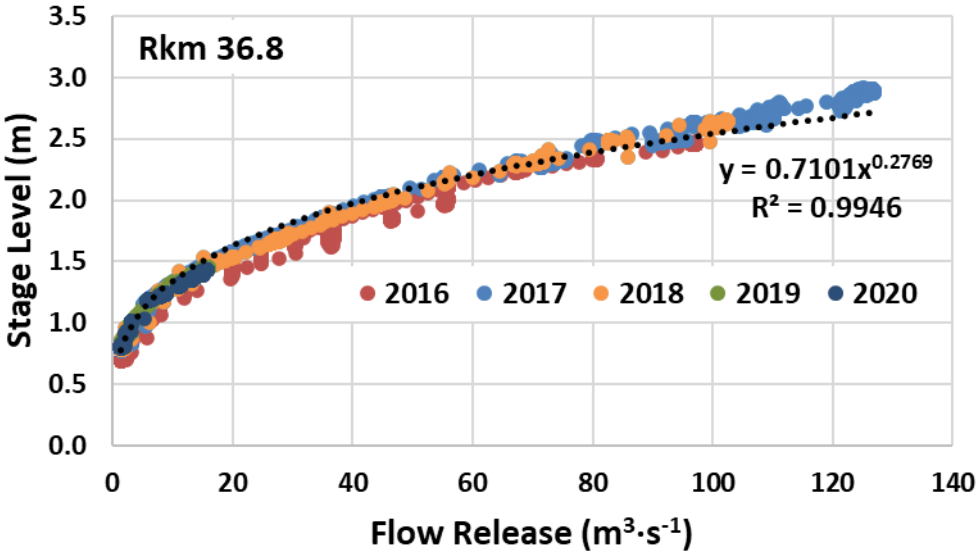

Figure 3.32 Discharge-stage relationship at 36.8 km (the compliance location) across the range of flows observed across all flow treatments. Separate data points for each Modified Operations monitoring year (2016-2020) are shown.

The curve drawn through the points has a good fit (R^2 = 0.995), such that the associated equation ($y = 0.7101x^{0.2769}$) may be useful for predicting stage changes for particular flow changes within

this range. Stage values for discharges between 10 $m^3 \cdot s^{-1}$ and 60 $m^3 \cdot s^{-1}$ tended to be a bit lower in 2016, possibly due to some channel changes at the gauging location that have occurred with the high flows since then, so the current curve is based on the 2017, 2018 and 2019 data points. The curve may underestimate stage elevations for discharges >100 $m^3 \cdot s^{-1}$. It is clear from the relationship that the greatest degree of stage changes occurs at the lowest discharges (i.e., the initial slope is the steepest). Above ~10 $m^3 \cdot s^{-1}$ the slope begins to decrease, and the discharge-stage relationship becomes close to linear across the higher flows.

As a result of the surveys conducted during the 2020 flow ramp down events, sites with the potential for fish stranding were documented at 3 fewer locations relative to the 20 locations that had been identified for the 15 to 1.5 $m^3 \cdot s^{-1}$ flow range during the previous Trial 2 and High flow years (2011 to 2018), bringing the current total to 17 unique locations to be monitored (in reaches 3 and 4 only; Figure 3.33). However, active fish salvaging was only required at 11 of the 17 sites in 2020. Crews noted that channel morphology or flow conditions had changed at several locations following the years of high flows, which resulted in the identification of four new sites in 2019 and rendered some others obsolete. An additional 35 locations were identified for the high flow range (>15 $m^3 \cdot s^{-1}$) across all four reaches of the Lower Bridge River during 2016–2018; however, fish salvaging was not required at these sites in 2019 or 2020 since flows did not exceed 15 $m^3 \cdot s^{-1}$ (± 5%).

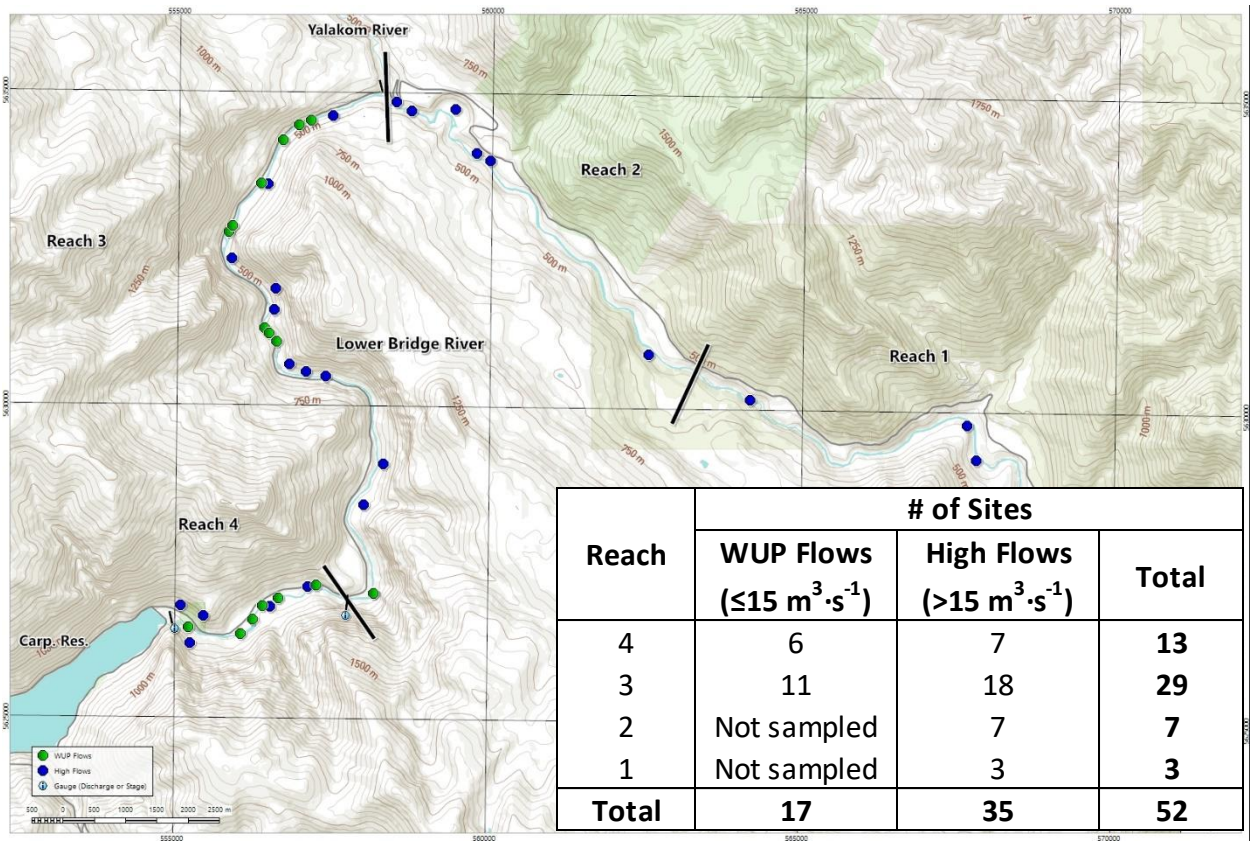

Reach	# of Sites		
	WUP Flows (≤15 $m^3 \cdot s^{-1}$)	High Flows (>15 $m^3 \cdot s^{-1}$)	Total
4	6	7	**13**
3	11	18	**29**
2	Not sampled	7	**7**
1	Not sampled	3	**3**
Total	**17**	**35**	**52**

Figure 3.33 Survey area map for ramp monitoring and fish salvage on the Lower Bridge River showing fish salvage locations for WUP flows in 2020 (green dots), and Modified Operations high flows (blue dots), which were not sampled in 2020. Discharge and stage gauging locations are represented by the blue information symbol (i). Solid black lines represent the reach breaks. A table summarizing the number of sites is also included (inset).

Fish salvage numbers for the ramp downs across the Trial 2 range (≤15 $m^3 \cdot s^{-1}$), including the 2020 data points, were generally higher relative to the results for the high flow range (>15 $m^3 \cdot s^{-1}$; Figure 3.34). In previous years (≤2016), crews had noted incidental catches (fish salvaged before their strand-risky habitat had become isolated from the main channel flow or dewatered); however, for consistency with the 2017–2019 results, these incidental catches were not included in the analyses or the results reported here.

Inclusive of the results from all available survey years, there appears to be a fairly distinct flow threshold where the fish stranding risk transitions from high risk (>100 fish per 1 $m^3 \cdot s^{-1}$ flow change) to moderate or low risk (10 to 99, and <10 fish per 1 $m^3 \cdot s^{-1}$ flow change, respectively), as defined in the Fish Stranding Protocol for the Lower Bridge River (Sneep 2016). This threshold flow appears to be at ~13 $m^3 \cdot s^{-1}$, similar to the flow value where the transition in the stage-discharge relationship occurs (see Figure 3.32), which was again apparent from the 2020 data. However, it must also be noted that substantially lower abundance of juvenile fish (particularly coho and steelhead fry that are generally the most vulnerable to stranding) were documented

for all three high flow years (see Section 3.4.2). Relative to the Trial 2 averages, abundance of coho and steelhead fry was down by 90% and 70%, respectively, during the high flow years. As such, the confounding effect of low abundance (due to displacement out of the survey area or poor survival) on the high flow fish salvage results cannot be ruled out.

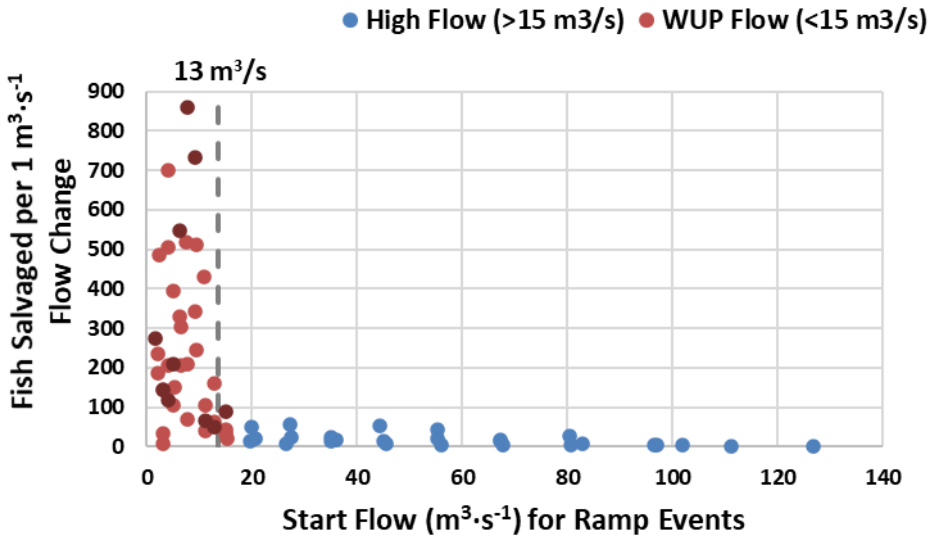

Figure 3.34 Relative differences in number of fish salvaged per increment of flow change for ramp downs from high flows (>15 $m^3 \cdot s^{-1}$) versus Trial 1 and 2 flows (≤15 $m^3 \cdot s^{-1}$). The vertical dashed line represents the approximate flow threshold (~13 $m^3 \cdot s^{-1}$) where the apparent break between high stranding risk and moderate or low stranding risk occurs. Circles with black border represent 2020 data; Plain circles are data from previous years.

Compared to survey results from the previous Trial 1 and Trial 2 years, relatively large areas of fish stranding habitat were documented within the high flow range (2018 total = 66,892 m^2), primarily due to the addition of stranding site reconnaissance and salvage surveys in reaches 2 and 1 (Table 3.23). Note: only the most recent high flow year is presented for comparison because stranding area changed to some degree with each consecutive high flow event. Potential stranding area contribution by reach was 4,887, 9,105, 22,900 and 30,000 m^2 for reaches 4, 3, 2, and 1, respectively. Under the trial flow range (≤15 $m^3 \cdot s^{-1}$) in 2020 when only reaches 3 and 4 were surveyed, the total stranding area was 8,493 m^2 (compared to 13,992 m^2 for those two reaches at the high flow range), and stranding area was again more prevalent in Reach 3 than Reach 4 (7,163 and 1,330 m^2, respectively).

Across the high flow range (>15 $m^3 \cdot s^{-1}$) in 2018, the highest proportion of salvaged fish per stranding habitat area was in Reach 3 (~8 fish per 100 m^2; Table 3.23). The values for the other reaches were relatively small (≤3 fish per 100 m^2). Within the Trial 2 flow range (≤15 $m^3 \cdot s^{-1}$) in 2020, fish stranding densities were greater, and the highest proportion was in Reach 4 followed by Reach 3 (57 and 46 fish per 100 m^2, respectively). These values were at the low end of the

range documented for the ≤15 $m^3 \cdot s^{-1}$ flows under the previous flow treatments that were characterized by much higher juvenile salmonid abundance (i.e., Trials 1 & 2 means = 81 (range = 51 to 123) and 63 (range = 48 to 75) fish per 100 m^2 of salvaged area in reaches 3 and 4, respectively; Sneep 2016). Reaches 1 and 2 have not been surveyed within the trial flow range.

Table 3.23 Summary of fish stranding area and numbers of fish salvaged by reach for 2018 high flow (>15 $m^3 \cdot s^{-1}$) and 2020 trial flow (≤15 $m^3 \cdot s^{-1}$) ranges. Note: there was no data for fish stranding or salvage in reaches 1 and 2 under the trial flows.

Flow Range	Reach	# of Sites	Area (m^2) (% Contribution)	# of Fish	# of Fish per 100 m^2
2018 High Flows (>15 $m^3 \cdot s^{-1}$)	4	7	4,887 (7%)	125	3
	3	11	9,105 (14%)	710	8
	2	4	22,900 (34%)	551	2
	1	3	30,000 (45%)	413	1
High Flow Totals		**25**	**66,892**	**1,652**	**3**
2020 Trial Flows (≤15 $m^3 \cdot s^{-1}$)	4	6	1,330 (21%)	753	57
	3	11	7,163 (79%)	3,272	46
	2	------ No data ------			
	1	------ No data ------			
Trial Flow Totals		**17**	**8,493**	**4,025**	**47**

With the benefit of fish salvage crews on the ground, some higher ramp rates (up to 4.6 cm/hr) were implemented in 2017, 2018 and 2019. In previous years, and in 2020, most ramp rates conformed to the ≤2.5 cm/hr threshold specified in the Water Use Plan (WUP; for when fish salvage crews are not present), even though crews were routinely deployed during all of those events. Based on the sample size available from 2017 and 2018, the higher ramp rates employed for ramp downs within the high flow range (>15 $m^3 \cdot s^{-1}$) did not increase the incidence of stranding at the flow levels tested (Figure 3.35). This suggests that for flows >15 $m^3 \cdot s^{-1}$ it may be possible to increase the ramp rate above the WUP threshold without unduly increasing the fish stranding risk.

For ramp downs within the Trial 2 range, the faster ramp rates implemented in 2019 were associated with greater incidence of stranding than for the high flows but were still within the range of salvage numbers for ramp rates ≤2.5 cm/hr for the other Trial 2 years. Collectively, these results suggest there can be some flexibility for strategically ramping flows down more quickly than would be possible using the WUP rate alone (i.e., to reach more optimal summer rearing flows, for instance). However, it is not possible to rule out the confounding effect of reduced abundance of the most strand-risky fish (i.e., coho and mykiss fry) in 2016 – 2019 relative to the Trial 2 years, as mentioned above. Testing faster ramp rates during years when juvenile salmonid

abundance is higher (e.g., similar to Trial 1 or 2 levels) would be necessary to address this uncertainty.

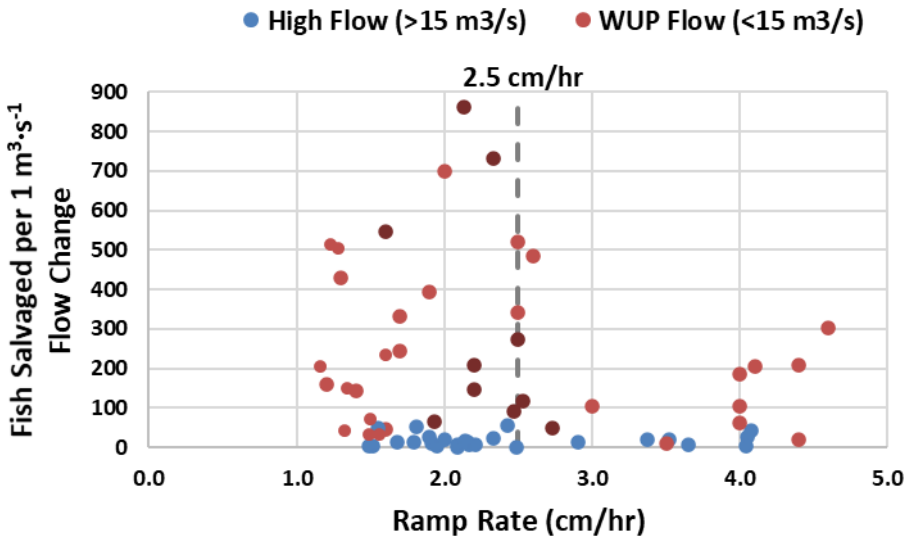

Figure 3.35 Relative incidence of fish stranding per increment of flow change according to different ramping rates under high flow (>15 $m^3 \cdot s^{-1}$; blue circles) and trial flow (≤15 $m^3 \cdot s^{-1}$; red circles) ranges. The vertical dashed line depicts the ramp rate (2.5 cm/hr) specified in the WUP when fish salvage crews are not present. Circles with black border represent 2020 data; Plain circles are data from past years.

Factoring in the reduced number of locations identified in 2020, the proportions of identified stranding sites on river left (76%) versus river right (24%) were not equal under the trial flows (≤15 $m^3 \cdot s^{-1}$), even though both banks were accessible to fish salvage crews across a significant part of that range (Table 3.24). Note that these proportions are based on reaches 3 and 4 only as reaches 1 and 2 were not surveyed at flows below 15 $m^3 \cdot s^{-1}$. Across the high flow range (>15 $m^3 \cdot s^{-1}$), the distribution was closer to equal with 44% on river left and 56% on river right based on the site reconnaissance conducted by staff from Coldstream Nature-Based Solutions (formerly Coldstream Ecology Ltd.) during 2016 – 2018.

Table 3.24 Proportions of sites on the river left bank versus the river right bank for trial flows (≤15 $m^3 \cdot s^{-1}$; based on reaches 3 and 4 only) and high flows (>15 $m^3 \cdot s^{-1}$; based on new site reconnaissance surveys during high flow years).

Flow Range	Left Bank		Right Bank	
	n	%	n	%
Trial Flows (≤15 $m^3 \cdot s^{-1}$) *Reaches 3 & 4 only	13	76%	4	24%
High Flows (>15 $m^3 \cdot s^{-1}$) *New Site Reconn.	8	44%	10	56%
All	**21**	**60%**	**14**	**40%**

As identified for past fish salvage surveys under flow trials 1 and 2 (≤15 $m^3 \cdot s^{-1}$), coho and mykiss were the most frequently encountered species under high flows (Sneep et al. 2019), and again under the WUP rampdown range in 2019 and 2020. Coho made up 50% of the total catch in 2019 and 45% in 2020 (Table 3.25). The contribution of mykiss fry to the salvage totals was also similar between 2019 and 2020 (47% and 49%, respectively). As noted in the Fish Stranding Protocol (Sneep 2016), coho and mykiss fry tend to be the most vulnerable to stranding because the habitat types preferred by this age class of these species (e.g., shallow edge areas and side channels/pools) are also among the habitat types that are most likely to dewater and result in fish stranding when flows are reduced. Fry may also remain in these habitats even as flows are dropping because they are less able to exploit deeper offshore areas where there are typically higher velocities, less cover, and increased risk of predation.

Table 3.25 Summary of numbers (and %) of fish salvaged by species-age class under WUP flow ramp downs (≤15 $m^3 \cdot s^{-1}$) in 2019 and 2020.

Species	WUP Flows (≤15 $m^3 \cdot s^{-1}$)	
	2019	2020
Chinook	13 (1%)	29 (1%)
Coho	1,012 (50%)	1,796 (45%)
Mykiss	948 (47%)	1,992 (49%)
Other spp.[a]	48 (2%)	208 (5%)
All	**2,021**	**4,025**

[a] Other species included: bull trout, mountain whitefish, redside shiner, and sculpins.

The least abundant of the target salmonid species in the salvage results were Chinook fry, which were encountered slightly more frequently in Reach 3 (2020 *n*= 17) than in Reach 4 (2020 *n*= 12) but contributed <1% to the total number of fish salvaged in 2019 and 2020 overall. Chinook fry can occupy some of the same habitats as coho and steelhead fry, but they tend to be larger (because they emerge earlier in the year) so they can exploit habitats further from the river margins that are less likely to dewater. Also, they have been much less abundant in the study area overall since the flow trials began, and particularly in reaches 3 and 4 (see Section 3.4.2).

Other species in the fish salvage catches were: bull trout (2019 *n*= 2; 2020 *n*= 13), mountain whitefish (2019 *n*= 2; 2020 *n*= 30), redside shiner (2019 *n*= 36; 2020 *n*= 157), and sculpin spp. (2019 *n*= 8; 2020 *n*= 8). The bull trout and mountain whitefish were almost exclusively salvaged in Reach 3 and the redside shiner and sculpin spp. were most prevalent in the Reach 4 catches. The low numbers of these species in the ramp down results relative to the target salmonid species was likely due to lesser abundance in the survey area, lower proclivity to stranding, or a combination of both. For the specific catch totals by species for each rampdown event, refer to Table F5 in Appendix F.

4. Discussion

4.1. Management Question 1

How does the instream flow regime alter the physical conditions in aquatic and riparian habitats of the Lower Bridge River ecosystem?

The data collected in 2020 added another set of results for the Post-High Flow period, which started in 2019. Flows in 2019 and 2020 followed the Trial 2 hydrograph throughout the year, rather than greatly exceeding 15 m^3/s peak flow in the spring, which characterized the 2016-2018 High Flow years. One of the goals of monitoring during the Post-High Flow years was to document how physical conditions, under a return to the Trial 2 hydrograph, compared to the previous Trial 2 years (i.e., 2011 to 2015) when flow releases were equivalent, as well as conditions under the preceding High flow years.

During the high spill years in 2016-2018, the volume of the Terzaghi flow releases during the peak flow period defined the physical and water chemistry of the entire Lower Bridge River. Terzaghi discharges during the peak flow period in 2016 – 2018 were 6- to 8-fold higher than the Trial 2 peak and were 3- to 7-fold higher than peak Yalakom inflows. These high flows had impacts on physical conditions within the study area including changes to wetted area, depths, velocities, water temperature, turbidity, bank erosion and substrate deposition (Sneep et al. 2019; Sneep et al. 2018; McHugh et al. 2017). Outside of the peak period, flow releases were the same as Trial 2 and in-season effects on physical conditions during those periods were the same as reported previously for Trial 2 (Soverel and McHugh 2016).

As reported by Ellis et al. 2018, the high flows were of sufficient magnitude to mobilize sediments in the river channel, coarsen the substrate in identified spawning areas (although subsequent monitoring has suggested that spawning habitat area is not limited relative to escapement sizes in the study area; Davey 2019), recruited sediments from active colluvial fans, and impacted embeddedness (increased interstitial pore depth but reduced pore density) within their monitored sites. For several of these measures there was a gradient of effect with greatest impacts closest to the dam, as well as spatial variability of both sediment grain size distributions and applied shear stress from the high flows. These changes associated with the 2016-2018 high flows (coupled with a declining trend in soluble-reactive phosphorus concentrations from upstream sources – see Figure 3.8) have altered physical habitat conditions in the study area relative to the pre-high flow conditions (i.e., during Trial 2) that may affect post-high flow recovery of the aquatic ecosystem and juvenile fish recruitment. This is the primary reason that conditions under the return to lower flows (i.e., according to the Trial 2 hydrograph) in 2019 and 2020 cannot be considered equivalent to the pre-high flow Trial 2 conditions even though the flow releases were equivalent. However, with only two years of Post-high flow data from 2019 and 2020 available to-date, understanding the linkages between these impacts and aquatic ecosystem recovery have just begun to be explored.

The Post-high flow sediment composition was characterized at the BRGMON-1 index monitoring locations (sites A-G and J-K in the LBR, and sites Yal_A and Yal_B in the Yalakom River) using the Wolman pebble count method for the first time in 2019. There was a slight difference in median particle size among the reaches with the largest D50 in Reach 4 (11.7 ±0.0 cm) and the smallest in the Yalakom River (3.5 ±0.4 cm). However, the sizes available at each of the sites were within the range of substrate classes that can support invertebrate colonization, salmon spawning and juvenile salmonid rearing. Further discussion of these results is included in the response to management question (MQ) #2, which follows. Unfortunately, this data collection was not repeated in 2020, but is recommended for monitoring years going forward in order to more fully characterize substrate composition at the monitoring sites and track changes among years and future flow treatments.

Estimated site-specific discharge estimates highlighted that flow conditions among sites in reaches 3 and 4 differed minimally throughout the year. The magnitude of combined tributary and groundwater inflows were relatively small in these reaches. However, the Yalakom River is a substantial contributor of inflow at the top of Reach 2, and this was again evident in 2020. As such, the estimated discharge rates for sites in Reach 2 were substantially higher (by 1.2 to 5.0x depending on the period of the year) than the estimates for the Reach 3 and 4 sites. During years with lower flow releases from Terzaghi Dam (including 2020), the Yalakom River inflow contributes a higher proportion of the total discharge in the lower reaches which dilutes or masks some of the physical and water chemistry characteristics of the release.

Under the Trial 2 hydrograph in 2020, river stage elevations varied by a total of 0.57 m between the spring peak and the winter low flows at the Rkm 36.8 monitoring location, and there was a gradient of effect with distance from the dam. Total stage changes across the Lower Bridge River were 92 cm at the Terzaghi Dam plunge pool (Reach 4; Rkm 40.9), 51 cm at the fish fence site (Reach 3; Rkm 26.1), 17 cm at horseshoe bend (Reach 2; Rkm 23.6) and 24 cm at Camoo (Reach 2; Rkm 20.0). Under the high flows from 2016 – 2018, the added discharge increased river stage by between 1.08 – 1.42 m above the Trial 2 peak (at the Rkm 36.8 site), but also reduced the proportional area of rearing habitat by increasing velocities beyond levels that juvenile fish could withstand throughout more of the channel. However, it was not possible to measure depths and velocities in mid-channel at the high flows using conventional field methods. Specific assessment of depths and velocities and changes to habitat area that meets rearing criteria will have to come from analysis of the 2D model outputs.

The water temperature profiles by reach during 2020 generally followed the patterns observed in other Trial 2 years: cooler temperatures in spring and warmer in the fall relative to the Pre-flow period (Trial 0) with a gradient of effect associated with distance from the dam. However, there were a couple of notable differences: temperatures were warmer than most other Trial 2 years in spring and summer, which was most evident in reaches 3 and 4, and there was also a period of warmer temperatures in September 2020 that was particularly evident in reaches 3, 2, 1 and the Yalakom River (Appendix D). The cause of the warmer water temperatures in

September 2020 were attributed to ambient temperature influence. Mean monthly air temperatures (recorded in Lillooet, BC) were warmer in September 2020 than they were in that month during the previous flow treatment periods.

The warmer temperatures in spring and summer may be due to an effect of "Modified Operations" on temperature profiles in Downton and Carpenter reservoirs (which are characterized by more frequent deep drawdowns and a reduced maximum fill elevation on Downton), since ambient temperatures in June to August in 2019 and 2020 were not notably warmer than this period during the previous flow trials. This effect was also observed during the High flow years and to a greater extent (Sneep et al. 2019). Nonetheless, the spring and summer temperatures recorded in 2019 and 2020 were still within optimal ranges reported in the literature for steelhead spawning and incubation, and rearing for each salmonid species (Brett 1952, Bjornn and Reiser 1991, Oliver and Fidler 2001).

Turbidity data were continuously recorded by loggers manufactured by RBR from March to November 2020. The pattern that emerged was relatively low turbidity (<10 NTU) in the mainstem LBR at the end of the winter period, rising to a snow-melt driven peak in the spring (value unquantified due to a firmware error with the loggers during this period), declining later in the summer (<10 NTU by August), rising to a second peak (near 60 NTU) in the fall as Carpenter Reservoir becomes isothermic and there is mixing among the depth layers, and then declining again to the winter low (<10 NTU) in November and December. Patterns of turbidity within the study area are primarily driven by the following factors: a) snow-melt (in the spring), b) Carpenter reservoir operations (low in the spring, filling and becoming thermally stratified in the summer, and then turning over in the fall), and c) inputs from the tributaries, primarily the Yalakom River, which have high turbidity during the freshet period (May to July) and low turbidity at other times of year (except during periodic rainfall events). These patterns and descriptions can be further fleshed out as additional turbidity monitoring data from subsequent monitoring years becomes available.

4.2. Management Question 2

How do differences in physical conditions in aquatic habitat resulting from the instream flow regime influence community composition and productivity of primary and secondary producers in the Lower Bridge River?

In the process of making structured decisions about what are preferred flows compared to others in the Bridge River, a technical working group suggested that benthic invertebrate diversity and abundance can be a useful proxy for river health (Failing et al. 2012). People believed that benthos provide insight into ecological processes centered not only on food for fish, particularly salmonids that are highly valued (Quinn 2018), but also on overall ecological processes. This belief is well founded in the scientific literature. The term, "river health" can be ambiguous (Boulton 1999), but in previous explanatory attempts, it refers to measurements that show

whether a river has sustainable and resilient structure and function (Costanza and Mageau 1999). Benthic invertebrates are particularly good indicators of these attributes because there are many taxa occupying many functional capacities (Cummins and Merritt 1996), they are relatively sedentary (data not confounded by movement), they are easily sampled, and responses to many types of disturbances are known among taxa (Norris and Thoms 1999). Links between benthic invertebrates and combinations of physical and chemical conditions are the basis of bioassessment that is favoured for testing river quality worldwide (e.g., Bailey et al. 2004, 2012; Nichols et al. 2014). The same arguments apply to algal periphyton. They have short life cycles, making them responsive to change in habitat, they are the first organisms to respond to environmental stress, and the first to recover from it (Lowe and Pan 1996, Smucker et al. 2013). In combination, periphytic algae and benthic invertebrates are ideal indicators of change to structure and function of the Lower Bridge River in relation to manipulation of flow.

The analytical foundation for testing effects of flow on the benthic communities was analysis of variance blocked among three categorical variables: Trial, Reach, and Pink salmon presence/absence. “Trial” was of particular interest because its four levels defined different flow regimes regulated by flow release from the Terzaghi Dam over years. A common approach for testing treatment effects on a large river is a Before After Control Impact design (Stewart-Oaten et al. 1986) in which a response variable is measured in years before and while (or after) a treatment is applied in a control and treatment reach (Johnston et al 1990, Rosario and Resh 2000, Smokorowski and Randall 2017). Statistical tests are then run to determine if the mean difference in the response variable between the control and treatment reach in the “before” years is different from the mean difference between the two reaches in the “after” years. Years are replicates in this layout. If the test shows a statistically significant difference, a conclusion is that treatment affected the response variable. This layout was not possible for the Bridge River because there was no suitable control reach (the entire set of reaches received the same flow treatment). As a result, we were limited to contrasting Trials, blocked by Reach and Pinks presence absence. Testing a Trial effect was similar to testing change in a response variable in a before - after layout. Given the large differences in flow regime between trials and no known regional change over years other than aspects of climate that would have affected all reaches the same way, this approach was considered reasonable. There is also a precedent. Bradford et al. (2011) used the same approach for testing the effect of flow trials on fish population metrics. We followed this approach.

Wetted habitat area increases logarithmically with flow in the Bridge River (Figure 3.3). This relationship is additive to the biotic response to flow for calculation of response over areas of whole reaches. A reported areal measure of biomass or density can be multiplied by change in wetted habitat area associated with flow to derive a reach-wide response. Given that all measurements of periphyton and benthic invertebrates occurred at the same low baseflow in the fall among years, there was little value in considering wetted area adjustments. Those

consistent fall flows produced similar wetted areas among biotic measurements among flow Trials and Reaches.

Although periphyton samples for taxonomic analysis in 2020 were lost (see explanation provided in Section 2.3), there is no reason to expect the assemblages would have differed greatly from those of previous years. Those earlier data showed that common benthic algae in the Lower Bridge River mostly included diatoms, blue greens, and chlorophytes (Sneep et al. 2020). These taxa are ubiquitous among mountain rivers (Wehr et al. 2014, Bowman et al. 2007, Goma et al 2005, Carpenter and Waite 2000, Hieber et al 2001). The small-celled genus *Achnanthidium* that occurred in all previous Bridge River samples has wide ranging environmental tolerances (Ponader and Potapova 2007). Other Bridge River diatoms including *Tabellaria* sp., and *Diatoma* sp. occur in widely varying nutrient conditions (Bothwell 1989) and *Encyonema, Eunotia, Gomphonema, and Nitzschia* are common in extreme physical conditions of alpine and mountain streams like the Bridge River (Rott et al. 2006). With the blue greens and chlorophytes that are also common in cool and fast streams (Bowman et al 2007), these diatoms are thought to be resilient due to fast recovery after scour events (Peterson 1996), formation of phosphatases to sequester phosphorus at extremely low concentrations and grow optimally at higher nutrient levels (Bothwell 1989), and shift assemblage patterns with temperature (DeNicola 1996). All taxa were potentially usable as food among grazing aquatic insects, particularly the EPT and dipterans that were common in the Bridge River (Junker and Cross 2014, Cummins and Merritt 1996).

The PB ANOVA followed by Tukey's test of paired contrasts showed the significant Trial effect was due to greater areal biomass during the Post-High Flow years compared to lower biomass during Trial 1. There was no difference in PB among the other Trial combinations. Most of this Trial effect was apparent in Reaches 3 and 4 (Figure 3.11). There was no significant decline in PB during the High Flow Years compared to the other flow periods, which shows the periphyton was either resistant to scour associated with those high spring and summer flows or it was resilient by declining at the High Flows but recovered by the time sampling occurred in the fall of each year.

Water velocity during the spring and summer high flows could modify amounts of benthic algal biomass (e.g., Townsend et al. 2012, Francoeur and Biggs 2006, Wellnitz and Poff 2006, Rinke et al 2001). The flow-biomass relationship can have a threshold wherein variation in flow at some low flows does not modify algal biomass, but once flow exceeds some higher value, biomass declines (Davie and Mitrovic 2014, Flinders and Hart 2009). The shape of this response curve can be related to mixtures of different growth forms in which tightly adhered, adnate, prostrate species such as *Achnanthidium* sp. may be highly resistant to sloughing, unless of course substrata movement occurs, while less tightly adhered taxa such as *Nitzschia* sp. may be more easily sloughed. Some form of step response may have occurred in the Bridge River during the spring and summer periods during the progression of rising flows associated with Trial. Afterwards in the fall of each year when sampling occurred, there was time for any flow related decline in biomass to recover from summer disturbance according to algal growth kinetics. In situ

accrual to some maximum biomass or temporary equilibrium that is defined by light, temperature, and nutrient supply and modified by cell loss can take two months (Grimm and Fisher 1989) with shorter times associated with reduced nutrient limitation (Perrin et al 1987, Bothwell 1989). The several weeks at low base flow in the fall when samplers were installed would have provided sufficient time for algal biomass to recover from any summertime disturbance. This process shows resilience to disturbance. The algal communities may be scoured at extreme flows but they can recover quickly, which is a trait found in other rivers (e.g. Grimm and Fisher 1989, Tornes et al. 2015). For the Bridge River, it means that extreme physical events may only exert a short - term change to autotrophy and do not have impacts on biomass over much more than a couple of months as periphyton production recovers following disturbance.

Within the fall sampling period, periphytic algae would have grown to reach PB defined by light (Hill 1996), temperature (Goldman and Carpenter 1974), and nutrient concentration (Bothwell 1989) with biomass being modified by physical sloughing according to flow and insect grazing. Flow is a product of water depth and velocity. Water depth can influence light attenuation and thus rate of photosynthesis in periphytic algae (Hill 1996). During sampler incubations in the fall, all water depths at the periphyton samplers were <0.35 m and they did not vary with Trial. The river substratum was visible and light attenuation from glacial turbidity declined during the fall, which is typical in the Bridge River. With this small range of water depths, there would be little to no difference in light limitation of algal growth between Trials. Water velocities at the plates were in the range where periphyton accrual can respond positively to change in velocity (~0.1 – 0.5 $m \cdot s^{-1}$, Stevenson 1996). At those velocities, nutrients are supplied to most cells in the algal mat (Townsend et al 2012) and shear is not enough to cause sloughing of the biofilm (Rinke et al. 2001). Water temperature at the sampling sites was relatively consistent within reaches between trials (**Error! Reference source not found.**) and would not be expected to impart a Trial effect on PB. Hence, physical conditions at the samplers in the fall were consistent and would not have caused change in periphyton accrual during sampling in the fall between Trial 1 and the Post-High Flow years.

Concentrations of DIN and SRP declined between Trial 1 and the Post-High Flow years, the two time periods that supported different PB (Table 3.7). At low nutrient concentrations, similar to those found in the Lower Bridge River, it is possible for algal growth or biomass to change with apparent absence of temporal or spatial change in measured nutrient concentrations. Nutrients are taken up by algae to support growth, usually according to Michaelis-Menten kinetics (Borchardt 1996, Earl et al. 2006). When a nutrient is in short supply relative to algal demand, rates of uptake can be much greater than when that same nutrient is in surplus. This physiological response to available nutrients means that the concentration of a growth-limiting nutrient in flowing water may be driven low while algae are growing at close to optimal rates, resulting in surprisingly high biomass in the presence of low concentration of a growth-limiting nutrient, until of course that nutrient supply is depleted to a point that growth cannot be supported. This inverse relationship will only occur at low nutrient concentrations that are less than those that

may saturate the nutrient uptake kinetics. It is intuitively rare given that water flow ensures a constant renewal of nutrient supply. It has, however, been observed (e.g., McKnight et al. 2004, Ensign and Doyle 2006) and may contribute to inconsistencies among typically positive relationships between nutrient concentration and periphyton biomass (Bowman et al. 2007). The nutrient band can be narrow and may have been present in the Bridge River at the low DIN and SRP concentrations during the Post-High Flow years. Luxury nutrient uptake leading to intercellular storage of nutrients coupled with this high nutrient demand within the narrow band of low nutrient concentrations may have supported higher algal biomass in the Post-High Flow years (possible high rates of nutrient uptake kinetics) compared to conditions in Trial 1 when nutrient concentrations were higher (possible lower rates of nutrient uptake kinetics).

Grazing by insects may have contributed to the difference in PB between Trial 1 and the Post-High Flow years, based on a review of studies on the topic by Feminella and Hawkins (1995). For grazers to exert differential control of PB between Trial 1 and the Post-High Flow years, an inverse difference in abundance of benthos and mean PB between the two periods would be expected, assuming that order level benthos counts are a reasonable surrogate for abundance of grazers. The higher PB during Post-High Flow years compared to lower PB in Trial 1 would be expected to occur with lower benthos abundance in the Post-High Flow years compared to that in Trial 1. That outcome was not found for any of the benthos metrics. Densities were the same (Table 3.11, Table 3.12, and Table 3.13). It shows grazing effects on periphyton may not have been temporally different enough to explain the difference in PB between Trial 1 and the Post-High Flow years, again assuming order level comparisons are a reasonable surrogate.

The Bridge River benthos (Tricoptera, Plecoptera, Ephemeroptera, chironomids, other true flies (Diptera), and a range of rarer taxa) can be ingested by salmonids (Hynes 1970, Scott and Crossman 1973, Wipfli and Baxter 2010, Quinn 2018) and were found at densities similar to or higher than those among other comparable rivers (Deegan et al. (1997), Wipfli et al. (1998), Rosario and Resh (2000), Dewson et al. (2007), Rader and Belish (1999). While this comparison implicitly suggests ample food was present for salmonids in the Bridge River, energetics calculations are required to examine extent of food limitation of fish growth and abundance (e.g., Kennedy et al. 2008). These calculations were beyond the scope of the present project.

Unlike periphyton biomass, the Bridge River benthic invertebrate density and diversity declined during the High Flow Years compared to the other flow periods. Values of benthos metrics were unchanged between Trials 1 and 2, as was predicted to some extent in early planning (Failing et al. 2004), but there was a 69% decline in the density among all benthos taxa between Trial 2 and the High Flow years. There was no event other than the high spring and summer flows that distinguished the High Flow years from the other blocks of years, which supports a conclusion that the high flows contributed to the decline in benthos density and diversity found in the fall following the spring and summer high flows of the High Flow years. This finding shows that flows during the High Flow Years exceeded capacity of habitat to sustain densities of benthos that were found during Trial 1, Trial 2, and the Post-High Flow years. The trial effect occurred despite a time

lag of more than two months between the time of high flows in summer and the time of sampling in the fall, which may be considered a low rate of recovery within the year of the flow event. This rate is lower than the two weeks to a month for recovery following disturbance reported by Figueroa et al. (2006) and Mackay (1992) but it is similar to evidence that more than a year may be needed for full recovery of community diversity following disturbance (Chapelsky et al. 2020).

The high flows of 2016 – 2018 moved bedload, resulting in coarsening of substrata with net loss of small particles in some places but net accumulation in others (Ellis et al 2018). This material movement may have contributed to lower benthos density and diversity during the High Flow Years compared to the other time periods. The patchy armouring declined with distance from the dam, generally resulting in larger particles in Reach 4 than in Reaches 3 and 2 based on the particle size measurements in 2019 (Table 3.2). Coarse substrata may trap less fine particulate organic matter (FPOM) that comes from periphyton and allochthonous detritus compared to absence of coarsening and limit the availability of food for many benthic invertebrates (Bundschuh and McKie 2016).

The measured differences among particle sizes between reaches in 2019, however, were small. The median size of 11.7 mm in Reach 4 comprised medium gravel while the sizes in Reaches 3 and 2 (7.6 mm and 9.1 mm respectively) were fine gravel (Wentworth scale: Bunte and Abt 2001). All sizes were suitable for colonization by benthic invertebrates (Williams and Mundie 1978) or were at the low end of optimum sizes (Quinn and Hickey 1990). They certainly were not larger than ideal sizes and they were suitable to support spawning by anadromous salmon (Davey 2019). The lack of a Reach effect on total benthos and EPT among Trials is evidence that these particle size differences between reaches were not enough to cause change at least among the EPT between different places in the river. Although chironomid density was lower in Reach 3 compared to the other reaches, substrata particle size was not likely a driving factor because Reach 3 particles remained close to optimum sizes for wide ranging taxa, including chironomids.

Loss of large woody material during the High Flow years may have reduced availability of invertebrate habitat and food associated with microbial films on and within surface complexities of wood. Amounts of wood in the river were not measured between flow trials but recent observations of scour and disturbance of riparian vegetation in Reaches 4 and 3 that occurred during High Flow years shows that organic matter was moved but remained at some other place in the river as part of benthic and other habitat (Photo 4.1).

Photo 4.1 A 2020 image of moved organic debris resulting from the High Flow years. C. Perrin photo.

Another consideration is lotic invertebrate recruitment mediated by drift from upstream. This drift may be limited by interruption of the flow continuum by the dam and reservoir (Jones 2010, Ellis and Jones 2013), commonly called serial discontinuity (Ward and Stanford 1995). With physical removal of benthos during the 2016 – 2018 high flows, this discontinuity may have caused recruitment to take longer for re-establishment of the benthic invertebrate communities following the High Flow years than might be expected in a river that is connected to headwaters. Indeed, the increasing family richness with distance from the dam among all flow trials suggests Reaches 4 and 3 were much like headwater streams in which invertebrate recruitment from tributary inflows and egg laying would gradually add diversity and community complexity with distance from stream source. We would expect Reach 2 to be less affected by serial discontinuity due to supplemental drift from the Yalakom River but lack of a Reach effect on total benthos and EPT density, despite the change in richness, suggests that supplemental drift from the Yalakom River was not enough to change density recruitment between reaches upstream and downstream of the Yalakom-Bridge confluence.

Unlike the EPT, chironomid density was significantly lower in Reach 3 compared to the other reaches. Reach 3 was within a confined canyon where wetted area relative to reach length increased less with rising flow than in the other reaches, which would result in greater water velocities in Reach 3 compared to the other reaches. The Ephemeroptera (mayflies) are particularly well suited to these conditions because many species have fusiform body shapes that enable them to move about on the tops of rocks in rapid water, while others are flattened dorsoventrally to hug rock surfaces (Edmonds and Waltz, 1996). The Plecoptera (stoneflies) and

Tricoptera (caddisflies) do not have these attributes to the same extent but they occurred in relatively small densities compared to the mayflies (Figure 3.12), making them less influential in the statistical test of Reach effects when combined with mayflies in the EPT group. Although chironomids can exist in almost any aquatic habitat, they are mainly burrowers and may be more susceptible to velocity driven drift with rising flow in a confined channel like Reach 3 than the mayflies. This difference of body shape and ability to remain in place may contribute to the mayfly dominated EPT not being affected by physical differences of the reaches while the chironomids were more sensitive. Water velocity in Reach 3 may be the differentiating factor.

Finding NH_4-N concentrations greater than 20 $\mu g \cdot L^{-1}$ in the absence of anthropogenic pollution was surprising because under well oxygenated conditions in the presence of organic matter, as in the Bridge River, NH_4-N is transient in its typically rapid oxidation to NO_3-N in surface waters of the temperate northwest, although this nitrification can be slowed at low temperature (Perrin et al. 1984). NH_4-N is the inorganic form of N that is the main nutrient limiting forest growth (Kimmins 1987, LeBauer and Treseder 2008, Bobbink et al 2010, Mahendrappa et al. 1986), which means it is tightly retained in forest soils and rarely gets above 10 $\mu g \cdot L^{-1}$ in pristine streams. Furthermore, NH_4-N is a preferred N source by phytoplankton (as in Carpenter Reservoir) and periphyton in the Bridge River because less energy is required to take up and metabolize NH_4-N compared to NO_3-N (Lachmann et al. 2018), thus putting more demand on its biological availability in solution. Given these conditions, the high NH_4-N concentrations of 28 – 70 $\mu g \cdot L^{-1}$ that were found during Trials 1 and 2 in Reaches 2 and 3 shows there must have been an anomalous NH_4-N source at those places and times. That NH_4-N did not come from the inflowing tributaries (a VALUES with a "≤" symbol were at or below the detection limit.

Table 3.8).

Concentrations of NH_4-N, SRP, and to a small extent NO_3-N, matched the timing and places of spawning by pink salmon. Highest NH_4-N and SRP concentrations coincided with presence of pink spawners in the odd years while lowest concentrations occurred in even years when pinks were absent. This coincidence shows that spawning pink salmon could be a source of the anomalous nutrient concentrations, particularly NH_4-N that is a primary product from decomposition of salmon carcasses. It follows that nutrient concentrations may be a rough indicator of pink run size. High concentrations may be expected during a strong run while low concentrations may be associated with a weak run. If this hypothesis is correct, the nutrient data suggest that run size was strong during the Trial 1 and 2 years but weak during Trial 0 and particularly weak during the High Flow years and the Post-High Flow years (Table 3.7, Figure 3.9). The high nutrient concentrations in odd years of Trials 1 and 2 would have benefitted biological production via trophic upsurge (e.g. Wipfli et al 1998, Johnston et al 2004, Ruegg et al. 2012, Harding et al 2014), while lower nutrient concentrations in even years of Trials 1 and 2 and all years of the High Flow years and the Post-High Flow years would have supported less biological production.

Lack of a "Pink" effect on periphyton PB, total benthos, EPT, and invertebrate family richness shows that trophic upsurge that may have occurred in the presence of Pinks was not enough among all years within flow trials to produce significant trophic upsurge among years. Trophic upsurge is driven by lowering nutrient deficiency (Bothwell 1989, Perrin et al 1987) that propagates through the food web and produces overall increased biomass of invertebrates that are fish food organisms (Johnston et al 1990, Perrin and Richardson 1997, Harvey et al. 1998, Ardon et al. 2020). While some years had high NH_4-N and SRP concentrations associated with presence of Pinks in Reaches 2 and 3, many more "Pink-on" years had little or no nutrient signal, potentially showing low spawner abundance in those years and little opportunity for trophic upsurge. This lack of enrichment was particularly noteworthy during the High Flow years and to a smaller extent in the Post-High Flow years (Figure 3.9), which would have diluted any trophic upsurge associated with what might have been stronger Pink runs during Trials 1 and 2.

Chironomid density did significantly increase in the presence of Pinks ($p=0.025$), unlike overall richness and responses by other taxa. Chironomid larvae are generally collector gatherers and filterers that can benefit directly by feeding on very small decomposing particles of fish tissue as well as other detrital matter, some of which would be suspended by wildlife feeding on carcasses. The caddisflies have similar feeding habits but their low numbers relative to other families of the EPT may have caused a Pink effect to be masked by different responses of the other taxa. This feeding habit is different from many of the mayflies and stoneflies. The mayflies were collector gatherers, like chironomids, but also scrapers due to body shapes and feeding appendages that facilitate grazing periphyton. Many of the stoneflies were shredders of leaf litter and facultative detritivores (e.g., Nemouridae, Capniidae) or predators of other insects (e.g., Perlidae, Perlodidae, Chloroperlidae). These functional capacities may be less directly influenced by the presence of Pink carcasses than those of the chironomids or caddisflies.

A factor that may have exacerbated flow induced decline in benthos density during the High Flow years compared to the other time periods was concentration of the bio-available N and P (DIN and SRP). The very low SRP concentrations in flow release from the Terzaghi Dam combined with little to no Pink effect on nutrient concentrations produced the highest potential nutrient deficiency for algal growth and thus food web production during the High Flow years compared to the other flow trials. These conditions coincided with lowest invertebrate density and lowest amount of food for fish among all flow trials. While high flows of the High Flow years likely scoured and displaced benthic biota as happens during a flood event (Robinson 2012), recovery of that biota may have been strongly limited by newly low nutrient concentrations. SRP concentration was particularly low in Reach 2 due to inorganic N loading from the Yalakom River, which shifted N:P ratios in Reach 2 upwards and into a range showing extreme phosphorus deficiency for algal growth. This condition was new and not observed in the earlier trials. Those SRP concentrations and N:P ratios were similar to those commonly associated with streams known to respond strongly and positively to nutrient addition (e.g., Johnston et al 1990, Perrin and Richardson 1997, Harvey et al. 1998, Ardon et al. 2020). An additive coupling was

coincidentally present: one part being lowest nutrient concentrations on record potentially due to low pink runs and more clearly due to declining phosphorus loading from Carpenter Reservoir combined with the second part being disturbance during the high flows of the High Flow Years.

There is uncertainty about cause of declining SRP concentrations and rising molar N:P over the past 10 years in water released from Carpenter Reservoir, a trend that may be increasing potential phosphorus limitation of biological production mainly in Reach 4 of the Bridge River (Figure 3.8). Uptake of soluble phosphorus by phytoplankton and P adsorption onto glacial flour (Hodson et al. 2004) in Carpenter Reservoir may be a sink for bioavailable P (Limnotek 2019). These processes have always been present but may be changing over time. There might be changes in the overall transport of P caused by the variation in what parent materials are being eroded as the Bridge glacier recedes at a remarkable rate of 118 m/year (Chernos 2014). This erosion would influence water chemistry in Downton Reservoir, the Middle Bridge River, Carpenter Reservoir, and ultimately the Lower Bridge River (Chernos 2014, Allen and Smith 2007). Downstream transport of P and other nutrients can be modified by management of flows and reservoir water surface elevations (Limnotek 2019) but larger scale processes driven by glacial melt may have larger influence (Hood and Scott 2008). Further investigation is required to determine if these or other explanations are plausible.

Reach 1 was sampled only during the Post-High Flow years resulting in a sample size of two based on the design for analysis using years as replicates. In those two years, nutrient concentrations were similar to those in Reach 2 but SRP concentrations were greater than those in the Yalakom River (Table 3.7), implying greater potential biological production in Reach 2 and Reach 1 compared to the Yalakom. PB and densities of the major groups of benthos were highly variable, which prevented comment on whether assemblage density differed between Reaches 1 and 2 and the Yalakom River. Composition was different. The EPT comprised most of the benthos in the Yalakom River while the EPT and chironomids were present in similar proportions, together making up most of total benthos in Reaches 1 and 2, as was found upstream in Reaches 3 and 4. While the Yalakom River is an important source for recruitment of EPT in Reaches 2 and 1, the upper reaches of the Lower Bridge River dominate recruitment of chironomids to the lower river. Sampling in additional years using the present layout is needed to gain further insight into temporal patterns in Reach 1, ideally using contrasts with those in Reach 2 and the Yalakom River.

4.3. Management Question 3

How do changes in physical conditions and trophic productivity resulting from flow changes together influence the recruitment of fish populations in Lower Bridge River?

The 2020 fish sampling data added another set of results for the Modified Operations years which started in 2016 but were considered another stand-alone year (along with 2019 results) in terms of the analyses since salmonid fry (Age-0+) sampled in 2019 and 2020 were spawned, incubated, and reared entirely under the low flow conditions (based on the Trial 2 hydrograph) and these

were the first two years of Post-high flow results. Conversely, the other Modified Operations years (2016 – 2018) were characterized by high flows that exceeded the Trial 2 peak and resulted in substantially different habitat conditions for fish within the study area during those years (Sneep et al. 2019) and have altered habitat conditions relative to the previous flow trials (see response to MQ #1).

Mean weight data provided an indication of fish size for each species and age class during the fall stock assessment (in September) for each flow treatment, which can be a reflection of growth. Mean weights were also used to transform the juvenile salmonid abundance data into biomass values for each of the target species and age classes. Mean weights of each species and age class were almost always highest (or among the highest) in each reach during the High Flow years (2016 – 2018) and were also high during the Post-high flow years (2019-2020) compared to the previous flow treatments. However, it should be noted that there was overlap in the standard deviation error bars among some treatments in certain reaches, suggesting that the statistical significance of these differences may be limited in some cases.

There are a few possible reasons why the mean sizes tended to be highest during the High Flow years: 1) despite reduced abundance of benthic invertebrates (Section 3.3; Sneep et al. 2019), the amount of forage available may still have been ample given the significantly reduced density of juvenile fish during the modified operations years and lower competition for the food resources that were available); 2) water temperatures were warmer during the spring and summer rearing period which may have improved growth conditions; or, 3) the high flows likely selected for the largest individuals, as fish compete for habitat areas that are available and the smallest individuals may more likely be displaced downstream or out of the study area. The high mean weights during the Post-high flow years were most likely due to reasons 1) and 2) above, which have continued to some extent, but also due to recovered benthic invertebrate abundance (see Figure 3.12 in Section 3.3) after two years of a return to Trial 2 flows.

Given the uncertainty about which of these explanations may have been correct, we also plotted mean condition factor (Fulton's K values) by reach and flow trial for each species. The condition factor data showed a different pattern than the mean weight data: Highest condition factors were generally during trials 0, 1, or 2 (according to species/age class) and the lowest were generally during the Mod. Ops. years (i.e., High flows and Post-high flows). Condition factor is a better metric for assessing the relative fitness of fish among the flow trials because it accounts for the relationship between fish length and weight. These results suggest that improved growth (i.e., reasons 1) and 2) above) is probably less likely the cause of the larger mean size of fish during the Mod. Ops years, and that size selection based on flow magnitude (i.e., reason 3) may be the more likely explanation.

Overall, juvenile salmonid abundance and biomass were substantially reduced under the three years of high flows (Trial 3), compared to flow trials 1 and 2 and the pre-flow baseline period, and remained low despite a return to lower flows (based on the Trial 2 hydrograph) in 2019 and 2020.

Total abundance of juvenile salmonids (Chinook, coho and mykiss combined) were highest under the flow trial releases (Trial 1 mean = ~312,000 fish; Trial 2 mean = ~284,000 fish), compared to the Pre-flow baseline, High flow and Post-high flow periods (means = ~189,000, ~69,000 and ~91,000 fish, respectively). Overall, the recruitment of juvenile salmonids was reduced by 70–80% under High flows (from 2016 to 2018) relative to trials 1 and 2, when production was greatest overall in each reach. Salmonid abundance data suggested modest recovery in 2019, but no further recovery in 2020. Total juvenile abundance for reaches 2, 3 and 4 was approx. 94,000 fish in 2019 and 87,000 fish in 2020, which was an increase of approx. 7,000 – 31,000 fish relative to the three preceding high flow years (or 22,000 more than the Trial 3 average). However, the 2019 and 2020 abundances were 82,000 – 248,000 fewer fish than the previous Trial 2 years (2011 – 2015), or 193,000 fewer fish than the Trial 2 average.

While all species and age classes declined during the Mod. Ops. years, the degree of effect varied among them. Under the high flows, the average production of mykiss fry was 20% relative to the two flow trials. Steelhead parr abundance was 30% of both the Trial 1 and 2 estimates. Chinook fry abundance was 30% of Pre-flow numbers, 60% of Trial 1, and equivalent to Trial 2. It is possible that Chinook fry abundance did not further decrease under the high flows (relative to the Trial 2 mean) since their abundance was already depressed due to early emergence effects on their survival or life history caused by the flow release (see Sneep and Evans 2022). Coho fry abundance was 10% of the Trial 1 and 2 numbers. Coho fry went from being the second most abundant species-age class, to the lowest under the high flows. This could have been due to the coincidence of the onset of high flows in May shortly after their emergence time in March or April (modelled; Figure 3.6) when their capacity to hold or select habitats in the high flows would be very limited. This same factor may also have been an issue for the mykiss fry, which would likely emerge during the high flow period (June – July).

Trends in biomass among flow treatments for all species and age classes generally followed those based on abundance (see Figure 3.18) because changes in average weight across flow treatments have been less significant than the changes in abundance. However, the higher mean weights during the High flow and Post-high flow years had a slight moderating effect on the change in biomass (relative to Trial 2) than the change in abundance. This moderating effect was evident for each species and age class during the High flow and Post-high flow treatments and was most notable for mykiss fry and parr since the increases in mean weight were more substantial for this species.

The increase in juvenile abundance from the High flow years to the Post-high flow years was entirely due to improved recruitment of mykiss fry and coho fry (i.e., by approx. 10,000–19,000 and 12,000–16,000 more fish relative to 2016 – 2018, respectively). Post-high flow abundances of mykiss parr (6,000 fish) and Chinook fry (9,000 fish) were each lower than the estimates for these species-age classes from the High flow years. The 2019 mykiss parr had recruited as Age-0+ fish under the last year of the High flows in 2018, so they were not expected to have recovered one year later. The 2020 mykiss parr were from the first year-class that recruited under the Post-

high flow conditions. They fared poorer than expected given the return to lower flows but it is difficult to draw conclusions from this single Post-high flow data point for this age class. In general, the mykiss fry-to-parr survival rate has remained quite consistent across the different flow treatments. Chinook fry production remained relatively low (between 11,000 and 15,000 fish) and stable for 10+ years (i.e., since the end of the Trial 1 period). The 2019 Chinook estimate (~12,000 fish) was on par with this range; however, the 2020 estimate was lower (~7,000 fish). At this point the reason for the drop in Chinook production in 2020 is not clear, but it may have been impacted by broodstock collection operations or the increased incidence of straying in 2019 (affecting spawning or recruitment for the Bridge River population). Overall, relative to the Trial 2 abundances for mykiss fry (162,000 fish), mykiss parr (33,000 fish) coho fry (76,000 fish) and Chinook fry (13,000 fish) the recovery in the first two years following high flows was quite limited (i.e., Post-high flow abundances were 30%, 20%, 30% and 70% of Trial 2 abundances for these species/age classes, respectively; Table 3.16, In terms of recovery post-high flows (i.e., in 2019 and 2020), all species and age classes have fared relatively poorly to-date. Since the return to low flow releases (i.e., the Trial 2 flow magnitudes and hydrograph shape) following the High flow years, mykiss fry and coho fry abundance and biomass increased modestly (+14K fish for each); however, the estimates for mykiss parr and Chinook fry actually decreased relative to the High flow period (-4K and -3K on average, respectively) (Table 3.16 and Table 3.17). The abundance and biomass estimates were fairly equivalent between 2019 and 2020 for all species/age classes and substantially lower than the Trial 2 estimates, particularly for mykiss (fry and parr) and coho fry (Figure 3.18). For Chinook, the 2019 and 2020 estimates were lower, but the Trial 2 estimates were already low (compared to the Pre-flow estimates) for this species.

Table 3.17 and Figure 3.19).

By reach during the Post-high flow years, highest juvenile abundances for mykiss (fry and parr) and coho (fry) were in Reach 3. Chinook abundance was highest in reaches 1 and 2. Among the reaches, the modest increase in abundance of juvenile fish in 2019 and 2020 was almost entirely attributable to Reach 3. Recovery of juvenile fish production in reaches 4 and 2 was negligible in the first two years following high flows, except for coho which increased by approx. 3,000 fish in Reach 4. Based on the redd survey data provided by BRGMON-3, Reach 4 is where the majority of coho spawning occurs (Figure 3.6; White et al. 2021).

The juvenile salmonid abundance and biomass results for each flow treatment period were run through a mixed effects model for the first time in 2020 to formally test for flow effects associated with each of the treatments. One model run was completed using data that were not stratified by reach (representing flow effects on the study area as a whole) and a second run was completed using reach-stratified data. The unstratified model combines the effects of rewetting Reach 4 with the effect of added flow in reaches 2 and 3 and the stratified model allows us to tease these effects among reaches apart. The intent of the two different approaches was to determine which one was better at explaining the variation in log density or biomass by the fixed effects (flow for the unstratified model; flow and reach for the stratified model) and random

effects (year). For the stratified model, the benefits of improving the fit of the model by adding more parameters (i.e., reach) must outweigh the costs to precision of adding extra parameters. The model outputs (plotted on Figure 3.21 and Figure 3.22 and summarized in Table 3.18 and Table 3.19) characterized the flow effects on log abundance and biomass and confirmed that the reach-stratified model was the better approach (lower DIC scores; higher FE_r^2 values) for each species and age class, except Chinook fry. For Chinook fry, both models were equivalent since their abundance and biomass have diminished among the reaches during each flow treatment.

Going forward the mixed effects model will also be a useful tool for including covariates that may be relevant for informing the variability among years and reaches within each flow treatment. This will also be highly useful for addressing MQ #3 by formally testing the relevance of each covariate for explaining the variation currently accounted for by year (γ_y) and reach-year ($\varepsilon_{r,t}$) effects in the model. Likely covariates could include nutrient concentrations, benthic invertebrate abundances, and spawner escapements (for Chinook and coho) since these data are available for most, if not all, monitoring years. If some or all of the covariates are good explanatory variables, it may change the estimated flow effect sizes, or at least change the certainty in those effect sizes. These additional analyses could not be included under the Year 9 scope and budget but have been recommended for inclusion in the Year 10 synthesis and reporting for next year (see Recommendation #5 in Section 5).

Adult salmon escapement estimates were provided by the BRGMON-3 program in order to evaluate stock-recruitment relationships according to flow release treatments and determine if spawner stock size was a potential limiting factor on recruitment. An apparent shift in escapement-fry stock-recruitment curves for Chinook and coho across the different flow treatments reflected the changes in fry abundance seen in the juvenile abundance analysis. However, because the curves associated with each treatment were different, and there was uncertainty in estimating egg-to-fry survival rates, there was limited information for defining the initial slope of the curves (which is essential for understanding the number of spawners required to “fully seed” the available habitat).

The stock-recruitment datapoint for 2020 (i.e., 2019 spawners vs. 2020 juvenile recruits) was added to the plots for Chinook and coho as a stand-alone point and was not factored into any of the existing curves, as was the case for the 2019 datapoint, since they represented the start of a new treatment (i.e., the first two years of the Post-high flow period). As such, there were not enough points to fit a new curve so we cannot draw any new conclusions other than that the 2019 and 2020 datapoints for Chinook reflected low spawner estimates in 2018 and 2019 (2018 *n*= 25; 95% CIs: 14–44; 2019 *n*= 161; 95% CIs: 84–310) and they were both nearest the asymptotes of the Trial 2 and High Flow curves. However, the escapement estimates in both those years were likely biased low (possibly by ≥50%) due to the effect of fish fence operations on the spawner surveys in those years (White et al. 2021). Another factor potentially affecting spawning (and subsequent recruitment in 2020) was the incidence of straying by Chinook spawners from other populations due to the migration obstruction on the Fraser River (upstream

of the Bridge River confluence) caused by the Big Bar slide. Spawner estimates in both of these Post-high flow years were close to a cluster of other low escapement values near the origin of the x-axis (even considering the caveats above), and the juvenile recruitment estimate was similar to all of the other values for trials 2 and 3 on the y-axis in 2019 but lower by about 6,000–8,000 fry in 2020.

The 2019 and 2020 stock-recruitment datapoints for coho were nearest the asymptote of the Pre-flow curve and approx. 45,000 fry below the asymptote of the Trial 2 curve despite a sizeable spawner return in 2018 (*n*= 1,245; 95% confidence intervals: 882–1,627) followed by a much lower return in 2019 (*n*= 214 (95% confidence intervals: 152–301), which were the back-to-back highest and second lowest coho escapements to the LBR since 2013. The Chinook broodstock collection fence did not impact coho spawners due to the difference in run timing for these species in the LBR. Also, the Big Bar slide should not have impacted the incidence of straying for coho as much as Chinook since the flows at the slide site were more passable during the coho migration window (DFO unpublished data), although data on coho straying were not available for this report. Given that recruitment of coho fry was nearly identical in 2019 (23,000 fish) and 2020 (21,000 fish) despite the large difference in spawner escapements (which were also in the range of escapements that resulted in much higher recruitment during the Trial 1 and 2 years), any evidence for stock size limitation during the Post-high flow period was not readily apparent.

The stock-recruitment analysis continues to be a bit of a crude tool for assessing whether spawner stock size was a factor in limiting juvenile recruitment among years and flow treatments in the Lower Bridge River (for the reasons described in Section 3.4.4). Because of these reasons, it would be worthwhile to include the annual spawner escapement estimates as a covariate in the fixed effects model to explicitly test the extent to which escapements explain the variability in the annual juvenile abundance and biomass estimates (for coho and Chinook) and assess whether escapement sizes among years and treatments alter the flow effect size and certainty for these species. See more on this in Section 5 – Recommendation #5.

Salmonid abundance data were collected in Reach 1 for the second time in 2020. Results for this year highlighted that all of the target species and age classes were again present in the reach, of which mykiss fry were the most abundant (~24,000 fish), followed by coho fry (~14,000 fish), Chinook fry (8,000 fish), and then mykiss parr (~3,000 fish). The patterns of abundance among the species in Reach 1 were most similar to their relative contributions in Reach 2, and the same general patterns were apparent during the first year of Reach 1 sampling in 2019 (Sneep et al. 2020); however, abundances for each species and age class were slightly higher in 2020. The total for all species and age classes (~49,000) in 2020 was just over 1/3 of all species in reaches 2, 3 and 4 combined (~87,000). Lineal densities in Reach 1 were on par with Reach 4 for mykiss fry, mykiss parr, and coho fry, and slightly higher than the other reaches for Chinook fry in 2020, at this stage of post-high flow recovery.

While the number of year replicates are still very limited for Reach 1 to-date, the lineal density results from 2020 may suggest that: a) densities in Reach 1 were less affected by the High flow years; b) recovery could be occurring more quickly in this reach than the upstream reaches; or c) that fish were additionally recruited to this reach from upstream (i.e., reaches 2, 3 and 4) or downstream (i.e., Fraser River) sources in 2020. Without the historical time series of data for Reach 1, however, it is not possible to know how current abundances in this reach compare with the earlier flow trials or how relative differences among the reaches may or may not have changed.

Given the expected increase in straying to the LBR by salmon from other populations due to the migration obstruction on the Fraser River caused by the Big Bar slide, samples for DNA analysis were collected from coho and Chinook juveniles in 2020 so they could be analyzed for genetic stock identification. The samples from juvenile Chinook (n= 117) were sent to the Molecular Genetics Lab at Pacific Biological Station for this analysis. From the original sample size of 117, three individuals failed to genotype and eight were identified as non-Chinook, reducing the viable sample size to 106 (Wetklo and Sutherland 2021). The following conclusion from their analyses comes directly from their summary report:

> "*Two analytical approaches have been applied to describe the ancestry of Bridge River juvenile Chinook sampled in 2020. The majority of the juveniles were the progeny of pure form Bridge parental pairings. We estimate that at least 13% of the juveniles were admixed and attributed to the successful spawning of mid and upper Fraser River Chinook salmon strays in Bridge River.*" (Wetklo and Sutherland 2021).

4.4. Management Question 4

What is the appropriate 'shape' of the descending limb of the 6 $m^3 \cdot s^{-1}$ hydrograph, particularly from 15 $m^3 \cdot s^{-1}$ to 3 $m^3 \cdot s^{-1}$?

Results from ramp down and fish salvage monitoring in 2020 were very similar to the results from 2019 and the Trial 2 years (2011 – 2015). As such, they did not provide significant *new* insights on the optimal 'shape' of the descending limb of the hydrograph from 15 $m^3 \cdot s^{-1}$ to 3 $m^3 \cdot s^{-1}$ beyond what has been reported for this flow range previously (Sneep et al. 2020; McHugh and Soverel 2017; Sneep 2016). Ramping across this range in 2020 conformed well to the timing and shape implemented during those previous years of Trial 2 flows, although the first 8 of 10 rampdown events occurred approx. 2 weeks earlier in 2020 (Figure 3.31).

Discharge Effect

The 2020 results reaffirmed that 13 $m^3 \cdot s^{-1}$ is the approximate flow threshold below which fish stranding risk tends to increase from low to moderate or high (as defined in the LBR fish stranding protocol (Sneep 2016)). As such, implementing the WUP rates (≤2.5 cm/hr) is likely warranted across most or all of this range. Above the 13 $m^3 \cdot s^{-1}$ threshold, there is flexibility to implement faster ramp rates (up to 4.1 cm/hr was tested in 2017, 4.0 cm/hr in 2018, and 4.6 cm/hr in 2019;

Table 3.22) to reduce flows more quickly without increasing fish stranding risk significantly (based on results for 2016–2019). Reducing flows more quickly (especially from high discharges >15 $m^3 \cdot s^{-1}$), can provide the opportunity to reach more optimal levels for summer rearing (i.e., the Trial 2 peak or lower) in less time, or over fewer days. Furthermore, field crews have reported that, because ramp down events can be completed more quickly, final gate changes can be implemented earlier in the day such that the river stabilizes at the new stage level before the end of the day, which facilitates the effectiveness of salvage efforts.

An important caveat that must be noted for the Modified Operations results, however, is that juvenile salmonid numbers were shown to be substantially reduced by the effects of the high flows overall (i.e., due to poor survival or displacement out of the study area) from 2016 – 2018, and only moderate recovery in the Post-high flow years (2019 and 2020), relative to the densities documented under trials 1 and 2. Although, given the effects of the high flows on physical habitat parameters, benthos production, and fish abundance (as noted in the sections above), this may be the case any time flow magnitudes in the range of the 2016 – 2018 discharges occur. For these reasons, the incidence of fish stranding and the effects of faster ramp rates on stranding risk should continue to be monitored for flows >15 $m^3 \cdot s^{-1}$ in order to build up a larger sample size of data and improve confidence in the results.

Reach Effect

Under flow ramp downs <15 $m^3 \cdot s^{-1}$ in previous years, differences in the number of fish salvaged among reaches were substantial: On average, the number of stranded fish in Reach 4 (mean = ~3,000) was nearly 1.5-fold higher than the number in Reach 3 (mean = ~2,000), and the amount of identified stranding area was nearly equivalent among them (4,865 and 4,540 m^2, respectively; Sneep 2016) despite the fact that Reach 3 is nearly four times longer than Reach 4 (~12 km vs ~3 km, respectively). Patterns in stranding risk among reaches were also apparent in the Post-high flow data, although they were different than the Trial 2 results, probably due to the significant physical changes to habitat that were caused by the high flows. The amount of fish stranding area was substantially greater in Reach 3 (7,163 m^2) versus Reach 4 (1,330 m^2) in 2020, and the numbers of fish salvaged were also larger in Reach 3 (3,272 vs 753); However, the fish stranding densities were highest in Reach 4 (57 fish per 100 m^2 of strand area), relative to Reach 3 (46 fish per 100 m^2).

Despite differences in sample size (i.e., # of years) for ramping and fish salvage data between modified operations years and the Trial 1 and 2 flows, there is little uncertainty that juvenile fish distribution and relative stranding risk varies among the reaches of the Lower Bridge River. Given the low abundance of juvenile salmonids in 2016–2020 overall, it would be worthwhile to characterize the relative stranding risk among the reaches at different high flow magnitudes (when fish abundance may be greater). However, based on assessment of stage changes in Reach 2 within the Trial 2 range (see Figure 3.4 and Table 3.21), total daily stage changes per event in that reach were approx. ⅓ to ½ the magnitude of changes at the top of Reach 3, and hourly changes were likely lower as well due to the mitigating influence of the Yalakom River and

other tributary inflows. This is one of the primary reasons that fish salvage efforts were focussed on reaches 4 and 3 and not on reaches 2 and 1 during implementation of the Trial 1 and 2 hydrographs, as well as flow ramp downs within that range in recent years. Considered together: the reduced stage changes, moderated ramping rate due to attenuated inflows, and generally low fish stranding risk documented for reaches 2 and 1 to-date, mutually support that fish stranding risk below the Yalakom confluence is lower than it is in the reaches above. However, it should be noted that fish stranding data in reaches 1 and 2 were available for ramp downs from flows >15 $m^3 \cdot s^{-1}$ but not within the 15 to 1.5 $m^3 \cdot s^{-1}$ range.

Ramping Rate Effect

Ramping rates implemented in 2020 were between 1.6 and 2.7 cm/hr (stage reduction per hour at the 36.8 km compliance location). These stage changes generally conformed to the target rates referenced in the WUP (i.e., ≤2.5 cm/hr). As before, fish salvage crews were on the ground to monitor the results, but generally avoided proactively moving fish out of strand-risky habitats in advance of isolation or dewatering (i.e., "incidental" catches) such that catch data would better reflect actual numbers of stranded fish. Fish salvage results at higher ramping rates within the Trial 2 range in 2019 were higher than the results for the high flow range in 2016 – 2018. However, the incidence of fish stranding did not change relative to the identified risk for flows ≤15 $m^3 \cdot s^{-1}$.

Currently the sample size for stranding monitoring at ramping rates >2.5 cm/hr is still relatively small. As was noted for the MQ above, juvenile fish abundances in 2017, 2018 and 2019 were low overall, which could have confounded the incidence of stranding despite the higher rates implemented in each of those years. However, the results to-date suggest that stranding risk is lower at flow releases >13 $m^3 \cdot s^{-1}$ (see above). As such, this should provide opportunity to further test higher rates across the high flow range going forward without unduly risking higher fish mortality. Increasing the number of ramp down events completed at higher ramp rates will be necessary to reduce uncertainty about the specific effects of higher ramp rates across the different high flow levels.

River Bank Effect

The distribution of sites between river left and river right was not equal for flows within the Trial 2 range. Based on the updated salvage survey data in 2020, the distribution of sites was 76% on river left and 24% on river right for ramp downs at flows ≤15 $m^3 \cdot s^{-1}$. Across the high flow range, based on site reconnaissance surveys, the distribution was 44% and 56%, respectively. Upon initial purview, differences in distribution of sites according to side of the river may seem unexpected, given that there is no known reason based in an understanding of channel morphological processes that more strand-risky habitats would naturally form on one side of the river versus the other across the length of these reaches. Rather, it's possible the reason could have more to do with human-caused effects than natural ones.

Other than at the very bottom of Reach 2 (i.e., at Camoo; km 20.0) and the bottom of Reach 1 up to the Applesprings off-channel habitat, road access along the entire length of the Lower Bridge River is along the river left side. The proportion of identified stranding sites on river left is likely influenced by this access and its associated human-caused effects, including: dam construction-, habitat enhancement- (i.e., spawning platforms, off-channel habitats), fish research-, river access-, and gold mining-related activities (to name a few).

At least some of the stranding sites that were likely created or altered by these activities include: the plunge pool, Eagle lake, Bluenose, Russell Springs, fish counter, Hippy pool, Horseshoe bend, and Camoo sites on river left; and the plunge pool, grizzly bar, and Camoo sites on river right. Given that the river was generally in a low flow, pre-release condition for 40 years following dam construction, most of these human-affected sites tend to occur within the lower flow range (≤15 $m^3 \cdot s^{-1}$). At higher flows (>15 $m^3 \cdot s^{-1}$), the distribution of sites appears to become more balanced on either side of the river – closer to what we would expect in the absence of human-caused interference.

Opportunities to minimize or mitigate the risk of fish stranding during ramp downs

The primary opportunity (or most conservative approach) for minimizing or mitigating the risk of fish stranding is by implementing the ramping rates referenced in the WUP (i.e., ≤2.5 cm/hr) and having fish salvage crews actively salvaging fish in each of the reaches downstream of the dam. This approach has been employed successfully in the Lower Bridge River for documenting the incidence of stranding and mitigating mortalities since the continuous flow release began. At these ramp rates, fish may have more opportunity to move out of strand-risky habitats with the changing flow level (similar to what occurs in unregulated systems), relative to faster rates, and fish salvage crews can more easily keep on top of salvaging fish from habitats as they become isolated (and before they dewater). Although, it must be acknowledged that fish stranding does occur on unregulated systems also, and it will never be possible to completely mitigate stranding with ramping rates alone. While being the most conservative from a fish stranding perspective, this approach is also the most time- and labour-intensive as the duration and number of ramp events are higher.

In some cases, such as in the 2016-2018 high flow years, there can be additional rationale for ramping the flows down faster in order to reach more optimal summer rearing flows (i.e., ≤15 $m^3 \cdot s^{-1}$) more quickly following peak flows. With the data for high flows available from 2016 to 2018, there is some evidence for when faster ramping rates can be applied without unduly increasing fish stranding risk. As described in the management question responses above, this could apply to ramping rates up to 4.6 cm/hr at discharges >13 $m^3 \cdot s^{-1}$ based on the information currently available. However, due to the factors noted in the sections above (low fish abundance during the Modified Operations years to-date; lower sample size at higher ramping rates), the application of these rates should be accompanied by ramp monitoring and fish salvaging (as was done in 2016–2020) to further characterize the fish stranding risk at flows

>15 $m^3 \cdot s^{-1}$ when fish abundances may be greater and expand the dataset from which conclusions are drawn.

4.5. Management Question 5

Do increased water temperatures and early emergence associated with Terzaghi Dam flow releases affect the survival of juvenile Chinook salmon in the Lower Bridge River?

A response to this question based on the current set of information available from BRGMON-1, as well as other studies, was provided in the Chinook Emergence Timing and Life History Review Memo Report that was prepared for St'at'imc Eco-Resources and BC Hydro (Sneep and Evans 2022). Since this Management Question was one of the focusses of that document, and there was additional context and detail provided within it (beyond what is in this report), we have not repeated that information here. Please refer to the Memo Report, which serves as a supplement to the BRGMON-1 reporting, for more information pertaining to this management question.

4.6. Management Question 6

What freshwater rearing habitats are used by Lower Bridge River juvenile Chinook salmon and is rearing habitat use influenced by Terzaghi Dam flow releases?

A response to this question based on the current set of information available from BRGMON-1, as well as other studies, was provided in the Chinook Emergence Timing and Life History Review Memo Report that was prepared for St'at'imc Eco-Resources and BC Hydro (Sneep and Evans 2022). Since this Management Question was one of the focusses of that document, and there was additional context and detail provided within it (beyond what is in this report), we have not repeated that information here. Please refer to the Memo Report, which serves as a supplement to the BRGMON-1 reporting, for more information pertaining to this management question.

4.7. Management Question 7

How does habitat use by juvenile salmonids change with discharge under the modified flow regime?

Spring (mid June) and summer (mid July) sampling in the off-channel habitats (Bluenose in Reach 4 and Applesprings in Reach 1) in 2020 further documented use of these sites by each of the target species during these two periods when flow releases from Terzaghi Dam were 15 $m^3 \cdot s^{-1}$. Coho fry were the most prevalent species at the Applesprings site and in the Bluenose outflow channel during both spring and summer surveys. Chinook fry were the next most abundant in the spring sample at Applesprings but were nearly absent in the summer survey and at Bluenose during both surveys. This change between spring and summer periods likely corresponds with the timing of outmigration for Chinook juveniles in the Bridge River. Mykiss (which were predominantly parr during the spring and summer surveys since they occurred during the timing of emergence for the new year class of fry) were most prevalent in the Bluenose

pool site and their abundance remained fairly consistent at both off-channel habitats among sessions. Some of the Applesprings sites were supplemented with a few recently emerged mykiss fry in the July session.

Under Trial 2 peak flows in 2020, there was no evidence of migration into these off-channel habitats for any of the target species and age classes. These data were intended to serve as baseline habitat use information for juvenile salmonids in these two offchannel habitats, against which use under future high(er) peak flows can be compared. The goal was to assess whether juvenile salmonids move into these habitats as refuge or if use is otherwise affected when rearing habitat areas in the mainstem LBR are reduced under high flows. Further analysis and discussion about these data will occur when additional high flow habitat use data are collected for comparison in the future.

Depletion sampling at riffle and pool sites in the two off-channel habitats was also completed in fall 2020, as it was in 2018 and 2019. Results from these surveys have indicated that mykiss (fry and parr) dominate the Bluenose habitat and coho fry dominate the Applesprings habitat in the fall. Chinook fry were absent at Bluenose and present only at the riffle sites in Applesprings at relatively low density. In general, densities of juvenile salmonids in these off-channel habitats were high (i.e., on par with mainstem densities in reaches 4 and 2 during the Trial 2 years), particularly in 2020 and 2018 (the last high flow year), and much higher than current densities in reaches 4 and 1 at this stage of post-high flow recovery in the mainstem.

These depletion sampling results have indicated that: a) the two selected offchannel habitats can support high densities of juvenile salmonids, b) each habitat has consistently had higher suitability for some species over others, and c) the overall densities have varied among years with the same flows in the mainstem (i.e., 2019 and 2020). Also, given that densities in these habitats were very similar between 2018 (a high peak flow year) and 2020 (a lower peak flow year), there is currently no evidence to suggest that fish move into these off-channel habitats in greater numbers during high flow years (e.g., seeking refuge); however, the number of year-replicates for assessing this is still quite low (*n*= 3 years).

Beyond a potential role as refuge habitats, the contributions from these off-channel habitats cannot compensate for the reduced production observed in the mainstem during years with high peak flows (e.g., 2016-2018) due to their limited size and availability in the LBR study area. Total mainstem production under Trial 2 was 256,000 fish (not including Reach 1 which was not sampled during that trial), so the 11,500 fish estimated for the two existing off-channel sites in 2020 would represent 4.5% of this Trial 2 abundance. To make-up for reduced mainstem production documented since the High flow years, a total of 165,000 additional fish are required (i.e., 256,000 Trial 2 average - 91,000 Post-high flow average). Assuming that the *maximum* densities of juvenile salmonids documented in the two off-channel areas from 2018 to 2020 are representative of what these habitats can produce, a total area of 119,000 m^2 (or approximately 103 Bluenose-sized sites) and 130,000 m^2 (equivalent to 15 Applesprings sites) would be required

to recover the lost mykiss and coho production in the mainstem. Off-channel recovery of lost Chinook production in the mainstem seems unlikely given the consistently low use of the existing off-channel habitats documented for this species to-date.

5. Recommendations

The following recommendations stem from the analysis and reporting of results for addressing the management questions up to, and including, Year 9 (2020):

1. There is much uncertainty about the role of changing melt patterns at the Bridge Glacier contributing to time course change in transport of nutrients, particularly phosphorus. This nutrient and others originate in geological formations that are eroded by the Bridge Glacier. They are transported downstream, supporting food webs and fish populations. Flow and water storage management can contribute to some change in system biogeochemistry (Limnotek 2019) but not to the degree seen in Figure 3.8. Larger more regional change may be active. To investigate the potential importance of these larger scale processes on nutrient availability for support of fish food webs, it is strongly recommended that monitoring of nutrient concentrations and transport be conducted over the continuum from the glacier including stations at the inflow to Downton reservoir, the Middle Bridge River, the inflow to Carpenter Reservoir, and the Carpenter Reservoir outflows. Some of this sampling has been done in past projects but it is not sufficient for tracking time course changes in system biogeochemistry that supports food webs and fish populations. New coordinated and longer-term sampling over the continuum is needed to assist with interpretations.
2. Calculation of a N and P budget for the Lower Bridge River. Concentrations of the various forms of N and P have been measured over years in both the Lower Bridge River mainstem and its tributaries. Site-specific flow has also been modelled for different places in the river. These two sets of data (nutrient concentrations and site-specific flow) need to be merged for calculation of nutrient loading rate at different places in the river. These calculations can be used to show the relative importance of sources and sinks of bioavailable N and P. That information will be needed for any consideration of mitigation using nutrient augmentation as a measure to increase fish growth and survival.
3. At present, it is unknown if fish are limited by food availability in the Lower Bridge River. Fish condition is known, and food abundance is known, but we don't know if addition of food would actually benefit fish populations. An energetics study is needed and recommended to answer this question. Procedures like those reported by Kennedy et al. (2008) could be investigated for application to the Bridge River. They involve using chemical signatures to estimate consumption rates along with bioenergetics modeling among juvenile salmonids.
4. If recommendation number 3 shows strong evidence of food limitation of salmonid growth and survival, we recommend that nutrient addition be examined as a fish enhancement strategy in the Lower Bridge River. There is a progressive decline in nutrient concentrations in Reach 4 due to declining nutrient loading from Carpenter Reservoir and potentially from further upstream) and in Reach 2 (due to high nutrient dilution from

Yalakom River inflows). Evidence from many fertilization studies shows that addition of nutrients may increase biological production of the salmonid food web, leading to larger fish with greater survival and greater abundance.

5. We can use the existing mixed effects model framework to test covariates other than flow (e.g., benthic invertebrate abundance, nutrient concentrations, spawner stock sizes) on juvenile salmonid density and biomass. We simply need to add another term to the model, such as $\beta \cdot SRP_{r,y}$ (for soluble reactive phosphorus), where β represents the overall effect of changing SRP concentrations, as an example. Other examples could include molar N:P ratios, benthic invertebrate abundances, or spawner escapement estimates as potential covariates. If any of these (or other options) are good explanatory variables, their inclusion may address some of the variation currently accounted for by year (γ_y) and reach-year ($\varepsilon_{r,t}$) effects. We did not add these parameters to the fixed effects models for this report since further discussion is required to identify and test the most relevant and informative covariates covering the entire suite of monitoring years. This effort would be best suited to include in the budget for the Year 10 final synthesis report.

   Note: the covariates do not need to be incorporated as purely linear effects, as described in the SRP example, above. For instance, if higher nutrient concentrations, benthic invertebrate abundances or spawner escapements provide diminishing returns relative to the effects at lower levels, then log-transformed covariate values can be used. Even binary variables could be used for covariates where the effect is either above (value=1) or below (value=0) a prescribed threshold level.

6. Preferably ensure that the collection of spawner escapement data for coho and Chinook under BRGMON-3 can be unimpeded by broodstock collection fence operations to the extent possible. When the completion of spawner surveys is compromised due to fence operations it increases bias and uncertainty in the stock recruitment relationships for assessing potential spawner stock size limitations. This issue may be mitigated by setting the fence up in a different location than the counter site at Rkm 26.1 (to reduce recycling over the counter) and allow for completion of the weekly spawner streamwalks throughout reaches 3 and 4 to ensure comparability of the data with the existing time series. The solution to these issues should involve input from all of the relevant parties (Chinook broodstock collection program manager, BRGMON-3 project manager, BRGMON-1 reporting manager, a St'at'imc Eco-Resources representative, the Joint Planning Forum group, etc.) to ideally find a compromise that balances the needs of the various programs.

7. Repeat the collection of Wolman pebble count data at each of the index monitoring sites on the LBR and Yalakom River. These data are useful for characterizing the substrate composition throughout the study area and tracking any changes among years and future flow treatments.

6. References Cited

Albers, S.J. and E.L. Petticrew. 2012. Ecosystem response to a salmon disturbance regime: Implications for downstream nutrient fluxes in aquatic systems. Limnology and Oceanography. 57: 113-123.

Allen, S.M. and D.J. Smith. 2007. Late Holocene glacial activity of Bridge Glacier, British Columbia Coast Mountains. Canadian Journal of Earth Science. 44: 1753-1773.

Anderson, R.O. and R.M. Neumann. 1996. Length, weight, and associated structural indices. Pages 447–482 in B.R. Murphy and D.W. Willis, eds. Fisheries techniques, 2nd edition. American Fisheries Society, Bethesda, MD.

APHA (American Public Health Association). 2011. Standard methods for the examination of water and wastewater. Available at: http://www.standardmethods.org American Public Health Association, American Water Works Association, and Water Environment Federation.

Ardon, M., L.H. Zeglin, R.M. Utz, S.D. Cooper, W.K. Dodds, R.J. Bixby, A.S. Burgett, J.F. Shah, N.A. Griffiths, T. K. Harms, S.L. Johnson, J.B. Jones, J.S. Kominoski, W.H. McDowell, A.D. Rosemond, M.T. Trentman, D.Van Horn, and A. Ward. 2020. Experimental nitrogen and phosphorus enrichment stimulates multiple trophic levels of algal and detrital-based food webs: a global meta-analysis from streams and rivers. Biological Reviews. doi: 10.1111/brv.12673.

Arscott, D.B., J.K. Jackson, & E.B. Kratzer. 2006. Role of rarity and taxonomic resolution in a regional and spatial analysis of stream macroinvertebrates. *Journal of the North American Benthological Society*, *25*(4), 977–997.

Bailey, R.C., G. Scrimgeour, D. Cote, D. Kehler, S. Linke, and Y. Cao. 2012. Bioassessment of stream ecosystems enduring a decade of simulated degradation: lessons for the real world. Can. Journal of Fish. Aquat. Sci. 69: 784-796.

Bailey, R.C., R.H. Norris, and T.B. Reynoldson. 2004. *Bioassessment of Freshwater Ecosystems: Using the Reference Condition Approach*. Kluwer Academic Publishers, Massachusetts, USA.

Bailey, R.C., R.H. Norris, & T.B. Reynoldson. 2001. Taxonomic resolution of benthic macroinvertebrate communities in bioassessments. *Journal of the North American Benthological Society*, *20*(2), 280–286.

Barbour, M.T. and J. Gerritsen. 1996. Subsampling of benthic samples: a defense of the fixed count method. *Journal of the North American Benthological Society*, 15 (3): 386-391.

BC Hydro. 2020. Scope of Services – 2020-2021 BRGMON-1 – Lower Bridge River Aquatic Monitoring and Reporting; WUP AND High Flow Monitoring. Prepared by Matt Casselman and Ira Hofer, BC Hydro Fish and Aquatic Issues Team, June 2020.

BC Hydro. 2018. BRGMON-1 Lower Bridge River Aquatic Monitoring – Monitoring Program Terms of Reference Revision 1. Bridge-Seton Water Use Plan. November 30, 2018.

BC Hydro. 2012. Bridge-Seton Water Use Plan Monitoring Program Terms of Reference – BRGMON-1 Lower Bridge River Aquatic Monitoring. Prepared for the Comptroller of Water Rights, Province of British Columbia, January 23, 2012.

BC Hydro. 2011. Bridge River power development water use plan: revised for acceptance for the Comptroller of Water Rights. pp. 1–79.

Biggs, B.J.F. 2000. Eutrophication of streams and rivers: dissoved nutrient-chlorophyll relationships for benthic algae. Journal of the North American Benthological Society. 19: 17-31.

Bobbink, R. K. Hicks, J. Galloway, T. Spranger, R. Alkemade, M. Ashmore, M. Bustamante, S. Cinderby, E. Davison, F. Dentener, B. Emmett, J.W. Erisman, M. Fenn, F. Gillian, A. Nordin, L. Pardo, and W. Devries. 2010. Global assessment of nitrogen deposition effects on terrestrial plant diversity: a synthesis. Ecological Applications. 20: 30-59.

Borchardt, M.A. 1996. Nutrients. In: R.J. Stevenson, M.L. Bothwell, and R.L. Lowe. (Ed). Algal Ecology. Academic Press. New York.

Bothwell, M.L. 1989. Phosphorus-limited growth dynamics of lotic periphyton diatom communities: areal biomass and cellular growth rate responses. *Canadian Journal of Fisheries and Aquatic Sciences*, 46:1293-1301.

Boulton, A.J. 1999. An overview of river health assessment: philosophies, practice, problems and prognosis. Freshwater Biology. 41: 469-479.

Bowman, M.F., P.A. Chambers, and D.W. Schindler. 2007. Constraints on benthic algal response to nutrient addition in oligotrophic mountain rivers. River Research and Applications. 23: 858-876.

Bradford, M.J. 1995. Comparative review of Pacific salmon survival rates. *Can. J. Fish. Aquat. Sci. 52:* 1327–1338.

Bradford, M.J., J. Korman, and P.S. Higgins. 2005. Using confidence intervals to estimate the response of salmon populations (*Oncorhynchus spp.*) to experimental habitat alterations. *Can. J. Fish. Aquat. Sci.* 62: 2716-2726.

Bradford, M.J., & P.S. Higgins. 2001. Habitat-, season-, and size-specific variation in diel activity patterns of juvenile chinook salmon (*Oncorhynchus tshawytscha*) and steelhead trout (*Oncorhynchus mykiss*). *Can. J. Fish. Aquat. Sci. 58*(2), 365–374. http://doi.org/10.1139/cjfas-58-2-365

Bradford, M.J., P.S. Higgins, J. Korman, and J. Sneep. 2011. Test of environmental flow release in a British Columbia river: does more water mean more fish? *Freshwater Biology* 56:2119-2134.

Bundschuh, M. and B.G. McKie. 2016. An ecological and ecotoxicological perspective on fine particulate organic matter in streams. Freshwater Biology. 61: 2063-2074.

Bunte, K. and S.R. Abt. 2001. Sampling surface and subsurface particle-size distributions in wadable gravel and cobble bed streams for analyses in sediment transport, hydraulics, and streambed monitoring. US Dept of Agriculture, Forest Service, Rocky Mountain Research Station General technical report RMRS-GTR-74.

Carpenter, K.D. and I.R. Waite. 2000. Relations of habitat-specific algal assemblages to land use and water chemistry in the Willamette Basin, Oregon. Environmental Monitoring and Assessment 64: 247-257.

Chapelski, A.J., M.M. Guzzo, L.E. Hrenchuk, and P.J. Blanchfield. 2020. Invertebrate colonization of a newly constructed diversion channel in the Canadian Shield. Canadian Journal of Fisheries and Aquatic Science. 77: 1477-1486.

Chernos, M. 2014. The relative importance of calving and surface ablation at a lacustrine terminating glacier. MSc. Thesis. University of British Columbia.

Chessman, B., S. Williams, & C. Besley. 2007. Bioassessment of streams with macroinvertebrates: effect of sampled habitat and taxonomic resolution. *Journal of the North American Benthological Society*, *26*(3), 546–565.

Costanza, R. and M. Mageau. 1999. What is a healthy ecosystem? Aquatic Ecology. 33: 105-115.

Crossin, G. T., S.G. Hinch, A.P. Farrell, M.P. Whelly, & M.C. Healey. 2003. Pink salmon (*Oncorhynchus gorbuscha*) migratory energetics: response to migratory difficulty and comparisons with sockeye salmon (*Oncorhynchus nerka*). *Canadian Journal of Zoology*, *81*(12), 1986–1995. http://doi.org/10.1139/z03-193

Cummins, K.W. and R.W. Merritt. 1996. Ecology and Distribution of Aquatic Insects. In: R.W. Merritt and K.W. Cummins (ed). An Introduction to the Aquatic Insects of North America. 3rd Edition. Kendall/Hunt Publishing.

Davey, C. 2019. Lower Bridge River Pilot Spawning Gravel Supplementation – Assessment of Spawning Habitat Availability in the Lower Bridge River. Technical Memorandum prepared by Kerr Wood Leidal Ltd. For BC Hydro and St'at'imc Government Services, July 9 2019. 22 p.

Davie, A.W. and S.M. Mitrovic. 2014. Benthic algal biomass and assemblage changes following environmental flow releases and unregulated tributary flows downstream of a major storage. Marne and Freshwater Research. 65: 1059-1071.

Decker, A.S., M.J. Bradford, & P.S. Higgins. 2008. Rate of biotic colonization following flow restoration below a diversion dam in the Bridge River, British Columbia. *River Research and Applications*, *24*(6), 876–883. http://doi.org/10.1002/rra.1076

Deegan, L.A., B.J. Peterson, H.Golden, C.C. McIvor and M.C. Miller. 1997. Effects of fish density and river fertilization on algal standing stocks, invertebrate communities, and fish production in an arctic river. Can. J. Fish. Aquat. Sci. 54: 269-283.

DeNicola, D.M. 1996. Periphyton responses to temperature at different ecological levels. In. R.J. Stevenson, M.L. Bothwell, and R.L. Lowe (Ed). Algal Ecology. Academic Press.

Dewson, Z.S., A.B.W. James, and R.G. Death. 2007. A review of the consequences of decreased flow for instream habitat and macroinvertebrates. *Journal of North American Benthological Society* 26(3): 401-415.

Earl, S.R., H.M. Valett, and J.R. Webster. 2006. Nitrogen saturation in stream ecosystems. Ecology. 87: 3140-3151.

Eaton, B.C., R.D. Moore, and L.G. MacKenzie. 2019. Percentile-based grain size distribution analysis tools (GSDtools) – estimating confidence limits and hypothesis tests for comparing two samples. Earth Surface Dynamics 7: 789-806.

Edmunds, G.F. and R.D. Waltz. 1996. Ephemeroptera. In: R.D. Merritt and K.W. Cummins (Ed). An Introduction to the Aquatic Insects of North America. 3rd Edition. Kendall Hunt Publishing. Dubuque. Iowa.

Ellis, E., C. Davey, A. Taleghani, B. Whitehouse, and B. Eaton. 2018. Lower Bridge River Sediment and Erosion Monitoring, 2017. Prepared by Kerr Wood Leidal Associates Ltd. for St'át'imc Eco-Resources and BC Hydro. 67p.

Ellis, L.E. and N.E. Jones. 2013. Longitudinal trends in regulated rivers: a review and synthesis within the context of the serial discontinuity concept. Environmental Reviews. 21: 136-148.

Ensign, S.H. and M.W. Doyle. 2006. Nutrient spiraling in streams and river networks. Journal of Geophysical Research. 111: 1-13.

Failing, L., G. Horn, and P. Higgins. 2004. Using expert judgment and stakeholder values to evaluate adaptive management options. *Ecology and Society* **9**:13.

Failing, L., R. Gregory, and P. Higgins. 2012. Science, uncertainty and values in ecological restoration: a case study in structured decision-making and adaptive management. *Restoration Ecology* 21:422-430.

Feminella, J.W. and C.P. Hawkins. 1995. Interactions between stream herbivores and periphyton: A quantitative analysis of past experiments. Journal of the North American Benthological Society. 14: 465-509.

Figueroa, R., V. Ruiz, X. Niell, E. Araya, and A. Palma. 2006. Invertebrate colonization patterns in a Mediterranean Chilean stream. *Hydrobiologia*. 571: 409-417.

Flinders, C.A. and D.D. Hart. 2009. Effects of pulsed flows on nuisance periphyton growths in rivers: A mesocosm study. River Research and Applications. 25: 1320-1330.

Francoeur S.N. and B.J.F. Biggs. 2006. Short-term effects of elevated velocity and sediment abrasion on benthic algal communities. Hydrobiologia. 561: 59-69.

Gelman, A. and I. Pardoe. 2006. Bayesian measures of explained variance and pooling in multilevel (hierarchical) models. Technometrics 48: 241-251.

Gelman, A., Carlin, J.B., Stern, H.S., and Rubin, D.B. 2004. Bayesian data analysis, 2nd Edition. Chapman & Hall/CRC, Boca Raton, FL. 668 p.

Goldman, J.C. and E. J. Carpenter. 1974. A kinetic approach to the effect of temperature on algal growth. *Limnology and Oceanography* 19(5): 756 – 766.

Goma, J., F. Rimet, J. Cambra, L. Hoffmann, and L. Ector. 2005. Diatom communities and water quality assessment in mountain rivers of the upper Segre basin (La Cerdanya, Oriental Pyrenees). Hydrobiologia. 551: 209-225.

Grant, S.C.H., M. Townsend, B. White, and M. Lapointe. 2014. Fraser River pink salmon (Oncyhynchus gorbuscha) data review: Inputs for biological status and escapement goals. Report prepared for Pacific Salmon Commission by Fisheries and Oceans Canada and Pacific Salmon Commission. 90pp.

Grimm, N.B. and S.G. Fisher. 1989. Stability of periphyton and macroinvertebrates to disturbance by flash floods in a desert stream. Journal of the North American Benthological Society. 8: 293-307.

Groves, P., J.A. Chandler, & T. Richter. 2008. Comparison of Temperature Data Collected from Artificial Chinook Salmon Redds and Surface Water in the Snake River. North American Journal of Fisheries Management. 28. 766-780. 10.1577/M07-045.1.

Guildford, S.J. and R.E. Hecky. 2000. Total nitrogen, total phosphorus, and nutrient limitation in lakes and oceans: Is there a common relationship? *Limnol. Oceanogr.* 45: 1213-1223.

Hall, A.A., S.B. Rood, & P.S. Higgins. 2011. Resizing a river: a downscaled, seasonal flow regime promotes riparian restoration. *Restoration Ecology*, *19*(3), 351–359. http://doi.org/10.1111/j.1526-100X.2009.00581.x

Harding, J.N. and J.D. Reynolds. 2014. Opposing forces: Evaluating multiple ecological roles of Pacific salmon in coastal stream ecosystems. Ecosphere. 5(12):157. http://dx.doi.org/10.1890/ES14-00207.1.

Harding, J.N., J.M.S. Harding, and J.D. Reynolds. 2014. Movers and shakers: nutrient subsidies and benthic disturbance predict biofilm biomass and stable isotope signatures in coastal streams. Freshwater Biology. doi:10.1111/fwb.12351.

Harvey, C.J., B.J. Peterson, W. B. Bowden, A.E. Hershey, M.C. Miller, L.A. Deegan, and J.C. Finlay. 1998. Biological responses to fertilization of Oksrukuyik Creek, a tundra stream. Journal of the North American Benthological Society. 17: 190-209.

Healey, F.P. 1985. Interacting effects of light and nutrient limitation on the growth rate of Synechococcus linearis (Cyanophyceae). *J. Phycol.* 21:134-146.

Heggenes, J., K. Alfredsen, J.E. Brittain, A. Adeva Bustos, A. Huusko, and M. Stickler. 2017. Temperature changes and biological responses to hydropower-regulated northern stream systems. University College of Southeast Norway. Publication series No. 21.

Hieber, M., C.T. Robinson, S.R. Rushforth, and U. Uehlinger. 2001. Algal communities associated with different alpine stream types. Arctic, Antarctic, and Alpine Research 33: 447-456.

Higgins, P.S. and J. Korman. 2000. Abundance, growth, standing stock, and components of variation of juvenile salmonids in the Bridge River: An analysis to define "baseline conditions" and optimal sampling designs. Report prepared by BC Hydro and Ecometric Research for Bridge River Water Use Planning Fisheries Technical Committee. 45p.

Higgins, P.S., & M.J. Bradford. 1996. Evaluation of a large-scale fish salvage to reduce the impacts of controlled flow reduction in a regulated river. *North American Journal of Fisheries Management*, *16*(3), 666–673. http://doi.org/10.1577/1548-8675(1996)016<0666:EOALSF>2.3.CO;2

Hill, W.R. 1996. Effects of light. In. R.J. Stevenson, M.L. Bothwell, and R.L. Lowe (Ed). Algal Ecology. Academic Press.

Hodson, A. J., P. N. Mumford, and D. Lister. 2004. Suspended sediment and phosphorus in proglacial rivers: bioavailability and potential impacts upon the P status of ice-marginal receiving waters. Hydrol. Process. **18**: 2409‐2422, doi:10.1002/hyp.1471

Holling, C. S. 1978. Adaptive environmental assessment and management. John Wiley and Sons, New York.

Holm-Hansen, O., C.J. Lorenzen, R.W. Holmes, and J.D.H. Strickland. 1965. Fluorometric determination of chlorophyll. *J. Cons. Perm. Int. Explor. Mer*. 30:3-15.

Holt, C.R., D. Pfitzer, C. Scalley, B.A. Caldwell, P. I. Capece, and D.P. Batzer. 2015. Longitudinal variation in macroinvertebrate assemblages below a large-scale hydroelectric dam. Hydrobiologia. 755: 13-26.

Hood, E. and D. Scott. 2008 Riverine organic matter and nutrients in southeast Alaska affected by glacial coverage. Nature Geoscience Letters. 1: 583-587.

Hynes, H.B.N. 1970. The ecology of running waters. University of Toronto Press, Toronto, Ontario.

Johnston, N.T., E.A. MacIsaac, P.J. Tschaplinski, and K.J. Hall. 2004. Effects of the abundance of spawning sockeye salmon (Oncorhynchus nerka) on nutrients and algal biomass in forested streams. Canadian Journal of Fisheries and Aquatic Science. 61: 384-403.

Johnston, N.T., C.J. Perrin, P.A. Slaney, and B.R. Ward. 1990. Increased juvenile salmonid growth by whole-river fertilization. Canadian Journal of Fisheries and Aquatic Science. 47: 862-872.

Jones, N.E. 2010. Incorporating lakes within the river discontinuum: longitudinal changes in ecological characteristics in stream – lake networks. Canadian Journal of Fisheries and Aquatic Sciences. 67: 1350-1362.

Jones, O.R. and J. Wang. 2010. COLONY: a program for parentage and sibship inference from multilocus genotype data. Molecular Ecology Resources 10: 551-555.

Junker, J.R. and W.F. Cross. 2014. Seasonality in the trophic basis of a temperate stream invertebrate assemblage: Importance of temperature and food quality. Limnology and Oceanography. 59: 507-518.

Kennedy, B.P., K.H. Nislow, and C.L. Folt. 2008. Habitat-mediated foraging limitations drive survival bottlenecks for juvenile salmon. Ecology. 89: 2529-2541.

Kennedy, T.A., J.D. Muehlbauer, C.B. Yackulic, D.A. Lytle, S.w. Miller, K.L. Dibble, E.W. Kortenhoeven, A.N. Metcalfe, and C.V. Baxter. 2016. Flow management for hydropower extirpates aquatic insects, undermining river food webs. BioScience. 66: 561-575.

Kimmins, J.P. 1987. Forest Ecology. Macmillan Publishing. New York.

King, N. and A. Clarke. 2015. The Life-History of Rainbow Trout in the Bridge River as Determined by Otolith Microchemistry. Unpublished report prepared for Coldstream Ecology, Ltd. 15pp + App.

King, R.S. and C.J. Richardson. 2001. Evaluating subsampling approaches and macroinvertebrate taxonomic resolution for wetland bioassessment. *Journal of the North American Benthological Society*, 21(1):150-171.

Korman, J. and A. Tompkins. 2014. Estimating regional distributions of freshwater stock productivity, carrying capacity, and sustainable harvest rates for Coho salmon using a hierarchical Bayesian modelling approach. CSAS Res. Doc. 2014/089.

Lachmann, S.C., T. Mettler – Altmann, and A. Wacker. 2019. Nitrate or ammonium: Influences of nitrogen source on the physiology of a green alga. Ecology and Evolution. 9: 1070-1082.

LeBauer, D.S. and K.K. Treseder. 2008. Nitrogen limitation of net primary productivity in terrestrial ecosystems is globally distributed. Ecology. 89: 371-379.

Limnotek. 2019. Carpenter Reservoir Productivity Model Validation and Refinement (BRGMON10): Final report. Report prepared for BC Hydro. 93p. plus appendices.

Lowe, R.L. and Y. Pan. 1996. Benthic algal communities as biological indicators. Pp. 705-733 In: Algal Ecology. R.J. Stevenson, M.L. Bothwell, R.L Lowe (Ed). Academic Press.

Mackay, R.J. 1992. Colonization by lotic macroinvertebrates: A review of processes and patterns. *Can. J. Fish. Aquat. Sci*. 49: 617-628.

Mahendrappa, M.K., N.W. Foster, G.F. Weetman, and H.H. Krause. 1986. Nutrient cycling and availability in forest soils. Canadian Journal of Soil Science. 66: 547-572.

Matthew, P.L. and R.W.J. Stewart. 1985. Summary of juvenile salmonid downstream trapping surveys; Spring, 1984. Report for Community Economic Development, Salmonid Enhancement Program, by Central Interior Tribal Fisheries, Kamloops, B.C., 69 p.

McCullough, D., Spalding, S., Sturdevant, D., & Hicks, M. 2001. Summary of Technical Literature Examining the Physiological Effects of Temperature on Salmonids. US Environmental Protection Agency, (May), 1–119.

McHugh, A.E., and N.O. Soverel. 2017. BRGMON-1 Lower Bridge River Aquatic Monitoring. Annual Report – 2015. Unpublished report by Coldstream Ecology, Ltd., Lillooet, BC, for BC Hydro Generation, Water Licence Requirements, Burnaby, BC. 45 pp. + Apps.

McHugh, A.E., and N.O. Soverel. 2015. Lower Bridge River Aquatic Monitoring. Year 2014 Data Report. Bridge Seton Water Use Plan. Prepared for St'át'imc Eco Resources, Ltd. and BC Hydro for submission to the Deputy Comptroller of Water Rights, August 2015.

McHugh, A.E., and N.O. Soverel. 2014. Lower Bridge River Aquatic Monitoring. Year 2013 Data Report. Bridge Seton Water Use Plan. Prepared for St'at'imc Eco Resources, Ltd. and BC Hydro for submission to the Deputy Comptroller of Water Rights, August 2014.

McHugh, A.E., and N.O. Soverel. 2013. Lower Bridge River Aquatic Monitoring. Year 2012 Data Report. Bridge Seton Water Use Plan. Prepared for St'at'imc Eco Resources, Ltd. and BC Hydro for submission to the Deputy Comptroller of Water Rights, August 2013.

McHugh, A.E., Soverel, N.O., and D. O'Farrell. 2017. Lower Bridge River (LBR) Aquatic Monitoring (2016 High Flow). Unpublished report by Coldstream Ecology, Ltd., Lillooet, BC, for BC Hydro Generation, Water Licence Requirements, Burnaby, BC. 48 pp. + Apps.

McKnight, D.M., R.L. Runkel, C.M. Tate, J.H. Duff, and D.L. Moorhead. 2004. Inorganic N and P dynamics of Antarctic glacial meltwater streams as controlled by hyporheic exchange and benthic autotrophic communities. Journal of the North American Benthological Society. 23: 171-188.

Merritt, R.W. and K.W. Cummins. 1996. An Introduction to Aquatic Insects of North America. 3rd ed. Kendall/Hunt Pub. Dubuque, Iowa.

Merritt, R.W., K.W. Cummins, & M.B. Berg. 2008. An introduction to the aquatic insects of North America. (K.W. Cummins & M.B. Berg, eds.) (4 ed.). Dubuque, Iowa: Kendall/Hunt.

Murray, C.B., T.D. Beacham, & J.D. McPhail. 1990. Influence of parental stock and incubation temperature on the early development of coho salmon (Oncorhynchus kisutch) in British Columbia. *Canadian Journal of Zoology* 68 347-358.

Myrick, C. A., & Cech, J. J. 2000. Temperature influences on California rainbow trout physiological performance. *Fish Physiology and Biochemistry*, 22(3), 245–254. https://doi.org/10.1023/A:1007805322097

Nelson, C.E., D.M. Bennett, and B.J. Cardinale. 2013. Consistency and sensitivity of stream periphyton community structural and functional responses to nutrient enrichment. Ecological Applications. 23: 159-173.

Nichols, S.J., T.B. Reynoldson, and E.T. Harrison. 2014. Evaluating AUSRIVAS predictive model performance for detecting simulated eutrophication effects on invertebrate assemblages. Freshwater Science. 33: 1212-1224.

Norris, R.H. and M.C. Thoms. 1999. What is river health? Freshwater Biology 41: 197-209.

Northcote, T.G., & D.Y. Atagi. 1997. Pacific salmon abundance trends in the Fraser River watershed compared with other British Columbia Systems. In D. J. Stouder, P. A. Bisson, & R. J. Naiman (eds.), *Pacific Salmon and their ecosystems status and future options* (pp. 199–218). Seattle.

Nusch, E.A. 1980. A comparison of different methods for chlorophyll and pheopigment analysis. *Arch. Hydrobiol. Beih. Ergebn. Limnol*. 14: 14-36.

O'Donnell B. 1988. Indian and Non-native use of the Bridge River: a historical perspective. Fisheries and Oceans Canada Native Affairs Division Publication No. 7.

Oliver, G.G. and L.E. Fidler. 2001. Towards a Water Quality Guideline for Temperature in the Province of British Columbia: 3.0 Effects of Temperature on Aquatic Biota. *Ministry of Environment, Lands and Parks, Water Management Branch*.

Perrin, C.J., M.L. Bothwell and P.A. Slaney. 1987. Experimental enrichment of a coastal stream in British Columbia: effects of organic and inorganic additions on autotrophic periphyton production. Can. J. Fish. Aquat. Sci. 44: 1247-1256.

Perrin, C.J. and J. S. Richardson. 1997. N and P limitation of benthos abundance in the Nechako River, British Columbia. Canadian Journal of Fisheries and Aquatic Science. 54: 2574-2583.

Perrin, C.J., K.S. Shortreed, and J.G. Stockner. 1984. An integration of forest and lake fertilization: transport and transformations of fertilizer elements. Canadian Journal of Fisheries and Aquatic Sciences. 41(2):253-262.

Peterson, C.G. 1996. Response of benthic algal communities to natural physical disturbance. In. R.J. Stevenson, M.L. Bothwell, and R.L. Lowe (Ed). Algal Ecology. Academic Press.

Ponader, K.C. and M.G. Potapova. 2007 Diatoms from the genus Achnanthidium in flowing waters of the Appalachian Mountains (North America): Ecology, distribution and taxonomic notes. Limnologica 37: 227-241.

Pritchard, J.K., M. Stephens and P Donnelly. 2000. Inference of Population Structure Using Multilocus Genotype Data. Genetics 155: 945–959.

Quinn, J.M. and C.W. Hickey. 1990. Characterization and classification of benthic invertebrate communities in 88 New Zealand rivers in relation to environmental factors. New Zealand Journal of Marine and Freshwater Research. 24: 387-409.

Quinn, T.P. 2018. The Behaviour and Ecology of Pacific Salmon and Trout. UBC Press.

Rader, R.B., and Belish, T.A. 1999. Influence of mild to severe flow alterations on invertebrates in three mountain streams. Regulated Rivers: Research and Management. 15: 353-363.

Recchia, A. 2010. R-squared measures for two-level hierarchical linear models using SAS. J. Stat. Soft. 32.

Reynoldson, T.B., D.M. Rosenberg, & V.H. Resh. 2001. Comparison of models predicting invertebrate assemblages for biomonitoring in the Fraser River catchment, British Columbia. *Canadian Journal of Fisheries and Aquatic Sciences*, *58*(7), 1395–1410. http://doi.org/10.1139/cjfas-58-7-1395

Rhee, G.-Y. 1978. Effects of N:P atomic ratios and nitrate limitation on algal growth, cell composition, and nitrate uptake. *Limnol. Oceanogr.* 23:10-25.

Rhee, G.-Y. and I.J. Gotham. 1980. Optimum N:P ratios and coexistence of planktonic algae. *J. Phycol.* 16:486-489.

Rinke, K., C.T. Robinson, and U. Uehlinger. 2001. A note on abiotic factors that constrain periphyton growth in alpine glacier streams. Internat. Rev. Hydrobiol. 86: 361-366.

Robinson, C.T. 2012. Long term changes in community assembly, resistance, and resilience following experimental floods. Ecological Applications. 22: 1949-1961.

Rosario, R., and V. Resh. 2000. Invertebrates in intermittent and perennial streams: is the hyporheic zone a refuge from drying? Journal of the North American Benthological Society. 19: 680-696.

Rott, E., M. Cantonati, L. Fureder, and P. Pfister. 2006. Benthic algae in high altitude streams of the Alps – a neglected component of the aquatic biota. Hydrobiologia. 562: 195-216.

Ruegg, J. D.T. Chaloner, P.S. Levi, J.L. Yank, S.D. Tiegs, and G.A. Lamberti. 2012. Environmental variability and the ecological effects of spawning Pacific salmon on stream biofilm. Freshwater Biology 57: 129-142.

Scrine, J., M. Jochum, J.S.Olafsson, and E.J. O'Gorman. 2017. Interactive effects of temperature and habitat complexity on freshwater communities. *Ecology and Evolution.* 7:9333–9346.

Scott, W.B. and E.J. Crossman. 1973. Freshwater fishes of Canada. Fisheries Research Board of Canada. Bulletin 184.

Smokorowski, K.E. and R.G. Randall. 2017. Cautions on using the Before – After – Control – Impact design in environmental effects monitoring programs. Facets. 2: 212-232.

Smucker, N.J., M. Becker, N.E. Detenbeck, and A.C. Morrison. 2013. Using algal metrics and biomass to evaluate multiple ways of defining concentration-based nutrient criteria for streams and ecological relevance. Ecological Indicators. 32: 51-61.

Sneep, J., and M. Evans. 2022. BRGMON-1 Lower Bridge River Aquatic Monitoring: Chinook Salmon Emergence Timing and Life History Review. Report prepared for St'at'imc Eco-Resources and BC Hydro. February 2022.

Sneep, J., C. Perrin, S. Bennett, and J. Korman. 2020. BRGMON-1 Lower Bridge River Aquatic Monitoring, Year 8 (2019) Results. Report prepared for St'at'imc Eco-Resources and BC Hydro. April 2020.

Sneep, J., C. Perrin, S. Bennett, and J. Korman. 2019. BRGMON-1 Lower Bridge River Aquatic Monitoring, Year 7 (2018) Results. Report prepared for St'at'imc Eco-Resources and BC Hydro. July 2019.

Sneep, J., J. Korman, C. Perrin, S. Bennett, and J. Harding. 2018. BRGMON-1 Lower Bridge River Aquatic Monitoring, Year 6 (2017) Results. Report prepared for St'at'imc Eco-Resources and BC Hydro. November 2018.

Sneep, J. 2016. Fish Stranding Protocol for BC Hydro's Bridge-Seton Generation Area. Prepared for BC Hydro, March 2016.

Sneep, J. and S. Hall. 2012a. Lower Bridge River Aquatic Monitoring, Year 2011 Data Report. Prepared for BC Hydro and the Deputy Comptroller of Water Rights. August 2012.

Sneep, J. and S. Hall. 2012b. Lower Bridge River 2011 Flow Ramping Report. Prepared for BC Hydro, Bridge River Generation. March 2012.

Soverel, N.O., and A.E. McHugh. 2016. Lower Bridge River Aquatic Monitoring. Year 2015 Data Report. Bridge Seton Water Use Plan. Prepared for St'át'imc Eco-Resources, Ltd. and BC Hydro for submission to the Deputy Comptroller of Water Rights, August 2016.

Spiegelhalter, D.J., Best, N.G., Carlin, B.P., and A. Van Der Linde. 2002. Bayesian measures of model complexity and fit. J. R. Statist. Soc. B. 64 (4): 583-639

Stevenson, R.J. 1996. An introduction to algal ecology in freshwater habitats. In: R.J. Stevenson, M.L. Bothwell, and R.L. Lowe. Editors: Algal Ecology. 3-30. Academic Press. San Diego.

Stewart-Oaten, A., W.W. Murdoch, and K.R. Parker. 1986. Environmental impact assessment: "Pseudoreplication" in time? Ecology 67: 929-940.

Stumm, W. and J.J. Morgan. 1996. Aquatic Chemistry: An introduction emphasizing chemical equilibria in natural waters. John Wiley and Sons. New York.

Thorp, J.H. and A.P. Covich. 2001. Ecology and classification of North American freshwater invertebrates. 2nd Ed. Academic Press. USA.

Tisdale Environmental Consulting. 2011a. Lower Bridge River Flow Monitoring, 2010. Report prepared for BC Hydro and Power Authority, May 2011.

Tisdale Environmental Consulting. 2011b. Lower Bridge River Flow Monitoring, 2009. Report prepared for BC Hydro and Power Authority, March 2011.

Tornes, E., V. Acuna, C. N. Dahm, and S. Sabater. 2015 Flood disturbance effects on benthic diatom assemblage structure in a semiarid river network. Journal of Phycology. 51: 133-143.

Townsend, S.A., E.A. Garcia, and M.M. Douglas. 2012. The response of benthic algal biomass to nutrient addition over a range of current speeds in an oligotrophic river. Freshwater Science. 31: 1233-1243.

Vinson, M.R. and C.P. Hawkins. 1996. Effects of subsampling area and subsampling procedure on comparisons of taxa richness among streams. JNABS 15(3): 392-399.

Walsh, C.J. 1997. A multivariate method for determining optimal subsampling size in the analysis of macroinvertebrate samples. Marine and Freshwater Research 48(3): 241-248.

Walters, C. J. 1986. Adaptive management of renewable resources. Blackburn Press, Caldwell, New Jersey.

Ward, J.V., and Stanford, J.A. 1995. The serial discontinuity concept: extendingthe model to floodplain rivers. Regulated Rivers: Research and Management, **10**: 159–168. doi:10.1002/rrr.3450100211.

Wehr, J.D., R.G. Sheath, and J. P. Kociolek. Eds. 2014. Freshwater algae of North America: Ecology and Classification. 2nd Edition. Elsevier Press Inc. New York.

Wellnitz, T. and N.L. Poff. 2006. Herbivory, current velocity and algal regrowth: how does periphyton grow when the grazers have gone? Freshwater Biology. 51: 2114-2123.

Wetklo, M. and B. Sutherland. 2021. Genetic stock identification of Bridge River 2020 juvenile Chinook – summary memo. Prepared for St'at'imc Eco-Resources and BC Hydro by the Molecular Genetics Lab at Pacific Biological Station, 22 March 2021.

White, C., D. Ramos-Espinoza, M. Chung, K. Cooke, S. Lingard, A. Putt and G. Poole. 2021. Lower Bridge River Adult Salmon and Steelhead Enumeration – Implementation Year 8 (2019). Ref. BRGMON-3. Report prepared for St'at'imc Eco-Resources by Instream Fisheries Research Inc.

Williams, D.D. and J.H. Mundie. 1978. Substrate size selection by stream invertebrates and the influence of sand. Limnology and Oceanography 23: 1030-1033.

Wipfli, M.S. and C.V. Baxter. 2010. Linking ecosystems, food webs, and fish production: subsidies in salmonid watersheds. *Fisheries*. 35: 373-387.

Wipfli, M.S., Hudson, J., and Caouette, J.P. 1998. Influence of salmon carcasses on stream productivity: response of biofilm and benthic macroinvertebrates in southeastern Alaska, USA. Canadian Journal of Fisheries and Aquatic Sciences **55**: 1503–1511.

Wolman. M. 1954. A method of sampling coarse bed material. American Geophysical Union Transactions. 35:951-956.

Appendix A – Locations of sampling sites in the Lower Bridge River.

Index Monitoring Site Locations

Reach	Index Site	Approx. River Km	UTM Coordinates	
			Easting	Northing
4	A	39.9	555649	5626314
3	B	36.5	558176	5627005
	C	33.3	558109	5629483
	D	30.4	556469	5631133
	E	26.4	556969	5634487
2	F	23.6	559356	5634485
	G	20.0	562537	5630967
1	H	11.3	567796	5629231
	I	7.5	570496	5627006
	J	3.9	572675	5624878
	K	1.2	574432	5623131
Yalakom River	Yal_A	3.8	555989	5637089
	Yal_B	0.1	558281	5635123

[a] UTM zone is 10U.

Off-channel Fish Sampling Locations

Field Component	Reach	Site	Approx. River Km	Bank	UTM Coordinates	
					Easting	Northing
Juvenile Salmonid Habitat Use	4	Bluenose Outflow	39.2	L	556654	5626903
		Bluenose Pond & Upper Intake	39.2	L	556651	5626901
	1	Applesprings Outflow	11.3	R	567992	5629097
		Applesprings Upper Sidechannel	11.3	R	567798	5629205
		Applesprings Middle Sidechannel	11.3	R	567832	5629153
		Applesprings Lower Sidechannel	11.3	R	567928	5629103
Offchannel Stock Assessment	4	Bluenose Riffle	39.2	L	556600	5626876
		Bluenose Pool	39.2	L	556626	5626888
	1	Applesprings Riffle	11.3	R	567955	5629095
		Applesprings Pool	11.3	R	567813	5629192

Juvenile Stock Assessment Site Locations (LBR Mainstem)

Reach	Site	Approx. River Km	Bank	UTM Coordinates	
				Easting	Northing
4	40500	40.5	L	555590	5626147
	40200	40.2	L	555649	5626314
	40100	40.1	R	555717	5626271
	39401	39.4	R	556482	5626807
	39400	39.4	R	556482	5626807
	39201	39.2	L	556759	5626389
	39200	39.2	L	556761	5626653
	37300	37.3	L	557900	5626750
	37200	37.2	R	558000	5626725
	37150	37.2	L	558075	5626750
	37001	37.0	L	558200	5626750
	37000	37.0	L	558225	5626775
3	35941	35.9	L	558174	5627021
	35940	35.9	R	558191	5627003
	33824	33.8	L	558250	5629725
	33800	33.8	L	558250	5629850
	32440	32.4	L	557800	5630250
	32432	32.4	L	557766	5630280
	32284	32.3	L	557725	5630314
	32211	32.2	L	557625	5630301
	32206	32.2	L	557627	5630344
	30721	30.7	L	556550	5631375
	30700	30.7	R	556550	5631375
	29300	29.3	L	556010	5632098
	29010	29.0	R	555733	5632232
	29000	29.0	R	555724	5632258
	28533	28.5	L	555900	5632500
	27600	27.6	R	556242	5633466
	27500	27.5	L	556291	5633555
	27450	27.5	L	556324	5633622
	26100	26.1	L	557174	5634605
	26000	26.0	L	557356	5634661

Reach	Site	Approx. River Km	Bank	UTM Coordinates	
				Easting	Northing
2	24841	24.8	L	558400	5634600
	24802	24.8	R	558450	5634575
	23900	23.9	L	559250	5634450
	23800	23.8	L	559350	5634550
	23602	23.6	L	559450	5634475
	23601	23.6	R	559450	5634475
	23301	23.3	L	559500	5634325
	22801	22.8	L	559743	5633911
	22800	22.8	L	559732	5633929
	21801	21.8	L	560494	5633459
	21800	21.8	R	560422	5633455
	21601	21.6	L	560748	5633331
	21600	21.6	R	560648	5633291
	21401	21.4	L	560849	5633130
	21400	21.4	R	560849	5633130
	20001	20.0	L	562500	5630900
	20000	20.0	R	562500	5630900
1	11350	11.4	R	567798	5629277
	11301	11.3	R	567817	5629276
	11300	11.3	R	567850	5629246
	7250	7.3	R	569867	5627075
	7201	7.2	L	569932	5627092
	7200	7.2	R	569888	5627048
	3999	4.0	L	572566	5625155
	3950	4.0	R	572636	5625094
	3901	3.9	L	572632	5625019
	1250	1.3	L	574437	5623140
	1200	1.2	L	574360	5623091
	1125	1.1	L	574377	5623127

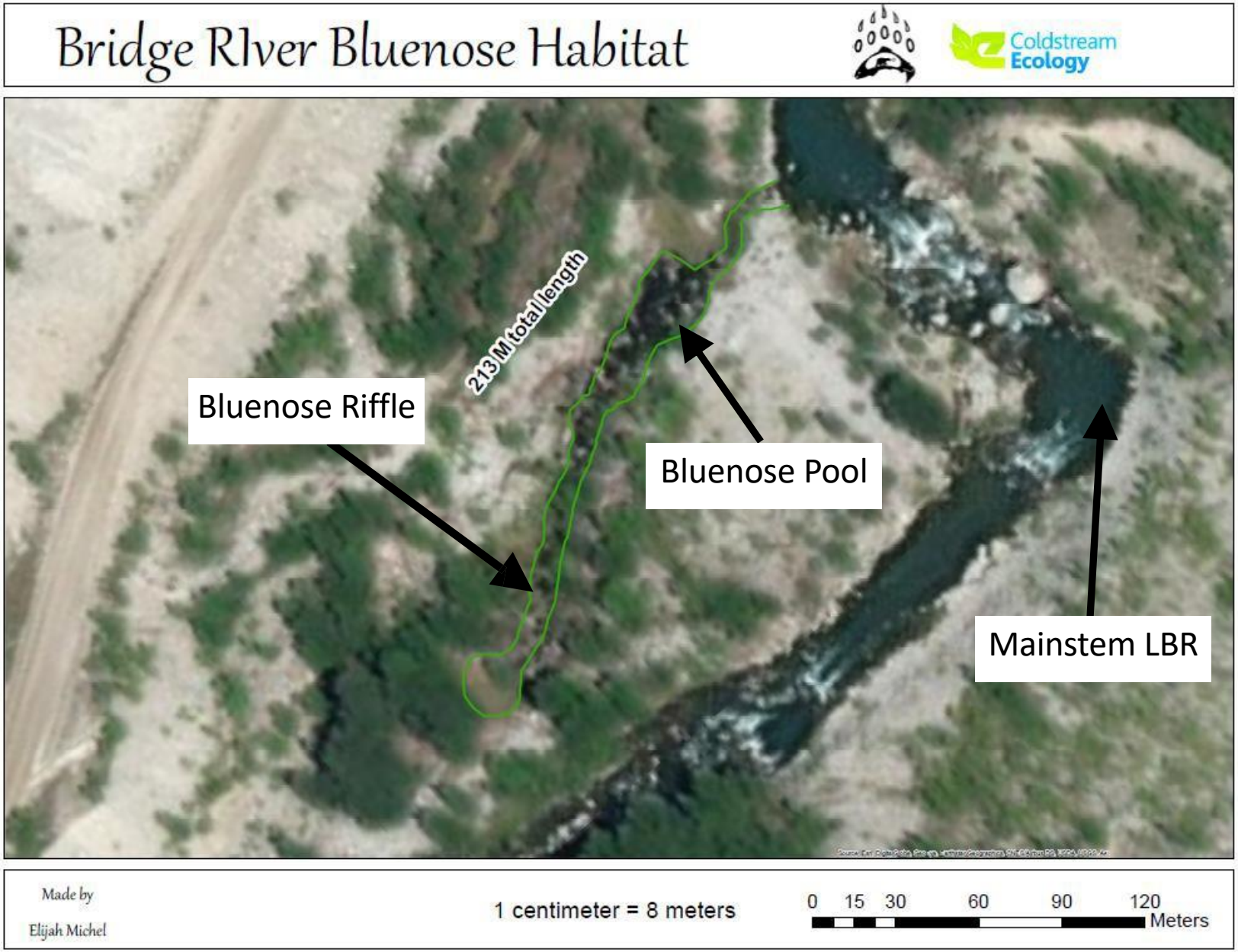
Bridge RIver Bluenose Habitat
Coldstream Ecology
213 M total length
Bluenose Riffle
Bluenose Pool
Mainstem LBR
Made by
Elijah Michel
1 centimeter = 8 meters
0 15 30 60 90 120
Meters

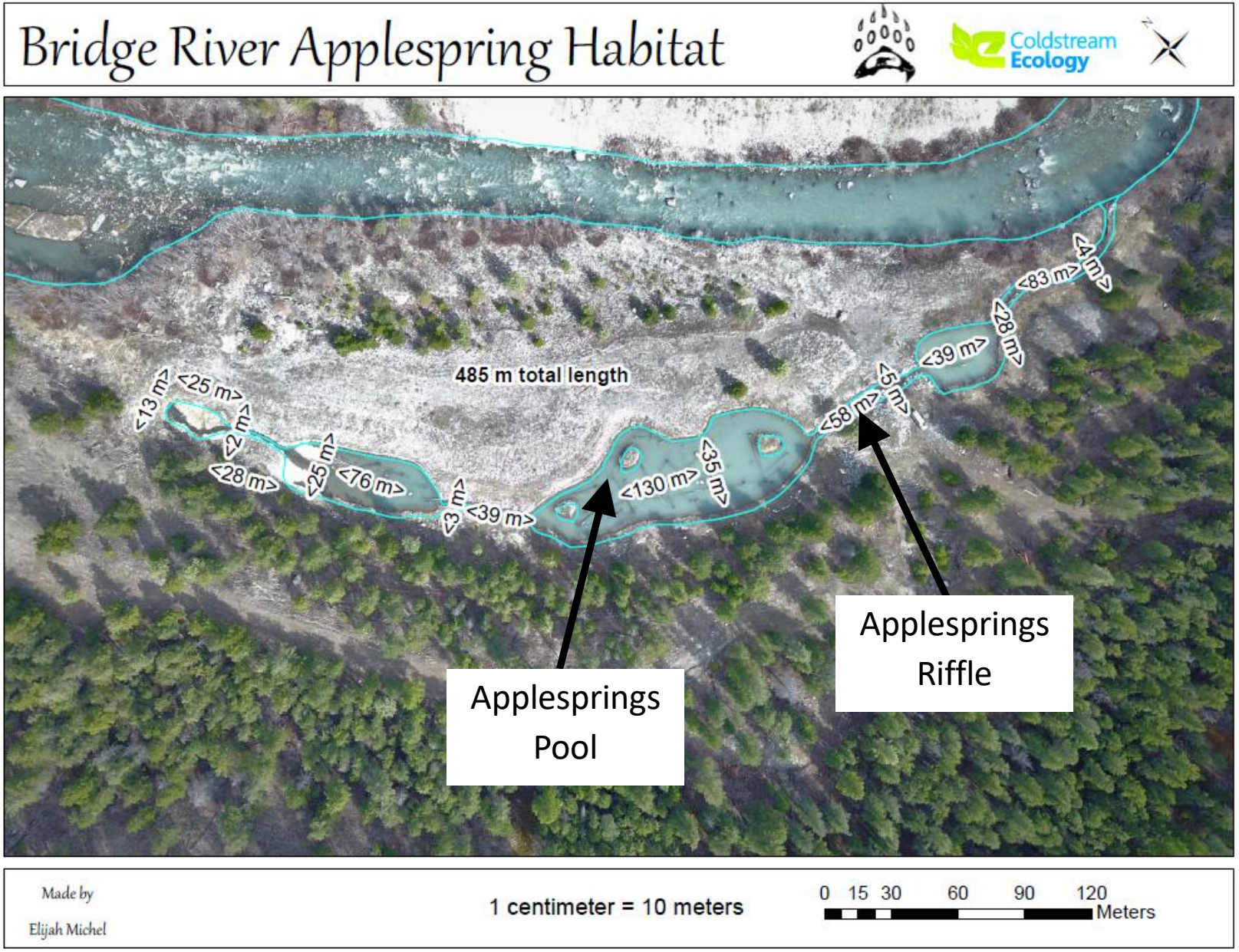
Bridge River Applespring Habitat
Coldstream Ecology
485 m total length
<13 m>
<25 m>
<2 m>
<28 m>
<25 m>
<76 m>
<3 m>
<39 m>
<130 m>
<35 m>
<58 m>
<5 m>
<39 m>
<28 m>
<83 m>
<4 m>
Applesprings Pool
Applesprings Riffle
Made by
Elijah Michel
1 centimeter = 10 meters
0 15 30 60 90 120
Meters

Appendix B – Description of Hierarchical Bayesian Model Estimating Juvenile Salmonid Abundance and Biomass in the Lower Bridge River

Our hierarchical Bayesian Model (HBM) is similar to model I of Wyatt (2002 and 2003). The model consists of two levels or hierarchies. Site-specific estimates of detection probability (also referred to as catchability) and densities at the lowest level of the hierarchy are considered random variables that come from hyper-distributions of catchability and density at the higher level. The HBM jointly estimates both site- and hyper-parameters. The process component of the model assumes that variation in fish abundance across sites can be modeled using a Poisson/log-normal mixture (Royle and Dorazio 2008). That is, abundance at-a-site is Poisson-distributed with a site-specific log-normally distributed mean. The observation component of the model assumes that variation in detection probability across sites can be modeled using a beta distribution, and that electrofishing catches across sites and passes vary according to a binomial distribution which depends on site-specific detection probability and abundance.

In the following description "fish" refers to one species-age group combination. Greek letters denote model parameters that are estimated. Capitalized Arabic letters denote derived variables that are computed as a function of parameters. Lower case Arabic letters are either subscripts, data, or prior parameter values.

We assumed that the number of fish captured, *c*, by electrofishing in year *y* at site *i* on pass *j* followed a binomial distribution (*dbin*) described by the detection probability (or catchability) θ, and the number of fish in the sampling arena, *N*:

(1) $$c_{y,i,j} \sim dbin(\theta_{y,i}, N_{y,i,j})$$

We assumed that detection probability was constant across passes but could vary among sites. The number of fish remaining in the sampling area after pass *j* was the difference between the number present prior to pass *j* and the catch on pass *j*:

(2) $$N_{y,i,j+1} = N_{y,i,j} - c_{y,i,j}$$

These two equations describe the binomial model on which removal estimators are based (e.g., Moran 1951, Otis et al. 1978). Inter-site variation in detection probability was assumed to follow a beta hyper-distribution (*dbeta*), with year-specific parameters:

(3) $\theta_{y,i} \sim dbeta(\alpha_y, \beta_y)$

Inter-site variation in fish density (λ) in log space was assumed to follow a normal (*dnorm*) hyper-distribution:

(4) $\log(\lambda_{y,i}) \sim dnorm(\mu_{\lambda_{y,r}}, \tau_{\lambda_{y,r}})$

Here μ and τ are the mean and precision of the normal probability distribution ($\tau = \sigma_\lambda^{-1}$) specifying the hyper-distribution of log density for each reach and year. The number of fish present at site *i* prior to the first electrofishing pass ($N_{y,i,1}$) followed a poisson distribution with an expected value determined by the product of site area, *a*, and fish density drawn from the hyper-distribution (Equation 4):

(5) $N_{y,i} = \lambda_{y,i} a_{y,i}$

To compute the total abundance of fish in a reach we also needed an estimate the number of fish in the areas of the river that we did not sample. As most of our sampling was conducted along the shorelines, we partitioned the wetted area of the river into one of 3 categories: the shoreline area that was sampled, the shoreline area that was not sampled, and the centre of the channel that in most cases was not sampled. The total abundance in reach *r* and year *y*, $Ntot_{y,r}$, was the sum of the estimates from sampled shoreline sites within the reach, *Nss*, the estimate for the unsampled shoreline, *Nus*, and abundance in the unsampled centre channel area (*Nuc*) for that reach and year:

(6) $Ntot_{y,r} = Nss_{y,r} + Nus_{y,r} + Nuc_{y,r}$

The number of fish in the sampled shoreline was the sum of abundances of all sites within the reach:

(7) $Nss_{y,r} = \sum_i N_{y,r,i,1}$

Abundance in the unsampled shoreline (*Nus*) was computed as the product of the transformed mean density from the log-normal density hyper distribution (μ_λ) with log-normal bias correction ($0.5\tau^{-1}_\lambda$), and the area of the unsampled shoreline in the reach. The area of the unsampled shoreline is the area of the shoreline zone (the product of twice the length of the reach (l) and the average width of sampled area, w, less the total area that was sampled in the reach:

(8) $$Nus_{y,r} = \exp\left[\mu_{\lambda_{y,r}} + 0.5\tau^{-1}_{\lambda_{y,r}}\right](2l_r w_{y,r} - \sum_i a_{y,i})$$

The number of fish in the centre of the channel (*Nuc*) was computed based on the abundance in the shoreline zone (*Nss*+*Nus*) and estimates of the proportion of the total population that was in the shoreline zone (ρ).

(9) $$Nuc_{y,r} = \left(Nss_{y,r} + Nus_{y,r}\right)(1 - \rho_{f,r})$$

The parameter ρ is calculated for each reach, *r*, and flow period, *f*, and depends on the average width of electrofishing sites in each reach relative to the distribution of fish from shore determined from the field study described earlier. We assumed that the number of fish in the micro-habitat study ($h_{f,r}$) between the shoreline and the average width of electrofishing sites ($w_{y,r}$) in any year-reach strata was a binomially distributed random variable that depended on $\rho_{y,r}$ and the total number of fish observed in the micro-habitat study for that strata ($m_{f,r}$).

(10) $$h_{f,y} \sim dbin(\rho_{y,r}, m_{f,r})$$

In Reach 3 during the baseline period the total wetted width was sampled. Hence $w_{y,r}$ is the average wetted width of the reach so the total wetted area of the reach is $l_3 w_3$ and the multiplier 2 in equation 8 is not used. Also $\rho = 1$ in Equation 9 and consequently *Nuc*=0.

We estimated the effect of the flow release in each reach as the difference in the estimated average abundance between the treatment and baseline years (Δ_r) for age-0 fish as:

$$\Delta_r = \frac{\sum_{y=2001}^{2008} N_{y,r}}{8} - \frac{\sum_{y=1996}^{1999} N_{y,r}}{4}$$

(11)

Data for the year 2000 were not used as the change in flow occurred midway through the growing season and it is unclear how age-0 fish would be affected. The overall effect of flow in the study area Δ, which includes the contribution from the re-wetted Reach 4, is the difference in the average abundance of three Reaches (2-4) during the treatment period and the average abundance for Reaches 2 and 3 for the baseline period:

$$\Delta = \frac{\sum_{y=2001}^{2008} \sum_{r=2}^{4} N_{y,r}}{8} - \frac{\sum_{y=1996}^{1999} \sum_{r=2}^{3} N_{y,r}}{4}$$

(12)

For age-1 trout we considered fish sampled in September 2000 to be part of the baseline period as they would have experienced the increased flows for only a month just before sampling, representing <10% of their life as free-swimming fish. We did not use data for 2001 for the treatment period as these fish would have experienced baseline flows during their first 2-3 months after emergence from spawning gravels, which may have affected survival during this important early life stage. The summation indices in Equations 11 and 12 were adjusted accordingly for this age group.

Posterior distributions of model parameters were estimated using WinBUGS (Spiegelhalter et al. 1999) called from the R2WinBUGS (Sturtz et al. 2005) library from R (R Development Core Team 2009). Prior distributions for hyper-parameters and related transformations are given in Table 1. Posterior distributions were based on taking every second sample from a total of 5000 simulations after excluding the first 2000 to remove the effects of initial values.

The HBM was able to converge in all years using uninformative priors for both age-0 rainbow trout and age-0 chinook salmon (Table 1). For age-1 rainbow trout and age-0 coho

salmon, depletion data were sparse for Reach 2 (there were small total catches at many sites within the reach). In these cases, the estimated abundance and detection probability at each site were highly confounded as the model was not able to distinguish estimates of high abundance and low detection probability with the converse. This uncertainty resulted in very low estimates of the precision of the hyper-distribution in log fish density across sites (τ_λ in Equation 4). To avoid unrealistically low estimates of precision, which in turn would lead to overestimates of abundance in the unsampled shoreline zone because of the bias correction term (Equation 8) we used a more informative distribution for these 2 species-age groups (Table 2). Following recommendations by Gelman (2006), the half-Cauchy or folded *t*-distribution prior was used to constrain σ_λ and achieve convergence.

The HBM had difficulty reaching convergence based on data from recent years due to low catches for some species and age groups (e.g. age-0 chinook). Site-specific estimates of capture probability, which drive estimates of the hyper-distribution of capture probability, depend on the magnitude of the reduction in catches across passes.There is no information about capture probabilty at a site if no fish of a given species-age class are captured, and very little information when the catch is very low. If this pattern occurs at many sites, the hyper-distribution of capture probability will be poorly defined and more information on capture probability in the prior distribution is required to obtain reliable estimates of capture probability and abundance.

In the original application of the HBM we used an uninformative prior for the mean capture probability across sites centered at 0.5 (beta distribution with parameters beta(1,1)), and a minimally informative prior for the standard deviation in capture probabilities across sites (half-cauchy distribution with scale parameters 0 and 0.3, see Gelman 2006). To obtain more reliable estimates, we used a more informative prior on the mean capture probability across sites. The prior was still centered at 0.5 (beta(50,50)), but has a uniform prior on the precison (inverse of variance) of capture probability across sites (unif(10,500)) which constrained the maximum extent of variation in capture probability aross sites. To be consistent, we applied the revised priors to all species and age classes.

In cases where capture probability was well defined in all years because the species-age class was abundant and widely distributed across sites (e.g. Rb-0), model estimates based on uninformative and minimally informative priors were very similar. Uncertainty in capture probability (Fig. A1) and abundance (Fig. A2) estimates was slightly lower when the more informative priors were used. In cases where catch was low and fish were absent from many sites (Ch-0 in years > 2003, Co-0 1996-2000), the more informative priors led to reduced variation in capture probability estimates across years. In the case of juvenile chinook salmon, the original priors resulted in a decline in capture probability over time (Fig. A1, bottom-right panel). That pattern was suspect because it was inconsistent with the stable trends for other species-age classes (Rb-0, Co-0) where capture probability was well defined. Both electrofishing methods and flows at the time of sampling were stable during this period, which should lead to stable capture probabilities. The revised priors stabilized and increased Ch-0 capture probability across years (Fig. A1) such that they were more consistent with trends from species-ages that were well determined. For the other species, revised capture probabilities tended to be higher when catches were low. This in turn resulted in a decrease in estimated abundance in many years and a large reduction in the uncertainty in annual abundance estimates.

To better understand the effects of low catch and occupancy on estimates of abundance from the HBM, we simulated a set of catch depletions across 50 sites based on a zero-inflated log-normal distribution of fish densities. We then applied the HBM to the simulated data and compared estimates of abundance and capture probability to the values used drive the simulation. We found that capture probability was underestimated and abundance was overestimated, and the extent of bias increased with the degree of zero-inflation in simulated fish densities. For example, when we assumed that 30% of the sample sites were unoccupied and mean density was low, abundance was overestimated by 50%. This occurred because the HBM assumes a log-normal distribution in fish density across sites and does not explicitly account for zero-inflation. When the true distribution of densities is a zero-inflated, a better fit is obtained by lowering the capture probability because this increases the likelihood for sites with low or zero catch. This in turn results in an overestimate of abundance. Increasing information on capture probability in prior distributions reduces the tendency of the model to underestimate capture

probability and therefore reduces the extent of positive bias in abundance. We attempted to revise the structure of the HBM to directly estimate the extent of zero-inflation, but this additional parameter was not estimable because the degree of zero-inflation and the magnitude of capture probability were confounded. That is, the model could not distinguish between cases where capture probabiltiy was high and a large fraction of sites were unoccupied, and the opposte pattern. Although directly accounting for zero-inflation in animal distributions can be accomodated in a mark-recapture framework (Conroy et al. 2008), confounding between capture probability and abundance precludes its use in depletion-based studies.

References

Conroy, M.J., Runge, J.P., Barker, R.J., Schofield, M.R., and C.J. Fonnesbeck. 2008. Efficient estimate of abundance for patchily distributed populations via two-phase, adaptive sampling. Ecology 89:3362-3370.

Gelman, A. 2006. Prior distributions for variance parameters in hierarchical models. Bayesian analysis 1: 515-533.

Royale, J.A., and R.M. Dorazio. 2008. Hierarchical modelling and inference in ecology. Academic Press, Amsterdam. 444 pp.

Spiegelhalter, D.J., Thomas A., Best, N.G., and Lunn, D. 1999. WinBUGS User Manual: Version 1.4. Cambridge: MRC Biostatistics Unit, 60 pp.

Sturtz, S., Legges U., and Gelman A. 2005. R2WinBGS: a package for running WinBUGS from R. Journal of Statistical Software 3: 1-16.

Wyatt, R.J. 2002. Estimating riverine fish population size from single- and multiple-pass removal sampling using a hierarchical mode. Can J. Fish. Aquat. Sci. 59:695-706.

Wyatt, R.J. 2003. Mapping the abundance of riverine fish populations: integrating hierarchical Bayesian models with a geographic information system (GIS). Can. J. Fish. Aquat. Sci. 60: 997-1007.

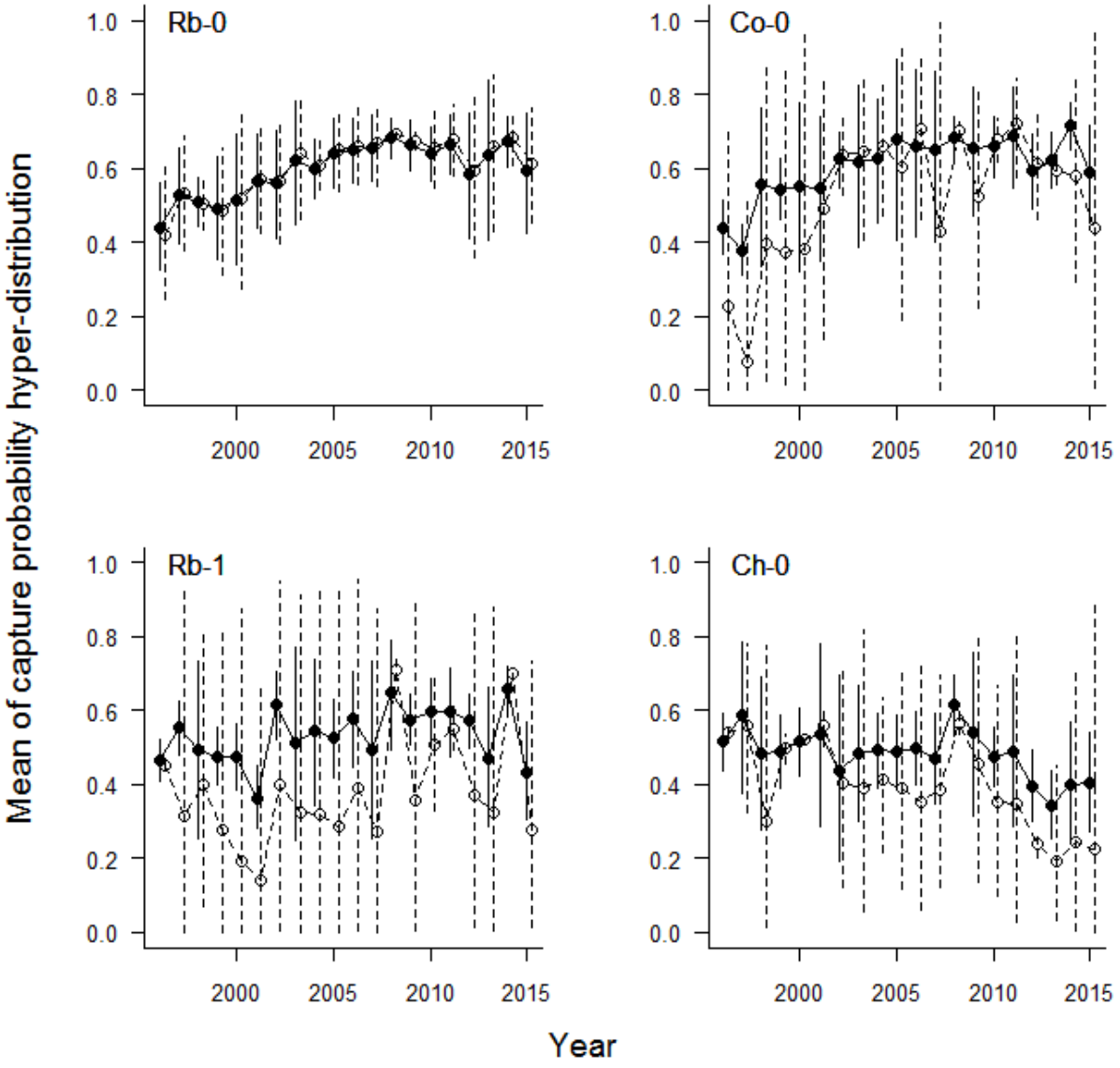

Figure B1. Annual estimates of the mean (with 90% credible interval) of the capture probability hyper-distribution (distribution of capture probability across sites) based on the HBM with more restrictive priors for the capture probability hyper-distribution (solid symbols). Also shown are estimates based on uninformative capture probability priors used in Bradford et al. (2011, open symbols).

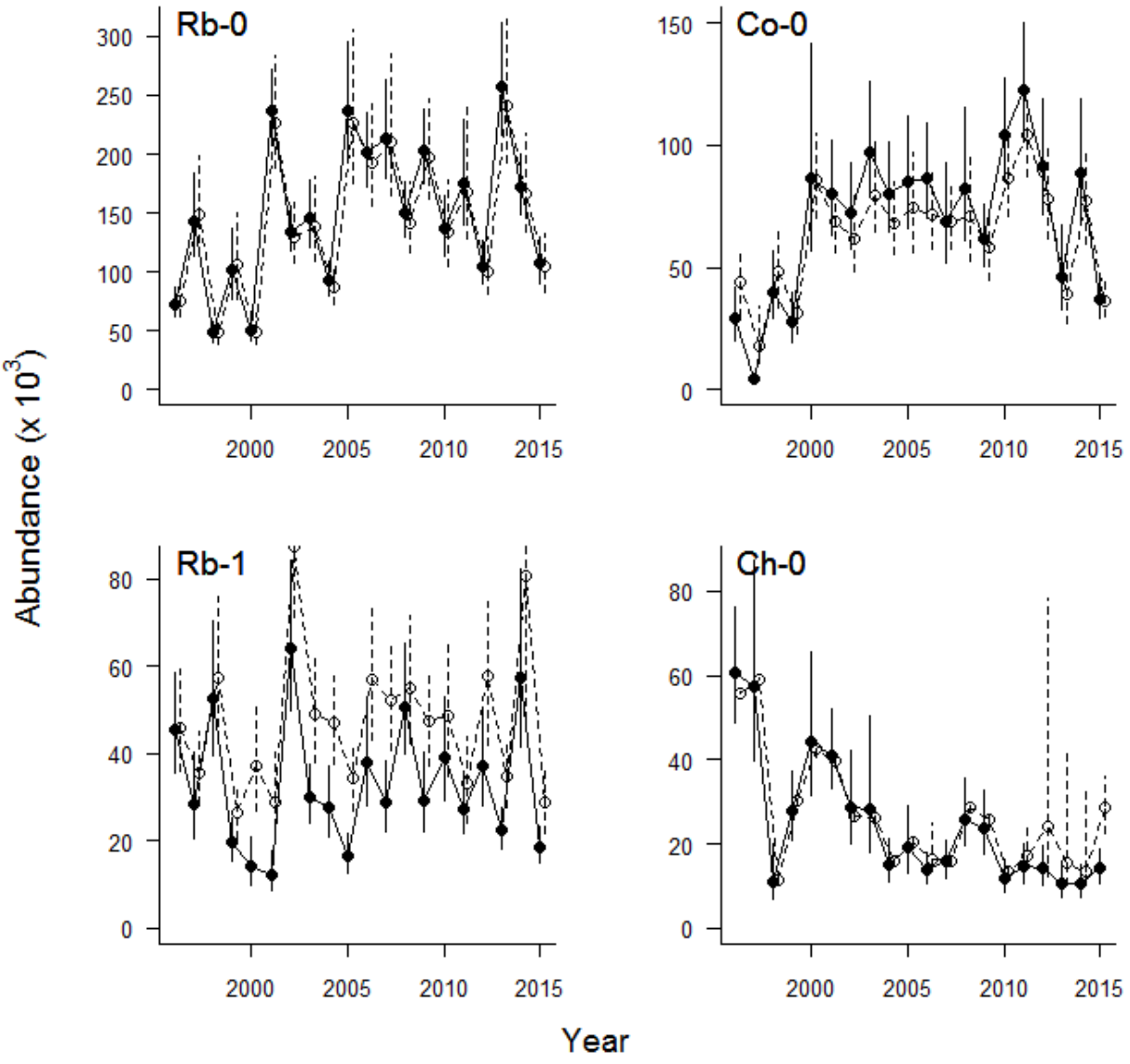

Figure B2. Annual estimates of abundance (all reaches combined) based on the HBM with a more restrictive prior (solid symbols). Also shown are estimates based on the uninformative priors used in Bradford et al. (2011, open symbols).

Appendix C – WinBUGS Source Code for Mixed Effects Model Predicting Log Density or Biomass.

Note: Text in black, blue, and green denotes data, statistical functions used as priors for fixed and random effects or the likelihood, and comments, respectively.

```
for(ir in 1:2) {BetaR[ir]~dnorm(0,1.0E-03)}           #fixed reach effects for trial 0 (0 cms)
BetaR[Nreaches]<-0                                    #reach effect for reach 4 (index 3) is 0 as it is dry
for(itr in 1:Ntreats){BetaF[itr]~dnorm(0,1.0E-03)}    #fixed treatment effects (relative to 0 cms)
yrSD~dunif(0.001,10);yrPrec<-pow(yrSD,-2)
for (i in 1:Nyrs) {BetaY[i]~dnorm(0,yrPrec)}          #random year effect
proSD~dunif(0.001,10);  proPrec<-pow(proSD,-2)        #process error

for(i in 1:LastTreat0){ #samples from flow trial 0 - 0 cms dam release
      pro_dev[i]~dnorm(0,proPrec)
      pred[i] <- BetaR[Reach[i]] + BetaY[Year[i]] + pro_dev[i]
      obs_mu[i]~dnorm(pred[i],obs_prec[i])
      RE[i]<-BetaY[Year[i]]+pro_dev[i]                #random effect component of prediction
}

for(i in (LastTreat0+1):Nsamps){    #samples from flow trials 1:3 (3, 6 and high flow dam release)
      pro_dev[i]~dnorm(0,proPrec)
      pred[i] <- BetaR[Reach[i]] + BetaF[Ftreat[i]] + BetaY[Year[i]] + pro_dev[i]
      obs_mu[i]~dnorm(pred[i],obs_prec[i])
      RE[i]<-BetaY[Year[i]]+pro_dev[i]
}
```

```
for(i in 1:Nsamps){     #Complete Fixed effect r2 computation and compute data r2
      ssRE[i]<-pow(RE[i]-sum(RE[]),2)            #squares of random effects
      ssTOT[i]<-pow(pred[i]-sum(pred[]),2)       #squares fixed + random effects
      data_res[i]<-pow(obs_mu[i]-pred[i],2)      #observed - predicted (squared residual)
      data_ssTOT[i]<-pow(obs_mu[i]-sum(obs_mu[]),2)
}
#Complete sums of squares calculation to finish FE_r2 computation, and compute data_r2
FE_r2<-1.0-sum(ssRE[])/sum(ssTOT[]) #Proportion of total sums of squares explained by fixed effects
data_r2<-1.0-sum(data_res[])/sum(data_ssTOT[]) #Proportion of total ss explained by model (Fixed + random)
```

Appendix D – Mean Water Temperatures in the Lower Bridge River (by Reach) and the Yalakom River for each Study Year

Note: Each year is coloured according to flow trial.

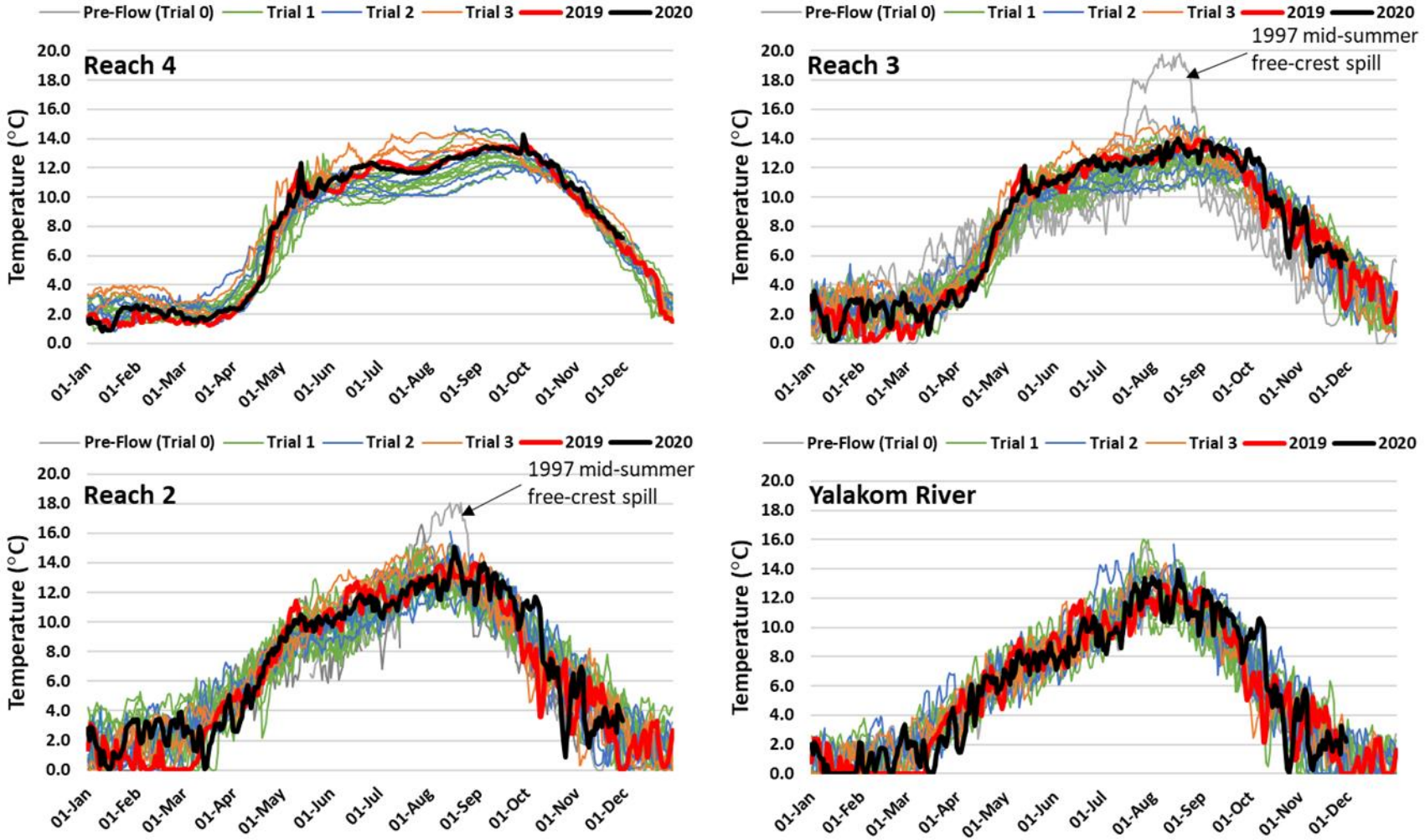

Appendix E – Genetic Stock Identification Results

Table E1: Chinook salmon microsatellite baseline samples used in the Structure analysis of the 2020 Bridge River juveniles (from Wetklo and Sutherland 2021).

Population or GU (genetic unit)	Stock	Stock abbreviation	Year	n
NOTH	North Thompson Mainstem	NThM	01	50
Brid	Bridge R	Brid	96	100
Brid	Bridge R juveniles	BriJ	20	93
Tase	Taseko R	Tase	02	50
GU3	Lower Caribou R	LCar	07	20
GU3	Lower Caribou R	LCar	08	30
GU3	Quesnel R	Ques	96	50
GU3	Upper Caribou R	Ucar	01	50
GU2	Baker Cr	Bake	08	30
GU2	Nazko R	Nazk	83	11
GU2	Nazko R	Nazk	84	10
GU2	Nazko R	Nazk	85	29
GU2	Baezaeko R	Baez	84	29
GU2	Baezaeko R	Baez	85	19
GU2	West Road R	West	97	20
GU2	West Road R	West	08	30
GU1	Nechako R	Nech	96	50
GU1	Stuart R	Stua	96	50
GU1	Kuzkwa R	Kuzk	07	4
GU1	Kuzkwa R	Kuzk	08	17
GU1	Kuzkwa R	Kuzk	09	29
GU4b	Bowron R	Bowr	03	36
GU4b	Bowron R	Bowr	09	14
GU4b	Indianpoint Cr	Indi	95	39
Tete	Tête Jaune	Tete	01	50
Total				910

Table E2: Microsatellite GSI assignment and Structure inferred genetic ancestry for the 2020 Bridge River Chinook juveniles (from Wetklo and Sutherland 2021).

		Microsatellite GSI assignment												
	Structure inferred ancestry	Bridge	NOTH	Taseko	GU3	GU2	GU1	GU4b	Tete Jaune	Reject (prob. < 75%)	Non-target species	Failed geno.	Assignments by Structure (n)	Assignments by Structure (%)
	Brid	43	1			1	7		1	22		1	76	71.7
Admixture source	NThM									1			1	0.9
	Tase			1									1	0.9
	GU3				1					2			3	2.8
	GU2					1				3			4	3.8
	GU1	2					5			5			12	11.3
	GU4b	2						1		1			4	3.8
	Tete									1			1	0.9
	Unknown	1								3			4	3.8
	Non-target species										8		8	
	Failed genotyping											3	3	
	Assignments by Microsatellite GSI (n)	48	1	1	1	2	12	1	1	38	8	4	117	
	Assignments by Microsatellite GSI (%)	45.7	1.0	1.0	1.0	1.9	11.4	1.0	1.0	36.2				

Table E3: Structure inferred genetic ancestry and GSI assignments for the 2020 Bridge River Chinook juveniles. Percentages 80% or higher are green, between 50 and 79% are yellow, and less than 49% are red (from Wetklo and Sutherland 2021).

FishID	Mean Bridge Ancestry (%)	Structure inferred ancestry	Accepted GSI assignment	Region Name	Prob 1 (%)
BriJ20_196	98%	Brid	GU1	GU1	96%
BriJ20_126	98%	Brid	GU1	GU1	95%
BriJ20_214	98%	Brid	GU1	GU1	96%
BriJ20_117	98%	Brid	GU1	GU1	89%
BriJ20_180	98%	Brid	TeteJaune	TeteJaune	93%
BriJ20_199	98%	Brid	Reject	Bridge	55%
BriJ20_90	97%	Brid	Reject	GU1	52%
BriJ20_184	97%	Brid	Reject	GU1	73%
BriJ20_191	97%	Brid	Reject	SOTH	66%
BriJ20_186	97%	Brid	Bridge	Bridge	92%
BriJ20_217	97%	Brid	Reject	Portage	68%
BriJ20_37	97%	Brid	Reject	GU6b	34%
BriJ20_7	96%	Brid	Reject	GU4b	46%
BriJ20_57	96%	Brid	NOTH	NOTH	100%
BriJ20_122	96%	Brid	Bridge	Bridge	94%
BriJ20_6	96%	Brid	Bridge	Bridge	100%
BriJ20_171	95%	Brid	Bridge	Bridge	100%
BriJ20_206	95%	Brid	Bridge	Bridge	100%
BriJ20_30	95%	Brid	Reject	LWFR-Sp	22%
BriJ20_198	95%	Brid	Bridge	Bridge	100%
BriJ20_175	94%	Brid	Bridge	Bridge	100%
BriJ20_61	94%	Brid	Bridge	Bridge	81%
BriJ20_95	94%	Brid	Bridge	Bridge	100%
BriJ20_176	94%	Brid	Bridge	Bridge	100%
BriJ20_67	94%	Brid	Bridge	Bridge	99%
BriJ20_190	94%	Brid	Bridge	Bridge	100%
BriJ20_189	93%	Brid	Bridge	Bridge	100%
BriJ20_141	93%	Brid	Reject	Bridge	62%
BriJ20_227	93%	Brid	Reject	Bridge	66%
BriJ20_225	93%	Brid	Bridge	Bridge	96%
BriJ20_222	92%	Brid	Bridge	Bridge	100%
BriJ20_178	92%	Brid	Bridge	Bridge	100%
BriJ20_201	92%	Brid	Bridge	Bridge	81%
BriJ20_10	92%	Brid	Bridge	Bridge	98%
BriJ20_193	91%	Brid	Bridge	Bridge	94%
BriJ20_125	91%	Brid	Bridge	Bridge	99%
BriJ20_123	90%	Brid	Bridge	Bridge	89%

Table E3 cont'd.

FishID	Mean Bridge Ancestry (%)	Structure inferred ancestry	Accepted GSI assignment	Region Name	Prob 1 (%)
BriJ20_183	89%	Brid	Bridge	Bridge	98%
BriJ20_208	89%	Brid	Bridge	Bridge	100%
BriJ20_187	89%	Brid	Bridge	Bridge	99%
BriJ20_192	89%	Brid	Bridge	Bridge	91%
BriJ20_224	88%	Brid	Bridge	Bridge	96%
BriJ20_202	88%	Brid	Bridge	Bridge	100%
BriJ20_76	87%	Brid	Bridge	Bridge	94%
BriJ20_215	87%	Brid	Reject	Bridge	60%
BriJ20_15	87%	Brid	Failed genotyping	Failed genotyping	
BriJ20_177	87%	Brid	Reject	GU2	54%
BriJ20_38	86%	Brid	Reject	GU4b	44%
BriJ20_120	85%	Brid	Reject	GU1	46%
BriJ20_129	84%	Brid	Bridge	Bridge	97%
BriJ20_92	84%	Brid	Reject	GU2	44%
BriJ20_80	82%	Brid	Reject	Bridge	48%
BriJ20_185	82%	Brid	Bridge	Bridge	93%
BriJ20_213	82%	Brid	Bridge	Bridge	100%
BriJ20_114	81%	Brid	Bridge	Bridge	90%
BriJ20_211	81%	Brid	Bridge	Bridge	99%
BriJ20_174	81%	Brid	Reject	L_Chilcotin	50%
BriJ20_45	80%	Brid	Bridge	Bridge	99%
BriJ20_39	79%	Brid	Bridge	Bridge	99%
BriJ20_205	79%	Brid	Bridge	Bridge	99%
BriJ20_118	78%	Brid	GU1	GU1	85%
BriJ20_173	78%	Brid	Bridge	Bridge	96%
BriJ20_194	78%	Brid	Bridge	Bridge	97%
BriJ20_275	78%	Brid	Reject	GU1	58%
BriJ20_212	78%	Brid	Bridge	Bridge	84%
BriJ20_128	77%	Brid	Reject	Bridge	61%
BriJ20_223	76%	Brid	Bridge	Bridge	94%
BriJ20_16	75%	Brid	Reject	Bridge	55%
BriJ20_210	74%	Brid	Reject	Bridge	71%
BriJ20_63	73%	Brid	GU2	GU2	93%
BriJ20_197	72%	Brid	GU1	GU1	79%
BriJ20_116	71%	Brid	Bridge	Bridge	99%
BriJ20_200	70%	Brid	Bridge	Bridge	78%
BriJ20_220	70%	Brid	Bridge	Bridge	100%
BriJ20_216	67%	Brid	GU1	GU1	83%

Table E3 cont'd.

FishID	Mean Bridge Ancestry (%)	Structure inferred ancestry	Accepted GSI assignment	Region Name	Prob 1 (%)
BriJ20_40	64%	Brid	Reject	GU2	38%
BriJ20_119	66%	GU1	Reject	Bridge	51%
BriJ20_182	61%	GU1	GU1	GU1	88%
BriJ20_203	56%	GU1	Bridge	Bridge	76%
BriJ20_181	56%	GU1	Reject	GU1	70%
BriJ20_219	53%	GU1	Reject	GU1	60%
BriJ20_124	47%	GU1	Reject	GU2	52%
BriJ20_195	43%	GU1	GU1	GU1	99%
BriJ20_218	43%	GU1	Bridge	Bridge	95%
BriJ20_12	42%	GU1	GU1	GU1	96%
BriJ20_127	32%	GU1	GU1	GU1	89%
BriJ20_188	28%	GU1	Reject	L_Chilcotin	55%
BriJ20_209	22%	GU1	GU1	GU1	81%
BriJ20_19	51%	GU2	GU2	GU2	98%
BriJ20_226	45%	GU2	Reject	GU4b	52%
BriJ20_35	32%	GU2	Reject	GU2	47%
BriJ20_82	71%	GU2	Reject	L_Chilcotin	59%
BriJ20_44	65%	GU3	Reject	GU3	41%
BriJ20_23	62%	GU3	GU3	GU3	76%
BriJ20_207	44%	GU3	Reject	Bridge	48%
BriJ20_221	79%	GU4b	Bridge	Bridge	99%
BriJ20_130	71%	GU4b	Bridge	Bridge	93%
BriJ20_204	39%	GU4b	Reject	Bridge	39%
BriJ20_179	23%	GU4b	GU4b	GU4b	87%
BriJ20_121	58%	NThM	Reject	Bridge	70%
BriJ20_62	12%	Tase	Taseko	Taseko	96%
BriJ20_172	18%	Tete	Reject	GU2	48%
BriJ20_59	62%	Admixed	Reject	GU1	63%
BriJ20_18	54%	Admixed	Bridge	Bridge	78%
BriJ20_115	47%	Admixed	Reject	Bridge	58%
BriJ20_53	47%	Admixed	Reject	GU1	54%
BriJ20_20		Failed genotyping			
BriJ20_281		Failed genotyping			
BriJ20_50		Failed genotyping			
BriJ20_17		non-target_species			

Table E3 cont'd.

FishID	Mean Bridge Ancestry (%)	Structure inferred ancestry	Accepted GSI assignment	Region Name	Prob 1 (%)
BriJ20_280		non-target_species			
BriJ20_29		non-target_species			
BriJ20_291		non-target_species			
BriJ20_295		non-target_species			
BriJ20_3		non-target_species			
BriJ20_81		non-target_species			

Figure E1: Structure inferred genetic ancestry for the 2020 Bridge River Chinook juveniles. Each juvenile or baseline individual is represented by a coloured vertical bar. Each colour represents a population (*k*) or ancestral genetic factor. Ten iterations (R) of the analysis are shown.

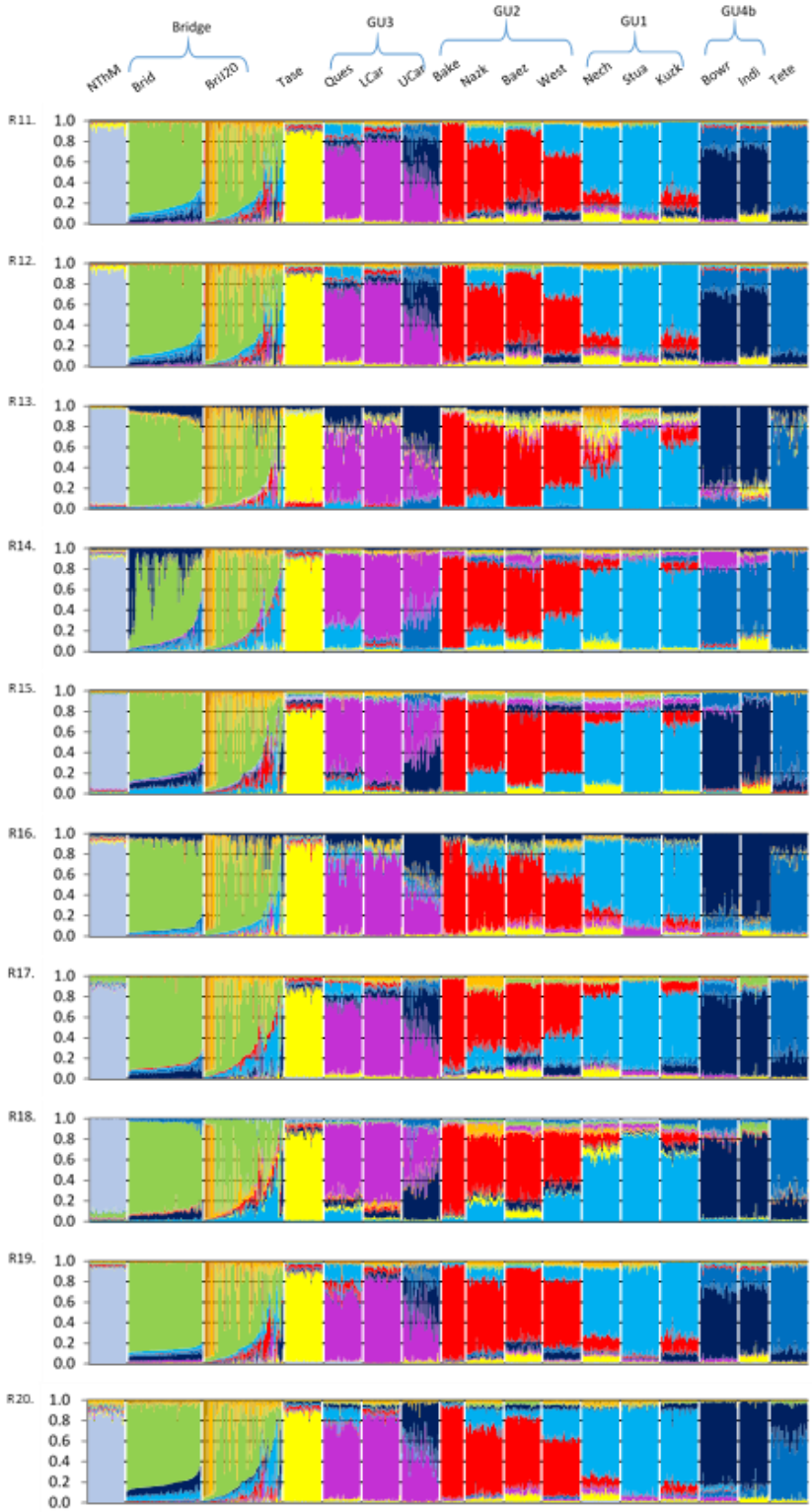

Table E4: Structure inferred genetic ancestry of 2020 Bridge River juvenile Chinook supported GSI analysis.

Structure inferred ancestry	**n**	**%**
Supported by GSI and Structure		
Bridge	43	64.2
Taseko	1	1.5
GU3	1	1.5
GU2	1	1.5
GU1	5	7.5
GU4b	1	1.5
Total	*52*	*77.6*
Not supported by GSI		
Total	*15*	*22.4*
Total	67	

Appendix F – Detailed Summary of Flow Rampdown Events and Fish Salvage Tallies

Table F1 Detailed Summary of Flow and Stage Changes, and Ramping Rates Associated with Individual Rampdown Events in 2019 and 2020.

Year	Date	Event #	Ramp Duration (hours)	Start Flow ($m^3 \cdot s^{-1}$)	End Flow ($m^3 \cdot s^{-1}$)	Flow Change ($m^3 \cdot s^{-1}$)	Start Stage (cm)	End Stage (cm)	Stage Change (cm)	Mean Daily Rate (cm/hr)
2020	21 Jul	1	4	15.1	12.9	-2.1	141	135	-6	-1.6
	22 Jul	2	4	13.0	11.0	-2.0	135	130	-6	-1.5
	28 Jul	3	4	11.1	9.3	-1.8	129	125	-3	-1.0
	29 Jul	4	5	9.3	7.7	-1.6	125	121	-4	-0.8
	4 Aug	5	4	7.7	6.4	-1.4	121	118	-4	-1.0
	5 Aug	6	4	6.4	5.1	-1.3	117	111	-6	-1.5
	6 Aug	7	4	5.1	4.1	-1.0	111	106	-5	-1.4
	7 Aug	8	5	4.1	3.0	-1.1	106	99	-6	-1.4
	5 Oct	9	7	3.0	1.7	-1.3	98	87	-11	-1.6
	6 Oct	10	3	1.7	1.5	-0.2	87	84	-3	-1.1
2020 Rampdown Summary			**4**	**15.1**	**1.5**	**-13.6**	**141**	**84**	**-57**	**-1.6 (Max.)**
2019	1 Aug	1	5	15.2	12.9	-2.3	144	138	-6	-1.1
	6 Aug	2	7	13.0	11.1	-1.9	138	133	-5	-0.7
	8 Aug	3	4	11.1	9.3	-1.8	133	128	-5	-1.3
	9 Aug	4	4	9.3	7.7	-1.6	128	123	-5	-1.3
	14 Aug	5	4	7.7	6.4	-1.3	122	118	-5	-1.2
	15 Aug	6	5	6.4	5.1	-1.3	117	111	-6	-1.3
	18 Aug	7	4	5.1	4.1	-1.1	111	106	-5	-1.3
	19 Aug	8	5	4.1	3.0	-1.1	106	99	-6	-1.3
	1 Oct	9	6	3.2	2.1	-1.0	98	91	-8	-1.3
	2 Oct	10	5	2.1	1.5	-0.6	90	84	-6	-1.2
2019 Rampdown Summary			**5**	**15.2**	**1.5**	**-13.7**	**144**	**84**	**-60**	**-1.3 (Max.)**

Table F2 Detailed Summary of Flow and Stage Changes, and Ramping Rates Associated with Individual Rampdown Events in 2018.

Year	Date	Event #	Ramp Duration (hours)	Start Flow ($m^3 \cdot s^{-1}$)	End Flow ($m^3 \cdot s^{-1}$)	Flow Change ($m^3 \cdot s^{-1}$)	Start Stage (cm)	End Stage (cm)	Stage Change (cm)	Mean Daily Rate (cm/hr)
2018	4 Jul	1	4	102.0	82.6	-19.4	265	248	-16	-4.0
	10 Jul	2	5	82.9	66.9	-15.9	247	229	-18	-3.6
	17 Jul	3	5	67.2	55.2	-12.0	229	215	-15	-2.9
	18 Jul	4	5	55.3	44.2	-11.0	215	197	-18	-3.5
	24 Jul	5	8	44.4	35.1	-9.3	197	182	-14	-1.8
	25 Jul	6	8	35.1	27.1	-8.0	182	168	-14	-1.8
	31 Jul	7	6	27.2	20.0	-7.2	168	153	-15	-2.4
	1 Aug	8	7	20.0	15.1	-4.9	153	142	-11	-1.6
High Flow Rampdown Summary		**8**	**6**	**102.0**	**15.1**	**-86.9**	**265**	**142**	**-123**	**-4.0 (Max.)**
2018	2 Aug	9	7	15.1	11.0	-4.1	142	132	-10	-1.5
	8 Aug	10	4	11.1	9.3	-1.8	132	126	-5	-1.3
	9 Aug	11	4	9.3	7.7	-1.6	126	121	-5	-1.2
	15 Aug	12	4	7.8	6.4	-1.3	122 [a]	116 [a]	-6	-1.4
	16 Aug	13	5	6.4	5.2	-1.3	116 [a]	110 [a]	-6	-1.2
	21 Aug	14	5	5.2	4.1	-1.1	110 [a]	103 [a]	-7	-1.3
	22 Aug	15	6	4.1	3.0	-1.1	103 [a]	96 [a]	-8	-1.3
	2 Oct	16	6	3.1	2.1	-1.0	96	87	-9	-1.6
	3 Oct	17	4	2.1	1.5	-0.6	87	80	-6	-1.6
WUP Rampdown Summary		**9**	**5**	**15.1**	**1.5**	**-13.6**	**142**	**80**	**-62**	**-1.6 (Max.)**

[a] These values are based on the discharge-stage relationship (see Figure 3.32 in Section **Error! Reference source not found.**) since stage values for the Rkm 36.8 logger were not available on these dates in 2018.

Table F3 Detailed Summary of Flow and Stage Changes, and Ramping Rates Associated with Individual Rampdown Events in 2017.

Year	Date	Event #	Ramp Duration (hours)	Start Flow ($m^3 \cdot s^{-1}$)	End Flow ($m^3 \cdot s^{-1}$)	Flow Change ($m^3 \cdot s^{-1}$)	Start Stage (cm)	End Stage (cm)	Stage Change (cm)	Mean Daily Rate (cm/hr)
2017	28 Jun	1	7	126.9	109.2	-17.7	290	272	-17	-2.5
	4 Jul	2	7	111.3	96.6	-14.7	278	263	-15	-2.1
	7 Jul	3	7	97.2	79.6	-17.5	263	247	-15	-2.2
	11 Jul	4	4	80.4	67.1	-13.3	247	231	-16	-4.0
	12 Jul	5	4	67.2	55.1	-12.2	232	218	-13	-3.4
	13 Jul	6	4	55.2	44.7	-10.5	218	202	-16	-4.1
	18 Jul	7	8	45.1	35.1	-10.1	203	186	-17	-2.2
	19 Jul	8	8	35.1	26.6	-8.5	186	171	-15	-1.9
	20 Jul	9	7	26.6	19.8	-6.8	171	157	-13	-1.9
	21 Jul	10	6	19.8	14.9	-4.9	157	147	-10	-1.7
High Flow Rampdown Summary		**10**	**6**	**126.9**	**14.9**	**-112.0**	**290**	**147**	**-143**	**-4.1 (Max.)**
2017	1 Aug	11	7	15.3	11.0	-4.3	147	136	-12	-1.6
	9 Aug	12	4	11.1	9.2	-1.8	136	131	-5	-1.2
	10 Aug	13	4	9.3	7.7	-1.6	130	125	-5	-1.3
	15 Aug	14	3	7.7	6.4	-1.4	125	120	-5	-1.7
	16 Aug	15	4	6.4	5.1	-1.3	120	110	-10	-2.5
	22 Aug	16	4	5.1	4.1	-1.0	110	103	-7	-1.7
	23 Aug	17	4	4.1	3.0	-1.1	103	96	-8	-1.9
	26 Sep	18	5	3.1	2.3	-0.8	95	88	-7	-1.4
	27 Sep	19	3	2.3	1.5	-0.7	88	80	-8	-2.6
WUP Rampdown Summary		**9**	**4**	**15.3**	**1.5**	**-13.7**	**147**	**80**	**-67**	**-2.6 (Max.)**

Table F4 Detailed Summary of Flow and Stage Changes, and Ramping Rates Associated with Individual Rampdown Events in 2016.

Year	Date	Event #	Ramp Duration (hours)	Start Flow ($m^3 \cdot s^{-1}$)	End Flow ($m^3 \cdot s^{-1}$)	Flow Change ($m^3 \cdot s^{-1}$)	Start Stage (cm)	End Stage (cm)	Stage Change (cm)	Mean Daily Rate (cm/hr)
2016	20 Jun	1	8	96.5	80.6	-15.9	245	233	-12	-1.5
	22 Jun	2	7	80.7	67.1	-13.6	234	223	-10	-1.5
	29 Jun	3	7	67.9	55.3	-12.6	224	209	-15	-2.1
	5 Jul	4	8	56.0	45.2	-10.9	210	195	-16	-2.0
	12 Jul	5	7	45.5	35.7	-9.8	196	180	-16	-2.2
	19 Jul	6	7	36.0	27.6	-8.4	180	165	-15	-2.1
	20 Jul	7	6	27.6	20.6	-7.0	165	151	-14	-2.3
	25 Jul	8	7	20.8	15.1	-5.7	151	137	-14	-2.0
High Flow Rampdown Summary		**8**	**7**	**96.5**	**15.1**	**-81.4**	**245**	**137**	**-108**	**-2.3 (Max.)**
2016	5 Aug	9	6	15.3	13.2	-2.2	137	131	-6	-1.0
	8 Aug	10	4	13.2	11.1	-2.1	131	124	-7	-1.8
	9 Aug	11	4	11.1	9.4	-1.7	124	118	-6	-1.5
	10 Aug	12	4	9.4	7.7	-1.6	118	111	-7	-1.8
	17 Aug	13	4	7.8	6.4	-1.3	111	105	-6	-1.5
	18 Aug	14	4	6.4	5.1	-1.3	105	99	-6	-1.4
	23 Aug	15	4	5.1	4.1	-1.0	99	93	-6	-1.5
	24 Aug	16	5	4.1	3.0	-1.2	93	83	-10	-2.0
	27 Sep	17	4	3.1	2.2	-0.8	95	87	-8	-2.0
	28 Sep	18	3	2.3	1.5	-0.7	87	78	-9	-3.0
WUP Rampdown Summary		**10**	**4**	**15.3**	**1.5**	**-13.8**	**137**	**78**	**-59**	**-3.0 (Max.)**

Table F5 Fish salvage tallies by species, ramp date and flow range – 2020 results (reaches 3 and 4 only).

Species	Ramp Date and Flow Range ($m^3 \cdot s^{-1}$)										Species Totals
	21 Jul (15.1–12.9)	22 Jul (13.0–11.0)	28 Jul (11.1–9.3)	29 Jul (9.3–7.7)	4 Aug (7.7–6.4)	5 Aug (6.4–5.1)	6 Aug (5.1–4.1)	7 Aug (4.1–3.0)	5 Oct (3.0–1.7)	6 Oct (1.7–1.5)	
Chinook			2	12	5	1		6	3		**29**
Coho	74	28	60	712	567	157	92	39	36	31	**1,796**
Mykiss	12	16	58	385	598	547	111	82	156	27	**1,992**
Bull trout				10	3						**13**
Mountain whitefish	1			23	4	2					**30**
Redside shiner	103	53			1						**157**
Sculpin spp.	4		1		1	1		1			**8**
Daily Totals	**194**	**97**	**121**	**1,142**	**1,179**	**708**	**203**	**128**	**195**	**58**	**4,025**